UNIVERSITAT DE BARCELONA

Design and characterization of topical ketorolac tromethamine formulations

Diseño y caracterización de formulaciones tópicas de Ketorolaco trometamina

Salima El Moussaoui El Masnaoui

UNIVERSITAT DE BARCELONA

UNIVERSIDAD DE BARCELONA

FACULTAD DE FARMACIA Y CIENCIAS DE LA ALIMENTACIÓN

PROGRAMA DE DOCTORADO DE BIOTECNOLOGÍA

SALIMA EL MOUSSAOUI EL MASNAOUI

2022

FACULTAD DE FARMACIA I CIÉNCIES DE LA ALIMENTACIÓN

PROGRAMA DE DOCTORADO EN BIOTECNOLOGÍA

DESIGN AND CHARACTERIZATION OF TOPICAL KETOROLAC TROMETHAMINE FORMULATIONS

Diseño y caracterización de formulaciones tópicas de Ketorolaco trometamina

Memoria presentada por Salima El Moussaoui El Masnaoui para optar al título de doctor por la Universidad de Barcelona

Directoras de Tesis:

Dra. Ana Cristina Calpena Campmany

Dra. Mireia Mallandrich Miret

Doctoranda: Salima El Moussaoui El Masnaoui

Tutora: Dra. Ana Cristina Calpena Campmany

SALIMA EL MOUSSAOUI EL MASNAOUI

2022

Dedicado a mi querida abuela Moumna, la persona que más ha confiado en mí y la que siempre me ha animado a seguir formándome.

Agradecimientos

Al Hamdullillah. Oh Allah gracias por permitir el cumplimiento de este proyecto y por iluminar siempre mi camino.

Con estas líneas quisiera agradecer a todas aquellas personas que con su esfuerzo, apoyo y tiempo han contribuido a que este proyecto se lleve a cabo. En primer lugar, un caluroso y especial agradecimiento a mis directoras de tesis, la Dra. **Ana Cristina Calpena Campmany** y Dra. **Mieria Mallandrich Miret**. Gracias por la confianza depositada en mí desde el minuto uno. Nunca olviadré el recibimiento tan afectuoso que me disteis. Enseguida me incluisteis en vuestro equipo como una más. Siempre habéis puesto vuestra experiencia y conocimiento a mi disposición y aprender de vosotras es siempre una gozada. Vuestra paciencia y cariño para conmigo me conmueven. Habéis estado allí siempre, tanto para lo profesional cómo lo personal, tirando de mí y apoyándome en mis momentos más flacos. Os llevo y os llevaré siempre en mi corazón.

A **Francisco Fernández Campos** por su gran profesionalidad, sus revisiones y sus valiosos consejos.

Gracias también a todos los compañeros con los que compartimos momentos en el laboratorio: **Cristina Cañadas, Álex, Núria, Cristina Alonso**. Sin vuestra ayuda y dedicación este proyecto no hubiera sido posible. Gracias de corazón.

Una especial mención a la directora del programa, la **Dra. Josefa Badia** por el apoyo constante y por facilitarnos siempre el trabajo, así como a la **Dra. María Luisa Garduño Ramírez** por su apoyo y por la oportunidad brindada al aceptarme en su laboratorio en la Universidad Autónomo del Estado de Morelos en México.

Agradecer también a mis padres**, Nassira** y **Houssein,** por habérmelo dado todo, vuestro tiempo, cariño y apoyo incondicional. Sé que cuando llego a vosotros con nuevos proyectos e ideas os preocupáis y sufrís conmigo todo el proceso, pero siempre estáis allí, apoyando, y eso es muy reconfortante. Sin vuestros rezos y

bendiciones no hubiera podido recorrer todo el camino hasta aquí. Os lo debo todo.

A mis segundos padres, mis suegros **Fátima** y **Mohamed,** a mis hermanos, **Youssef, Bilal, Mohamed** y **Hanan** y mis cuñadas **Nassira** y **Siham** por preocuparos, preguntar y escuchar. Vuestros ánimos en los momentos críticos han sido cruciales.

Pero en especial gracias a ti **Youssef**, mi otra mitad. Eres mi compañero de vida, el que me aguanta en los momentos de bajón y el que me sacude y tira hacia adelante. Sin tu ayuda y tu apoyo este proyecto no hubiera visto la luz. Siempre dispuesto a ayudar y escuchar, aunque no siempre entiendas muy bien los tecnicismos. Has estado en los momentos difíciles y celebrando conmigo los logros. Tú y nuestro pequeño **Karim** sois mi motivación para seguir siempre hacia adelante. Gracias por estar allí y no dejarme desistir.

A mis amigos y compañeros de trabajo. Gracias a ti **Sheimah** por mantener la amista aún y la distancia y por preocuparte siempre.

Y a todos los que me dejo, a todos ellos, ¡GRACIAS!

ÍNDICE

Agradecimientos IV

Abstract 1

Resumen 2

Abreviaturas 3

INTRODUCCIÓN 6

1.1.- Dolor e inflamación 7

1.1.1.- El dolor. Conceptos básicos 7

1.1.2.- Tipos de dolor 9

1.1.3.- Inflamación 11

1.2.- Analgesia 14

1.2.1.- Antiinflamatorios no esteroidales (AINE) 14

1.3.- Piel 18

1.3.1.- Estructura 18

1.3.2.- Propiedades y funciones 21

1.4.- Mucosas 23

1.4.1.- Mucosa oral 23

1.4.2.- Mucosa vaginal 26

1.4.3.- Permeabilidad de las mucosas y de la piel 28

1.5.- Condiloma acuminado 32

1.5.1.- Descripción 32

1.5.2.- Características clínicas y diagnóstico 33

1.5.3.- Tratamiento 35

1.6.- Hidrogeles mucoadhesivos 41

1.6.1.- Propiedades y aplicaciones 41

1.6.2.- Polímeros gelificantes 43

1.7.- Nanopartículas 47

1.7.1.- Elaboración de Nanopartículas 48

1.7.2.- Caracterización de nanopartículas..... 50

OBJETIVOS 52

RESULTADOS..... 54

3.1.- Artículo 1..... 55

3.2.- Artículo 2..... 78

3.3.- Artículo 3.....101

DISCUSIÓN.....126

CONCLUSIONES.....138

BIBLIOGRAFÍA.....142

Abstract

Pain and inflammation are the most common and recurrent side effects after surgery and, understandably, the patient's most feared, affecting treatment adherence.

The present work aims to characterize in vitro, ex vivo, and in vivo different ketorolac tromethamine mucoadhesive topical formulations to be applied to the skin and mucous membranes for the pain and inflammation management associated with surgical, chemical, and/or ablative processes, such as it may be that of the eradication of condyloma acuminata. For this, different gelling polymers with mucoadhesive properties that were biocompatible, and biodegradable, were chosen. Sodium alginate and chitosan were the polymers we worked with in addition to other ingredients such as hyaluronic acid. Additionally, PLGA (polylactic glycolic acid) nanoparticles were made where ketorolac tromethamine was encapsulated with the possibility that it could be applied as a spray.

The in vitro characterization was carried out by studying the organoleptic characteristics, pH, rheological behavior, morphology, and release study of each formulation. The ex vivo studies consisted of Franz-type cell permeation tests of the formulations on different tissues (human skin and mucous membranes). The in vivo studies included applying some of the formulations in live pigs and their subsequent histological analysis, anti-inflammatory efficacy studies in the ear of mice, and tolerability studies in human skin and pigs oral mucosa.

The results show how all ketorolac tromethamine formulations meet the requirements for application on skin and mucous membranes, showing easy applicability, excellent tolerability, and good topical anti-inflammatory efficacy.

Resumen

Dolor e inflamación son los efectos secundarios más comunes y recurrentes tras una cirugía y comprensiblemente, los más temidos por el paciente, lo cual repercute en la adherencia al tratamiento.

El presente trabajo pretende caracterizar in vitro, ex vivo e in vivo diferentes formulaciones tópicas mucoadhesivas de ketorolaco trometamina con el fin de ser aplicados sobre piel y mucosas para el manejo del dolor y la inflamación asociado a procesos quirúrgicos, químicos y/o ablativos, como puede ser el de la erradicación del condiloma acuminado. Para ello se escogieron diferentes polímeros gelificantes con propiedades mucoadhesivas que fueran biocompatibles y biodegradables. El alginato de sodio y el chitosan fueron los polímeros con los que trabajamos a de más de otros ingredientes como el ácido hialurónico. Adicionalmente, se elaboraron nanopartículas de PLGA (ácido polilácticoglicólico) donde se encapsulo el ketorolaco trometamina con la posibilidad de que pudiera aplicarse en forma de spray.

La caracterización in vitro se llevó a cabo mediante el estudio de las características organolépticas, pH, comportamiento reológico, morfología, y estudio de liberación de cada formulación. Los estudios ex vivo consistieron en ensayos de permeación en celdas tipo Franz de las formulaciones sobre diferentes tejidos (piel humana y mucosas). Los estudios in vivo incluyeron la aplicación de algunas de las formulaciones en cerdos vivos y el posterior análisis histológico, estudios de eficacia antinflamatoria en oreja de ratones y estudios de tolerabilidad en piel humana y en mucosa oral de cerdo.

Los resultados muestran cómo todas las formulaciones de ketorolaco trometamina cumplen con los requisitos necesarios para su aplicación sobre piel y mucosas, mostrando una fácil aplicabilidad, excelente tolerabilidad, así como una buena eficacia antinflamatoria tópica.

Abreviaturas

ADP	adenosina fosfato
AH	ácido hialurónico
AINE	antiinflamatorio no esteroideo
ALA	5-aminolevulínico
ATC	ácido tricloracético
CA	condiloma acuminado
cm	centímetro
cm^2	centímetro cuadrado
COCE	carcinoma orofaríngeo de células escamosas
COX	ciclooxigenasa
CTS	chitosan
DLS	Dynamic lihgt scattering (dispersión de luz dinámica)
EMA	*european medicines agency* (agencia europea del medicamento)
ETS	enfermedad de transmisión sexual
FDA	*food and drug administration*
G	residuos de ádico L-gulurónico
h	hora
kg	kilogramo
KT	ketorolaco
L	litro
log P	coeficiente de partición de n-octanol/agua
LOX	lipooxigenasa

LTs	leucotrienos
M	residuos de ácido D-manurónico
m^2	metros cuadrados
MAL	ácido metil-aminolevulinato
mm	milímetro
nm	nanómetro
PGI_2	prostaciclinas
PGs	prostaglandinas
Ph. Eur.	farmacopea europea
PI	*polidispersity index* (índice de polidispersidad)
PLA	ácido poliláctico
PLGA	ácido poliláctico-co-glicólico
PVA	alcohol de polivinilo
QSAR	*quantitative structure-activity relationship* (relación cuantitativa estructura-actividad)
SEM	*scanning electron microscopy* (microscopio electrónico de barrido)
TEM	*transmisión electron microscopy* (microscopio electrónico de transmisión)
TEWL	*transepidermal water los* (pérdida de agua transepidérmica)
t_{max}	tiempo hasta la concentración máxima en plasma
TMWL	*transmucosal water los* (pérdida de agua transmucosa)
TXAs	tromboxanos
V_d	volumen de distribución aparente
VG	verruga genital
VIH	virus de la inmunodeficiencia humana

VPH	virus del papiloma humano
Zave	tamaño de partícula
ZP	potencial Z

INTRODUCCIÓN

1.1.- Dolor e inflamación

1.1.1.- El dolor. Conceptos básicos

La Real Academia Española define dolor cómo" sensación molesta y aflictiva en una parte del cuerpo por causa interior o exterior" (Real Academia Española, 2021, definición 1).

Desde siempre, el ser humano ha intentado aliviar y controlar esta sensación molesta, para lo cual, el entendimiento y conocimiento del proceso doloroso era imprescindible. Para las sociedades primitivas, el dolor físico resultante por accidentes o eventos traumáticos era comprensible, ya que la causa era clara y tangible. Sin embargo, el dolor más emocional y psicológico o el dolor crónico causado por motivos no tan obvios, se asociaba a figuras divinas, dioses, espíritus y demonios. No es de extrañar entonces, el papel que jugaron sacerdotes, chamanes y otras figuras espirituales en el tratamiento del dolor durante tantos años [1]. Con el paso del tiempo y el avance del conocimiento sobre medicina y el cuerpo humano se esclareció el funcionamiento del sistema nervioso, cómo funciona el mecanismo del dolor y se desarrollaron tratamientos funcionales capaces de aliviarlo y controlarlo.

La existencia de muchos tipos de dolor pueden entenderse mediante la identificación de cuatro amplias categorías: nocicepción, percepción del dolor, sufrimiento y conductas de dolor [2].

Nocicepción: el dolor de una herido o lesión no puede ocurrir sin la nocicepción. Ésta consiste en la detección de estímulos potencial o realmente dañinos seguidos de un retiro reflejo. Dicha detección se lleva a cabo a través de receptores transductores especializados denominados nociceptores que transmiten la detección en forma de potenciales de acción a través de los nervios hacia el sistema nervioso central, dónde será procesada [3]. Estos transductores pueden estar sesgados por cambios inflamatorios y neurales en su entorno inmediato.

La **percepción del dolor** es la percepción que el sujeto experimenta, con todos sus componentes sensoriales y emocionales. Cuando se presenta dolor agudo,

inicialmente se asocia a reflejos autonómicos y somáticos específicos, pero estos desaparecen en pacientes con dolor crónico. El dolor puede ocurrir sin nocicepción, es decir, sin la presencia de una lesión o de un estímulo nocivo y la intensidad del dolor crónico frecuentemente tiene poca o ninguna relación con la extensión de la lesión tisular de otra patología cuantificable, lo que indica la compleja relación entre lesión y dolor.

Sufrimiento: Eric J. Cassel [4] decía que el sufrimiento era causado por la amenaza de la integridad física o psíquica de la persona. Consiste en una respuesta afectiva negativa inducida por el miedo, la ansiedad, el estrés, otros estados psicológicos y por supuesto el dolor. No todo sufrimiento es causado por el dolor, pero en nuestra cultura medicalizada describimos el sufrimiento en el lenguaje del dolor.

Los **comportamientos del dolor** incluyen todas aquellas conductas que un individuo adopta al experimentar o sufrir dolor: gritar, llorar, hacer muecas, acostarse, recurrir a la atención médica, dejar de hacer una actividad concreta como trabajar, etc. Tales comportamientos son observables por otros y por ende pueden cuantificarse.

A de más de los conceptos descritos anteriormente, hay otros aspectos que son importantes para poder entender y clasificar el dolor. Estos son la duración, la intensidad, la localización, la cualidad y el afecto.

La **duración** es el tiempo durante el cual se percibe el dolor. Este puede ser continuo o intermitente y, en la mayoría de los casos, la duración está relacionada directamente con la nocicepción. En clínica se ha convenido en denominar al dolor, de acuerdo con su duración, como agudo y crónico, siendo el agudo aquel que tiene una duración de hasta 3 meses y el crónico aquel dolor con una durabilidad, ya sea de manera continua o intermitente de más de tres o seis meses.

La **intensidad** es la magnitud del dolor percibido. La intensidad del dolor es un fenómeno subjetivo que puede estar influenciado por diversos factores tanto personales como ambientales. Para poder cuantificarla se usan escalas numéricas dónde la intensidad del dolor es determinada por el mismo paciente sobre una escala del 0 al 10. El número 0 indica ausencia del dolor, y 10 se refiere al dolor más intenso que el sujeto pueda imaginar.

La **localización** se refiere al lugar del cuerpo donde el dolor es percibido. En ocasiones el lugar de percepción no coincide con el lugar dónde se origina el dolor,

debido a la Ley de la Proyección. El dolor originado por estímulos nocivos en estructuras profundas (musculares o viscerales), en muchos casos se percibe en áreas superficiales, sanas, correspondientes a dermatomas relacionados con la víscera afectada (dolor proyectado) o en dermatomas vecinos (dolor irradiado). Estas dos clases de dolor se conocen globalmente como dolor referido. Cuando el dolor referido se origina en estructuras somáticas o viscerales se divide en dos tipos: dolor referido sin hiperalgesia (dolor segmentario) y dolor referido con hiperalgesia (dolor parietal).

La **cualidad** del dolor describe cómo es el dolor percibido: punzante, calambre, quemante, opresivo, etc. El **afecto** es positivo o negativo según si la sensación que acompaña a una percepción es de agrado o desagrado. En el caso del dolor el afecto suele ser negativo.

1.1.2.- Tipos de dolor

Son muchos los aspectos a tener en cuenta a la hora de clasificar los tipos de dolor; durabilidad, fisiopatología, intensidad, etc. De forma simple y generalizada podemos distinguir 3 tipos de dolor.

Por un lado, tendríamos el dolor que actúa cómo respuesta fisiológica normal del organismo frente a lesiones traumáticas, físicas y químicas. Tiene función de protección biológica constituyendo un sistema de alarma de primer orden que advierte de la existencia de peligro, permitiendo poner en marcha mecanismos de evitación o protección [5]. Dichas lesiones pueden a su vez tener una localización somática o visceral, siendo el dolor somático aquel cuyo origen es la información nociceptiva procedente de cualquier tejido que constituye la estructura del cuerpo: huesos, músculos, articulaciones, tendones, tronco y extremidades; y el dolor visceral el que proviene de órganos internos como el corazón y vasos, los pulmones y las vías respiratorias, el hígado, los riñones, etc. A de más el dolor visceral se caracteriza por ser difuso y estar mal localizado. Debido a que este dolor está relacionado con la detección de estímulos nocivos, se denomina **dolor nociceptivo**, un dolor de alto umbral que solo se activa en presencia de estímulos intensos [6]. El dolor nociceptivo se presenta como algo que se debe evitar ahora y, cuando se activa, el sistema anula la mayoría de las demás funciones neuronales [7].

El segundo tipo de dolor es causado por la activación del sistema inmunitario por lesión o infección tisular, por lo que se denomina **dolor inflamatorio**. Este dolor también es adaptativo y protector. Después de un daño tisular aumentar la sensibilidad sensorial del dolor y esto ayuda en la curación de la parte del cuerpo lesionada al crear una situación que desalienta el contacto físico y el movimiento, reduciendo el riesgo adicional de daño y promoviendo la recuperación [7]. De hecho, el dolor es una de las características cardinales de la inflamación.

Por último, tendríamos el **dolor patológico** que no es un síntoma de algún trastorno sino un estado de enfermedad del sistema nervioso. Éste puede ocurrir después de un daño en el sistema nervioso, dolor neuropático, o en condiciones en las que no hay daño o inflamación, dolor disfuncional. Las condiciones que provocan dolor disfuncional incluyen fibromialgia, síndrome del intestino irritable, dolor de cabeza de tipo tensional, enfermedad de la articulación temporomandibular, cistitis intersticial y otros síndromes en los que existe un dolor sustancial pero ningún estímulo nocivo y ninguna patología inflamatoria periférica o mínima. Este dolor patológico es en gran parte la consecuencia de señales sensoriales amplificadas en el sistema nervioso central y es un dolor de bajo umbral.

Debido a que los procesos que impulsan cada tipo de dolor son bastante diferentes, los tratamientos deben dirigirse a los distintos mecanismos responsables.

A de más de los tipos de dolor descritos anteriormente, también podemos clasificar el dolor teniendo en cuenta la durabilidad. Por un lado, el **dolor agudo**, que sería aquel dolor activado por nocicepción delimitado en el tiempo y que persiste durante el proceso de curación o cicatrización de los tejidos implicados (generalmente hasta 3 meses) [8] y por otro lado el **dolor crónico,** un dolor persistente que transcurre más de 3-6 meses desde el momento de la agresión tisular, e incluso, en ausencia de ella [5]. Suele ser refractario a los tratamientos y se asocia a importantes síntomas psicológicos.

1.1.3.- Inflamación

La inflamación es un fenómeno patológico protector, complejo y cuidadosamente regulado diseñado para minimizar los efectos dañinos de estímulos nocivos mediante dilución, localización, destrucción y, si es posible, eliminación del mismo. La respuesta inflamatoria genera una respuesta humoral y celular (complemento, cininas, coagulación y cascada fibrinolítica) en el foco inflamatorio [9]. Los mecanismos involucrados en este proceso se caracterizan por una serie compleja de eventos que implican vasodilatación, aumento de la permeabilidad vascular, activación/adhesión celular e hipercoagulabilidad [10]. La vasodilatación y el incremento de la permeabilidad microvascular en el lugar de la inflamación aumentan la disponibilidad local de nutrientes y de oxígeno, produciendo calor, hinchazón y edema tisular. Los cambios hemodinámicos producen los cuatro síntomas clásicos asociados a la inflamación local: rubor (eritema), tumor (edema), calor y dolor [11].

Las células endoteliales juegan un rol importante en la respuesta inflamatoria facilitando la extravasación de leucocitos de la sangre a las zonas de inflamación. Los neutrófilos y macrófagos se suman y ejercen su acción fagocítica, además de liberar al medio extracelular sustancias como prostaglandinas, leucotrienos y citoquinas que amplifican la respuesta inflamatoria.

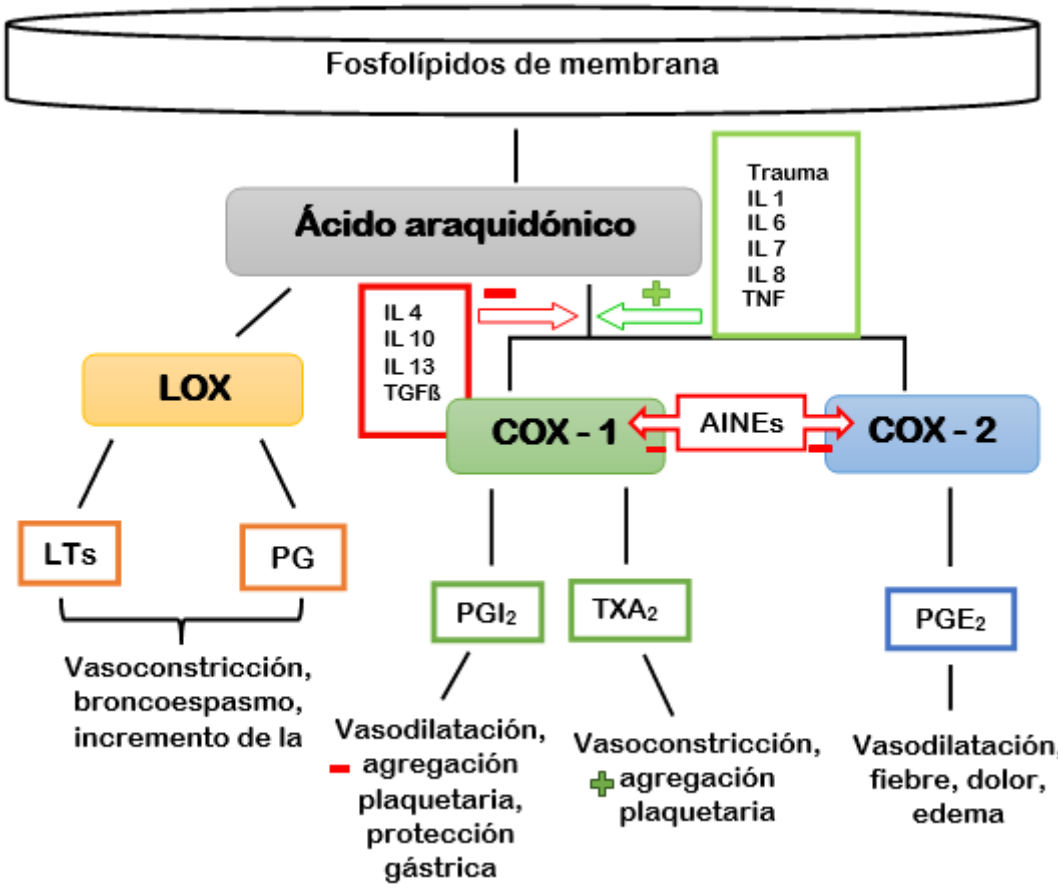

***Figura 1**. Síntesis de eicosanoides a partir de COX-1, COX-2 y LOX.*

La familia de las ciclooxigenasas, COX-1 y COX-2, es un grupo de enzimas bifuncionales que contienen actividad ciclooxigenasa y peroxidasa, que catalizan la síntesis de eicosanoides, prostaglandinas (PG_S), prostaciclinas (PGI_2) y tromboxanos (TXA_2) a partir de la oxidación del ácido araquidónico, un ácido graso insaturado de 20 carbonos, que es liberado de la membrana plasmática por fosfolipasas. COX-1, o constitutiva, fue la primera enzima en identificarse. Está presente en casi todos los tejidos en niveles constantes y se encarga de la producción fisiológica normal de prostaglandinas. Sus metabolitos a partir del ácido araquidónico son los responsables de mantener las condiciones fisiológicas básicas del organismo, tales como la protección gastrointestinal, la homeostasia vascular y renal y la función plaquetaria [12]. COX-2, o inducible, en cambio, no se encuentra en la mayoría de los tejidos, sino en focos inflamatorios, neoplasias o bajo determinadas condiciones fisiológicas. Está implicada en la síntesis de prostaglandinas que participan en procesos inflamatorios, patológicos y de estrés, y su expresión es inducida por estímulos proinflamatorios como determinadas citoquinas, factores de crecimiento o agentes tumorogénicos [13][14] pudiendo ésta aumentar entre 10 y 80 veces [15].

Hay cuatro prostaglandinas bioactivas principales: prostaglandina E_2 (PGE_2) que causa vasodilatación, calor, fiebre y edema; prostaciclina (PGI_2) que provoca vasodilatación, contribuye a la protección gástrica e inhibe la agregación plaquetaria; prostaglandina D_2 (PGD_2) y prostaglandina $F_{2\alpha}$ ($PGF_{2\alpha}$) que causan vasodilatación y edema. Durante una respuesta inflamatoria, tanto el nivel como el perfil de producción de prostaglandinas cambian drásticamente. La producción de prostaglandinas es generalmente muy baja en tejidos no inflamados, pero aumenta inmediatamente en la inflamación aguda antes del reclutamiento de leucocitos y la infiltración de células inmunitarias [13].

La producción de prostaglandinas (Figura 1) depende de la actividad de la COX-1 y COX-2. La PGH2 es producida por ambas isoformas de COX y es el sustrato común para las enzimas isomerasas y sintasas específicas que producen PGE_2, PGI_2, PGD2, $PGF_{2\alpha}$ y TXA_2. El perfil de producción de prostanoides está determinado por la expresión diferencial de estas enzimas dentro de las células presentes en los sitios de inflamación [16].

Paralelamente, el ácido araquidónico puede ser convertido a leucotrienos (LTs) o a eicosanoides por la vía de la lipooxigenasa (LOX) que acabarían ocasionando vasoconstricción e incremento de la permeabilidad vascular.

1.2.- Analgesia

La analgesia es el alivio del dolor. Para ello existen diferentes tipos de fármacos que, mediante distintos mecanismos de acción, consiguen mitigar la sensación dolorosa.

Por un lado, tendríamos a los opioides. Éstos actúan sobre los receptores opioides de las neuronas del sistema nervioso, imitando el poder analgésico de los opiáceos endógenos. Unos son naturales (opiáceo) como la morfina, y otros artificiales (opioide) como el fentanilo. Son los fármacos analgésicos más potentes conocidos, no presentan techo terapéutico, por lo que se puede aumentar la dosis según la presencia de dolor y tolerancia del paciente, pero presenta el inconveniente de que son sustancias estupefacientes y deprimen el sistema nervioso central, así como un alto potencial de dependencia y abuso [17].

Los Antiinflamatorios No Esteroidales (AINEs) son un grupo heterogéneo de analgésicos ampliamente prescritos y utilizados para tratar diferentes tipos de dolores. A de más del efecto analgésico, presentan efecto antipirético, antiinflamatorio y antiagregante plaquetario [15]. Sus efectos secundarios limitan su uso.

Por otro lado, tendríamos los fármacos adyuvantes que, aunque no son analgésicos cuando se administran aisladamente, potencian la acción de cualquier analgésico en asociación. En este grupo tendríamos a los corticoides, antidepresivos (sobre todo los antidepresivos tricíclicos) y anticonvulsivantes.

El dolor es imprescindible para mantener la integridad corporal. Aunque usamos analgésicos para reducirlo, hay que tener cuidado de que el dolor de los pacientes no sea tan mitigado por la terapia, que pierda su función protectora [7].

1.2.1.- Antiinflamatorios no esteroidales (AINE)

1.2.1.1.- Mecanismo de acción

El mecanismo de acción de los AINEs fue descrito por primera vez en 1971 por Vane y Piper, quienes demostraron que los AINEs ejercen sus efectos a través de la inhibición de la biosíntesis de prostaglandinas y prostanoides por parte de las enzimas

COX [16]. Las isoenzimas COX son las primeras en convertir el ácido araquidónico en PGG_2. Luego, la peroxidasa metaboliza PGG_2 a PGH_2 que, a su vez, se convierte mediante isomerasas específicas de tejido en prostanoides primarios, incluidos PGD_2, PGE_2, $PGF_{2\alpha}$, PGI_2 y tromboxano A_2. Tanto los efectos terapéuticos como los adversos de los AINE son causados por la inhibición de la enzima COX y el consiguiente bloqueo de la formación de PGs y compuestos relacionados. Los efectos analgésicos, antipiréticos y antiinflamatorios de los AINEs se atribuyen a la reducción en la producción de PGE_2 y PGI_2 [16].

La actividad analgésica de los AINE es de intensidad media/moderada y tiene lugar a nivel periférico. Los prostanoides provocan una hipersensibilización de las terminaciones nerviosas aferentes nociceptivas frente a los mediadores del dolor (especialmente bradicinina). Es por ello que los AINEs son especialmente eficaces en todos aquellos dolores asociados con procesos inflamatorios y otras situaciones donde participen de forma destacada las prostaglandinas (migrañas asociadas con la menstruación, dismenorreas, dolores articulares, musculares y vasculares, dolor postoperatorio, dolor canceroso, dolor postraumático), ya que actúan, precisamente, disminuyendo el efecto hiperalgésico de los prostanoides. La eficacia analgésica es una peculiaridad de cada molécula, no es normalmente dependiente de dosis y no guarda ninguna relación con la capacidad antiinflamatoria. Para evaluar la eficacia antiálgica de un determinado AINE es necesario considerar el tipo de dolor y su intensidad y cabe destacar que las dosis recomendadas para conseguir la analgesia suelen ser menores que las recomendadas por su efecto antiinflamatorio [18].

1.2.1.2.- Ketorloaco

El Ketorolaco (KT) es un agente no esteroidal con un potente efecto analgésico y una actividad antiinflamatoria moderada. Se administra en forma de sal de trometamina, por vía oral, intramuscular, intravenosa y por vía tópica como solución oftálmica. El ketorolaco trometamina es un fármaco AINE que pertenece a la clase de los derivados heterocíclicos del ácido acético. Es un inhibidor no selectivo de la COX, que se comercializa en forma de racemato. La mayor parte de su actividad analgésica e inhibidora de la COX se retiene en el isómero S.

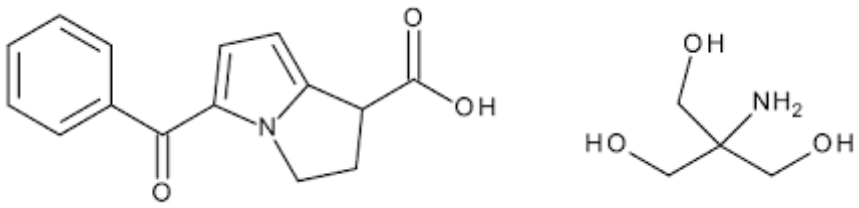

***Figura 2**: Estructura molecular de la sal ketorolaco trometamina. Izquierda: ketorolaco. Derecha: trometamina.*

El KT se absorbe rápidamente, con un tiempo hasta la concentración máxima en plasma (t_{max}) de unos 30 a 40 minutos después de la administración oral, y de 45 a 50 minutos después de la administración intramuscular. La disponibilidad sistémica de KT es aproximadamente entre un 80-90% después de la administración oral y los alimentos parece que reducen la tasa de absorción. Al igual que con otros AINE, el KT se une casi por completo a las proteínas plasmáticas (>99 %), lo que da como resultado un volumen de distribución aparente (Vd) pequeño [<0,3 L/kg]. En sujetos sanos, su aclaramiento plasmático es de 0,021-0,037 L/h/kg y la semivida de eliminación terminal va de 4 a 6 horas. Parece que el KT traviesa la placenta aproximadamente un 10 %, pero no se encuentra en leche materna en cantidades significativas. La principal vía metabólica en los seres humanos es la conjugación con ácido glucurónico e hidroxilación en el hígado. Aproximadamente el 90 % de la dosis se recupera en la orina, y el resto en las heces [19].

El KT es soluble en agua y tiene un pKa de 3,5 permitiendo de este modo, que se absorba rápidamente en un medio ácido como el estómago. Una vez absorbido en la circulación (pH 7,4), la mayor parte del fármaco está en forma ionizada. Su coeficiente de partición de n-octanol/agua (logP) es de 0,26, sugiriendo que está distribuido internamente por todo el cuerpo después de alcanzar el equilibrio. Comercialmente se presenta como sal de trometamina que tiene una solubilidad en agua mayor en comparación con el KT base. El peso molecular de la sal de trometamina es de 376,4.

1.2.1.3.- Propiedades del Ketorolaco

La eficacia analgésica del KT ha sido ampliamente evaluada en pacientes postoperatorios con dolor moderado a intenso después de una cirugía mayor abdominal, ortopédica o ginecológica, aunque existe una variación interoperatoria e interpaciente sustancial en la respuesta de los pacientes a la terapia. La

administración preoperatoria de KT reduce el dolor en el postoperatorio inmediato. La terapia combinada con KT y opioides da como resultado una reducción significativa del 25 al 50 % en los requerimientos de morfina y fentanilo en los primeros 1 a 2 días posteriores a la operación y puede ir acompañada de una reducción de los eventos adversos inducidos por los opioides. Además, algunos pacientes experimentan un regreso más rápido a la función gastrointestinal normal y un tiempo de hospitalización más corto [20].

Estudios clínicos demuestran que, tanto en régimen de dosis única, cómo de dosis múltiple, su eficacia analgésica es, como mínimo, comparable a la de los opioides cómo la morfina en dolores postoperatorios de moderados a severos, y con evidencias de un perfil de efectos secundarios más favorable al de la morfina [21][22][23]. Además, no actúa a nivel central cosa que lo convierte en una buena alternativa a agentes opioides en dolores post quirúrgicos.

Los efectos secundarios notificados en un régimen de dosis múltiples tanto por vía oral como intramuscular incluyen somnolencia, aumento de la sudoración, náuseas, dolor de cabeza, mareos, vómitos, vasodilatación y alteraciones gastrointestinales tales como sangrado, úlceras pépticas y perforaciones [19].

Por vía oftálmica, se utiliza tanto en el tratamiento de la conjuntivitis alérgica estacional, como en postoperatorio y en el dolor e inflamación ocular.

Además, se usa para aliviar el dolor en el cólico renal agudo asociado a un traumatismo y en el dolor visceral asociado al cáncer.

También parece que inhibe la agregación plaquetaria inducida por ácido araquidónico y/o colágeno, pero no la inducida por adenosina fosfato (ADP) ni por prolongación del tiempo medio de sangrado [24]. Las preocupaciones sobre el sangrado posoperatorio han limitado su uso aun y mostrar un perfil analgésico tan bueno durante el pre- y postoperatorio pero, un metaanálisis del 2014 de ensayos aleatorios controlados que examinaba si había aumento del sangrado postoperatorio con la administración de KT, mostró cómo dicho sangrado no aumentó significativamente con KT en comparación con los controles, ni tampoco los efectos adversos [25].

1.3.- Piel

La piel es uno de los órganos más importantes de nuestro organismo. Si llegase a faltar más del 40 %, este hecho sería incompatible con la vida. La piel, además, es el más extenso órgano que tenemos. Pesa entre 3 y 5 kg, y completamente extendida puede llegar a ocupar un área de hasta 18 m^2.

1.3.1.- Estructura

Estructuralmente, la piel consta de tres capas bien diferenciadas, la epidermis, la dermis y la hipodermis

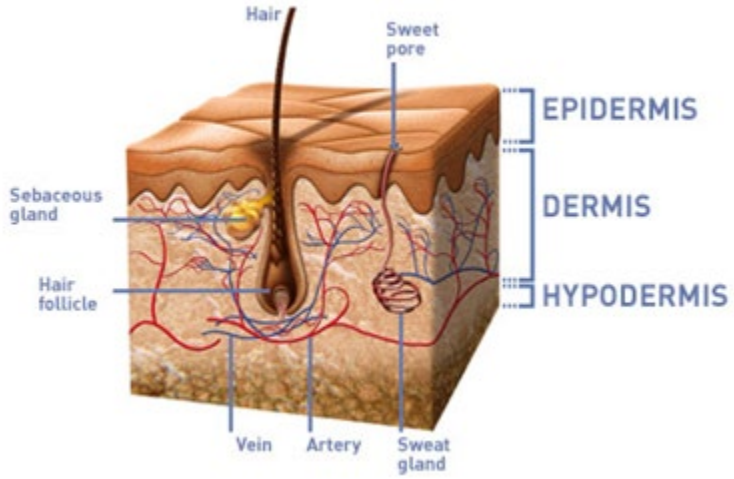

***Figura 3**. Estructura de la piel.*

Epidermis: es la capa más externa. Tiene un grosor de un milímetro, aunque en las palmas de las manos y en las plantas de los pies puede medir un poco más, y menos en los párpados de los ojos.

Está constituida por varias capas de células llamadas queratinocitos, dispuestas unas sobre otras constituyendo una barrera impermeable para casi todas las sustancias.

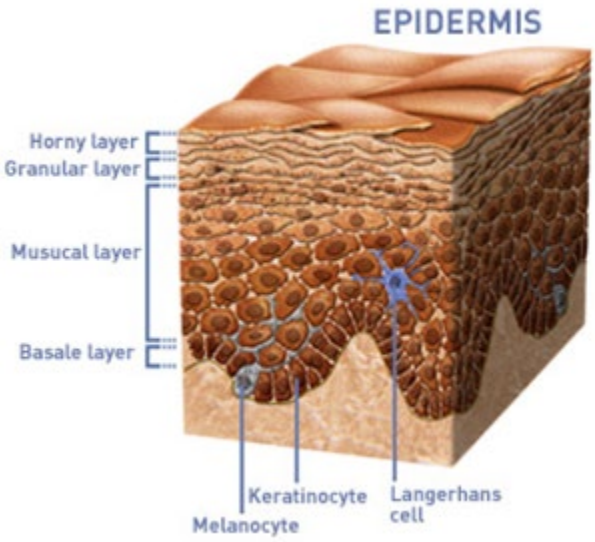

***Figura 4**. Estructura de la epidermis*

Se regenera cada 2 meses y su función es mantener la piel hidratada, así como protegernos de la radiación solar. La epidermis se encuentra constituida por diferentes capas, que reciben distintos nombres; de un nivel más profundo a más superficial, encontramos:

- Capa basal o germinativa**:** está formada por una hilera de células vivas que desarrollan una gran actividad y que constantemente regeneran la epidermis. En esta capa se encuentran los melanocitos, células de forma estrellada con prolongaciones llamadas dendritas. Son las células responsables de la fabricación de melanina, un pigmento que contribuye al color de la piel y nos protege de los posibles efectos negativos de los rayos solares. Además, en esta capa también se encuentran células del sistema inmunológico conocidas como células de Langerhans, encargadas de presentar los antígenos en los linfocitos e iniciar así la respuesta inmunológica de defensa.

- Capa espinosa: se sitúa por encima de la capa basal y está constituida por varias hileras de células que representan otro estadio de evolución de las células basales. Las células de la capa espinosa se unen entre sí y con las de la capa basal constituyendo una sólida armadura.

- Capa granulosa: está formada por elementos celulares aplanados que contienen gránulos de queratohialina, sustancia córnea característica de esta capa. Estas células no poseen capacidad de dividirse, puesto que están dedicadas exclusivamente a la síntesis y formación de queratina.

- Capa córnea: está constituida por capas de células muertas denominadas corneocitos que constituyen el último paso en la evolución de los queratinocitos desde su origen en la capa basal. Está en constante descamación, aunque en condiciones normales este fenómeno es imperceptible. Así la piel se renueva constantemente. Esta capa aparece en toda la piel, excepto en las mucosas (labios, vulva, boca, etc.).

La dermis: forma la mayor proporción de la piel y constituye el verdadero soporte de este órgano. Tiene un grosor de unos cuatro milímetros. Se encuentra dividida en tres zonas que, de un nivel más superficial a más profundo, reciben los siguientes nombres; dermis papilar, dermis reticular y dermis profunda. Ya no se trata de capas de células superpuestas, como sucedía en la epidermis, sino de un complicado sistema de fibras entrelazadas, rodeadas por una sustancia denominada *sustancia fundamental*, en la que se sitúan una extensa variedad de tipos de células. En la dermis se encuentran también los anexos cutánicos, que son de dos tipos: córnicos (pelos y uñas) y glandulares (glándulas sebáceas y glándulas sudoríparas). También encontramos los vasos sanguíneos que irrigan la piel y las terminaciones nerviosas.

Los tipos de fibras que constituyen la armadura de la dermis y que dan lugar a la finura, flexibilidad y elasticidad de la piel son:

- Fibras de colágeno: son el principal componente de la dermis y proporcionan resistencia a la tensión y flexibilidad.
- Fibras elásticas: más escasas que las anteriores, pero tienen su importancia, ya que son las responsables de la elasticidad de la piel.
- Fibras reticulares: son las más escasas y se disponen en torno a los anexos (pelos, uñas, glándulas) y de los vasos sanguíneos. Se trata de pequeñas fibras delgadas de un diámetro de 30 a 40 nm que se asocian formando redes. Estas redes actúan como tejido de soporte.

Las células que forman principalmente la dermis se llaman fibroblastos. Son las que se encargan de producir las fibras de colágeno, elásticas y la sustancia fundamental. Existen además distintas células del sistema inmunológico (linfocitos, macrófagos, eosinófilos y mastocitos) presentes en número variable dependiendo de las circunstancias de la piel, aumentando cuando existe inflamación. En este supuesto, además, encontramos células extravasadas desde los vasos sanguíneos, hematíes y leucocitos. La sustancia fundamental se encuentra entre las fibras y está constituida por proteínas, electrolitos (como el sodio y el potasio), glucosa y agua.

La hipodermis: es la capa más profunda de la piel. También se llama tejido celular subcutáneo. Se encuentra constituido por gran multitud de adipocitos, dispuestas en lóbulos y separadas por fas de fibras de colágena y elásticas que reciben el nombre de trabéculas. La grasa forma un tejido metabólico muy activo que además protege al organismo proporcionándole amortiguación y aislamiento térmico [4].

1.3.2.- Propiedades y funciones

La piel es esencialmente la cubierta exterior del organismo, que funciona de forma permanente y que cumple dos importantes misiones; la de relacionarnos con el mundo exterior y la de protegernos de las agresiones del exterior.

En cuanto a la función de relación, en ella se encuentra uno de los sentidos que tenemos más desarrollados, el tacto. La piel es la encargada de recibir los estímulos del exterior a través de las terminaciones nerviosas que se sitúan en ella y de ahí se dirigen hacia el cerebro que nos dice cómo debemos reaccionar. Cada centímetro cuadrado de piel contiene unos 5.000 receptores sensitivos. La piel es responsable de que sintamos una caricia o de que notemos el calor producido por el fuego o el frío de la nieve. Pero también la piel es el espejo de los sentimientos y emociones. Ponernos rojos porque algo nos dé vergüenza, “tener la piel de gallina” o sudar por algo que nos dé miedo, son algunas de las muchas respuestas emocionales que se ponen de manifiesto a través de la piel. Por este motivo, no es de extrañar que este órgano constituya una pieza clave en la imagen exterior de una persona.

La piel posee otras funciones básicas para el buen funcionamiento del organismo. Tiene una función protectora, ya que es capaz de seleccionar lo que resulta perjudicial para el organismo y lo que, por el contrario, es beneficioso para nosotros. Esto se produce gracias a su disposición de barrera que impide la entrada de sustancias nocivas (millones de bacterias que viven sobre ella, cuerpos extraños y, en parte, radiaciones solares perjudiciales) y a un sistema inmunológico propio. También tiene una función reguladora del metabolismo: impide la salida de sustancias (líquidos, células) imprescindibles para el organismo, regula la temperatura corporal protegiéndonos de los cambios de temperatura ambientales y transforma los rayos del sol en vitamina D, vitamina necesaria para el buen funcionamiento de nuestros huesos, entre otras muchas funciones [5].

1.4.- Mucosas

1.4.1.- Mucosa oral

La cavidad oral es una estructura que se encuentra comunicada con el exterior, requiere entonces una membrana mucosa de recubrimiento superficial húmeda. La humedad es proporcionada por las glándulas salivales principales y accesorias y resulta fundamental para el mantenimiento de la estructura normal de los tejidos. La mucosa oral, al igual que todas las mucosas, está conformada por 2 capas de tejidos, de estructura y origen embriológico diferente:

- Tejido epitelial: capa superficial de origen ectodérmico. Es de tipo plano o escamoso pluriestratificado. Puede ser queratinizado, paraqueratinizado o no queratinizado, y según la ubicación presenta diferencias estructurales y funcionales. Sus células se encuentran firmemente unidas entre sí, conformando una barrera funcional de protección.
- Tejido conectivo (lámina propria o corion): capa subyacente de origen ectomesenquimático. Corresponde a una capa de tejido conectivo de espesor y densidad variable, dependiendo de la zona de la cavidad oral. Tiene por función la nutrición, la inervación y el sostén del epitelio que se apoya sobre ella. Presenta numerosas papilas o invaginaciones del corion, que aproximan vasos y nervios hacia las capas más superficiales del epitelio. Las terminaciones nerviosas sensoriales reciben información sobre la percepción de temperatura (termo-receptores), tacto y presión (mecano-receptores) y dolor (nocireceptores). Los mecano-receptores son los corpúsculos de Meissner y las células de Merkel del epitelio.

Entre ambos tejidos se encuentra la membrana basal, que se observa ondulada por la presencia de papilas del corion y crestas epiteliales, que facilitan la nutrición entre el epitelio avascular y el conectivo vascular.

Puede existir una tercera capa de tejido conectivo laxo, la submucosa, presente en algunas zonas de la mucosa oral. Esta capa está compuesta por tejido conectivo más denso destinado a unir la mucosa a los tejidos subyacentes. La submucosa puede

estar presente o no como capa definida. La podemos encontrar en zonas que requieren movimiento y que no estén expuestas directamente al choque masticatorio, pero no en zonas donde el corion está firmemente adherido a la estructura ósea subyacente.

En la Figura 5 se presenta la imagen de la histología de la mucosa bucal, sublingual y vaginal, dónde se pueden apreciar las diferentes capas y tejidos mencionados anteriormente.

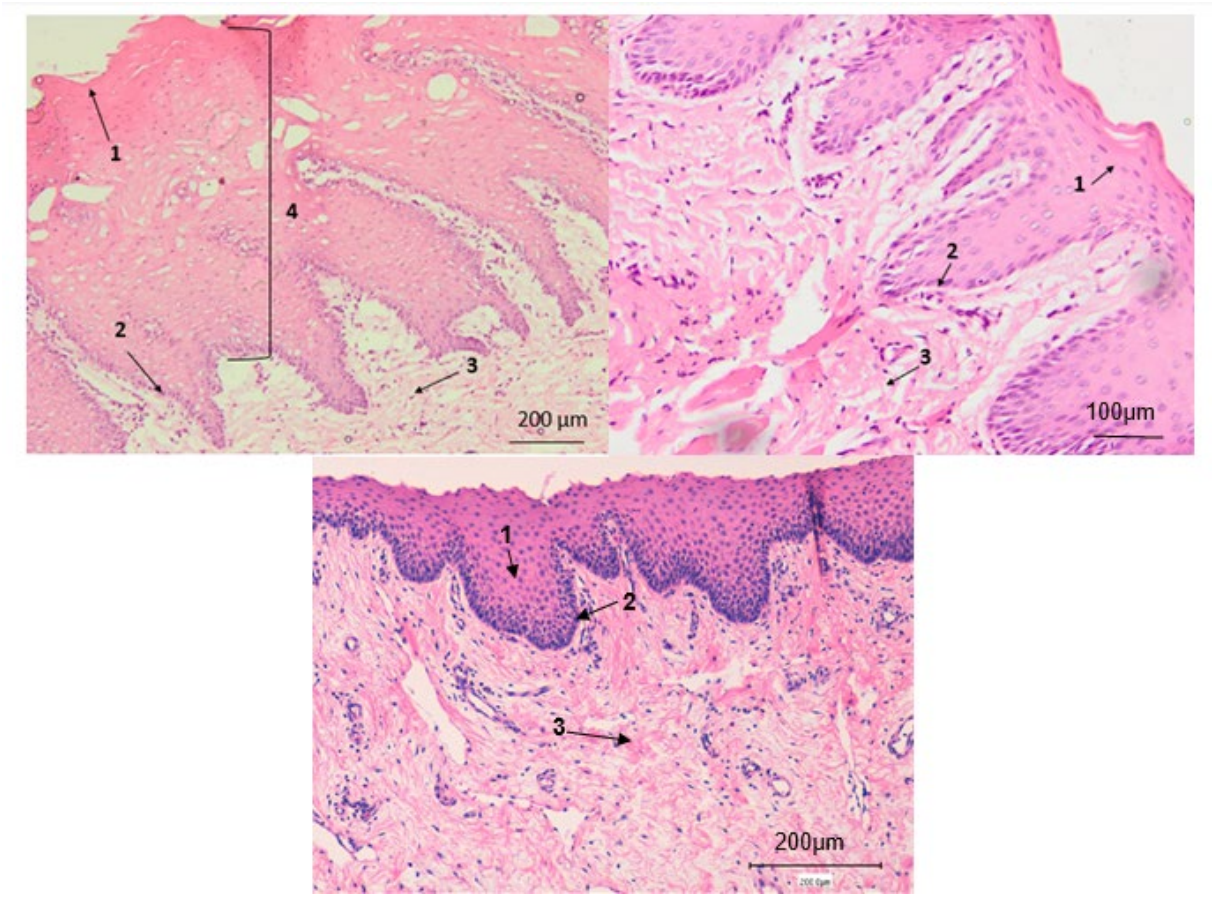

Figura 5. *Arriba izquierda: mucosa bucal a 200x; Arriba derecha: mucosa sublingual a 100x; abajo centro: mucosa vaginal a 200x. (1) estrato escamoso queratinizado o no queratinizado; (2) lámina basal; (3) lámina propria*

Según la adaptación funcional a la influencia mecánica que actúa sobre las mucosas, se puede dividir la mucosa oral en tres tipos principales:

- Mucosa de revestimiento: Esta mucosa reviste zonas de la cavidad oral que no están expuestas a fricción o presión (cara interna del labio, mejilla, paladar blando, piso de la boca, superficie ventral de la lengua, mucosa alveolar y

vestibular). Cumple funciones de protección. El epitelio es de tipo no queratinizado, con un corion laxo o semidenso, presentando una submucosa de tejido conectivo laxo bien definida. Presenta la capacidad de distenderse y de adaptarse a la contracción y relajación de las mejillas, labios y lengua, y a los movimientos del maxilar inferior, producidos durante la masticación.

- Mucosa masticatoria: Esta mucosa se ubica en zonas sometidas a fenómenos de presión y fricción, producto del proceso de masticación (encía y paladar duro). Se encuentra adherida al hueso y no experimenta estiramiento. El epitelio que posee es de tipo queratinizado o paraqueratinizado. La submucosa está ausente, excepto en los bordes laterales del paladar duro, donde existe tejido adiposo y glandular.
- Mucosa especializada: Esta mucosa recubre la superficie dorsal y lateral de la lengua y se caracteriza por presentar una superficie muy irregular, por la presencia de numerosos levantamientos denominados papilas linguales. La lámina propria es relativamente densa y muy inervada. La submucosa de tejido conectivo laxo, se ubica entre los fascículos musculares, muy abundantes en la lengua. Esta capa aloja botones gustativos intraepiteliales, de función sensitiva, encargados de la recepción de estímulos gustativos. En la zona profunda de la mucosa especializada se ubican numerosos adenómeros de secreción mixta (glándulas de Blandin y Nuhn) que mantienen la humedad del epitelio y de las papilas gustativas [26].

1.4.2.- Mucosa vaginal

***Figura 6**. Sistema reproductor femenino. Capas de la mucosa vaginal.*

Los órganos genitales femeninos incluyen la vagina, el útero, las trompas de Falopio y los ovarios.

El tracto reproductivo femenino (Figura 6) consta del tracto reproductivo superior, compuesto por los ovarios, las trompas de Falopio y el útero, y el tracto reproductivo inferior, que incluye la vagina, el exocérvix y los genitales externos (vulva). El cuello uterino es una porción del útero que se estrecha y termina en la vagina en una protuberancia cónica conocida como exocérvix. El revestimiento mucoso del útero se denomina endometrio y la mucosa del cuello uterino es más específicamente el endocérvix [27].

El endometrio se encuentra dentro del miometrio, que consiste principalmente en células de músculo liso. El tracto reproductivo femenino superior está revestido con una capa de epitelio cilíndrico que posee uniones estrechas. El cuello uterino se recubre aún más con moco, secretado por células epiteliales en las glándulas endocervicales. El grosor de la capa de moco y la consistencia del moco dependen de la fase del ciclo menstrual [28].

El tracto reproductivo femenino inferior consta del exocérvix y vagina. La vagina es un tubo muscular que se extiende desde el exocérvix del útero hasta la abertura vaginal y se encuentra entre la uretra y el recto. El tejido fibromuscular configura las paredes de la vagina y la dota de una gran elasticidad, muy necesaria para alguna de sus funciones. Este órgano femenino desempeña un papel fundamental en la reproducción humana y, por tanto, en el ciclo reproductor de la mujer. Sus funciones se pueden resumir en:

- Paso y salida natural al flujo menstrual durante la regla.
- Conducto a través del cual se elimina el moco cervical que se secreta en el cuello del útero antes y después de la ovulación.
- Cavidad en la que, a través de la vulva, penetra el pene durante la relación sexual y en la que se deposita el semen tras la eyaculación.
- Constituye el denominado canal del parto, por el que sale el feto en el momento del parto y se elimina la placenta.

El revestimiento, o mucosa, de la vagina consiste en un epitelio escamoso estratificado no queratinizado, adherido a una membrana basal o lámina propria. El epitelio vaginal consta de aproximadamente 28 capas de células en los días 1 a 12 del ciclo menstrual, con un ligero adelgazamiento a 26 en los días 19 a 24 del ciclo. Este epitelio escamoso estratificado es la principal barrera de permeabilidad de la vagina. Esta función de barrera está respaldada por la producción y presencia de lípidos intercelulares amorfos y gránulos de revestimiento de membrana que extruyen ceramidas, glucosilceramidas y colesterol [29].

La vagina se lubrica con fluido vaginal, que es una mezcla de líquidos del tracto reproductivo superior, como el moco cervical y fluidos endometriales y trasudados de las paredes vaginales. Las glándulas de Bartolino, situadas a ambos lados de la sección posterior de la apertura vaginal también sirven para ayudar a la lubricación de la vagina, secretando cantidades relativamente pequeñas de líquido durante la excitación sexual. Posicionadas a ambos lados de la parte anterior de la abertura vaginal se encuentran las glándulas de Skene, que realizan una función similar. Los constituyentes del fluido vaginal son agua (90-95 %), mucinas, carbohidratos, urea, sales, inmunoglobulinas, ácidos grasos, albúmina, enzimas proteolíticas y otros componentes menores. El fluido vaginal se renueva constantemente y sus funciones principales son la lubricación y la protección de la vagina contra infecciones.

Otra protección la proporciona el pH ácido de la vagina (entre 4,0 y 5,0), caracterizada por la presencia de *Lactobacillus spp* que forman parte del microbiota vaginal natural [29].

Godley [30] evaluó la cantidad media de flujo vaginal producida durante un ciclo menstrual en 22 voluntarias sanas. La media fue de 1,55 g/8 h, aunque la cantidad varió significativamente entre los diferentes días del ciclo. El máximo se produjo a mitad del ciclo (1,96 g/8 h) y se observaron valores medios bajos el día 7 (1,38 g/8 h) y el día 26 (1,37 g/8 h). Esta variación cíclica fue estadísticamente significativa ($P < 0,02$) en mujeres célibes que no usaban anticonceptivos, pero fue menos marcada en mujeres sexualmente activas que tomaban la píldora anticonceptiva oral combinada.

1.4.3.- Permeabilidad de las mucosas y de la piel

Los fármacos atraviesan la piel y/o mucosa a través del mecanismo de difusión pasiva. Es necesario distinguir 2 rutas distintas, la transcelular y la paracelular.

La primera supone la difusión en las membranas lipídicas de las células y es la vía mayoritaria. La vía intercelular es de naturaleza fundamentalmente lipídica, por lo que el fármaco pasa a través de la matriz lipídica entre los corneocitos del estrato corneo. Los fármacos lipófilos difunden a través de estos lípidos extracelulares y los más polares a través de la parte hidrófila de dichos lípidos. La ruta paracelular, en cambio, es el paso de los solutos a través del espacio que existe entre las células; supone que el epitelio tenga una matriz accesible y que el soluto pueda difundir en el medio intercelular [31].

Los fármacos para ser bien absorbidos a través de piel y mucosas deben de tener un coeficiente de reparto log P (octanol/agua) menor a 5 (idealmente entre 1 y 3) [32]. El log P y el reparto en la piel mantienen una relación parabólica. Los compuestos con un bajo log P presentan una baja permeabilidad, y por lo tanto un bajo reparto con los lípidos de la piel, provocando que el fármaco tienda a quedarse en el vehículo. Sin embargo, un log P elevado facilita la salida del fármaco del vehículo hacia la piel, pero poseen también una baja permeabilidad por su incapacidad de reparto fuera del estrato corneo, quedando retenido en este [33].

El coeficiente de difusión es inversamente proporcional al tamaño de la molécula. Por tanto, los fármacos con un bajo peso molecular son más susceptibles de penetrar a

través del epitelio. En general se estima que un fármaco tiene que tener un tamaño no mayor a 500 Da para poder ser permeado a través de piel y mucosa [34].

El grado de dispersión influye de forma considerable la penetración de fármacos poco solubles en los vehículos porque afecta al coeficiente de difusión, por tanto, al aumentar el grado de dispersión en el vehículo, aumenta el coeficiente de difusión y en consecuencia la penetración.

Las moléculas muy hidrófilas son demasiado polares y sólo penetran en la mucosa al dosificarlas en altas concentraciones, y las lipófilas tienen una solubilidad en agua demasiado baja y esto provoca que su absorción se encuentre limitada por su velocidad de disolución.

El grado de ionización del fármaco también es un factor que influye en la absorción, el cual depende del pKa del fármaco y del pH de la zona, que en el caso de la piel va de 4,1 a 5,8 [35]–[37], en la boca se mantiene entre 6,2 y 7,2 [38] y en la mucosa vaginal entre 4 y 5 [29]. Si se quisiera modificar dicho pH se puede hacer incorporando reguladores del pH en los excipientes del medicamento.

Hay considerables diferencias en la permeabilidad entre las diferentes regiones de la cavidad oral, debido a las diversas estructuras y funciones de las diferentes mucosas. En general, la permeabilidad de las mucosas seguirían la siguiente clasificación decreciente: mucosa sublingual seguida de la bucal, palatal y por último la mucosa gingival con la menor permeabilidad. Este orden de clasificación se basa en el espesor relativo y el grado de queratinización de estos tejidos. La mucosa sublingual es relativamente delgada y no queratinizada, la bucal más gruesa y no queratinizada, y la palatal intermedia en espesor, pero queratinizada.

Un factor importante a tener en cuenta es la gran secreción de saliva que se produce en la cavidad oral. Este hecho conlleva a que la boca este permanentemente húmeda, lo cual influye en la velocidad de disolución de la forma farmacéutica y en la capacidad de absorción [40]. Además de estos condicionantes, no pueden administrarse sustancias con mal sabor o amargas, porque condicionan un aumento de secreción salival, que redundaría en la deglución de parte de la dosis.

Con relación a la mucosa vaginal, un estudio mostró que la vagina es aproximadamente 16 veces más permeable al agua que la piel [41] y en otro [42] que la penetración del agua tritiada a través del epitelio vaginal humano no es

estadísticamente diferente de la permeación a través de la mucosa bucal humana ex vivo.

La administración de fármacos a través de la piel y/o mucosas para lograr un efecto terapéutico sistémico se encuentra actualmente bajo intensa investigación. Dichos tejidos ofrecen ventajas y limitaciones únicas para la entrada de fármacos en el cuerpo [43]. A continuación, se enlistan las principales ventajas e inconvenientes de la administración transdérmica y transmucosa de fármacos.

Beneficios

- Evitar el metabolismo de primer paso y otras variables asociadas con el tracto gastrointestinal, como el pH y el tiempo de vaciamiento gástrico.
- Liberación sostenido y controlado durante un período de tiempo prolongado.
- Reducción de los efectos secundarios asociados con la toxicidad sistémica, es decir, minimización de los picos y valles en la concentración de fármacos en sangre.
- Acceso directo al sitio objetivo o target, y por lo tanto facilidad de finalización de la dosis en caso de reacciones adversas, ya sean sistémicas o locales.
- Administración conveniente, sencilla e indolora, facilitando el uso y reduciendo los costos generales del tratamiento de atención médica.
- Proporcionar una alternativa a la contraindicación de la dosificación oral (en pacientes inconscientes o con náuseas).

Limitaciones

- Un peso molecular inferior a 500 Da es esencial para garantizar la facilidad de difusión a través del estrato córneo, ya que la difusividad del soluto está inversamente relacionada con su tamaño.
- Suficiente solubilidad acuosa y lipídica. Un Log P (octanol/agua) entre 1 y 3 es necesario para que el principio activo atraviese con éxito el estrato córneo y sus capas acuosas subyacentes para que se produzca la administración sistémica.
- Intravariabilidad e intervariabilidad asociada con la permeabilidad de la piel humana intacta y enferma. Esto implica que habrá perfiles de absorción cutánea rápidos, lentos y normales que darán como resultado respuestas biológicas variables.

- Metabolismo presistémico; la presencia de enzimas en la piel, como peptidasas y esterasas, podría metabolizar el fármaco en una forma terapéuticamente inactiva, reduciendo así la eficacia del fármaco.
- Irritación y sensibilización de la piel y mucosas. La piel como barrera inmunológica puede ser provocada por la exposición a ciertos estímulos, esto puede incluir fármacos, excipientes o componentes de los dispositivos de administración que dan como resultado eritema, edema, etc. [26].

1.5.- Condiloma acuminado

1.5.1.- Descripción

El Condiloma Acuminado (CA) o Verruga Genital (VG) es una Enfermedad de Transmisión Sexual (ETS) causada por determinados genotipos del Virus del Papiloma Humano (VPH).

Hay más de 200 genotipos del VPH descritos hasta la fecha, de los cuáles, aproximadamente unos 40 son sexualmente transmitidos afectando la región anogenital [44]. Los genotipos 6 y 11 son los responsables de las VG en la gran mayoría de casos (90-95 %) [45]. Los genotipos 16 y 18 son importantes por poseer un fuerte carácter oncogénico y son los responsables de causar cáncer cervical a de más de estar relacionados con otros cánceres del aparato reproductor, de cabeza y orofaríngeos [46].

La coinfección por tipos de VPH de alto riesgo oncogénico con tipos de bajo riesgo es posible. Que un condiloma acuminado pase a ser maligno y derive en cáncer es un caso aislado, pero no se descarta una asociación entre el hecho de haber tenido condilomas con un incremento del riesgo para neoplasia anogenital y de cabeza y cuello [47].

El CA es la ETS más frecuente. Estudios y revisiones publicados en diversos países muestran un incremento de la incidencia de la enfermedad hasta antes de la introducción de la vacuna del VPH tetravalente en el calendario de vacunación. En una revisión sistemática de la eficacia de la vacuna del VPH, publicada en el año 2016, se reporta una reducción significativa de la incidencia de CAs tras la implementación de la misma [48]. Aun así, en los últimos años, la incidencia de la enfermedad parece ser que va en aumento en todos los países [49]. La tasa de incidencia máxima en las mujeres se observa entre los 20 y 24 años y en los hombres entre los 25 y 29 años [50].

1.5.2.- Características clínicas y diagnóstico

Aunque el acto sexual es considerada la vía principal de transmisión, la vía no-sexual por contacto directo entre piel y/o mucosas ha ido cogiendo fuerza en revisiones recientes [51]. También se han dado casos de transmisión vertical, de la madre infectada al recién nacido, durante el parto [47]. Se han relacionado varios genotipos del VPH con verrugas nasales y orofaríngeas [52] así como con el Carcinoma Orofaríngeo de Células Escamosas (COCE) [53]. Dichas infecciones orales se cree que han podido ser transmitidas mediante sexo oral, pero la evidencia reciente respalda también su transmisión horizontal de boca a boca [54].

La transmisión del VPH se lleva a cabo por contacto directo de piel y mucosas. El VPH penetra el epitelio mediante microabrasiones o pequeños traumatismos infectando así las células de la capa basal [46][53]. Una vez dentro, el genoma vírico entra en el núcleo de la célula iniciando así su transcripción. La replicación viral tiene lugar en paralelo a la replicación de la célula basal infectada, quedando el genoma viral anclado al cromosoma de la célula huésped, propagándose así a una nueva célula hija [53]. A medida que las células infectadas se diferencian de células basales a queratinocitos, las copias del genoma viral se amplifican y se ensamblan (Figura 7). Cuando los queratinocitos se descaman de las capas epiteliales superiores, las células están repletas de miles de virus, listos para infectar al próximo huésped, estableciéndose así la proliferación viral y epitelial que se traduce clínicamente en la lesión condilomatosa [46][47].

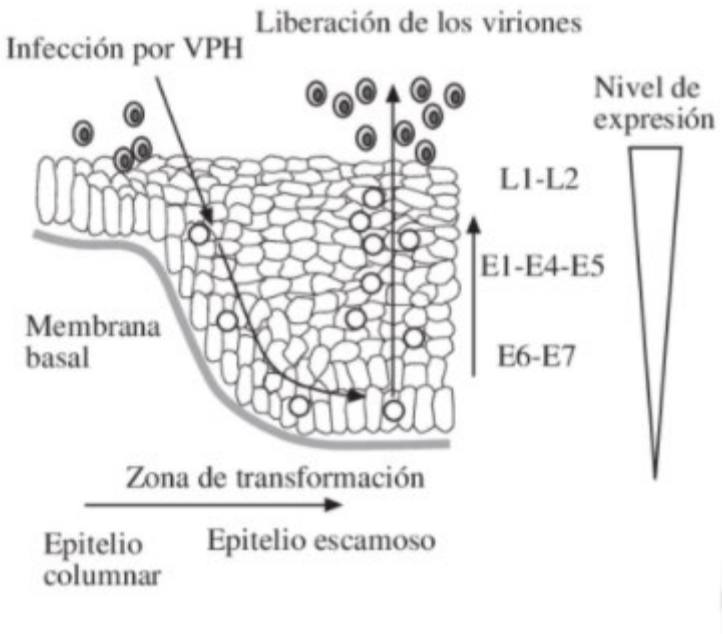

***Figura 7**. Replicación del VPH en las células del huésped*.

El efecto citopático de la replicación viral provoca la vacuolización de las células formando la coilocitosis típica por infección por VPH [46][47]. Dichos coilocitos es común encontrarlos tanto en mucosa vaginal [47] cómo en mucosa oral y/o sublingual [53][55].

Los síntomas asociados al CA van a depender sobre todo de la localización, número y tamaño de las lesiones [56]. Los síntomas pueden ir desde no notar nada hasta complicaciones cómo cáncer u obstrucción cuando se trata de verrugas gigantes o hay una gran agrupación de ellas.

En la gran mayoría de casos los síntomas cursan de forma leve, el más frecuente suele ser el prurito, seguido por orden de frecuencia el aumento de leucorrea, la sensación de incomodidad, el sangrado y el dolor. En las mucosas de cérvix y vagina, los CAs suelen cursar de forma asintomática [47] así como en la mucosa oral [57]. No se debe de olvidar la afectación del estado psicológico que esta enfermedad conlleva. Son frecuentes la preocupación, vergüenza, afectación de la autoestima y de la esfera sexual [47].

El periodo de latencia entre la infección inicial y la aparición de las lesiones oscila entre tres semanas y 8 meses. Si no se tratan, los condilomas acuminados pueden

resolverse de forma espontánea, permanecer sin cambios o aumentar en número y/o tamaño [52].

El diagnóstico del CA se realiza mediante exploración física. Normalmente se suelen encontrar entre 5 y 15 lesiones, aisladas o en placas, de entre 1 y 10 mm de grosor cada una, más o menos sobreelevadas, con una superficie espiculada o plana. Se ha observado que con el paso del tiempo la superficie de las lesiones va perdiendo rugosidad y se va tornando más redondeada y la coloración pasa de un tono rosado inicial (debido a la hipervascularización) a uno más pigmentado, pudiendo llegar a hacerse marrones [47] (Figura 8). En el caso de condilomas orales, la localización más común son los labios, paladar y la lengua, aunque pueden aparecer en cualquier lugar de la superficie oral [58].

Figura 8. *Verruga anogenital (VG) o condiloma acuminado (CA).*

1.5.3.- Tratamiento

Existe un gran arsenal terapéutico para tratar o erradicar las VG. No hay suficiente evidencia que demuestre mayor eficacia de una terapia sobre otra [56]. Para escoger el tratamiento adecuado se ha de analizar cada situación teniendo en cuenta forma, localización y número de verrugas, experiencia y técnica del personal facultativo, situación y estilo de vida del paciente, costo económico, entre otros.

El tratamiento se puede clasificar según si es aplicado por un profesional sanitario en un centro médico o, por el contrario, si es aplicado por el paciente en su domicilio [45]. Otra clasificación posible es según el objetivo terapéutico. Aquí tendríamos por un lado fármacos que pretenden mediante acción directa o inmunomodulación eliminar el virus, y por otro lado, aquellas terapias que pretenden eliminar las verrugas a través de la destrucción de las células infectadas [59].

1.5.3.1.- Tratamiento administrado por el profesional

- Ácido tricloroacético (ATC) (80-90 %). Agente cáustico que destruye los condilomas desnaturalizando, mediante coagulación química, las proteínas del virus y dañando su ADN [47][60]. La solución es una fórmula magistral. La solución de ATC se aplica semanalmente hasta que se aclaren las verrugas o hasta un máximo de 10-12 semanas. La mayoría de lesiones se aclaran tras 4-6 aplicaciones [47].

- **Crioterapia**. Técnica que con el uso de temperaturas subcero (-196ºC) consigue congelar el agua que se encuentra dentro de las mitocondrias y así desencadena la necrosis de los tejidos con los que entra en contacto [45][62]. Los criógenos más usados son el nitrógeno líquido y el óxido nitroso [63]. La crioterapia es apta para tratar verrugas anogenitales tanto internas como externas [47]. La posología suele ser semanal, realizando 2-3 secuencias de congelación/reposo por sesión. El tratamiento se puede repetir cada 2-3 semanas hasta un máximo de 3-4 meses [47]. El dolor después de la aplicación ha sido reportado en numerosos casos y en menor medida la aparición de ampollas y úlceras [62]. Para tratar el dolor durante la aplicación del criógeno se suele aplicar un anestésico tópico local antes de congelar la verruga [45]. En la mayoría de los casos la eliminación de las lesiones se produce antes de la tercera sesión [56]. Las recurrencias son frecuentes [47].

- **Tratamiento quirúrgico**. Cuenta con la ventaja de eliminar más de una verruga en una sola visita, aunque las recurrencias son elevadas [52].

- Escisión / extirpación. Incisión tangencial bien sea con tijera, legra o bisturí que separa la base de la verruga de la capa superior de la dermis de la piel [45]. Este método es apropiado para cualquier verruga genital, pero puede ser particularmente útil cuando las verrugas son pediculadas o exofíticas [61], o para lesiones grandes que causan obstrucción [63]. Dado que el procedimiento puede ser doloroso, se requiere de anestesia ya sea local, regional o general [56].

- Láser de CO_2: La energía emitida por el haz láser de CO_2 vaporiza las lesiones por ebullición del agua contenido en los tejidos sobre los que se aplica dicho láser [47][63]. La técnica requiere anestesia regional o sedación y un aprendizaje previo específico. Puede usarse para el tratamiento de condilomas en cualquier área del tracto anogenital [47]. Después de la cirugía con láser, es probable que las personas

experimenten dolor e irritación en el sitio donde se encontraban las verrugas.. El tratamiento puede repetirse si es necesario [64].

- Electrocoagulación. Consiste en aplicar, sobre el tejido a destruir y bajo anestesia local, corriente eléctrica con un electrobisturí. La corriente eléctrica aplicada calienta y quema el tejido, destruyendo la lesión [65]. Está indicado para el tratamiento de condilomas en número y extensión limitadas situados en cualquier área del tracto anogenital. No resulta viable ante lesiones múltiples o gran volumen de enfermedad [47].

1.5.3.2.- Tratamiento aplicado por el paciente

- **Podofilotoxina**. Su acción farmacológica es la de bloquear el ensamblaje de microtúbulos durante la mitosis al unirse a la tubulina [66]. La podemos encontrar en forma de crema al 0,15% y en forma de solución cutánea al 5% [47]. Se aplica dos veces al día durante tres días consecutivos [67], seguido de un periodo de descanso de cuatro días. Esta pauta se repite hasta un máximo de cuatro ciclos para la crema y dos ciclos para la solución. La crema se puede aplicar con los dedos y la solución con un hisopo de algodón, siendo la aplicación lo más selectiva posible sobre las lesiones [47]. La podofilotoxina tiene una toxicidad local y sistémica mínima [66][67]. Se han descrito reacciones cutáneas en el lugar de administración y destrucción de tejido, pero en caso de aplicación excesiva (sobre todo en la formulación en solución), así como toxicidad neurológica sistémica, especialmente si se aplica en lesiones ulceradas que faciliten la absorción del fármaco. Las preparaciones de podofilotoxina están indicadas para el tratamiento de condilomas en genitales externos, perineales y perianales, no voluminosos y extensos. Está contraindicado su uso sobre mucosas para evitar una posible absorción sistémica así como en la gestación y durante la lactancia [47].

- **Imiquimod (3,75 % - 5,0 %)**. Es un inmunomodulador que activa directamente células inmunitarias innatas a través del receptor TLR-7 [68]. La crema al 5 % es aplicado por el paciente en su domicilio 1 vez al día, normalmente por la noche [47], tres veces por semana (lunes-miércoles-viernes o martes-jueves-sábado) hasta la desaparición de las verrugas o hasta un máximo de 16 semanas [68]. Después de 6-10 horas debe de lavarse la zona con agua y jabón [61]. Está indicado para el tratamiento de CA de genitales externos, perineales y perianales. El uso sobre

mucosas no se recomienda por posible riesgo de mucositis [47]. Imiquimod al 3,75 % a diferencia de la crema al 5 % deberá ser aplicado una vez al día por dos semanas, repitiendo este ciclo después de dos semanas de descanso.

- **Sinecatequinas (Polifenol E).** Se trata de un extracto estandarizado de las hojas del té verde (Camellia sinensis) [59]. Interviene en múltiples vías de señalización celulares, consiguiendo inhibir la transcripción del VPH y activar la inmunidad celular [47][69]. Al combinar todas estas actividades se eliminan tanto las células clínicamente afectadas como aquellas con infección subclínica [45]. Las sinecatequinas se administran en forma de pomada. Según el país, hay presentaciones del 10 % (España) o del 15 % (Estados Unidos) [47]. Están aprobadas para el tratamiento de las verrugas anogenitales externas y su uso sobre mucosas está contraindicado por alto riesgo de mucositis y absorción sistémica [47]. La posología es de 3 aplicaciones diarias durante un máximo de 16 semanas. Los resultados empiezan a observarse a partir de la tercera semana, haciéndose más evidentes a partir de la cuarta o sexta semana [45]. Los efectos adversos locales como eritema y el prurito son los más comunes y suelen manifestarse a partir de la tercera semana de tratamiento, pero por lo general son bien tolerados [70].

1.5.3.3.- Tratamiento profiláctico: Vacunas

Actualmente existen en el mercado 3 vacunas profilácticas para la prevención de la infección por VPH y para la inmunidad frente a CA y lesiones precancerosas y canceres que afectan al cuello de útero, vulva, vagina y ano. Cervarix® de laboratorios GSK, es una vacuna bivalente contra los genotipos de alto riesgo oncogénico 16 y 18; Gardasil® o Silgard® de laboratorios Merck, es tetravalente contra los genotipos 6, 11, 16 y 18 y Gardasil9® o Silgard9® inmuniza frente los genotipos 6, 11, 16, 18, 31, 33, 45, 52 y 58. Las vacunas están constituidas por la proteína estructural L1 de cada genotipo del VPH purificada obtenida mediante recombinación genética [59]. Las vacunas han sido incluidas en el calendario de vacunación de numerosos países y están indicadas tanto para mujeres como hombres. En una revisión sistémica publicada en el 2015 sobre la efectividad de la vacuna tetravalente durante sus primeros 10 años se reporta una importante reducción (aproximadamente un 90 %) de la incidencia de la infección de los genotipos 6, 11, 16 y 18 del VPH así como de los CA y de las anomalías histológicas de cérvix, tanto de bajo como de alto grado [48][71].

1.5.3.4.- Otros tratamientos

- **Inmunoterapia intralesional.** Esta terapia lo que pretende es estimular la respuesta inmune del huésped mediante la inyección intralesional de vacunas y/o antígenos que sean capaces de desarrollar una respuesta de hipersensibilidad retardada contra varios antígenos entre los cuales estaría el VPH [59]. El mecanismo de acción no es claro, pero se cree que estaría mediado por la estimulación de los linfocitos Th1 que liberarían citoquinas e interleucinas que a su vez activarían linfocitos CD8 y células natural Killer necesarios para erradicar la infección por VPH [59][72]. Los antígenos usados en la inmunoterapia incluyen el antígeno de Candida albicans (candidina); el del sarampión, paperas y rubéola (MMR); Trichophyton y antígenos de la tuberculina tales como derivado proteico purificado (PPD), vacuna Mycobacterium w, y Bacilo Calmette-Guérin (BCG) [72]. En la literatura podemos encontrar diferentes casos tanto en adultos como en niños en los que se aplicó esta técnica con resultados muy esperanzadores [73][74][75][76].

Las infiltraciones se realizan habitualmente cada 1-3 semanas en un máximo de 3-5 sesiones. Los efectos secundarios más frecuentemente descritos son leves y consisten en una reacción inflamatoria en el sitio de la inyección y síntomas pseudogripales [59].

- **Terapia Fotodinámoca.** El ácido 5-aminolevulínico (ALA) y el ácido metil-aminolevulinato (MAL) son los agentes fotodinámicos más usados. Son fármacos fotosensibles que se activan por irradiación con luz con el objetivo de causar daño citotóxico y activar una respuesta inmune que acabe produciendo destrucción tisular selectiva [77]. Se ha observado que el ácido 5-aminolevulínico (ALA) se acumula en mayor cantidad en las células infectadas por el VPH que en la piel normal adyacente [45], lo cual confiere a esta técnica una cierta selectividad. Los efectos secundarios más descritos son dolor, quemazón y eritema [78].

- **Cidofovir** es un nucleósido fosfonato acíclico que actúa inhibiendo la ADN-polimerasa viral y celular [79]. El mecanismo de acción del cidofovir en las células infectadas por VPH no se comprende por completo, pero en estudios *In Vitro* se han descrito que actúa induciendo la apoptosis de dichas células [80]. Cidofovir está aprobado para el tratamiento de retinitis causada por citomegalovirus en pacientes infectados por el virus de la inmunodeficiencia humana (VIH) y se ha utilizado en el tratamiento de infecciones causadas por VPH, incluyendo algunos casos de verrugas

anogenitales [81] mostrando resultados esperanzadores. Aun así, la evidencia científica sigue siendo escasa. La concentración de cidofovir tópica recomendada es del 1 % al 3 % aplicado 1 a 2 veces al día. El tratamiento debe interrumpirse si no hay respuesta a la semana 10. Los efectos secundarios más comunes son dolor, prurito y erupción en el lugar de aplicación [79].

Como se observa las opciones terapéuticas son muchas. Para evaluar la eficacia del tratamiento hay dos aspectos primordiales que se tienen en cuenta. El aclaramiento de las lesiones condilomatosas, es decir la eliminación visible de las verrugas, y las recurrencias. Éstas últimas aparecen en mayor o menor medida en todos los tratamientos y es uno de los mayores problemas con el que se encuentran los profesionales y los pacientes a la hora de abordar el tratamiento de los CAs. Los efectos secundarios y la duración de los procedimientos son otra de las limitaciones. La mayoría de los procedimientos son dolorosos y molestos, lo que acaba afectando a la adherencia al tratamiento y por consiguiente a la eficacia. Mientras los tratamientos administrados por el profesional parecen tener mejores resultados de aclaramiento, los tratamientos administrados por el paciente (por ejemplo, imiquimod, podofilotoxina) son soluciones útiles para pacientes que les cuesta cumplir con el tratamiento [82]. También se ha presentado la posibilidad de combinar terapias ablativas con terapias citotóxicas o inmunomodulativas con el fin de mejorar la tasa de aclaramiento y de recurrencia. Los datos disponibles, sin embargo, no son concluyentes a la hora de determinar si la combinación de tratamientos aporta mejoras clínicamente significativas.

1.6.- Hidrogeles mucoadhesivos

1.6.1.- Propiedades y aplicaciones

Los hidrogeles son redes tridimensionales, hidrofílicos y poliméricos capaces de absorber grandes cantidades de agua o fluidos biológicos. Las redes están compuestas por homopolímeros o copolímeros, y son insolubles debido a la presencia de entrecruzamientos químicos (puntos de enlace, uniones) o entrecruzamientos físicos, como enredos. Los hidrogeles presentan una compatibilidad termodinámica con el agua que les permite hincharse en medios acuosos. Son numerosas sus aplicaciones, en particular en los sectores médico y farmacéutico. Los hidrogeles se parecen más al tejido vivo natural que a cualquier otra clase de biomateriales sintéticos, debido a su alto contenido de agua y su consistencia blanda, similar al tejido natural. Además, el alto contenido de agua de los materiales contribuye a su biocompatibilidad. Por lo tanto, los hidrogeles se pueden usar como lentes de contacto, membranas para biosensores, revestimientos para corazones artificiales, materiales para piel artificial y dispositivos de administración de fármacos [83].

El término de bioadhesión describe la capacidad de ciertas macromoléculas, sintéticas o biológicas, de adherirse a los tejidos del organismo. Cuando el tejido biológico es una mucosa, entonces hablamos de mucoadhesión. La investigación y el desarrollo de las formas bioadhesivas intenta lograr los siguientes objetivos:

1) Localizar el sistema medicamentoso en la región deseada superando, hasta cierto punto, los procesos naturales de eliminación.
2) Incrementar el tiempo de permanencia del medicamento en dicha región, consiguiendo un aumento neto del tiempo de efectividad del medicamento.
3) Mejorar el contacto del fármaco disuelto con la mucosa a través de la cual se realizará el fenómeno de absorción.
4) Formular sistemas de liberación prolongada o controlada de la sustancia activa.

La capa de mucus y la mucina en concreto son el componente de mayor implicación en el fenómeno de adhesión. El mucus es una secreción viscosa, translúcida que forma una capa continua, delgada y adherente en la superficie de la mucosa epitelial. Las funciones principales son la lubrificación y la protección de las células epiteliales

de agresiones de tipo mecánico o químico y a la degradación bacteriana. El mucus está en constante renovación habiéndose establecido un equilibrio dinámico entre la cantidad continuamente secretada por las células y la pérdida por acción mecánica o proteólisis. En su composición destacan las mucinas, glicoproteínas de alto peso molecular, sales inorgánicas, proteínas y lípidos [39].

La dilucidación de los mecanismos de interacción entre substratos biológico y los agentes bioadhesivos son fundamentales para el desarrollo de estas formas farmacéuticas.

- Interacciones físicas o mecánicas. Se producen a través del contacto íntimo entre el polímero bioadhesivo y la superficie irregular del mucus. Se trata de uniones semipermanentes, no específicas, que, si bien no pueden considerarse de importancia en bioadhesión, suponen una primera fase que promueve la posterior interacción química propiamente bioadhesiva.

- Enlaces químicos. Los de tipo covalente, o primarios, son enlaces muy estables de interés en odontología y ortopedia. Los enlaces secundarios, de menor energía, poseen características más idóneas a la bioadhesión por su transitoriedad. Para que pueda ocurrir mucoadhesión, la fuerza atractiva debe ser mayor que la repulsión no específica. Las interacciones atractivas provienen de las fuerzas de Van der Waals, atracciones electrostáticas, enlaces de hidrógeno e interacciones hidrófobas. Las interacciones repulsivas ocurren por la repulsión electrostática y estérica [39][84].

Los sistemas bioadhesivos deben sus propiedades a moléculas poliméricas que, en condiciones apropiadas, establecen interacciones con la superficie biológica. Dichas condiciones apropiadas dependen de las características químicas y estructurales del polímero bioadhesivo, de factores fisiológicos y variaciones experimentales. Una de las características estructurales es el peso molecular, donde los que tienen un bajo peso ven favorecido su difusión a través de la mucosa, aunque éste no parece ser un parámetro determinante. En cuanto a estructura y grupos funcionales, las moléculas de mucina están cargadas negativamente a pH neutro, por tanto, debido a las fuertes interacciones que se establecen entre electrolitos de carga contraria, los policatiónicos podrían ser excelentes mucoadhesivos a pH neutro; por el contrario, a bajos valores de pH, donde la mucina no se encuentra cargada, los policatiónicos serán poco

efectivos. También es importante mencionar otros factores como la flexibilidad de las cadenas del polímero para la interpenetración, donde, a mayor densidad de enlaces cruzados, la longitud efectiva de la cadena que puede penetrar en el mucus disminuye reduciéndose así la fuerza mucoadhesiva. Altas concentraciones del polímero manifiestan poca adhesión con el mucus porque el polímero adquiere una conformación replegada no disponiendo de grupos suficientes para el establecimiento de interacciones adhesivas. La consideración de factores de tipo fisiológico contribuye al éxito del diseño mucoadhesivo. La renovación de mucina produce un sustancial incremento de moléculas solubles de mucina. Éstas interaccionan con el sistema mucoadhesivo antes de que tengan la oportunidad de realizarlo con la capa de mucus, lo que supone una contaminación de la superficie y un hecho desfavorable a la mucoadhesión con la superficie de los tejidos. El estado patológico también es un factor a tener en cuenta. Se sabe que las propiedades fisicoquímicas del mucus se modifican. Dado que los mucoadhesivos han de usarse en estados patológicos las características de los mucoadhesivos han de evaluarse bajo las mismas condiciones [39].

1.6.2.- Polímeros gelificantes

1.6.2.1.- Alginato de sodio

Los alginatos son polímeros de polisacáridos naturales aislados de algas pardas (*Phaeophyceae spp.*). El alga se extrae con una solución alcalina diluida que solubiliza el ácido algínico presente. El ácido algínico libre se obtiene por tratamiento de la masa espesa y viscosa resultante con ácidos minerales. El ácido algínico se puede convertir luego en una sal de la cual el alginato de sodio es la forma principal que se usa actualmente.

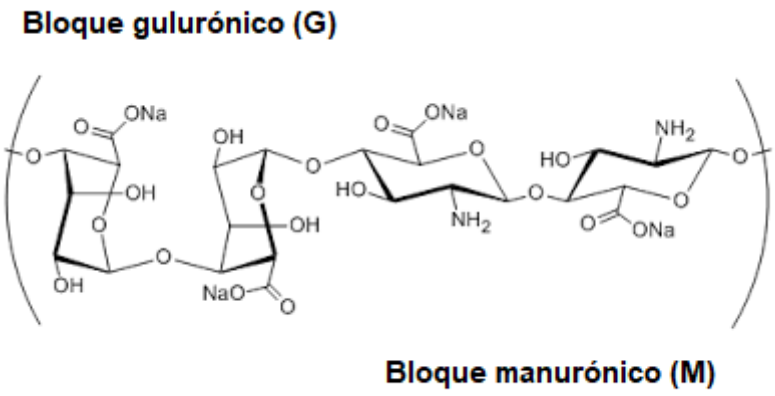

***Figura 9**. Estructura molecular del alginato de sodio*

El ácido algínico es un polímero lineal que consta de residuos de ácido D-manurónico (M) y ácido L-gulurónico (G) (Figura 9) que están dispuestos en bloques en la cadena del polímero. Estos bloques homogéneos (compuestos solo por residuos de ácido) están separados por bloques hechos de unidades aleatorias o alternas de ácidos manurónico y gulurónico.

Los alginatos con un alto contenido de bloques de ácido gulurónico dan geles de una fuerza considerablemente mayor en comparación con los alginatos ricos en manuronato, ya que los residuos G muestran una mayor afinidad por los iones divalentes que los residuos M. La transmitancia, la hinchazón y la viscoelasticidad de las membranas de gel de alginato se ven muy afectadas por la relación M/G [85].

La hidratación del ácido algínico conduce a la formación de un "gel ácido" de alta viscosidad debido a la unión intermolecular. Después de la gelificación, las moléculas de agua quedan atrapadas físicamente dentro de la matriz de alginato, pero aún pueden migrar libremente [85]. Esto es de gran importancia en muchas aplicaciones como, por ejemplo, geles de alginato para la inmovilización/encapsulación de células. La capacidad de retención de agua del gel se debe a las fuerzas capilares. Los geles termoestables pueden desarrollarse a temperatura ambiente.

Las propiedades fisicoquímicas del sistema polimérico y el proceso de hinchamiento para activar la liberación de fármacos dependerán del tipo de gel formado. El ácido algínico y sus sales de sodio y calcio son considerados generalmente como no tóxicos y biocompatibles. Estos productos están disponibles comercialmente y se fabrican más de 200 grados diferentes de alginato, además de ácido algínico y varias sales correspondientes. Los alginatos se utilizan ampliamente en la industria farmacéutica, cosmética y alimentaria. Sin embargo, dado que los alginatos se obtienen de una fuente natural, es posible que estén presentes diversas impurezas. Estos incluyen metales pesados, proteínas y endotoxinas. Para aplicaciones farmacéuticas, particularmente para administración parenteral, estas impurezas deben eliminarse. En la Farmacopea Europea (Ph.Eur.) se incluye una monografía para el ácido algínico, pudiendo obtener Alginato aprobado por Ph.Eur..

Su aplicación generalmente depende de las propiedades espesantes, formadoras de gel y estabilizantes, así como su propiedad mucoadhesiva [86]. Como ejemplos se puede mencionar que el alginato de sodio se puede utilizar como agente aglutinante

y desintegrante en comprimidos, como agente de suspensión y espesante en geles, lociones y cremas miscibles en agua, y como estabilizador de emulsiones.

1.6.2.2.- Chitosan

El interés por el chitosan (CTS), o quitosano, un polímero biodegradable, no antigénico, no tóxico, natural y biocompatible derivado de la chitina (o quitina), se debe a los diversos efectos beneficiosos para la salud del mismo, incluido el alto poder antioxidante y actividades antimicrobianas [87].

La quitina se extrae de la concha y los caparazones de los artrópodos, principalmente de los crustáceos, y también está presente en pequeña cantidad en la pared de algunos hongos y levaduras. Sin embargo, el chitosan solo se encuentra de manera natural en un reducido grupo de hongos, por este motivo, el origen principal del CTS comercial se obtiene a partir de la desacetilación de la quitina [88].

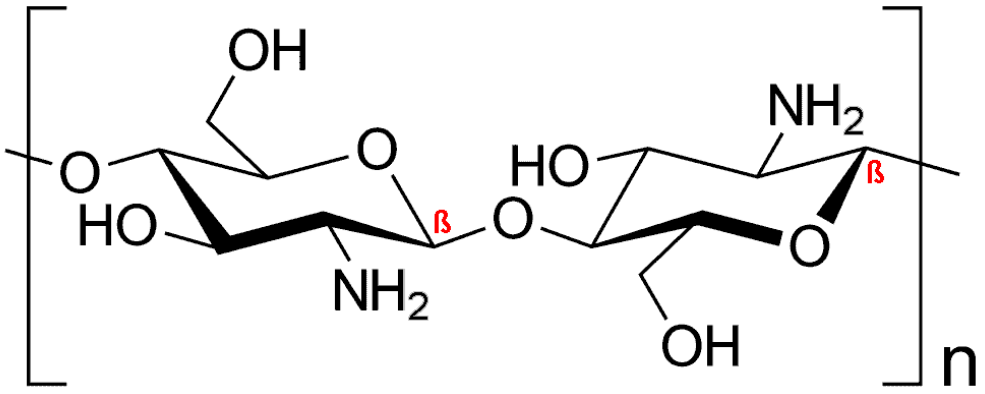

***Figura 10**. Estructura química del chitosan.*

Es un polisacárido lineal dispuesto de manera aleatoria compuesto por cadenas de D-glucosamina y N-acetilglucosamina, unidas mediante enlace β-(1-4). Se trata de un polímero catiónico natural, propiedad que le permite crear estructuras multicapa o complejos electrostáticos con otros polímeros sintéticos o naturales cargados negativamente.

El peso molecular del CTS y el grado de desacetilación influyen significativamente en sus actividades biológicas. La proporción de unidades estructurales de N-acetilglucosamina a D-glucosamina tiene un impacto en la extensión de la distribución de carga, la absorción de humedad, la viscosidad intrínseca y la solubilidad del quitosano en soluciones acuosas [87].

Debido a sus actividades biológicas únicas, el CTS ha ganado una atención considerable en las últimas décadas. Éste es ampliamente utilizado en varias aplicaciones biomédicas y biológicas, entre otros cabe destacar el de vehículo portador de fármacos. Su capacidad de incorporar grandes cantidades de agua en su estructura lo convierten en un gran agente gelificador. A de más, tiene propiedades mucoadhesivas [89], propiedad que permite desarrollar sistemas de liberación controlada de fármacos. A todo esto, hay que añadir otras propiedades tales como una muy buena biocompatibilidad, biodegradabilidad, baja inmunogenicidad, propiedades antifúngicas y antimicrobianas, efecto cicatrizante, hemostático e incluso un efecto antiinflamatorio [86][88][89].

Todas estas propiedades hacen del CTS un excelente polímero para la formulación de hidrogeles mucoadhesivos en donde vehiculizar otros fármacos de diferente índole con el fin de tratar diferentes patologías tisulares, e incluso patologías que requieran niveles sistémicos de fármaco.

1.7.- Nanopartículas

Las nanopartículas (NPs) cómo vehículo de liberación de fármacos son estructuras (cápsulas o esferas) de diferente naturaleza con un tamaño aproximado de 100 nm, generalmente huecas, capaces de acumular en su interior fármacos, proteínas, material genético, etc.

La administración de fármacos y el desarrollo farmacéutico relacionado en el contexto de la nanomedicina deben verse como ciencia y tecnología de sistemas complejos a escala nanométrica (10–1000 nm), que consta de al menos dos componentes, uno de los cuales es un ingrediente farmacéuticamente activo, aunque también son posibles las formulaciones de NPs del propio fármaco [92]. Todo el sistema conduce a una función especial relacionada con el tratamiento, la prevención o el diagnóstico de enfermedades, a veces denominadas drogas inteligentes o teragnósticas. Los objetivos principales de la investigación de nanobiotecnologías en la administración de fármacos incluyen:

- Dirección y administración de fármacos más específicos.
- Reducción de la toxicidad manteniendo los efectos terapéuticos.
- Mayor seguridad y biocompatibilidad.
- Desarrollo más rápido de nuevos medicamentos seguros.

En definitiva, los sistemas nanoparticulares para la liberación de fármacos persiguen la finalidad de mejorar la eficacia y seguridad del medicamento. Para ello, se diseñan sistemas para proteger al principio activo de su degradación prematura y conseguir así una liberación más prolongada en el tiempo. A de más, se tiene en cuenta que presenten una permeabilidad adecuada para atravesar las membranas fisiológicas y se intenta que tengan, si procede, una liberación dirigida para disminuir los efectos secundarios, la toxicidad y aumentar la concentración del fármaco en el lugar de acción [93]. Por consiguiente, el empleo de NPs para vehiculizar fármacos presenta importantes ventajas respecto a los sistemas convencionales.

Existe gran variedad de vehículos nanoestructurados, pero en particular, las NPs poliméricas biodegradables han sido utilizadas ampliamente durante las últimas décadas para potenciar la biodisponibilidad de fármacos en aplicación tópica. El polímero derivado del ácido poliláctico-co-glicólico (PLGA) es biocompatible y biodegradable, de naturaleza no tóxica, y, además, está aprobado tanto por la FDA (*Food and Drug Administration*) como por la EMA (*European Medicin Agency*) como excipiente en productos farmacéuticos.

El PLGA es uno de los más exitosos polímeros biodegradables utilizados ya que su hidrólisis da lugar a metabolitos monómeros; ácido láctico y ácido glicólico. Debido a que estos dos monómeros son endógenos y fácilmente metabolizados por el cuerpo a través del ciclo de Krebs, se asocia una toxicidad sistémica mínima al uso de PLGA para la administración de fármacos o aplicaciones de biomateriales. El PLGA está disponible comercialmente con diferentes pesos moleculares y composiciones de copolímero, influyendo éstos en el tiempo de degradación, que puede variar de varios meses a varios años. Las formas de PLGA generalmente se identifican por la proporción de monómeros utilizada. Por ejemplo, PLGA 50:50 identifica un copolímero cuya composición es 50 % ácido láctico y 50 % ácido glicólico. El poli(ácido láctico) (PLA) también se ha utilizado en menor medida que el PLGA debido a la menor tasa de degradación [93].

El PLGA se puede procesar en casi cualquier forma, y puede encapsular moléculas de prácticamente cualquier tamaño. Permite incorporar moléculas hidrófilas e hidrofóbicas y obtener una liberación sostenida del fármaco, así como protegerlo de la degradación. Es soluble en una amplia gama de disolventes comunes, incluyendo disolventes clorados, tetrahidrofurano, acetona o acetato de etilo. En el agua, PLGA se biodegrada por hidrólisis de sus enlaces éster. La biodistribución y la farmacocinética del PLGA sigue un perfil lineal y dosis-dependiente.

1.7.1.- Elaboración de Nanopartículas

Existen numerosos métodos para elaborar NPs poliméricas que permitan la encapsulación de moléculas. Estos métodos pueden ser clasificados en dos grandes categorías; los de elaboración directa y aquellos a base de polímeros preformados. Entre los métodos de elaboración directa se pueden mencionar la polimerización de

una emulsión, que permite crear nanoesferas, y la polimerización interfacial a partir de monómeros, para formar nanocápsulas.

Dentro de los métodos que emplean polímeros preformados destaca la emulsión por evaporación de solvente. Éste fue el primer método desarrollado para la preparación de NPs basadas en polímeros en el sector farmacéutico. Consiste en la preparación de soluciones de polímeros en disolventes volátiles y la obtención de emulsiones. En un inicio los disolventes más usados eran el diclorometano y el cloroformo, pero actualmente estos han sido reemplazados por el acetato de etilo ya que presenta un mejor perfil toxicológico.

La emulsión por preparar puede ser simple o doble, permitiendo obtener así nanoesferas si se opta por la emulsión simple, y nanocápsulas mediante emulsiones dobles [94]. Si el principio activo es hidrófobo se emplea una emulsión w/o simple, por el contrario, en el caso de principios activos hidrosolubles se forma una emulsión doble w/o/w.

1.7.1.1.- Método de doble emulsión

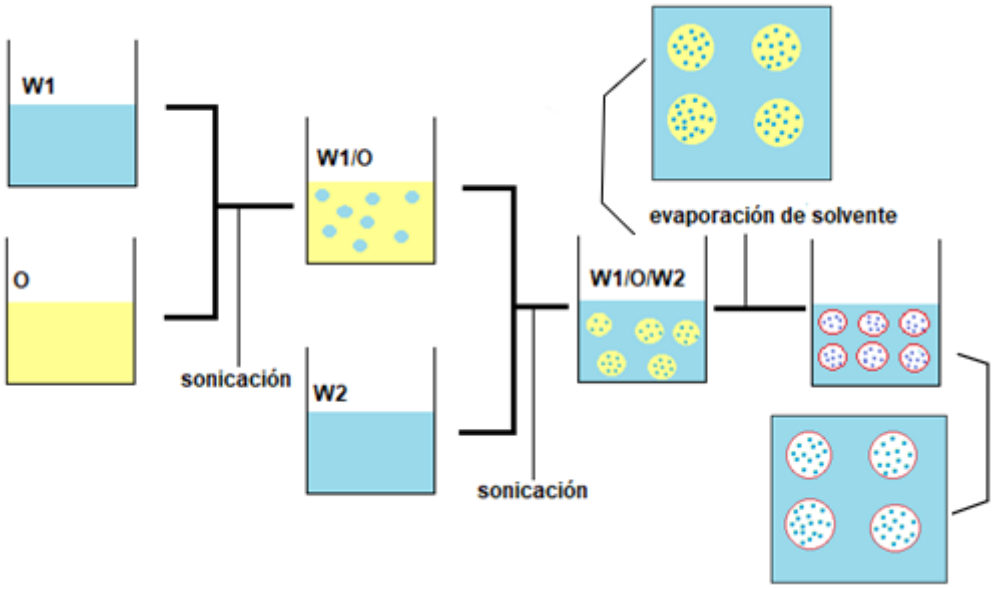

Figura 11. *Esquema de la Técnica de doble emulsión.*

Esta técnica consiste en elaborar una primera emulsión en donde se dispersa una fase acuosa sobre una fase hidrófila continua w_1/o mediante la ayuda de una sonda de ultrasonido. El principio activo o sustancia para encapsular se disuelve en la fase

acuosa (w_1), mientras que el polímero destinado a la formación de la matriz suele ir en la fase orgánica junto con el solvente volátil (o). A esta emulsión w_1/o se le añade una segunda fase hidrófila (w_2) que viene a ser la misma que la w_1 sólo que sin principio activo, obteniendo así una doble emulsión $w_1/o/w_2$. Una vez formada la doble emulsión, el solvente orgánico es evaporado, por lo que debe ser suficientemente volátil. La evaporación del solvente puede realizarse mediante agitación magnética a temperatura ambiente durante varias horas o mediante rotavapor [95]. El polímero que se encontraba disuelto en dicho solvente precipita atrapando al fármaco, lo que permite la formación de las NPs (Figura 11) [96][97].

1.7.2.- Caracterización de nanopartículas

Las variables que afectan a la estabilidad y aplicabilidad de las NPs son numerosas. Por un lado, está el polímero seleccionado para la encapsulación del principio activo. Sus propiedades físico y bioquímicas determinarán el comportamiento de las NPs en términos de encapsulación, degradación, liberación de moléculas así como en el **tamaño de partícula (Zave)** final [98]. Este parámetro es uno de los más importantes ya que si lo que se quiere lograr es una absorción rápida, el tamaño de la NP debe ser de 100 nm o menos. Por lo general, en la aplicación transdérmica, las vesículas con un diámetro de 600 nm o superior no pueden transportar el material encapsulado a las capas más profundas de la piel, tendiendo a permanecer dentro o sobre el estrato córneo. Las NPs con un diámetro de 300 nm o menos pueden entregar su contenido, hasta cierto punto, en las capas más profundas de la piel. Sin embargo, las NP con un diámetro de 70 nm o menos han mostrado una máxima deposición de contenido tanto en capas dérmicas como epidérmicas [99]. Otras variables que pueden afectar al tamaño de partícula son el surfactante por utilizar y la concentración del mismo [100], tiempo e intervalo de sonicación a la hora de preparar las emulsiones [101], el disolvente orgánico escogido [102], etc.

El **índice de polidispersidad (PI)** es una medida de la heterogeneidad de una muestra basada en el tamaño. El PI es un parámetro que se obtiene de manera simultánea con el tamaño de partícula y provee información sobre la muestra. Este índice es adimensional y está escalado de tal manera que los valores inferiores a 0,05 se observan principalmente con estándares altamente monodispersos. Los valores de PI superiores a 0,7 indican que la muestra tiene una distribución de tamaño de

partícula muy amplia y probablemente no sea adecuada para ser analizada mediante la técnica de dispersión de luz dinámica (DLS). Los diferentes algoritmos de distribución de tamaño funcionan con datos que se encuentran entre estos dos valores extremos de PI (es decir, 0,05–0,7) [99].

El estudio de la morfología y estructura de las NPs es otro parámetro importante por determinar a la hora de caracterizar NPs. Para ello se utiliza un microscopio electrónico de transmisión (TEM). Con las imágenes obtenidas se observa la estructura y forma de las nanopartículas y si todas tienen una estructura parecida. Además de pasada puede medirse también el tamaño de partícula.

La información sobre la carga superficial de las nanopartículas en dispersión se puede obtener a partir del **potencial zeta (ZP)**. La carga superficial de una partícula en solución se compensa con la acumulación de iones del medio circundante, que forma una doble capa electroquímica. La capa interna consta de contraiones que están fuertemente unidos a la superficie de la partícula. Esta capa se llama capa de Stern y está rodeada por otra capa difusa de iones menos unidos. A cierta distancia de la superficie de la partícula, esta capa difusa tiene un límite más allá del cual los iones enlazados ya no la siguen debido a las fuerzas de cizallamiento cuando la partícula se mueve. Esto significa que la carga de la partícula ya no está equilibrada y se produce un potencial eléctrico en este límite, que es lo que se denomina potencial zeta. La importancia del potencial zeta es que su valor está relacionado con la estabilidad de las dispersiones coloidales. Para las moléculas y partículas que son lo suficientemente pequeñas, un alto potencial zeta es sinónimo de estabilidad ya que la solución o dispersión se resistirá a la agregación. Cuando el potencial es bajo, se tiene atracción entre las partículas, se supera a la repulsión y se forman agregados. Por lo tanto, los coloides de alto potencial zeta se estabilizan eléctricamente, mientras que, los coloides con bajos potenciales zeta tienden a coagular [103].

OBJETIVOS

The main objective of this doctorate is to develop mucoadhesive formulations of KT and their physicochemical, morphological, and biopharmaceutical characterization for topical administration on the skin and different mucous membranes as an alternative for the management of pre-and postoperative pain of different tissue injuries, such as condyloma acuminata.

To fulfill this objective, the doctoral work was divided into different secondary objectives:

- Design and prepare different mucoadhesive topical formulations of Ketorolac Tromethamine. Mucoadhesive and biodegradable gelling polymers such as sodium alginate and chitosan were chosen to formulate hydrogels and PLGA to produce nanoparticles.

- Characterize the organoleptic, morphological, and physicochemical properties of the formulations.

- Determine the kinetic profile of the different formulations through in vitro release studies and modelling.

- Study KT's ex vivo penetration capacity from the formulations in different tissues: skin, buccal, sublingual, and vaginal mucosa.

- Evaluate the anti-inflammatory efficacy of some formulations through in vivo studies in mouse ears.

- Observe the tissue's histological structure after applying some formulations to show their tolerability.

- Analyze the impact of some formulations on the skin and mucous biomechanical properties by monitoring the following parameters: TEWL/TMWL and hydration.

- Examine the harmlessness and safety of some formulations through in vitro cell cultures.

RESULTADOS

3.1.- Artículo 1

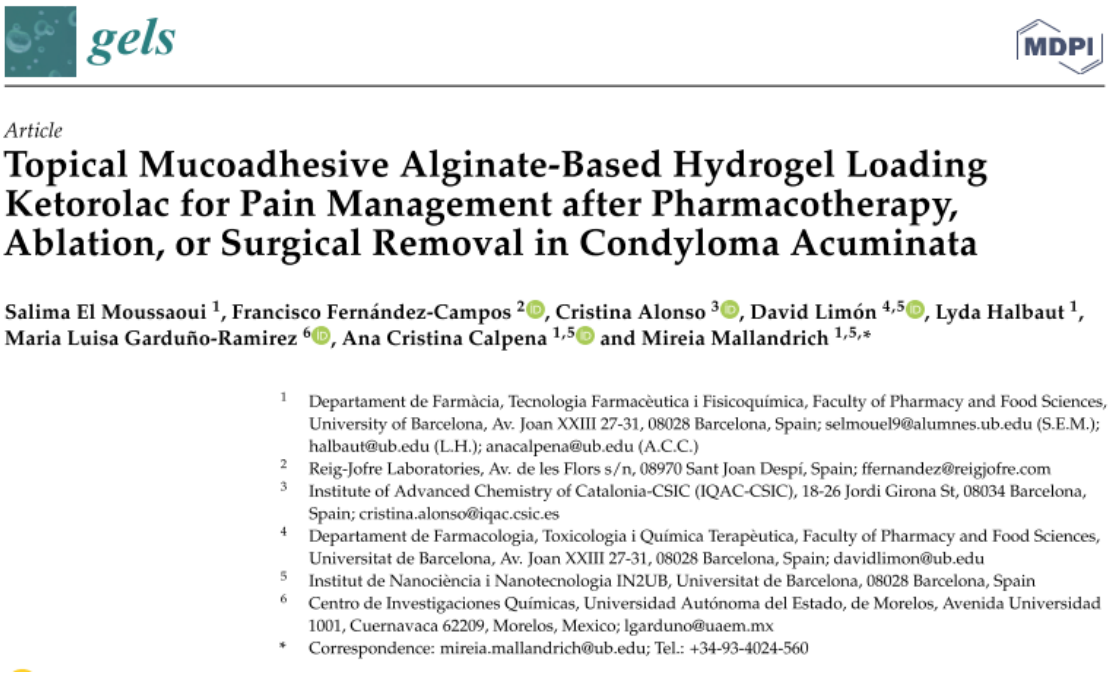

gels

MDPI

Article

Topical Mucoadhesive Alginate-Based Hydrogel Loading Ketorolac for Pain Management after Pharmacotherapy, Ablation, or Surgical Removal in Condyloma Acuminata

Salima El Moussaoui [1], Francisco Fernández-Campos [2], Cristina Alonso [3], David Limón [4,5], Lyda Halbaut [1], Maria Luisa Garduño-Ramirez [6], Ana Cristina Calpena [1,5] and Mireia Mallandrich [1,5,*]

1 Departament de Farmàcia, Tecnologia Farmacèutica i Fisicoquímica, Faculty of Pharmacy and Food Sciences, University of Barcelona, Av. Joan XXIII 27-31, 08028 Barcelona, Spain; selmouel9@alumnes.ub.edu (S.E.M.); halbaut@ub.edu (L.H.); anacalpena@ub.edu (A.C.C.)
2 Reig-Jofre Laboratories, Av. de les Flors s/n, 08970 Sant Joan Despí, Spain; ffernandez@reigjofre.com
3 Institute of Advanced Chemistry of Catalonia-CSIC (IQAC-CSIC), 18-26 Jordi Girona St, 08034 Barcelona, Spain; cristina.alonso@iqac.csic.es
4 Departament de Farmacologia, Toxicologia i Química Terapèutica, Faculty of Pharmacy and Food Sciences, Universitat de Barcelona, Av. Joan XXIII 27-31, 08028 Barcelona, Spain; davidlimon@ub.edu
5 Institut de Nanociència i Nanotecnologia IN2UB, Universitat de Barcelona, 08028 Barcelona, Spain
6 Centro de Investigaciones Químicas, Universidad Autónoma del Estado, de Morelos, Avenida Universidad 1001, Cuernavaca 62209, Morelos, Mexico; lgarduno@uaem.mx
* Correspondence: mireia.mallandrich@ub.edu; Tel.: +34-93-4024-560

Current Impact Factor	JCR category rank
4.702	Q1 Polymer Science

Resumen

En este trabajo se desarrolló un hidrogel tópico biocompatible que contiene ketorolaco trometamina al 2% y alginato de sodio cómo polímero gelificante. El hidrogel se caracterizó física, mecánica y morfológicamente, mostrando características adecuadas para una formulación tópica. Se pudo liberar hasta el 73 % del KT del gel siguiendo un modelo exponencial de fase uno. Tras la aplicación en piel humana y mucosa vaginal, el KT pudo penetrar a través de ambos tejidos y quedar retenido en ellos, particularmente en la mucosa vaginal. Otra ventaja es que no se deben esperar efectos secundarios sistémicos después de la aplicación del gel. El hidrogel demostró ser bien tolerado in vivo cuando se aplicó en humanos y no causó ninguna irritación visible. Finalmente, el hidrogel de KTmostró una actividad antiinflamatoria del 53 %, lo que sugiere que es una formulación estable y adecuada para el tratamiento de procesos inflamatorios, como los que ocurren con la extirpación química o quirúrgica de las verrugas anogenitales.

gels

MDPI

Article

Topical Mucoadhesive Alginate-Based Hydrogel Loading Ketorolac for Pain Management after Pharmacotherapy, Ablation, or Surgical Removal in Condyloma Acuminata

Salima El Moussaoui [1], Francisco Fernández-Campos [2], Cristina Alonso [3], David Limón [4,5], Lyda Halbaut [1], Maria Luisa Garduño-Ramirez [6], Ana Cristina Calpena [1,5] and Mireia Mallandrich [1,5,*]

1 Departament de Farmàcia, Tecnologia Farmacèutica i Fisicoquímica, Faculty of Pharmacy and Food Sciences, University of Barcelona, Av. Joan XXIII 27-31, 08028 Barcelona, Spain; selmouel9@alumnes.ub.edu (S.E.M.); halbaut@ub.edu (L.H.); anacalpena@ub.edu (A.C.C.)
2 Reig-Jofre Laboratories, Av. de les Flors s/n, 08970 Sant Joan Despí, Spain; ffernandez@reigjofre.com
3 Institute of Advanced Chemistry of Catalonia-CSIC (IQAC-CSIC), 18-26 Jordi Girona St, 08034 Barcelona, Spain; cristina.alonso@iqac.csic.es
4 Departament de Farmacologia, Toxicologia i Química Terapèutica, Faculty of Pharmacy and Food Sciences, Universitat de Barcelona, Av. Joan XXIII 27-31, 08028 Barcelona, Spain; davidlimon@ub.edu
5 Institut de Nanociència i Nanotecnologia IN2UB, Universitat de Barcelona, 08028 Barcelona, Spain
6 Centro de Investigaciones Químicas, Universidad Autónoma del Estado, de Morelos, Avenida Universidad 1001, Cuernavaca 62209, Morelos, Mexico; lgarduno@uaem.mx
* Correspondence: mireia.mallandrich@ub.edu; Tel.: +34-93-4024-560

Citation: El Moussaoui, S.; Fernández-Campos, F.; Alonso, C.; Limón, D.; Halbaut, L.; Garduño-Ramirez, M.L.; Calpena, A.C.; Mallandrich, M. Topical Mucoadhesive Alginate-Based Hydrogel Loading Ketorolac for Pain Management after Pharmacotherapy, Ablation, or Surgical Removal in Condyloma Acuminata. *Gels* **2021**, *7*, 8. https://doi.org/10.3390/gels7010008

Received: 30 December 2020
Accepted: 20 January 2021
Published: 23 January 2021

Abstract: Condyloma acuminata is an infectious disease caused by the human papilloma virus (HPV) and one of the most common sexually transmitted infections. It is manifested as warts that frequently cause pain, pruritus, burning, and occasional bleeding. Treatment (physical, chemical, or surgical) can result in erosion, scars, or ulcers, implying inflammatory processes causing pain. In this work, a biocompatible topical hydrogel containing 2% ketorolac tromethamine was developed to manage the painful inflammatory processes occurring upon the removal of anogenital condylomas. The hydrogel was physically, mechanically, and morphologically characterized: it showed adequate characteristics for a topical formulation. Up to 73% of ketorolac in the gel can be released following a one-phase exponential model. Upon application on human skin and vaginal mucosa, ketorolac can permeate through both of these and it can be retained within both tissues, particularly on vaginal mucosa. Another advantage is that no systemic side effects should be expected after application of the gel. The hydrogel showed itself to be well tolerated in vivo when applied on humans, and it did not cause any visible irritation. Finally, ketorolac hydrogel showed 53% anti-inflammatory activity, suggesting that it is a stable and suitable formulation for the treatment of inflammatory processes, such as those occurring upon chemical or surgical removal of anogenital warts.

Keywords: *Condyloma acuminata*; ketorolac; pain management; alginate hydrogel; topical delivery; transdermal; mucosal delivery; mucoadhesive; anti-inflammatory

1. Introduction

Condyloma acuminata (CA) is one of the most common sexually transmitted infections [1] caused by various genotypes of Human Papilloma Virus (HPV) [2]. There are more than 180 genotypes described, around 40 of which have been related to anogenital warts, most particularly genotypes 6 and 11 [3]. Genotypes 16 and 18 attracted attention because of their oncogenic nature and they have been associated to vaginal cervix cancer and anus cancer [4].

Although the introduction of the tetravalent vaccine against HPV caused a significant reduction in its incidence [5], the disease incidence is still high, especially in certain countries with socio-economic issues [5]. CA can affect both sexes at any age, being the

maximum incidence is between 20- and 24-year-old women and between 25- and 29-year-old men [6]. Symptoms associated to CA depend on anatomical location, number, and size of the lesions [3], being pruritus the most frequent, followed by leukorrhea, discomfort, bleeding and pain. In addition, CA usually involves psychological aspects such as concern, shame, and lack of self-esteem in the sexual sphere [1].

On some occasions CA can be resolved spontaneously or will remain with no change, but in other cases lesions need to be treated, specially to prevent future outcomes such as cancer. In these cases, a therapeutic intervention should be carried out, considering location of the disease, number of warts, and patient related aspects such as life-style, and economic considerations, among others [6]. Several theories are described in the literature but there is not enough scientifical evidence demonstrating one treatment to be superior over others [7]. Pharmacological treatment involves an immunomodulatory approach (topical imiquimod, podophyllotoxin, and sinecatechins of tea extract), physical agents (cryotherapy, trichloroacetic acid, electrocoagulation, and CO_2 laser), and/or surgery. Other treatments backed up less scientific evidence due to the few clinical trials, involve intralesional interferon, photodynamic therapy, and topical cidofovir [8]. Unfortunately, when there is intravaginal or intra-anal CA, the treatment alternatives are reduced, and on some occasions, surgery is the only option.

Pain management is under extensive study so that it may improve patient quality of life and reduce the post-surgery discomfort. Ambulatory and minor surgeries usually combine anesthetics, analgesics, and anti-inflammatory drugs in different pre, intra, or post-operative regimes. Ketorolac is a non-steroidal anti-inflammatory drug with potent analgesic properties close to those of opioids, with no addictiveness potential and no sedative properties [9]. Several authors injected surgery ketorolac at the anatomical site (colon or vaginal), with local effect, in haemorrhoidectomy [10] and other colon and vaginal surgical procedures [11]. It resulted in successful pain management and improvement in the patient's recovery. Ketorolac demonstrated to be effective in the management of postoperative pain when administrated in a single dose [12]. It is also administrated topically as preoperative medication in eye laser keratectomy and cataracts [13–15]. In fact, one of the most common applications of topical ketorolac has been in ophthalmology, with very low topical administration in skin and mucosa. Considering the successful results in pain management after local injection in colon and vaginal surgeries, as previously described, topical ketorolac is proposed is proposed for intravaginal application, pre-vaginal applications and/or anal application in CA removal.

Two main events modulate the successful topical delivery: diffusion through the vehicle towards the surface of the tissue (in this case, skin or vaginal mucosa) and the partitioning between the vehicle and the tissue. For this reason, several aspects should be considered during the development. On one hand, the physicochemical properties of the drug modulate its intrinsic permeability, being the molecular weight and the log P (octanol–water partitioning) the main parameters used to predict successful permeation. On the other hand, characteristics of the formulation also modulate the permeation, such as the complete solution of the drug in the vehicle, the particle size (in suspensions), pH, relative polarity between formulation-drug-body surface, and the presence of permeation enhancers.

As well, the biocompatibility of the formulation is essential for treatment tolerance and patient compliance. Hydrogels are traditional formulations composed of different polymers types, natural ones (different cellulose grades and other polysaccharides) or synthetic ones (polyacrylates, polyvinyl pyrrolidone, etc.) All these polymers are able to retain water in their 3D network by creating hydrogen bonds between water molecules and polymer molecules. Alginate is a natural linear copolymer formed by (1,4)-β-D-mannuronic acid and α-L-guluronic acid residues, which can be arranged as homopolymeric sequences of each residue, or with alternating residues. Alginate-based gels show interesting mucoadhesive properties and a very good compatibility profile [16], having been extensively used in topical drug delivery systems with successful results.

In this work, we designed and developed a hydrogel using sodium alginate as the gelator polymer and ketorolac tromethamine (Figure 1) as a potent non-steroidal anti-inflammatory drug, as a candidate for the local pre- or post-treatment of inflammatory processes derived from CA surgical removal. The hydrogel has been extensively characterized in terms of appearance, microscopic morphology, and mechanical properties, among others. As well as this, its biopharmaceutical properties have also been investigated in terms of drug release, drug permeation across the skin and vaginal mucosa, and the amount of drug retained within the tissue after application for performing a local therapeutical activity. Moreover, the biocompatibility of the formulation has been tested by measuring the trans-epidermal water loss (TEWL) in humans, and the anti-inflammatory efficacy of the ketorolac hydrogel (KT hydrogel) has been evaluated in mice. Results from this work show that this hydrogel is a promising candidate for the described indication.

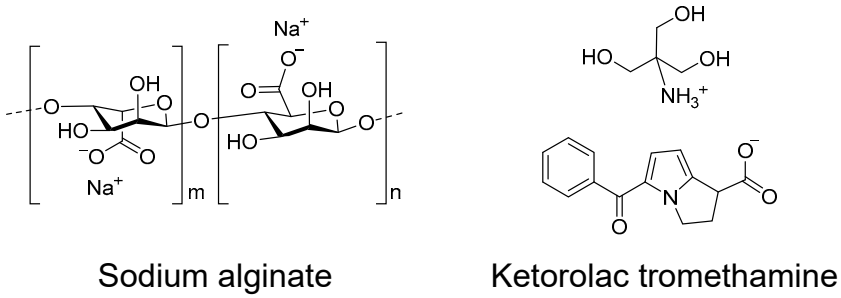

Figure 1. Chemical structures of sodium alginate polymer and ketorolac tromethamine.

2. Results and Discussion

2.1. Physical Characterization of KT Hydrogel

2.1.1. Appearance and pH Evaluation

KT hydrogel when freshly prepared showed a yellowish-translucent color, stickiness and limited flowability. The gel showed a neutral pH of 7.3. None of these aspects changed after two month-storage at room temperature.

2.1.2. Optical Stability

The stability of the hydrogel was studied by observing if any change occurred in the backscattered light from the hydrogel using TurbiScanLab® equipment. The analysis of changes in backscattered light, from the bottom to the top of the sample permits the detecting of sedimentation/creaming processes of colloidal dispersions, as well as coalescence/flocculation processes, with a much higher sensitivity as compared to the naked eye [17,18].

The hydrogels (with ketorolac tromethamine and without the drug) freshly prepared were examined every hour for 24 h to observe potential changes in the short term. After two-months of storage at room temperature (23 ± 2 °C), the analysis was repeated to assess the stability in the long term. Figure 2 shows the backscattered light from a hydrogel without drug (A–B) and with ketorolac tromethamine (C–D), both at day 1 (A,C) and at day 60 (B, D), where the color of the lines shows the hourly evolution within the day of analysis, being magenta the first and red the last analysis after the 24-h study.

As it can be observed in the figure, both the hydrogel alone and with ketorolac tromethamine are mainly translucent, as the mean backscattered light is only around 6% in all cases, indicating that the inclusion of ketorolac tromethamine in the formulation does not affect the structure of the hydrogel and the drug remains in perfect solution. Moreover, neither the hydrogel alone nor the hydrogel with ketorolac tromethamine undergo sedimentation or creaming processes, as no significant increase/decrease in the backscattered light in the bottom/top of the sample is observed. For colloidal samples having a particle size bigger than 0.6 μm in diameter, flocculation is detected by the decrease of the mean backscattering values throughout the sample [17]. In this case, the

24-h evolution shows very little change (<1%) in the mean backscattered light of the freshly prepared KT hydrogel (day 1), suggesting a reversible restructuration of the gel fibers during the first 24 h, but with no evident flocculation process occurring, as the mean backscattered light on day 60 remained stable. These results therefore show that the KT hydrogel can be considered stable.

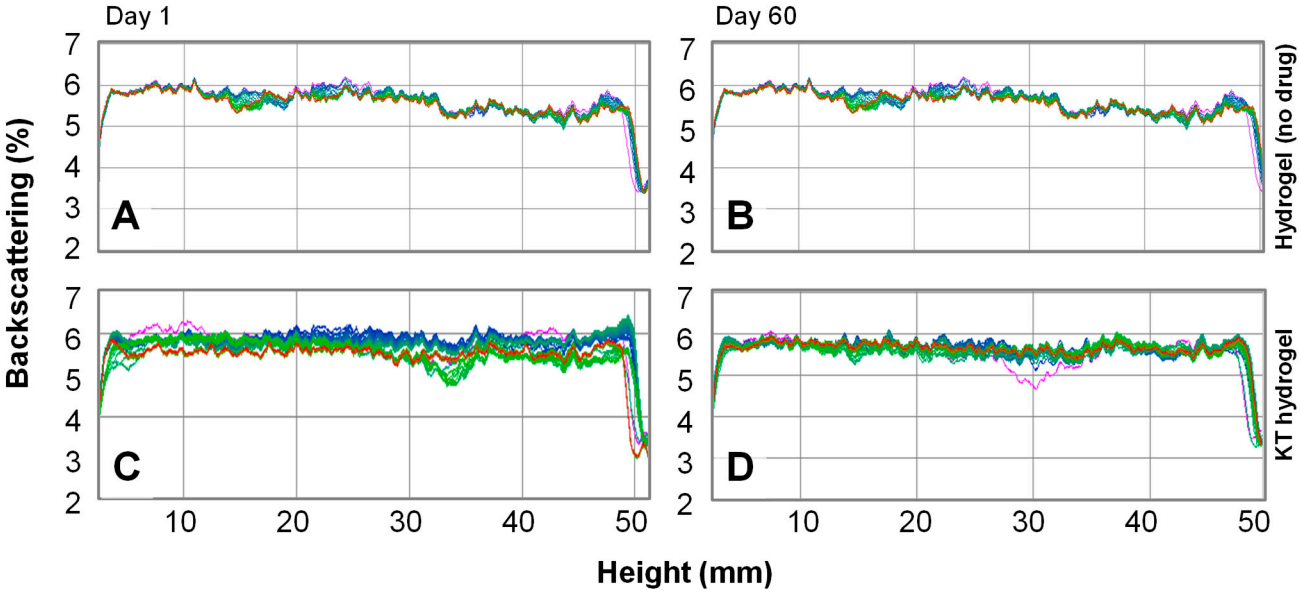

Figure 2. Hourly backscattering profiles over 24 h for (**A**) hydrogel without drug at day 1; (**B**) hydrogel without drug at day 60; (**C**) ketorolac hydrogel (KT hydrogel) at day 1; and (**D**) KT hydrogel at day 60. The color of the lines shows the hourly evolution within the day of analysis, being magenta the first and red the last analysis after the 24-h study.

2.1.3. Morphological Studies

Scanning Electron Microscopy (SEM) was used to evaluate the morphology of the KT hydrogel. Figure 3 shows that the gel is composed of sodium alginate polymer that self-assembles in the presence of water forming fibers that can be as thin as 80 nm in diameter. The sodium alginate-fibers can grow resulting in two different arrangements and therefore morphologies (Figure 3A,B). Fibers can grow longitudinally to several micrometers in length and can gradually attach to each other to form thicker fibers. Fibers of different thicknesses are intertwined and create pores with diameters ranging between 400 nm and up to one micrometer.

The high porosity as well as the hydrophilic behavior of the fibers is ideal from a drug delivery point of view, as it could permit the incorporation of solvent, and explains the high and fast swelling observed. In addition, it could predict a fast diffusion of the drug during drug release experiments (see below).

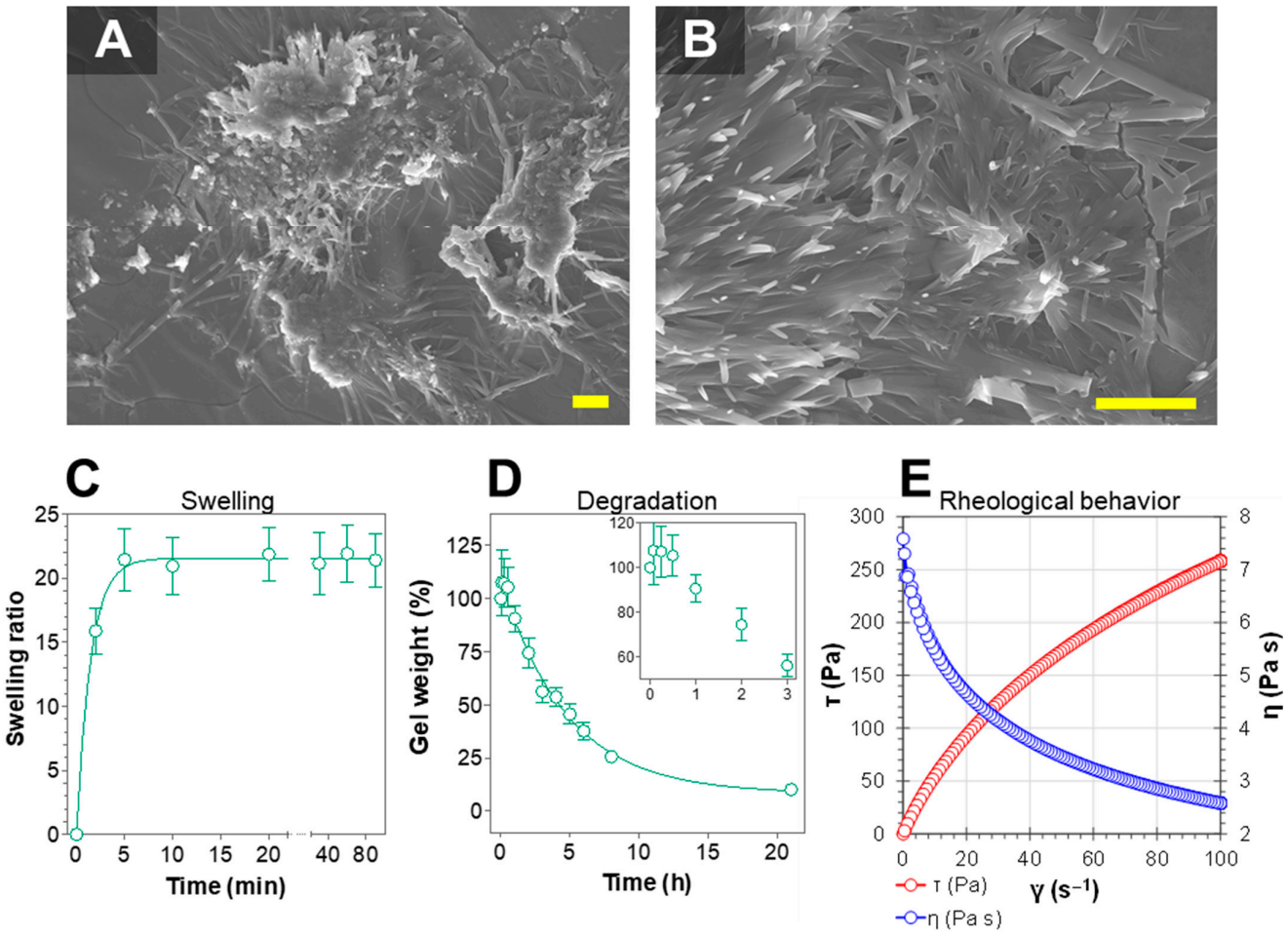

Figure 3. Characterization of KT hydrogel. (**A**,**B**) SEM images of KT hydrogel at different magnifications. The gel is formed by sodium alginate polymers that self-assemble to form fibers with diameters of around 100 nm. Scalebar represents 5 µm. (**C**) Swelling ratio of KT hydrogels upon immersion in PBS. The kinetics followed a first-order (one-phase exponential association) model (**D**) Degradation of KT hydrogels in PBS. Inset shows a 7% weight increase during the first hour, in accordance to swelling results. After one hour, degradation follows a one-phase exponential decay kinetics. Values represent Means ± SD (n = 3). (**E**) Rheogram of KT hydrogel at 32 °C. The flow curve represents shear stress (τ in Pa) (left axis) or viscosity (η in Pa·s) (right axis) as a function of the shear rate (γ in s^{-1}).

2.1.4. Swelling and Degradation Tests

Swelling experiments were performed in KT hydrogels to evaluate their ability to incorporate solvent beneath the matrix. Briefly, previously dehydrated KT hydrogels were immersed in PBS, and their weight was recorded at certain intervals. Figure 3C shows that previously dehydrated gels are highly hygroscopic, as they can incorporate up to 20 times their weight in water in less than 5 min. The weight increase followed a first order kinetics (one-phase exponential association), with a constant value k = 0.68 min^{-1}.

Moreover, degradation experiments were performed by immersing the KT hydrogels in PBS and recording their weight at certain intervals. Figure 3D shows an initial 7% weight increase during the first hour upon immersion, corresponding to the incorporation of PBS into the matrix, and which is in accordance with swelling experiments. After the first hour, the gel weight decreased following a first-order kinetics (one-phase exponential decay), with a degradation constant value of 0.21 h^{-1}, therefore achieving 10% of the original weight after 21 h. This weight loss corresponds to the gradual diffusion of the components of the hydrogel into the medium, indicating that the formulation could be successfully degraded when immersed in the biological medium.

2.1.5. Rheological Behavior

The mechanical properties of the KT hydrogel were studied by performing rheology studies, where the shear rate was first increased and subsequently decreased, while shear stress (τ) and the viscosity (η) were measured. The flow curve of KT hydrogels (Figure 3E) (n = 2) indicated no thixotropic behavior in the system as the rheogram did not display any hysteresis loop. The mathematical model that provided the best overall match of the experimental data according to the highest correlation coefficient of regression (r) was *Cross*, which indicates a shear thinning (pseudoplastic) behavior. Additionally, the results indicated that the viscosity of the different samples at 100 s^{-1} was 2555.5 ± 28.5 mPa·s, showing good repeatability of the rheological results between samples and indicating an adequate formulation protocol.

2.2. In Vitro Release of Ketorolac from the Hydrogel

In vitro drug release experiments were performed using Franz-type cells to evaluate the ability of the hydrogel to release the drug according to previously reported methodologies [19]. Figure 4 shows the cumulative amount of ketorolac released from the hydrogel. Different models were fitted (Zero-order, first-order and Higuchi) (see Appendix A, Tables A1 and A2), and the best-fitting model was chosen according to the determination coefficient (r^2). Ketorolac released from the hydrogel followed a first order (one-phase exponential association) kinetics, and the release parameters can be seen in Table 1.

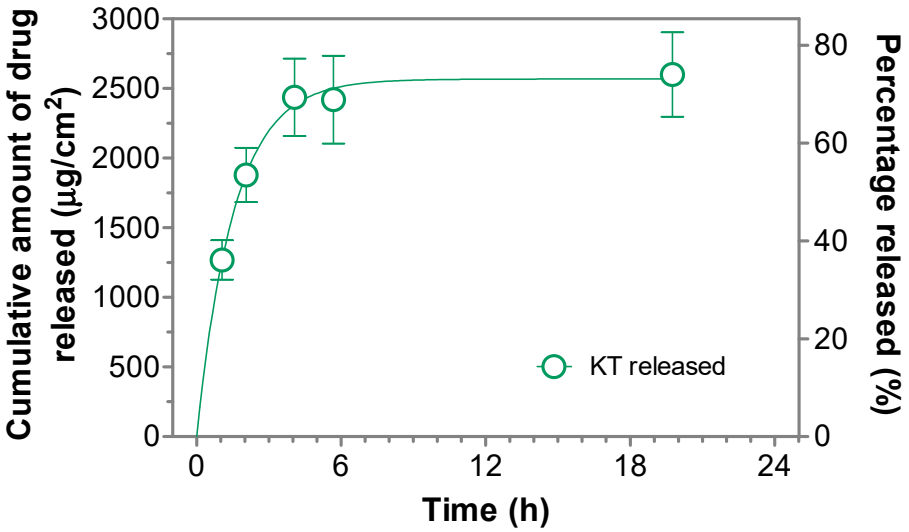

Figure 4. Cumulative amount of ketorolac released. Data followed a first-order (One-phase exponential association) kinetics. Values represent Means ± SD (n = 6).

Table 1. Drug release parameters from KT hydrogel according to a first order kinetics. Ymax = total amount of drug released; K = release rate constant. Values represent Means ± 95% confidence interval (n = 6).

Best-Fit Values	
Ymax (µg/cm^2)	2568 ± 14
K (h^{-1})	0.64 ± 0.12
Half-time (h)	1.08
R^2	0.9908

Results show that the hydrogel can release up to 2568 µg/cm^2 of ketorolac, corresponding to 73% of the total dose seeded, and this maximum amount is already achieved within 4 h, showing a release rate of 0.64 h^{-1}. This fast drug release is in accordance with

the wide and numerous pores created by the fibers arrangement, as observed in the SEM images (Figure 3A,B), which allow the easy diffusion of the drug.

2.3. Ex Vivo Permeation of Ketorolac through Human Skin and Vaginal Mucosa

Permeation experiments were performed ex vivo to assess the permeation of ketorolac across human skin as well as across vaginal mucosa according to previously reported methodologies [9,20,21], in both cases under an infinite-dose regimen [22]. The cumulative amount of ketorolac permeated through each tissue along time is shown in Figure 5A, and the permeation parameters calculated can be seen in Table 2.

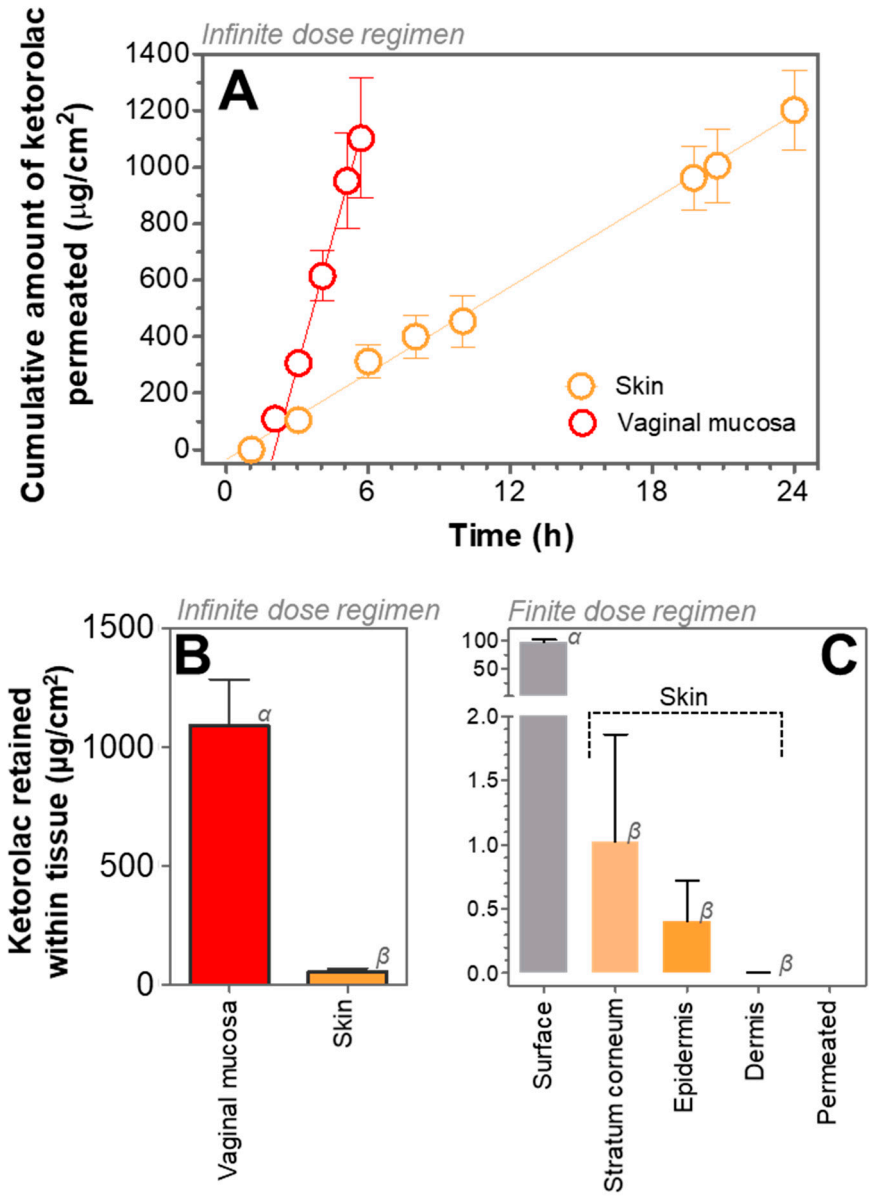

Figure 5. (**A**) Cumulative amount of ketorolac permeated (μg/cm^2) through human skin and through vaginal mucosa upon application of KT hydrogel. (**B**) Total amount of ketorolac retained within the tissue (μg/g cm^2) (skin or vaginal mucosa) 24-h after application of KT hydrogel under an infinite dose regimen. (**C**) Biodistribution of ketorolac 24 h after application of KT hydrogel using a finite dose regimen. Around 95% ketorolac remains outside the skin while the successfully penetrated ketorolac is retained within the stratum corneum and epidermis layers. All values represent Means ± SD (n = 6). Different Greek letters represent significant differences ($p < 0.001$).

Permeation of ketorolac across different tissues (skin or vaginal mucosa) upon application of KT hydrogel showed significant differences. In case of permeation across skin tissue, the permeation parameters indicate that ketorolac permeation reached the steady state from the very beginning, with an estimated T_{lag} of 0.67 h, and showing a transdermal flux of 50.92 μg/h·cm^2, leading to a total amount of ketorolac permeated of 1202.46 μg/cm^2 after 24 h. In contrast, permeation through vaginal mucosa indicated a slightly longer Tlag (2.04 h) while a significantly higher flux (306.00 μg/h·cm^2) led to a similar amount of ketorolac permeated (1102.20 μg/cm^2) in only 6 h.

Table 2. Transdermal/transmucosal permeation parameters of ketorolac 24 h/6 h after application of KT hydrogel under an infinite dose regimen. Results are expressed as Mean ± SD (n = 6). A_P: amount of ketorolac permeated after 24 h/6 h. A_R amount retained after 24 h/6 h. Css: plasma concentration at steady state. Tlag: lag time. Jss: transdermal/transmucosal flux.

	Skin	**Vaginal Mucosa**
A_P (μg/cm^2)	1202.46 ± 143.99	1102.20 ± 212.08
A_R (μg/cm^2)	52.54 ± 14.71	1090.42 ± 196.27
Css (μg/mL)	0.22 ± 0.01	1.30 ± 0.05
T_{lag} (h)	0.67 ± 0.003	2.04 ± 0.50
Jss (μg/h·cm^2)	50.92 ± 1.44	306.00 ± 6.95
K_p (cm/h)	2.55 × 10^{-3}	1.53 × 10^{-2}

These results can be explained by the fast release of ketorolac from KT hydrogel (Figure 4) as well as by the physicochemical properties of the drug (QSAR). For instance, it is considered that drugs with a molecular weight below 500 Da, an octanol: water partitioning coefficient (log P) below 5, less than 5 hydrogen bound donors, and less than 10 hydrogen bound acceptors, can successfully permeate through skin tissue [23,24]. These properties change when the drug is in its neutral form (ketorolac) or in the salt form (ketorolac tromethamine). For instance, the salt form has a higher molecular weight than the neutral form (376.4 vs. 255.27 g/mol), more hydrogen bond donors (5 vs. 1), more hydrogen bond acceptors (7 vs. 3), and although the log P for the salt form is not reported, it is expected to be much lower than that of the neutral form (1.9) [25,26]. It is true that the drug in contact with biological medium may change its form (and thus its properties), being in an equilibrium that depends on the concentration of the drug and the composition of the medium in which it is dissolved. Changes can include exchange of the cationic moiety (tromethamine) for other cations or protonation of the carboxylate group of ketorolac to a neutral carboxylic acid. Nonetheless, the use of the salt form in KT hydrogel may initially influence a higher proportion of ketorolac molecules in the salt form. For this reason, the faster permeation of ketorolac through the vaginal mucosa may be especially related to the highly hydrophilic behavior of the salt form (ketorolac tromethamine), as it does not find an important lipophilic barrier against the penetrating of the tissue and permits high fluxes across the mucosa. In contrast, permeation of ketorolac through the skin is compromised by the barrier effect produced by the epidermis (especially the highly lipophilic stratum corneum), leading to smaller fluxes. Examples of gels for topical application can be found in the literature showing that the physicochemical properties of the drug highly influence their ability to permeate through the skin. When applied using the same gel and at the same concentration, neutral, lipophilic drugs such as the corticoids betamethasone 17-valerate or triamcinolone acetonide tend to permeate faster than cationic drugs such as gemcitabine hydrochloride or anionic drugs such as methotrexate sodium [20].

Moreover, local anti-inflammatory activity with a rapid action onset may be achieved by a sufficient amount of drug retained in the tissue in short time. In this regard, short T_{lag} was observed in both tissues, and the total amount of ketorolac retained within the skin was 52.54 μg/cm^2, whereas within vaginal mucosa was around 20 times higher (1090.42 μg/cm^2). These results confirm the suitability of KT hydrogel for local application

in either tissue but especially on vaginal mucosa, as the higher retention is most probably related to the higher contents of water in the tissue.

In order to assess a possible systemic effect after application of KT hydrogel under an infinite-dose regimen, either on skin or vaginal mucosa, the steady state plasma concentration (Css) after application of ketorolac gel was estimated, considering the human plasma clearance of ketorolac (1840 mL/h) [27] for a mean 80-kg individual. For instance, the expected Css achieved after application of these hydrogel considering a hypothetical area of application of 5 cm^2 would be 0.22 µg/mL when applied on human skin, whereas 1.30 µg/mL when applied on vaginal mucosa. The therapeutic plasma concentration range reported is 0.3 to 5 µg/mL [28]; thus, the Css expected after a dermal application would be below the therapeutic plasma concentration range. On the contrary, the Css calculated after a 5 cm^2 vaginal application would be within this reported range. However, no side effects would be expected since the Css is close to the lower limit. Additionally, topical products are not used in exaggerated use conditions (infinite dose approach) but in finite dose conditions. All this suggests that the KT hydrogel could be safely used for the local healing of inflammation. The equations for the calculation of Css and of the absorption parameters can be seen in the Appendix A (permeation parameters and calculation of the Css upon application of KT hydrogel).

2.4. Distribution of Ketorolac within the Skin Layers

A permeation experiment under finite dose regimen [22] was performed to study the skin biodistribution of ketorolac. For instance, around 10 µL of gel was applied on the skin, the dose of ketorolac trometamine being only 102 µg/cm^2. After 24-h permeation, the receptor fluid was collected. Ketorolac remaining on the surface of the skin was carefully recovered, adhesive tape was used to perform stripping procedures to detach the *stratum corneum*, and the epidermis was then separated from the dermis by means of heat. Ketorolac contained in the adhesive tapes, the epidermis, and the dermis was extracted using a water:methanol mixture from the different layers and finally was analyzed (Figure 5C). Detailed absolute and relative amounts can be seen Table 3. After application of a small amount of KT hydrogel, most of the ketorolac could be recovered (92–101%). Approximately 95% of the dose applied was not absorbed, rather it was found on the surface, which can be related to the barrier effect produced by the highly lipophilic *stratum corneum* [29].

Table 3. Distribution of ketorolac within the skin layers 24 h after application of KT hydrogel under a finite-dose regimen. b.l.q. stands for 'below limit of quantification'

KT Hydrogel Application	µg/cm^2	%
Ketorolac trometamine dosed	102.09	100.00
Surface	96.72 ± 4.07	94.75 ± 3.99
Stratum corneum	1.02 ± 0.84	1.00 ± 0.82
Percutaneous absorption	0.40 ± 0.32	
Epidermis	0.40 ± 0.32	0.39 ± 0.32
Dermis	0.002 ± 0.001	0.002 ± 0.001
Receptor fluid	b.l.q.	b.l.q.
Total recovery	98.14 ± 4.69	96.14 ± 4.60

Regarding the drug penetrated into the skin, around 1% was found in the stratum corneum, 0.4% was found in the epidermis, and only 0.002% in the dermis, whereas no ketorolac was detected in the receptor fluid. This indicates no drug is absorbed into the systemic circulation when applying a small dose. This biodistribution suggests that upon application of small doses, finding the drug in the outer layers of the skin is not related to the affinity of the drug for these (lipophilic) layers, but is due to the low dose applied. In the beginning, the high drug concentration gradient at the surface of the skin promotes the

diffusion inside the skin, but the low dose leads to a rapid decrease in the concentration gradient, impeding the further diffusion along the inner epidermis layers.

Therefore, the application of a small dose such as 10 μL on the skin would probably lead to anti-inflammatory activity in the outer layers of the skin only; however, when the KT hydrogel is applied in higher quantities, such as those used under the infinite dose regimen (~200 μL), it should be effective for the topical relieve of inflammatory processes, either applied through the skin or through vaginal mucosa.

2.5. In Vivo Anti-Inflammatory Efficacy Evaluation

To assess if the ketorolac retained within the skin after application (Sections 2.3 and 2.4 ex vivo permeation experiments under finite and infinite-dose approaches) is sufficient to develop a local anti-inflammatory effect, an in vivo study was carried out in mice. Groups of mice (n = 6) were processed in parallel. In all groups, acute skin edema was induced upon application of TPA in both ears of the mice. At the same time, in one of the groups, KT hydrogel was applied to the right ear of the mice as a treatment, whereas 2% solution of ketorolac tromethamine in water was applied to the right ear in a second group, and finally, hydrogel without drug was applied to the right ear in a third group.

The inhibition of inflammation achieved by the KT hydrogel as well as by the ketorolac tromethamine solution or the hydrogel without drug was calculated and is shown in Figure 6C.

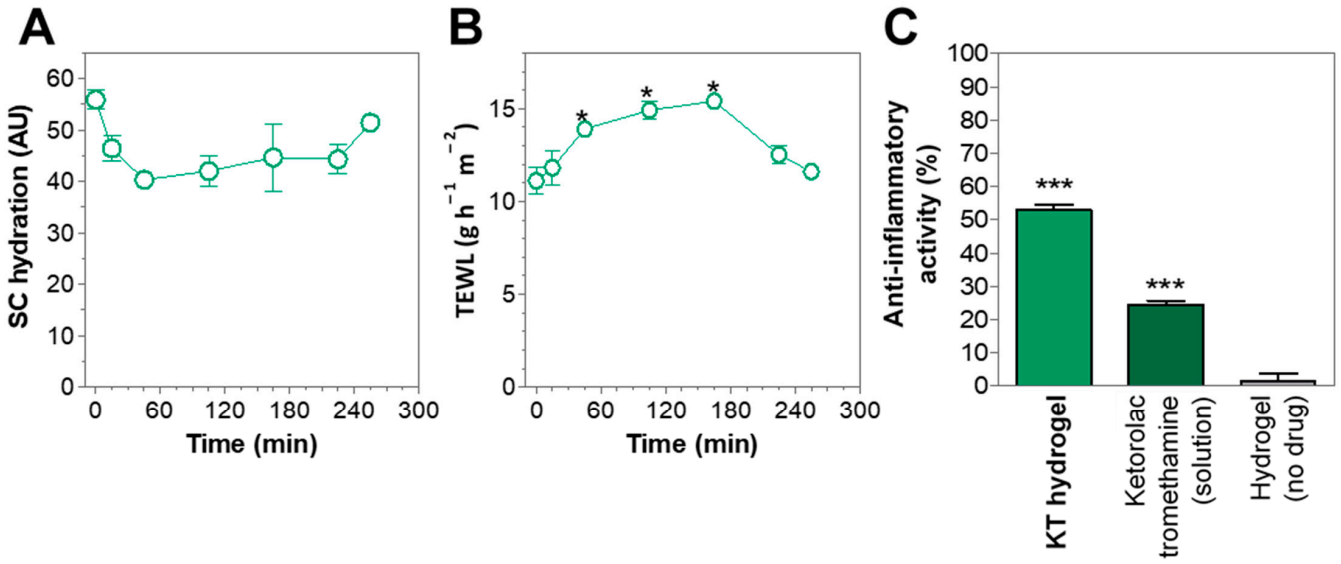

Figure 6. (**A**) Hydration of the *stratum corneum* upon application of KT hydrogel in humans. (**B**) Trans-epidermal water loss (TEWL) expressed in g of water per hour per m^2 of skin, upon application of KT hydrogel in humans. (**C**) Anti-inflammatory activity expressed as inhibition (%) of TPA-induced inflammation upon application of a treatment (KT hydrogel, ketorolac tromethamine in solution, and hydrogel without drug). Values represent Means ± SD (n = 6). * Significant differences ($p < 0.05$); *** Significant differences ($p < 0.001$) as compared to control (hydrogel without drug).

The application of KT hydrogel led to a 52.9% reduction of inflammation as compared to the positive control, while application of ketorolac tromethamine in solution led to a 24.5% reduction of inflammation. However, KT hydrogel showed itself to be 2.16 times more effective than ketorolac tromethamine in solution, suggesting that the clinical application of KT hydrogel could be suitable for producing local anti-inflammatory activity.

2.6. In Vivo Tolerance Study

The preservation of the integrity of the skin upon application of KT hydrogel was studied using a corneometer. Parameters such as the hydration of the *stratum corneum* or the trans-epidermal water loss (TEWL) were analyzed and are shown in Figure 6A,B. Re-

sults show that upon application of the hydrogel, the basal hydration levels of the *stratum corneum* (55.9 ± 1.9 AU) decreased by 28%, reaching values of 40.3 ± 1.3 AU, 45 min after application, but gradually recovered to the initial values after 4 h. According to the normal values of skin hydration [30], values comprehended between 30 and 45 AU could be related to moderately dry conditions, while values above 45 AU could be related to a sufficiently hydrated skin. Thus, the application of KT hydrogel may result in only moderate dehydration, a condition that is reversible in the short term. The moderate dehydration of the stratum corneum could be explained by the highly hydrophilic behavior of the sodium alginate fibers forming the gel, that in contact with the stratum corneum may absorb the water from the surroundings, a behavior that was also observed in swelling experiments.

Likewise, TEWL is an indirect measure of skin permeability and the barrier function of the *stratum corneum* by observing the speed at which water is being evaporated from the surface [31]. It is generally accepted that TEWL values from patients with intact skin can range between 6 and 13 g h^{-1} m^{-2}. In this study, untreated patients showed TEWL values of 11.1 + 0.7 g h^{-1} m^{-2}, while upon application of KT hydrogel, TEWL values increased to 13.9 + 0.1 after 45 min and reached a maximum of 15.4 + 0.4 after 2.7 h but later decreased to basal values after 3.7 h. These results show that the application of KT hydrogel may slightly disrupt the barrier function of the stratum corneum but only to an extent which does not represent any threat to the physiological function of the skin, since TEWL values revert to the basal one in a few hours. The diffusion across a lipophilic structure, such as the stratum corneum, may be challenging for a highly water-soluble drug such as ketorolac tromethamine, and the hydrogel might be exerting a boost action on the Ketorolac's penetration by modifying the vehicle-skin partition coefficient in a reversible manner by promoting the water content in the stratum corneum, and the water embedded in the hydrogel might drive the Ketorolac diffusion through the stratum corneum.

Studies have shown that skin variables such as TEWL, pH, and skin temperature in humans are dependent on circadian rhythms, interestingly finding that the skin permeability is higher during the evening and late night than in the morning [32]. Moreover, it has been shown in hairless rats that changes in the environmental temperature and light have an effect on skin function [33]. This suggests that the reversible TEWL values of the skin after application of KT hydrogel might be influenced by circadian rhythms and/or environmental factors such as temperature, and this suggests that its application during the evening might lead to higher analgesic and anti-inflammatory efficacy.

In addition, the application of KT hydrogel on patients' skin did not lead to any visual irritation and was well tolerated.

3. Conclusions

An alginate-based hydrogel was extensively characterized in terms of morphology, pH, physical stability, and mechanical properties, showing adequate characteristics for a topical formulation.

Drug release studies show that up to 73% of the total amount of ketorolac in the gel can be released in less than 6 h from the hydrogel following the one-phase exponential model.

Permeation experiments under an infinite-dose approach were performed using human skin and vaginal mucosa, demonstrating that ketorolac contained in the hydrogel can permeate through both tissues successfully, showing almost 7 times faster permeation through vaginal mucosa (306.0 μg/h·cm^2) than through human skin (50.92 μg/h·cm^2). Moreover, ketorolac is retained within the tissue 24 h/6 h after application, showing an up to 20-times higher amount of drug retained within vaginal mucosa (1090.42 μg/cm^2) than in human skin (52.54 μg/cm^2).

The topical application of this hydrogel, in general, should not cause any systemic side effects, and therefore, it can be considered safe.

The hydrogel was well tolerated in vivo when applied in humans, showing no important alterations in the skin barrier function such as hydration and TEWL. Additionally, the hydrogel did not cause any visible irritation. These results show that KT hydrogel is a

sults show that upon application of the hydrogel, the basal hydration levels of the *stratum corneum* (55.9 ± 1.9 AU) decreased by 28%, reaching values of 40.3 ± 1.3 AU, 45 min after application, but gradually recovered to the initial values after 4 h. According to the normal values of skin hydration [30], values comprehended between 30 and 45 AU could be related to moderately dry conditions, while values above 45 AU could be related to a sufficiently hydrated skin. Thus, the application of KT hydrogel may result in only moderate dehydration, a condition that is reversible in the short term. The moderate dehydration of the stratum corneum could be explained by the highly hydrophilic behavior of the sodium alginate fibers forming the gel, that in contact with the stratum corneum may absorb the water from the surroundings, a behavior that was also observed in swelling experiments.

Likewise, TEWL is an indirect measure of skin permeability and the barrier function of the *stratum corneum* by observing the speed at which water is being evaporated from the surface [31]. It is generally accepted that TEWL values from patients with intact skin can range between 6 and 13 g h^{-1} m^{-2}. In this study, untreated patients showed TEWL values of 11.1 + 0.7 g h^{-1} m^{-2}, while upon application of KT hydrogel, TEWL values increased to 13.9 + 0.1 after 45 min and reached a maximum of 15.4 + 0.4 after 2.7 h but later decreased to basal values after 3.7 h. These results show that the application of KT hydrogel may slightly disrupt the barrier function of the stratum corneum but only to an extent which does not represent any threat to the physiological function of the skin, since TEWL values revert to the basal one in a few hours. The diffusion across a lipophilic structure, such as the stratum corneum, may be challenging for a highly water-soluble drug such as ketorolac tromethamine, and the hydrogel might be exerting a boost action on the Ketorolac's penetration by modifying the vehicle-skin partition coefficient in a reversible manner by promoting the water content in the stratum corneum, and the water embedded in the hydrogel might drive the Ketorolac diffusion through the stratum corneum.

Studies have shown that skin variables such as TEWL, pH, and skin temperature in humans are dependent on circadian rhythms, interestingly finding that the skin permeability is higher during the evening and late night than in the morning [32]. Moreover, it has been shown in hairless rats that changes in the environmental temperature and light have an effect on skin function [33]. This suggests that the reversible TEWL values of the skin after application of KT hydrogel might be influenced by circadian rhythms and/or environmental factors such as temperature, and this suggests that its application during the evening might lead to higher analgesic and anti-inflammatory efficacy.

In addition, the application of KT hydrogel on patients' skin did not lead to any visual irritation and was well tolerated.

3. Conclusions

An alginate-based hydrogel was extensively characterized in terms of morphology, pH, physical stability, and mechanical properties, showing adequate characteristics for a topical formulation.

Drug release studies show that up to 73% of the total amount of ketorolac in the gel can be released in less than 6 h from the hydrogel following the one-phase exponential model.

Permeation experiments under an infinite-dose approach were performed using human skin and vaginal mucosa, demonstrating that ketorolac contained in the hydrogel can permeate through both tissues successfully, showing almost 7 times faster permeation through vaginal mucosa (306.0 μg/h·cm^2) than through human skin (50.92 μg/h·cm^2). Moreover, ketorolac is retained within the tissue 24 h/6 h after application, showing an up to 20-times higher amount of drug retained within vaginal mucosa (1090.42 μg/cm^2) than in human skin (52.54 μg/cm^2).

The topical application of this hydrogel, in general, should not cause any systemic side effects, and therefore, it can be considered safe.

The hydrogel was well tolerated in vivo when applied in humans, showing no important alterations in the skin barrier function such as hydration and TEWL. Additionally, the hydrogel did not cause any visible irritation. These results show that KT hydrogel is a

stable and suitable formulation for the treatment of inflammatory processes, such as those occurring upon chemical or surgical removal of anogenital warts.

4. Materials and Methods

4.1. Materials

4.1.1. Reagents

Sodium alginate was purchased from Fagron Iberica (Terrassa, Spain). Ketorolac tromethamine and Nipagin were obtained from Sigma-Aldrich (Barcelona, Spain). Nipasol was acquired from Acofarma (Barcelona, Spain), and Na_2HPO_4 and KH_2PO_4 were supplied by Panreac (Barcelona, Spain). PBS pH 7.6, gentamicin sulphate, and bovine serum albumin were provided by Sigma (St. Louis, MO, USA); methanol was obtained from Merck, Darmstadt, Germany. The adhesive tapes were obtained from D-squame, (Cuderm Co., Dallas, TX, USA).

The purified water was obtained from a Milli-Q1 Gradinet A10 system apparatus (Millipore Iberica S.A.U., Madrid, Spain). All the other chemicals and reagents used in the study were of analytical grade.

4.1.2. Tissues and Experimental Animals for Ex Vivo and In Vivo Assays

Human skin was obtained from abdominoplasties on healthy women (Barcelona SCIAS Hospital, Barcelona, Spain). The Bioethics Committee of the Barcelona-SCIAS Hospital approved the Study protocol (Nº001; approved on 20/01/2016), and volunteers provided written informed consent forms.

Following the surgery, the skin was stored at -20 °C until the experiments; then, the skin was dermatomed (GA630, Aesculap, Tuttlingen, Germany) at 500 µm-thick. The human skin barrier integrity of all skin discs was determined by transepidermal water loss (TEWL) using a TEWL-meter (Dermalab) prior to the permeation studies. Those skin discs that failed in the skin barrier integrity stage (TEWL values above 13 g/m^2 h) were discarded and replaced.

Vaginal mucosa (Landrace Large White race) was provided by the Bellvitge animal facility services. The Ethics Committee of Animal Experimentation of the University of Barcelona approved the Study Protocol (approved on 10/01/2019). Full-thickness mucosa was used in the permeation studies.

Male Swiss CD-1 mice weighing 20–25 g (Círculo ADN S.A. de C.V.; Coyoacan D.F., Mexico) were used for the in vivo anti-inflammatory efficacy evaluation after a 7-day quarantine period. The animals were housed in plastic cages with soft bedding, controlled diet, and tap water ad libitum. Environmental conditions were controlled at 24 $\pm$ 1 °C, and the relative humidity was kept at 50–60%. Light conditions were also controlled, being 12 h light and 12 h dark every 24 h.

The study was performed according to the Mexican Official Normative for Animal Care and Handling (NOM-062-ZOO-1999), and the Academic Ethics Committee of the Vivarium at the Universidad Autónoma del Estado de Morelos (Mexico) approved the Study Protocol (BIO-UAEM:012:2013; approved on 21/12/2015).

4.2. Preparation of Sodium Alginate Hydrogels

Drug-loaded hydrogels were prepared at laboratory scale at a concentration of 2% *w/v* by dissolving ketorolac tromethamine in aqua conservans. Sodium Alginate (4%) was gradually added to the ketorolac tromethamine solution with continuous stirring, until a thin dispersion without residual powder was formed. The dispersions were allowed to equilibrate in a water bath at 37 °C for 24 h so that they would undergo the swelling process that led to the formation of a cross-linked polymeric network, obtaining KT hydrogel. The gel was stored at room temperature.

4.3. Physical Characterization of KT Hydrogel

4.3.1. Appearance

The hydrogel formulation was visually observed directly for color, odor, and viscosity, at preparation and again 2 months afterwards.

4.3.2. pH Measurements

The pH of the hydrogel was measured at room temperature using the pH meter micro-pH 200 (Crison Instruments S.A., Barcelona, Spain). Measurements were conducted with the gel freshly prepared and at 2 months after preparation.

4.3.3. Optical Stability

The physical stability of the KT hydrogel was monitored by Dynamic Backscattering using a TurbiScanLab® (Turbiscan T-Lab Expert (Formulaction Co., L'Union, France). The optical sensor comprises a pulsed near-infrared light source and two synchronous optical sensors: one for backscattering and one for transmission.

A volume of 20 mL of KT hydrogel was filled into flat-bottom cylindrical glass measuring cells, and backscattered light at λ = 880 nm was measured from the top to the bottom of the vial, hourly for 24 h at 25 °C to evaluate the short-term stability. Measurements were repeated two months later to assess the long-term stability. Hydrogel without drug was analyzed similarly as a control [34].

4.3.4. Morphological Studies

The micro-structure of the hydrogel was examined by Scanning Electron Microscopy (SEM) in a JSM-7100F (JEOL Inc., Peabody, MA, USA) by coating the sample with a thin layer of carbon in an Emitech K950 coater (Quorum Technologies Ltd., Kent, UK).

4.3.5. Swelling and Degradation Tests

The swelling test evaluates the hydrogel capacity of absorbing water within its structure. The PBS uptake was carried out in triplicate by determining the swelling ratio (SR) by a gravimetric method [9] according to Equation (1):

$$SR = \frac{W_s - W_d}{W_d} \quad (1)$$

where W_d is the weight of dried hydrogel, and W_s is the weight of the swollen hydrogel at different times.

Briefly, the dried hydrogel was immersed in PBS (pH = 7.4) at 37 °C for 90 min. At different times (2, 5, 10, 20, 30, 60, and 90 min), the gel was removed from the incubation, and the excess PBS on the gel surface was soaked up and then weighed (W_s).

The degradation test aims to monitor the weight loss as a function of time. The weight loss (WL) was calculated by incubating known amounts of fresh hydrogel in PBS (pH = 7.4) at 37 °C for 21 h. Three replicates of hydrogel were removed, blotted, and weighed at the following time points: 0.08, 0.25, 0.5, 1, 2, 3, 4, 5, 6, 8, and 21 h. The weight loss was expressed as the percentage of weight loss with respect to the freshly prepared hydrogel. It was calculated based on Equation (2):

$$WL(\%) = \frac{W_i - W_d}{W_i} 100\% \quad (2)$$

where W_i is the initial weigh of hydrogel and W_d the weight of hydrogel at different times.

4.3.6. Rheological Behavior

The rheological properties of the sodium hydrogel containing 2% ketorolac tromethamine were determined by a rotational Haake RheoStress 1 rheometer (Thermo Fisher Scientific, Karlsruhe, Germany) equipped with cone-plate geometry (Haake C60/2°

Ti, 60 mm diameter, 0.105 mm gap between cone-plate). Measurements were performed in duplicate at 32 °C (Thermo Haake Phoenix II + Haake C25P), the program consisted of a 3 steps shear profile: (1) a ramp-up period from 0 to 100 s^{-1} during 3 min, (2) followed by a constant shear rate period at 100 s^{-1} for 1 min, and (3) the ramp-down period from 100 to 0 s^{-1} for 3 min. Steady-state viscosity, determined at $t_{0,}$ at 32 °C, was also calculated from the constant shear stretch at 100 s^{-1}.

The flow data obtained were fitted to different mathematical models (Table 4) to describe the flow curve and characterize the flow properties:

Table 4. Mathematical models for the flow characterization by regression analysis.

Flow Curve—Models: τ=*f*($\dot{\gamma}$)	
Newton	$\tau = \eta \cdot \dot{\gamma}$
Bingham	$\tau = \tau_0 + (\eta_0 \cdot \dot{\gamma})$
Ostwald–de Waele	$\tau = K \cdot \dot{\gamma}^n$
Herschel–Bulkley	$\tau = \tau_0 + K \cdot \dot{\gamma}^n$
Casson	$\tau = \sqrt[n]{\left(\tau_0^n + (\eta_0 \cdot \dot{\gamma})^n\right)}$
Cross	$\tau = \dot{\gamma} \cdot (\eta_\infty + (\eta_0 - \eta_\infty)/(1 + (\dot{\gamma}/\dot{\gamma}_0)^n)$

where, τ is the shear stress (Pa), η is the dynamic viscosity (mPa·s), $\dot{\gamma}$ is the shear rate (1/s), τ_0 is the yield shear stress (Pa), η_0 is the zero-shear rate viscosity, η_p is a constant plastic viscosity (mPa·s), η_∞ is the infinity shear rate viscosity, n is the flow index, and K is the consistency index. The goodness of fit was determined by correlation coefficient (r) by linear regression analysis of the flow plots.

4.4. In Vitro Release of Ketorolac from the Hydrogel

The in vitro release assay was conducted using amber glass Franz diffusion cells (Franz Diffusion cells (FDC 400, Crown Glass, Somerville, NY, USA) with an active diffusion area of 1.77 cm^2 (n = 6). The receptor fluid consisted of 0.06M PBS (pH 7.4), which was continuously stirred with magnetic beads at 500 rpm to keep the contents of the receptor compartment homogeneous throughout the tests. The system was thermostatted at 37 ± 0.5 °C by a circulating water jacket. Sink conditions were held throughout the experiments, and 310 mg ± 10 mg of KT hydrogel was accurately applied to the membranes (mixed ester cellulose 0.45 µm pore size) in the donor compartment. Air bubbles entrapped below the membranes were removed, and the system was allowed to equilibrate for at least 30 min before applying the hydrogel. Parafilm was used to avoid evaporation by sealing the donor compartment and the sampling ports. Samples (300 µL) were collected at specific time intervals for about 20 h (1, 2, 4, 5.5, and 19.75 h), and the same volume was immediately replaced with PBS after the removal of each sample. The ketorolac was determined by High Performance Liquid Chromatography (HPLC) following the norms of a validated method, and the experimental data were fitted to different mathematical models (Zero-order, First-order, and Higuchi) (See Appendix A, Mathematical models fitted to drug release experiments). The best fitting model was chosen according to the correlation coefficient (r^2) value.

4.5. Ex Vivo Permeation of Ketorolac through Human Skin and Vaginal Mucosa

The penetration and permeation of Ketorolac into and through the skin was evaluated by infinite dose and by finite dose approaches. The former provided information about the kinetics and permeation parameters (Sections 4.5.1–4.5.3), and the finite dose setup provided information about the distribution of Ketorolac within the skin, in its different layers with a realistic application approach (Section 4.6).

4.5.1. Infinite Dose Approach Ex Vivo Permeation Assay in Human Skin

To study the rate and extend of Ketorolac that diffused through the skin, an ex vivo permeation assay was performed. The experiment was conducted as designed for the release assay except that 500-µm dermatomed frozen skin was used instead of synthetic membrane ($n = 6$). The skin was thawed at room temperature, and skin discs were punched and mounted on the Franz cell (0.64 cm^2 of diffusion area) with the Stratum Corneum facing up to the donor compartment and the dermis in contact with the receptor fluid [35]. Hydrogel (200 mg) was applied to the skin, and samples (300 µL) were collected at the time intervals: 0, 3, 6, 8, 10, 19.75, 20.75, and 24 h and stored at −20 °C until sample analysis by HPLC was carried out.

4.5.2. Infinite Dose Approach Ex Vivo Permeation Assay in Porcine Vaginal Mucosa

The ex vivo permeation test with full-thickness porcine vaginal mucosa aimed at investigating the capacity of ketorolac to diffuse through the vaginal tissue. It was conducted in the same manner as in Section 4.5.1, adjusting the sampling times to: 1, 2, 3, 4, 5, and 5.7 h. Samples were stored and analyzed by HPLC.

Results from the permeations assays fitted to a zero-order kinetic model, by means of a linear least squares regression, and the permeation parameters were calculated according to the equations described in Appendix A (Permeation parameters and calculation of the Css upon application of KT hydrogel).

4.5.3. Amount of Ketorolac Retained in the Skin and in the Vaginal Mucosa

At the end of the permeation assays, the residual hydrogel on the skin or mucosa was removed by a swab, and the tissues were taken out of the Franz cells, cleaned with a gauze soaked in 0.05% solution of sodium lauryl sulfate and rinsed 3 times with distilled water. The permeation area of the skin/vaginal mucosa was then cut and weighed and perforated by a thin needle and incubated with 1 mL of methanol: water (1:1) to extract the Ketorolac remaining in the tissues. The mixtures were sonicated for 20 min., and the supernatants were pipetted and analyzed by the HPLC method, yielding the amount of ketorolac retained in the tissues.

4.6. Distibution of Ketorolac within the Skin Layers

The distribution of Ketorolac within the skin layers was assessed by ex vivo permeation assays in finite dose approach using human skin dermatomed at 500 µm. Skin discs were placed on thermostated (32 °C) Franz static diffusion cells (3 mL, 1.86 cm^2 of exposed area, Lara-Spiral, Courtenon, France). The sink conditions were guaranteed throughout the assay by adding bovine serum albumin 1% (w/v) in the receptor fluid, which was PBS at pH 7.6, gentamicin sulphate 0.04% (w/v) was also added to prevent skin degradation [9]. The receptor fluid was under magnetic stirring throughout the assay. A volume of 10 µL of hydrogel was applied to the skin. Control cells were also used with placebo hydrogel to evaluate any potential interferences in the sample analysis of the receptor fluid samples or skin samples. After 24 h of exposition, the skin discs were demounted from the Franz cells and the residual hydrogel (either with or without Ketorolac) remaining on the skin surface was recovered. The receptor fluid was recovered, and the *stratum corneum* was isolated by the tape-stripping technique. Twelve strips were carried out to remove most of the *Stratum corneum*. The epidermis was separated from the dermis by heat treatment [9]. The skin samples were incubated in water:methanol (1:1, v/v) and sonicated for 20 min to extract the Ketorolac. The extraction solvent volume was 10 mL for the skin surface, 2 mL for the *Stratum corneum* and Epidermis, and 1 mL for the Dermis. The supernatants were pipetted and analyzed by the HPLC method. The amounts of ketorolac in each compartment are expressed as µg/cm^2 and % of the applied dose.

4.5.1. Infinite Dose Approach Ex Vivo Permeation Assay in Human Skin

To study the rate and extend of Ketorolac that diffused through the skin, an ex vivo permeation assay was performed. The experiment was conducted as designed for the release assay except that 500-µm dermatomed frozen skin was used instead of synthetic membrane ($n = 6$). The skin was thawed at room temperature, and skin discs were punched and mounted on the Franz cell (0.64 cm^2 of diffusion area) with the Stratum Corneum facing up to the donor compartment and the dermis in contact with the receptor fluid [35]. Hydrogel (200 mg) was applied to the skin, and samples (300 µL) were collected at the time intervals: 0, 3, 6, 8, 10, 19.75, 20.75, and 24 h and stored at −20 °C until sample analysis by HPLC was carried out.

4.5.2. Infinite Dose Approach Ex Vivo Permeation Assay in Porcine Vaginal Mucosa

The ex vivo permeation test with full-thickness porcine vaginal mucosa aimed at investigating the capacity of ketorolac to diffuse through the vaginal tissue. It was conducted in the same manner as in Section 4.5.1, adjusting the sampling times to: 1, 2, 3, 4, 5, and 5.7 h. Samples were stored and analyzed by HPLC.

Results from the permeations assays fitted to a zero-order kinetic model, by means of a linear least squares regression, and the permeation parameters were calculated according to the equations described in Appendix A (Permeation parameters and calculation of the Css upon application of KT hydrogel).

4.5.3. Amount of Ketorolac Retained in the Skin and in the Vaginal Mucosa

At the end of the permeation assays, the residual hydrogel on the skin or mucosa was removed by a swab, and the tissues were taken out of the Franz cells, cleaned with a gauze soaked in 0.05% solution of sodium lauryl sulfate and rinsed 3 times with distilled water. The permeation area of the skin/vaginal mucosa was then cut and weighed and perforated by a thin needle and incubated with 1 mL of methanol: water (1:1) to extract the Ketorolac remaining in the tissues. The mixtures were sonicated for 20 min., and the supernatants were pipetted and analyzed by the HPLC method, yielding the amount of ketorolac retained in the tissues.

4.6. Distibution of Ketorolac within the Skin Layers

The distribution of Ketorolac within the skin layers was assessed by ex vivo permeation assays in finite dose approach using human skin dermatomed at 500 µm. Skin discs were placed on thermostated (32 °C) Franz static diffusion cells (3 mL, 1.86 cm^2 of exposed area, Lara-Spiral, Courtenon, France). The sink conditions were guaranteed throughout the assay by adding bovine serum albumin 1% (w/v) in the receptor fluid, which was PBS at pH 7.6, gentamicin sulphate 0.04% (w/v) was also added to prevent skin degradation [9]. The receptor fluid was under magnetic stirring throughout the assay. A volume of 10 µL of hydrogel was applied to the skin. Control cells were also used with placebo hydrogel to evaluate any potential interferences in the sample analysis of the receptor fluid samples or skin samples. After 24 h of exposition, the skin discs were demounted from the Franz cells and the residual hydrogel (either with or without Ketorolac) remaining on the skin surface was recovered. The receptor fluid was recovered, and the *stratum corneum* was isolated by the tape-stripping technique. Twelve strips were carried out to remove most of the *Stratum corneum*. The epidermis was separated from the dermis by heat treatment [9]. The skin samples were incubated in water:methanol (1:1, v/v) and sonicated for 20 min to extract the Ketorolac. The extraction solvent volume was 10 mL for the skin surface, 2 mL for the *Stratum corneum* and Epidermis, and 1 mL for the Dermis. The supernatants were pipetted and analyzed by the HPLC method. The amounts of ketorolac in each compartment are expressed as µg/cm^2 and % of the applied dose.

4.7. Analysis of Ketorolac in Solution

The samples generated in the in vitro release and in vitro permeation studies were analyzed by a validated HPLC method. The chromatographic conditions were the following: the mobile phase consisted of acetonitrile (+0.065% triethylamine) and purified water (+0.165% acetic glacial acid), in an isocratic elution (1:1) at flux 1 mL/min. The column used was Symmetry C18 75 mm × 4.6 mm and 3.5 µm. The volume injected was 10 µL, and Ketorolac was determined at the wavelength of 314 nm.

4.8. In Vivo Anti-Inflammatory Efficacy Evaluation

The anti-inflammatory efficacy of the hydrogel was evaluated in accordance with the methodology described by Mallandrich et al. [9], which consisted of inducing an ear oedema inflammation on mice by 12-O-detradecanoylphorbol-13-acetate TPA. Swelling is caused by fluid accumulation in the interstitial tissue after vasodilation; this greater fluid retention, in turn, increases the weight of the ear, and it is correlated with the inflammatory/anti-inflammatory response.

Briefly, a TPA solution was prepared in ethanol at 0.05%. The animals were divided in 3 groups (n = 6), which were processed in parallel: group 1, KT hydrogel; group 2, 2% solution ketorolac tromethamine in water; and finally, group 3, hydrogel without drug. In all groups, acute skin edema was induced upon application of 5 µL TPA in the mice's left ears, which served as 100% inflammation control. An equivalent volume of TPA was applied to the right ear of the animals and subsequently, 100 mg of formulation (KT hydrogel, ketorolac solution or placebo hydrogel, depending on the group) was also applied to the mice's right ear as treatment.

At 4 h post-application, the animals were slaughtered, and 7-mm circular sections were cut from both ears and weighed to determine the anti-inflammatory activity. The inhibition of inflammation achieved by the KT hydrogel as well as by the ketorolac tromethamine solution or the hydrogel without drug was calculated according to the Equation (3):

$$Inhibition\ (\%) = \left(\frac{Weight\ control\ ear\ -\ Weight\ treated\ ear}{Weight\ control\ ear} \right) \times 100 \quad (3)$$

4.9. In Vivo Tolerance Study

Variations in the skins biomechanical properties were evaluated after the hydrogel application compared to the basal conditions. The parameters assessed were the Transepidermal water loss (TEWL–Dermalab), and the *Stratum corneum* hydration (SCH–Corneometer Courrage CM825). To this end, healthy subjects participated as volunteers in this study with prior approval of the Study Protocol by the Ethics Committee University of Barcelona (IRB00003099; approved on 20/03/2018). Six women—aged between 21 and 64—who gave their informed consent were asked to abstain from the application of cosmetics 6 h prior to the test. They had a 20 min adaption period to acclimate themselves to the room conditions before each measurement. Prior to the hydrogel application, the site of application was marked by a template, and the basal values of TEWL and SCH were recorded for the test areas. Then, the hydrogel was applied homogenously as a thin layer to each volunteer's left forearm. The following readings were performed at different time points for about 4 h (15, 45, 105, 165, 225, and 255 min).

4.10. Statistical Analysis

The cumulative amounts of the drug released and permeated over time were determined using linear regression analysis. The influence of the KT hydrogel on the TEWL and hydration of the skin was analyzed by one-way analysis of variance (ANOVA) at the time points. The significance level was set to 0.05.

GraphPad Prism®, v. 5.00 software (San Diego, CA, USA) was used for all statistical calculations.

Author Contributions: Conceptualization, A.C.C.; methodology, A.C.C., F.F.-C.; software, D.L. and M.M.; validation, C.A., A.C.C., and M.M.; formal analysis, A.C.C., F.F.-C., D.L. and M.M.; investigation, S.E.M. and C.A.; resources, A.C.C., M.L.G.-R., and L.H.; data curation, D.L. and F.F.-C.; writing—original draft preparation, D.L.; writing—review and editing, D.L., A.C.C., F.F.-C., and M.M.; visualization, D.L.; supervision, F.F.-C. and M.M.; project administration, F.F.-C. and M.M.; funding acquisition, A.C.C. All authors have read and agreed to the published version of the manuscript.

Funding: This research received no external funding.

Institutional Review Board Statement: The study was conducted according to the guidelines of the Declaration of Helsinki, and approved by the Bioethics Committee of the Barcelona-SCIAS Hospital (protocol code Nº001 and date of approval 20/01/2016); the Academic Ethics Committee of the Vivarium at the Universidad Autónoma del Estado de Morelos (protocol code BIO-UAEM:012:2013 and date of approval 21/12/2015); and the Ethics Committee University of Barcelona (protocol code IRB00003099 and date of approval 20/03/2018).

Informed Consent Statement: Informed consent was obtained from all subjects involved in the study.

Data Availability Statement: The data presented in this study are available on request from the corresponding author. The data are not publicly available due to they take part in a Doctoral Thesis, and they will be available once the Thesis will be published.

Acknowledgments: The authors would like to thank Alvaro Gimeno from the Bellvitge Animal Facility Services for providing the porcine mucosa; we also thank Harry Paul for the English editing services.

Conflicts of Interest: The authors declare no conflict of interest.

Abbreviations

°C	Degree Celsius
µL	Microliter
µm	Micrometer
ANOVA	One-way analysis of variance
AP	Amount ok ketorolac permeated
AR	Amount ok ketorolac retained
C_0	Initial concentration
CA	California
CA	Condyloma acuminata
Clp	Human plasma clearance
cm	Centimeter
cm^2	Square centimeters
CO_2	Carbon dioxide
Css	Plasma concentration at steady state
Da	Dalton
g	Gram
h	Hour
HPLC	High Performance Liquid Chromatography
HPV	Human Papilloma Virus
J	Flux
Jss	Flux at steady state
K	Release rate constant
Kg	Kilogram
KH_2PO_4	Potassium dihydrogen phosphate
Kp	Permeability coefficient
KT	Ketorolac tromethamine

Appendix A

Appendix A.1. Mathematical Models Fitted to Drug Release Experiments

The amount of ketorolac released from the gels was fitted to the following model equations [36]:

Table A1. Equations of the kinetic models fitted.

Zero-order	$Rt = R\infty + Ko \times t$
First-order	$Rt = R\infty \times \left(1 - e^{k \times t}\right)$
Higuchi	$Rt = R\infty + Kh \times t^{1/2}$

where Rt is the amount of drug released at time t, $R\infty$ is the maximum amount of drug released, K is the release rate constant expressed in units of concentration/time, and n is the diffusion release exponent that can be used to characterize the different release mechanisms. It has been established that $n \leq 0.43$ (Fickian diffusion mechanism), $0.43 < n < 0.85$ (anomalous transport) and $n \geq 0.85$ (Super case II transport, i.e., zero, order release) [36].

The best fitting model was chosen according to the correlation coefficient (r^2) value (Table A1), for which drug release was determined to follow a First-order (one-phase exponential association) kinetics.

Table A2. Correlation factors of the fitted mathematical models.

	$\mathbf{R^2}$
Zero-order	0.4380
First-order	0.9908
Higuchi	0.6000

Appendix A.2. Permeation Parameters and Calculation of the Css upon Application of KT Hydrogel

The steady state plasma concentration (Css) was calculated assuming an area of application of 5 cm^2 according to the Equation (4):

$$\text{Css} = \frac{\text{J} \cdot \text{TSA}}{\text{Clp} \cdot \text{A}} \quad (4)$$

where Css is the steady state plasma concentration (Css), J (μg/h) is the flux, TSA (cm^2) is the theoretical surface area of application, Clp (mL/min) is the human plasma clearance of ketorolac, and A (cm^2) is the diffusion area of the Franz cells. An area of application of 5 cm^2 was assumed.

The permeability coefficient was calculated in accordance with the Equation (5).

$$\text{Kp} = \frac{\text{J}}{\text{C}_0} \quad (5)$$

where Kp is the permeability coefficient of ketorolac through the membranes; J (μg/h) is the flux, and C_0 (μg/mL) is the initial concentration of ketorolac in the gel.

References

1. *Asociación Española de Patología Cervical y Colposcopia Condilomas Acuminados*. 2015. Volume Noviembre. Publicaciones AEPCC. Madrid. Available online: http://www.aepcc.org/wp-content/uploads/2019/04/AEPCC_guiaCONDILOMAS-ACUMINADOS-ISBN.pdf (accessed on 1 November 2015).
2. Lacey, C.J.; Woodhall, S.; Wikstrom, A.; Ross, J. 2012 European guideline for the management of anogenital warts. *J. Eur. Acad. Dermatol. Venereol.* **2012**, *27*, e263–e270. [CrossRef]
3. *Centers for Disease Control and Prevention Sexually Transmitted Diseases Treatment Guidelines*; Department of Health and Human Services: Atlanta, GA, USA, 2015; Volume 64.

4. Martínez, G.G.; Troconis, J.N. Tratamiento de las verrugas genitales: Una actualización. *Rev. Chil. Obstet. Ginecol.* **2015**, *80*, 76–83. [CrossRef]
5. Bouscarat, F.; Pelletier, F.; Fouéré, S.; Janier, M.; Bertolloti, A.; Aubin, F. Verrues génitales (condylomes) externes. *Annales Dermatologie Vénéréologie* **2016**, *143*, 741–745. [CrossRef]
6. Scheinfeld, N.; Lehman, D.S. An evidence-based review of medical and surgical treatments of genital warts. *Dermatol. Online J.* **2006**, *12*, 5.
7. Karnes, J.B.; Usatine, R.P. Management of external genital warts. *Am. Fam. Physician* **2014**, *90*, 90.
8. Muñoz-Santos, C.; Pigem, R.; Alsina, M. Nuevos tratamientos en la infección por virus del papiloma humano. *Actas Dermo-Sifiliográficas* **2013**, *104*, 883–889. [CrossRef]
9. Mallandrich, M.; Fernández-Campos, F.; Clares, B.; Halbaut, L.; Alonso, C.; Coderch, L.; Garduño-Ramírez, M.L.; Andrade, B.; Del Pozo, A.; Lane, M.E.; et al. Developing Transdermal Applications of Ketorolac Tromethamine Entrapped in Stimuli Sensitive Block Copolymer Hydrogels. *Pharm. Res.* **2017**, *34*, 1728–1740. [CrossRef]
10. O'donovan, S.; Ferrara, A.; Larach, S.; Williamson, P. Intraoperative use of toradol® facilitates outpatient hemorrhoidectomy. *Dis. Colon Rectum* **1994**, *37*, 793–799. [CrossRef]
11. Coloma, M.; White, P.F.; Huber, P.J.; Tongier, W.K.; Dullye, K.K.; Duffy, L.L. The Effect of Ketorolac on Recovery After Anorectal Surgery: Intravenous Versus Local Administration. *Anesthesia Analg.* **2000**, *90*, 1107–1110. [CrossRef]
12. De Oliveira, G.S.; Agarwal, D.; Benzon, H.T. Perioperative Single Dose Ketorolac to Prevent Postoperative Pain: A meta-analysis of randomized trials. *Anesth. Analg.* **2012**, *114*, 424–433. [CrossRef]
13. McCormack, P.L. Ketorolac 0.45% Ophthalmic Solution. *Drugs Aging* **2011**, *28*, 583–589. [CrossRef]
14. Katsev, D.A.; Katsev, C.C.; Pinnow, J.; Lockhart, C.M. Intracameral ketorolac concentration at the beginning and end of cataract surgery following preoperative topical ketorolac administration. *Clin. Ophthalmol.* **2017**, *11*, 1897–1901. [CrossRef]
15. Kim, S.K.; Hong, J.P.; Nam, S.M.; Stulting, R.D.; Seo, K.Y. Analgesic effect of preoperative topical nonsteroidal antiinflammatory drugs on postoperative pain after laser-assisted subepithelial keratectomy. *J. Cataract. Refract. Surg.* **2015**, *41*, 749–755. [CrossRef]
16. Gorshkova, M.Y.; Volkova, I.F.; Vanchugova, L.V.; Valuev, I.L.; Valuev, L.I. Sodium Alginate Based Mucoadhesive Hydrogels. *Appl. Biochem. Microbiol.* **2019**, *55*, 371–374. [CrossRef]
17. Formulaction Turbiscan LAB: Stability Analysis of Emulsions, Suspensions and Foams—Formulation Stability—Particle Size Analysis Methods. Available online: http://www.formulaction.com/stability-turbiscan-lab.html (accessed on 3 November 2014).
18. Celia, C.; Trapasso, E.; Cosco, D.; Paolino, D.; Fresta, M. Turbiscan Lab® Expert analysis of the stability of ethosomes® and ultradeformable liposomes containing a bilayer fluidizing agent. *Colloids Surf. B Biointerfaces* **2009**, *72*, 155–160. [CrossRef]
19. Sathyanarayanan, G.; Rodrigues, M.; Limón, D.; Rodriguez-Trujillo, R.; Puigmartí-Luis, J.; Pérez-García, L.; Amabilino, D.B. Drug-Loaded Supramolecular Gels Prepared in a Microfluidic Platform: Distinctive Rheology and Delivery through Controlled Far-from-Equilibrium Mixing. *ACS Omega* **2017**, *2*, 8849–8858. [CrossRef]
20. Limón, D.; Domínguez, K.T.; Garduño-Ramírez, M.L.; Andrade, B.; Calpena, A.C.; Pérez-García, L. Nanostructured supramolecular hydrogels: Towards the topical treatment of Psoriasis and other skin diseases. *Colloids Surf. B Biointerfaces* **2019**, *181*, 657–670. [CrossRef]
21. Limón, D.; Jiménez-Newman, C.; Calpena, A.C.; González-Campo, A.; Amabilino, D.B.; Pérez-García, L. Microscale coiling in bis-imidazolium supramolecular hydrogel fibres induced by the release of a cationic serine protease inhibitor. *Chem. Commun.* **2017**, *53*, 4509–4512. [CrossRef]
22. Lau, W.M.; Ng, K.W. Finite and Infinite Dosing. In *Percutaneous Penetration Enhancers Drug Penetration Into/Through the Skin*; Springer: Berlin/Heidelberg, Germany, 2017; Volume 37, pp. 35–44.
23. Lipinski, C.A.; Lombardo, F.; Dominy, B.W.; Feeney, P.J. Experimental and computational approaches to estimate solubility and permeability in drug discovery and development settings. *Adv. Drug Deliv. Rev.* **2012**, *64*, 4–17. [CrossRef]
24. Ghose, A.K.; Viswanadhan, V.N.; Wendoloski, J.J. A Knowledge-Based Approach in Designing Combinatorial or Medicinal Chemistry Libraries for Drug Discovery. 1. A Qualitative and Quantitative Characterization of Known Drug Databases. *J. Comb. Chem.* **1999**, *1*, 55–68. [CrossRef]
25. PubChem Database Ketorolac | C15H13NO3—PubChem. Available online: https://pubchem.ncbi.nlm.nih.gov/compound/3826 (accessed on 19 December 2020).
26. PubChem Database Ketorolac Tromethamine | C19H24N2O6—PubChem. Available online: https://pubchem.ncbi.nlm.nih.gov/compound/Ketorolac-tromethamine (accessed on 19 December 2020).
27. *TORADOL (Ketorolac Tromethamine Tablets)*; Roche Laboratories Inc.: Branchburg, NJ, USA, 2008; pp. 1–27.
28. Cordero, J.A.; Alarcón, L.; Escribano, E.; Obach, R.; Doménech, J. A Comparative Study of the Transdermal Penetration of a Series of Nonsteroidal Antiinflammatory Drugs. *J. Pharm. Sci.* **1997**, *86*, 503–508. [CrossRef]
29. Raney, S.G.; Hope, M.J. The effect of bilayer and hexagonal HII phase lipid films on transepidermal water loss. *Exp. Dermatol.* **2006**, *15*, 493–500. [CrossRef]
30. Constantin, M.-M.; Poenaru, E.; Poenaru, C.; Constantin, T. Skin Hydration Assessment through Modern Non-Invasive Bioengineering Technologies. *Maedica* **2014**, *9*, 33–38.
31. Halkier-Sorensen, L.; Thestrup-Pedersen, K.; Maibach, H.I. Equation for conversion of transepidermal water loss (TEWL) to a common reference temperature: What is the slope? *Contact Dermat.* **1993**, *29*, 280–281. [CrossRef]

32. Yosipovitch, G.; Xiong, G.L.; Haus, E.; Sackett-Lundeen, L.; Ashkenazi, I.; Maibach, H.I. Time-Dependent Variations of the Skin Barrier Function in Humans: Transepidermal Water Loss, Stratum Corneum Hydration, Skin Surface pH, and Skin Temperature. *J. Investig. Dermatol.* **1998**, *110*, 20–23. [CrossRef]
33. Flo, A.; Díez-Noguera, A.; Calpena, A.C.; Cambras, T. Circadian rhythms on skin function of hairless rats: Light and thermic influences. *Exp. Dermatol.* **2014**, *23*, 214–216. [CrossRef]
34. Limon, D.; Amirthalingam, E.; Rodrigues, M.; Halbaut, L.; Andrade, B.; Garduño-Ramírez, M.L.; Amabilino, D.B.; Pérez-García, L.; Calpena, A.C. Novel nanostructured supramolecular hydrogels for the topical delivery of anionic drugs. *Eur. J. Pharm. Biopharm.* **2015**, *96*, 421–436. [CrossRef]
35. Limón, D.; Jiménez-Newman, C.; Rodrigues, M.I.A.; González-Campo, A.; Amabilino, D.B.; Calpena, A.C.; Pérez-García, L. Cationic Supramolecular Hydrogels for Overcoming the Skin Barrier in Drug Delivery. *ChemistryOpen* **2017**, *6*, 585–598. [CrossRef]
36. Costa, P.; Lobo, J.M.S. Modeling and comparison of dissolution profiles. *Eur. J. Pharm. Sci.* **2001**, *13*, 123–133. [CrossRef]

3.2.- Artículo 2

International Journal of
Molecular Sciences

MDPI

Article

HPV Lesions and Other Issues in the Oral Cavity Treatment and Removal without Pain

Salima El Moussaoui [1], Mireia Mallandrich [1,2,*], Núria Garrós [1], Ana Cristina Calpena [1,2], Maria José Rodríguez Lagunas [3] and Francisco Fernández-Campos [4]

1 Departament de Farmàcia, Tecnologia Farmacèutica i Fisicoquímica, Faculty of Pharmacy and Food Sciences, University of Barcelona, Av. Joan XXIII 27-31, 08028 Barcelona, Spain; selmouel9@alumnes.ub.edu (S.E.M.); nuriagarros98@gmail.com (N.G.); anacalpena@ub.edu (A.C.C.)
2 Institut de Nanociència i Nanotecnologia IN2UB, Universitat de Barcelona, 08028 Barcelona, Spain
3 Departament de Bioquímica i Fisiologia, Faculty of Pharmacy and Food Sciences, University of Barcelona, Av. Joan XXIII 27-31, 08028 Barcelona, Spain; mjrodriguez@ub.edu
4 Reig-Jofre Laboratories, Av. de les Flors s/n, 08970 Sant Joan Despí, Spain; ffernandez@reigjofre.com
* Correspondence: mireia.mallandrich@ub.edu; Tel.: +34-93-4024-560

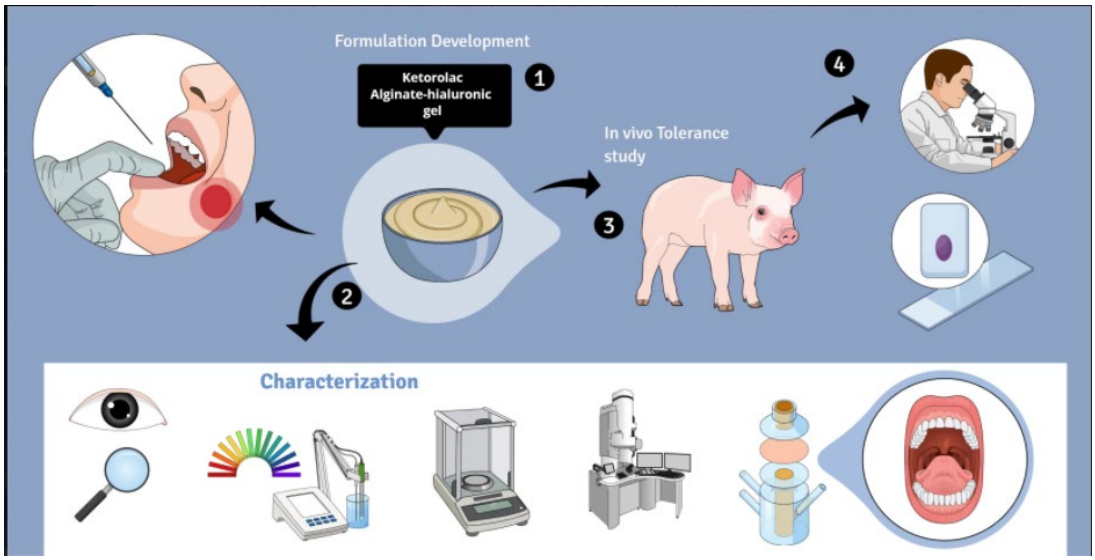

Current Impact Factor	JCR category rank
5.924	Q1 Biochemistry & Molecular Biology

Resumen

Para este artículo se ha desarrollado un hidrogel a base de alginato de sodio y ácido hialurónico que contiene un 2% de ketorolaco trometamina. La indicación sugerida es el tratamiento y manejo del dolor e inflamación asociados a procesos quirúrgicos sobre mucosas de la cavidad oral. Dicho hidrogel se caracterizó física, mecánica y morfológicamente. Los resultados reológicos sugieren que la formulación se puede aplicar fácil y suavemente. Los estudios de permeación ex vivo muestran que el KT es capaz de penetrar a través de las mucosas bucal y sublingual, además de ser retenido en la estructura de estas. Mediante una prueba in vitro pudimos evaluar el papel que juega la saliva en la biodisponibilidad del fármaco, observando que más de la mitad de la dosis aplicada se elimina en una hora por acción de la misma. Los estudios histológicos y citotóxicos realizados en cerdos in vivo mostraron el excelente perfil de seguridad de la formulación, así como su alta tolerabilidad. Paralelamente se evaluó una membrana artificial biomimética (PermeaPad®) que mostró un alto grado de correlación con la mucosa oral y sublingual.

International Journal of
Molecular Sciences

MDPI

Article

HPV Lesions and Other Issues in the Oral Cavity Treatment and Removal without Pain

Salima El Moussaoui [1], Mireia Mallandrich [1,2,*], Núria Garrós [1], Ana Cristina Calpena [1,2], Maria José Rodríguez Lagunas [3] and Francisco Fernández-Campos [4]

1 Departament de Farmàcia, Tecnologia Farmacèutica i Fisicoquímica, Faculty of Pharmacy and Food Sciences, University of Barcelona, Av. Joan XXIII 27-31, 08028 Barcelona, Spain; selmouel9@alumnes.ub.edu (S.E.M.); nuriagarros98@gmail.com (N.G.); anacalpena@ub.edu (A.C.C.)
2 Institut de Nanociència i Nanotecnologia IN2UB, Universitat de Barcelona, 08028 Barcelona, Spain
3 Departament de Bioquímica i Fisiologia, Faculty of Pharmacy and Food Sciences, University of Barcelona, Av. Joan XXIII 27-31, 08028 Barcelona, Spain; mjrodriguez@ub.edu
4 Reig-Jofre Laboratories, Av. de les Flors s/n, 08970 Sant Joan Despí, Spain; ffernandez@reigjofre.com
* Correspondence: mireia.mallandrich@ub.edu; Tel.: +34-93-4024-560

Abstract: Due to different oral and dental conditions, oral mucosa lesions such as those caused by the human papilloma virus and temporomandibular joint pathologies often have to be treated by surgical, ablative or extractive procedures. The treatment and control of pain and inflammation during these procedures is essential to guarantee the patient's well-being. For the foregoing reason, a hydrogel based on sodium alginate and hyaluronic acid containing 2% of ketorolac tromethamine has been developed. We characterized it physically, mechanically and morphologically. The rheological results suggest that the formulation can be easily and gently applied. Ex vivo permeation studies show that Ketorolac Tromethamine is able to penetrate through the buccal and sublingual mucosae, in addition to being retained in the mucosae's structure. Through an in vitro test, we were able to evaluate the role that saliva plays in the bioavailability of the drug, observing that more than half of the applied dose is eliminated in an hour. The histological and cytotoxic studies performed on pigs in vivo showed the excellent safety profile of the formulation, as well as its high tolerability. In parallel, a biomimetic artificial membrane (PermeaPad®) was evaluated, and it showed a high degree of correlation with the oral and sublingual mucosa.

Keywords: oral condyloma; Human Papilloma Virus; Ketorolac; pain; inflammation; sodium alginate; hyaluronic acid

Citation: El Moussaoui, S.; Mallandrich, M.; Garrós, N.; Calpena, A.C.; Rodríguez Lagunas, M.J.; Fernández-Campos, F. HPV Lesions and Other Issues in the Oral Cavity Treatment and Removal without Pain. *Int. J. Mol. Sci.* **2021**, *22*, 11158. https://doi.org/10.3390/ijms222011158

Academic Editor: Philip W. Wertz

Received: 10 September 2021
Accepted: 9 October 2021
Published: 16 October 2021

1. Introduction

Various lesions in the oral cavity have been related to the Human Papilloma Virus (HPV) infection: verruca vulgaris (VV), squamous cell papilloma (SP), condyloma acuminatum (CA), and multifocal epithelial hyperplasia (MFEH) [1]. All of them are a benign hyperplastic exophytic proliferation of the oral epithelium [2], caused by different HPV genotypes. Subtypes 6 and 11, with a low-oncogenic risk, are the most commonly found and cause CA in both the oral cavity [2] and in the anogenital region [3]. Labial mucosa, soft palate and lingual frenum are the most common locations of CA [4] and koilocytes can be observed in histopathologic sections [5]. All HPV-related oral lesions present clinical similarities, and therefore, a biopsy is necessary for a precise diagnosis.

Although CA is considered a benign lesion, clinical infections with the high-risk genotypes 16 and 18 have been found to cause oral and genital CA and have been associated with malignant lesions [6]. Spontaneous remission of oral CA is possible [5], but if this is not the case, there are different treatments to eliminate it. Surgical therapy seems to be the preferred treatment over Trichloroacetic acid (TCA), cryotherapy, and CO_2 laser because these methods often induce artifactual changes that compromise the diagnostic capabilities

of the pathologist [1]. Surgical or ablation treatments have the advantage in that the lesion (s) are removed in a single session and, typically, are quick interventions. However, they are procedures that generally require anesthesia and the control of pain and inflammation. The possibility of recurrences should not be ruled out. In addition to lesions caused by HPV, there are a variety of conditions and diseases of the oral cavity requiring surgical, ablative, or extractive interventions that involve mild to severe pain and inflammation, such as certain tumors of the oral mucosa, temporomandibular joint pathologies, facial trauma, and which could require dental interventions, etc. Pain management in minor surgical and ablative treatments does not always attract the attention it deserves, even though it is crucial for patient satisfaction in that they feel well and are mightily encouraged to follow treatment adherence. Surgery and ablative techniques usually require prior local anesthesia, and the postoperative pain and inflammation should also be controlled. For pain management of these processes, analgesics, anesthetics, and anti-inflammatory drugs can be combined in various regimens.

Ketorolac is a non-steroidal anti-inflammatory drug (NSAID) with a potent analgesic effect and a moderate anti-inflammatory action. It is indicated to treat moderate to severe pain. The analgesic ketorolac potency has been equated to that of several opioids [7] without presenting the problems associated with these drugs, such as tolerance or sedation [8]. Its use both pre [9] and postoperatively [10] has been analyzed, showing successful results. Ketorolac is marketed as tromethamine salt and can be administered orally, intramuscularly, intravenously, and by nasal or ophthalmic processes. Several authors have studied the analgesic safety and efficacy of ketorolac tromethamine (KT) after its topical application in different mucoadhesive formulations on the oral mucosa [11,12]. The results were satisfactory and promising. Therefore, we are able to propose its use during the removal of oral condyloma.

Mucoadhesive topical formulations have advantages over the most common routes, such as a simple and painless application and a better bioavailability of the active ingredient, allowing formulations with lower doses and inducing fewer side effects [13]. However, when formulating drugs intended to be applied to the oral mucosa, certain aspects need to be considered and may limit the success of our formula. One of them is the biology and histology of the mucosa. The lining of the oral cavity includes the buccal (cheeks), sublingual, gingival, palatal, and labial mucosa. These are made up of closely compacted epithelial cells, which help fulfill the mucosa's primary function: to protect the underlying tissues from external agents and fluid loss [14]. The drug to be designed must be able to cross the mucosal barrier. There are different factors to consider, such as the tissue's permeability, the drug's molecular weight, the partition coefficient (octanol/water) log P, and all aspects that are related to the formulation: the release capacity of the drug from the vehicle to tissue, pH, and the formulation's biocompatibility with the target tissue.

In this work, we designed and formulated a 2% ketorolac tromethamine hydrogel composed of sodium alginate as a polymer to be applied to the buccal and sublingual mucosae to treat pain and inflammation before, during, and after surgical, ablative, or extractive procedures. In order to reduce damage to the mucous membranes, hyaluronic acid (HA) was incorporated into the formulation, taking advantage of its well-known and well-documented regenerative and moisturizing action, as well as its role in strengthening cell resistance to mechanical damage [15]. In addition, HA also has gelling properties, which are excellent for the type of formulation to be made. High and low molecular weight HA have been used. The low-molecular-weight HA can penetrate to slightly deeper layers and there it acts regeneratively, while the high-molecular-weight HA acts at a more superficial level. The physicochemical, mechanical, and morphological characteristics of the gel have been analyzed, and the biopharmaceutical properties were examined by ex vivo permeation tests and in vivo administration.

The results show that alginate-HA hydrogel with 2% KT is a promising formulation for combating pain and inflammation, the two common side effects of surgical, ablative, and extractive treatments of the oral cavity.

2. Results

2.1. Alginate Gel-Ketorolac Characterization

2.1.1. Appearance and pH Evaluation

The finished prepared hydrogel had a translucent light yellowish appearance, considerable consistency, and poor flowability. After allowing it to stand untouched for 24 h, no bubbles or undissolved suspended particles were seen. The pH was 7.2, which is within the normal intraoral pH range (6.8–7.8) [16].

2.1.2. Swelling and Degradation Studies

To determine KT hydrogel's capacity to incorporate solvent in the matrix, the swelling ratio (SR) was measured. The previously dehydrated KT hydrogel was immersed in PBS, and the weight gain was noted at predetermined time intervals.

As shown in Figure 1a, the KT hydrogel can incorporate up to 15 times its weight in 5 min, showing great hygroscopy. The increase in weight caused by incorporating water in the matrix follows a first kinetic order (one phase association) with a kinetic constant value Kd = 1.012 min^{-1}.

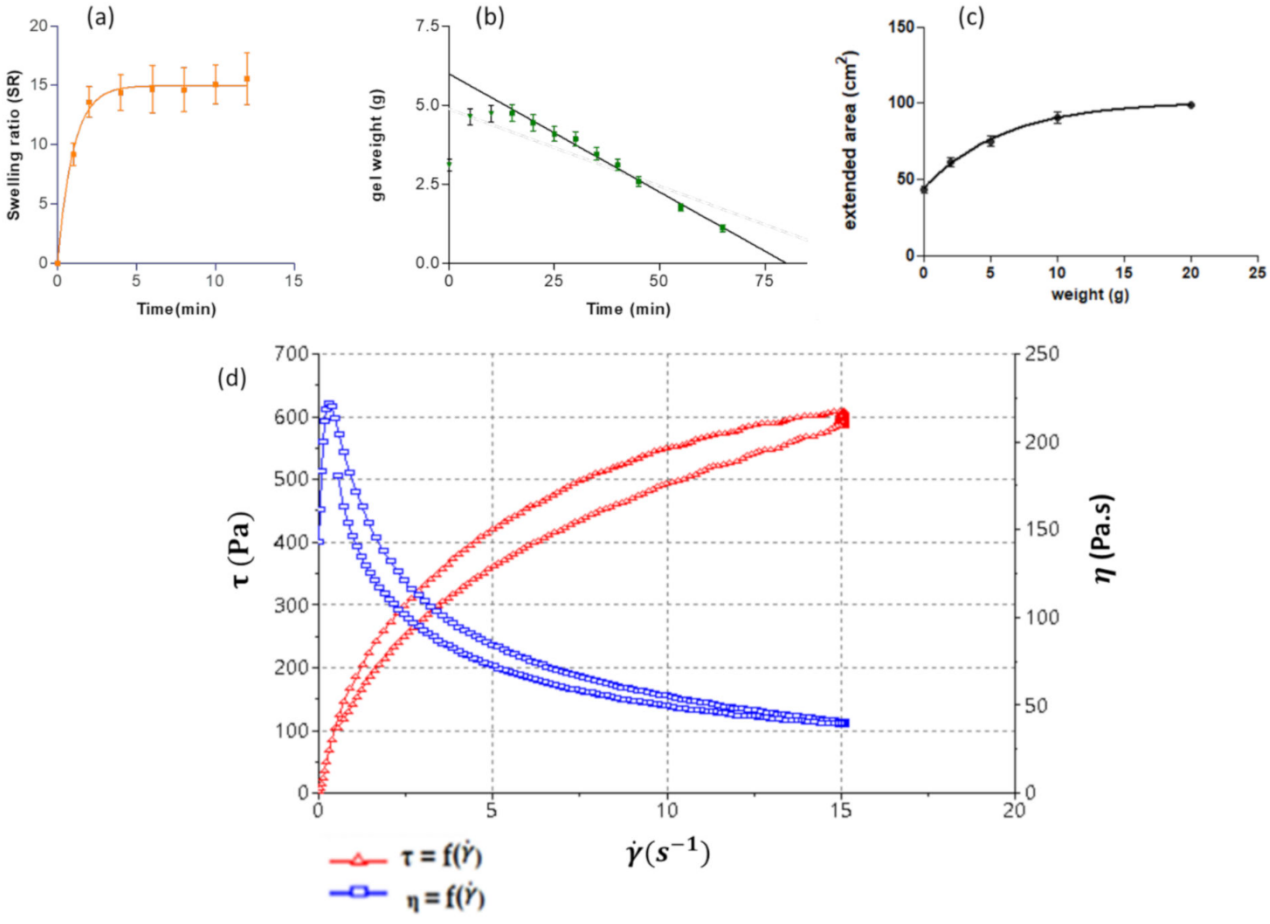

Figure 1. Characterization of the alginate-HA-gel KT 2%: (**a**,**b**) Modelling plots represented as variations in the hydrogel's weight over time: Swelling Ratio (SR) and degradation assay, respectively. (**c**) Extended area in cm^2 after applying 2, 5, 10, and 20 g of weight. Expressed as means ± standard deviation (n = 3). (**d**) Flow Curve of alginate-HA hydrogel KT 2%. The blue curve represents the formulation viscosity. The red curve represents the shear stress of the formulation.

The degradation kinetics was determined by immersing the fresh hydrogel in PBS and evaluating the weight changes. In the first minutes, the hydrogel's weight increases because the polymers are able to include more water in their structure, due to their hygroscopic nature, as previously described. The degradation begins to be appreciated from minute 20 (Figure 1b). The hydrogel degradation followed a zero-order kinetics, with a kinetic constant degradation value (Kd) of 0.075 min^{-1} (r^2 = 0.993). After about one hour, about 84% of the total hydrogel weight was degraded.

2.1.3. Extensibility

The extensibility was determined by observing the area over which the hydrogel extended after applying specific weights (0, 2, 5, 10, and 20 g). The results are shown in Figure 1c, where it is observed how the formulation extends to cover an area of 98.87 cm^2. The increase in extension was 51.61 cm^2. This increase followed a pseudo-first-order association with a constant value of 0.013 g^{-1}. These results show how the KT-hydrogel has good extensibility for the treatment's target condylomatous lesions.

2.1.4. Rheological Profile

To carry out an adequate characterization of semi-solid products, it is essential to evaluate rheological behavior. In the oscillatory study, a strain sweep of 0 to 500 Pa, at 1 Hz, was first performed to determine the linear viscoelastic zone. This said linearity was observed to be between 0.4 and 100 Pa. To perform the frequency sweep, which allows how the product behaves at low and high frequencies to be determined, the shear is set to a value within the linear viscoelastic zone, in our case 10 Pa. Initially, at low frequency, the viscous mode predominates up to the value of 0.8 Hz; from there, the elastic mode predominates. At 0.7902 Hz, the two modules G′ = G″ = 329.2 Pa (crossover point) are equalized.

Figure 1d shows the flow curves. It can be seen that the shear stress does not increase linearly with the shear rate, so it is concluded that the fluid is non Newtonian pseudoplastic. To confirm the rheological profile, the experimental data were fitted to different equations (Table A1).

The model that best fits is the Cross equation in both up and down curves, which usually explain the behavior of pseudoplastic material in a broad range of shear rates. Under certain assumptions, the Cross equation could be simplified to the power law equation [17]. This is the reason why in the ramp-down curve, the regression coefficient of the Cross equation is the same as the Herschel-Bulkley equation. In fact, in the ramp-up curve, the regression coefficient of Herschel-Bulkley exhibits a good fit, and considering that the Cross equation has four parameters, in contrast with the three parameters of the Herschel-Bulkley equation, the latter could be more appropriate to describe the flow behavior (avoiding an overparameterization) of the produced hydrogel. Nevertheless, both equations confirmed that the formulation exhibits a pseudoplastic flow (exponent $n < 1$) with yield stress around 150 Pa.s.

As shown in Figure 1d, the flow curve presents a hysteresis loop, which denoted a thixotropic behavior or a viscosity time-dependence, indicating that the microstructure of the gel is altered as it was sheared with a disturbance degree of Δa = 1582 Pa/s. The medium viscosity determined at 15 s^{-1} is 39.61 $\pm$ 0.44 Pa.s.

2.1.5. Morphological Study

To determine the hydrogel morphology, the formulation was analyzed by Scanning Electron Microscopy (SEM). In SEM, an electron beam with low energy is radiated onto the material and scans the sample's surface. It can be seen that the hydrogel has a very compact structure, and no pores are observed in its microstructure. In the 40.000× magnification (Figure 2), small cavities are seen, in which the KT in solution could be lodged.

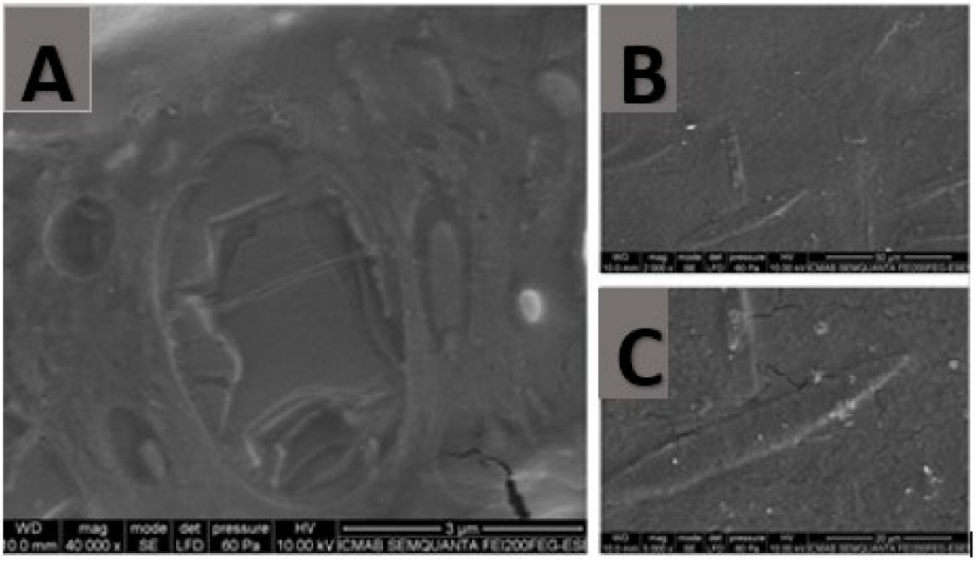

Figure 2. SEM images of sodium alginate and hyaluronic acid gel with 2% KT. (**A**) Magnification 40.000×, scale bar 3 µm; (**B**) magnification 2.000×, scale bar 50 µm; (**C**) magnification 5.000×, scale bar 20 µm.

2.2. In Vitro Release Assay on Membranes and Biomimetic Membranes

The hydrogel's ability to release the KT was evaluated using Franz-type cells according to the reported methodologies [18]. In a previous study, two synthetic membranes, nylon and polyethersulfone (PES), were evaluated to select the membrane that allows a greater release of a free drug solution (at the same KT concentration as the hydrogel). Nylon was discarded for presenting major resistance to the release of KT (data not shown). Thus, the in vitro release assay of the alginate-HA 2% KT was conducted with the PES membrane and the synthetic biomimetic membrane.

Figure 3a shows the release profile of KT from the hydrogel in the PES membrane and in a synthetic biomimetic membrane, called PermeaPad®, which is claimed to mimic the permeability behavior of oral mucosa [19]. The membrane is composed of two cellulose membranes, and there is one lipidic barrier between them.

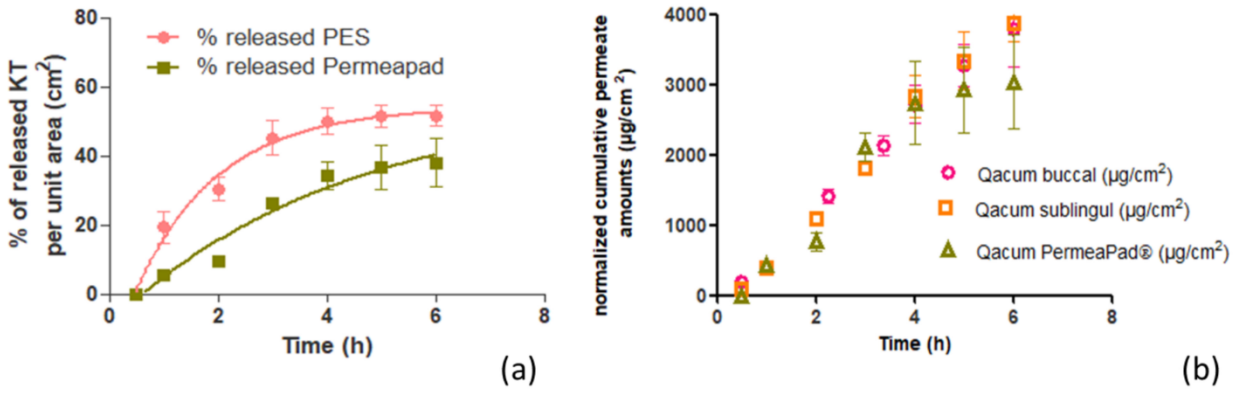

Figure 3. In vitro and ex vivo assays. (**a**) Representation of the percentage of released KT per unit area (cm^2) from the PES membrane (pink curve) and the PermeaPad® biomimetic membrane (green curve). (**b**) Cumulative amount of KT permeated ($\mu g/cm^2$) under an infinite dose regimen through buccal and sublingual mucosae and biomimetic membrane upon application of KT hydrogel. Values represent means ± SD (n = 3).

After the assay, the results show that the hydrogel can release up to 4.12 mg/cm^2 of KT through the PES membrane, corresponding to 51.6% of the total dose seeded (8.00 mg) per unit area, which was achieved within 6 h, showing a release rate of 0.66 h^{-1}. At the

same time, regarding the results obtained with the biomimetic membrane, 38.0% of KT was released through this membrane, which corresponds to a total amount of 3.04 mg/cm^2. This amount was achieved in 6 h with a release constant of 0.23 h^{-1}. The differences were statistically significant (p-value for t-test of 0.001).

The release curves were adjusted to different kinetics showing the best fit and correlation for first-order kinetics (see r^2 values in Table 1).

Table 1. Drug release parameters from KT hydrogel according to a first order kinetics. Values represent means ± standard error (n = 3).

Best-Fit Values	PES	PermeaPad®
Ymax (%/cm^2)	51.6 ± 3.2	38.0 ± 6.9
K (h^{-1})	0.66 ± 0.12	0.23 ± 0.14
$t^{1/2}$ (h)	1.05 ± 0.11	3.01 ± 0.27
r^2	0.98	0.96

Ymax = total amount of drug released; K = release rate constant; $t^{1/2}$ = half time.

2.3. Ex Vivo Transmucosal Permeation Assay

The KT permeations across porcine buccal and sublingual mucosae were performed ex vivo according to previously reported methodologies [20] under an infinite-dose regimen [21]. Figure 3b shows the permeation profiles of KT from the alginate-HA gel through the buccal and sublingual mucosae as well as through the biomimetic membrane.

The results between the two mucosae, buccal and sublingual, were compared by a t-test statistical analysis. The permeated amounts through the buccal and sublingual mucosae after 6 h exposure to the KT hydrogel were very similar: 3790.61 µg/cm^2 of KT (47.4% of the total dose applied) in the case of the buccal mucosa and 3864.93 µg/cm^2 (48.3%) within the sublingual mucosa (p value = 0.836). The permeability coefficients (Kp) were also very similar: 0.052 cm/h and 0.056 cm/h, respectively (p = 0.183). The same happens with the other calculated biopharmaceutical parameters (see values in Table 2). The transmucosal flow values (Jss) obtained were high: 666 µg/h·cm^2 and 714.59 µg/h·cm^2, respectively (p = 0.192). Said values are in agreement with the release test results, in which a great capacity of KT to be released from the hydrogel formulation in which it had been dissolved was observed. The latency time was low in both tissues. In the buccal mucosa, the steady state is reached quickly, after the first 8 min (0.13 h) of the test and in the sublingual mucosa after approximately 23 min (0.38 h) (p = 0.004). The estimated steady-state plasma concentration (Css) was calculated considering a hypothetical area of application of 5 cm^2, the human plasma clearance of ketorolac (1840 mL/h) [22] for an individual with a mean weight of 80 kg. For the buccal mucosa, the estimated Css was 1.13 µg/mL, and for the sublingual mucosa, it was 1.21 µg/mL (p = 0.219). These values are within the therapeutic range of 0.3 to 5 µg/mL of KT [23], so the studied formulation would allow sufficient transmucosal permeability to achieve systemic therapeutic concentrations. The extraction study determines the amount of KT that the tissues subjected to the permeation test are capable of retaining. Both mucous tissues can retain a certain amount of KT. The buccal mucosa was able to retain a total of 127.34 µg/cm^2 of KT and the sublingual mucosa 150.97 µg/cm^2. The statistical study (t-test) gave a p-value greater than 0.05 (0.377), so we can conclude that both mucosae have the same KT retention capacity.

The differences in the results were not statistically significant, except for the Tlag values. Therefore, it can be concluded that the transmucosal permeation of KT through both mucosae, buccal and sublingual, are the same, only that through the buccal mucosa, the therapeutic effect would be achieved more rapidly.

The cumulative amount of ketorolac permeated through each tissue over a long time is shown in Figure 3, and the permeation parameters are calculated in Table 2.

Table 2. Transmucosal biopharmaceutical permeation parameters of ketorolac 6 h after applying KT hydrogel under an infinite dose regimen according to first-order kinetics, and *p*-values from statistical analysis (one-way ANOVA). Results are expressed as Mean ± SD (n = 3).

Parameter	Buccal Mucosa	Sublingual Mucosa	PermeaPad®	*p*-Values
AP (μg/cm^2)	3790.61 ± 0.24	3864.93 ± 0.25	3041.70 ± 0.67	0.943
AR (μg/cm^2)	127.34 ± 37.94	150.97 ± 16.13	35.48 ± 13.67	0.003 **
Css (μg/mL)	1.13 ± 0.04	1.21 ± 0.05	1.36 ± 0.14	0.167
Tlag (h)	0.13 ± 0.02	0.38 ± 0.01	0.23 ± 0.04	0.005 **
Jss (μg/h·cm^2)	666.00 ± 22.74	714.59 ± 27.23	798.80 ± 85.02	0.181
Kp(cm/h)	0.052 ± 0.002	0.056 ± 0.002	0.062 ± 0.007	0.216

** Means statistically significant difference. AP: amount of KT permeated after 6 h. AR amount of KT retained after 6 h. Css: plasma concentration at steady state. Tlag: lag time. Jss: transmucosal/transmembrane flux. Kp: permeability coefficient.

In Vitro—Ex Vivo Correlation

In order to analyze the biocompatibility of the PermeaPad® synthetic membrane with the mucosa of the oral cavity, the correlation of the permeation results through the buccal and sublingual mucosae with the results of the release test through the biomimetic membrane (Figure 4a,b) was calculated. The regression coefficient (r^2) was 0.94 between PermeaPad® and buccal mucosa and 0.95 between the PermeaPad® membrane and sublingual mucosa, showing a strong positive correlation.

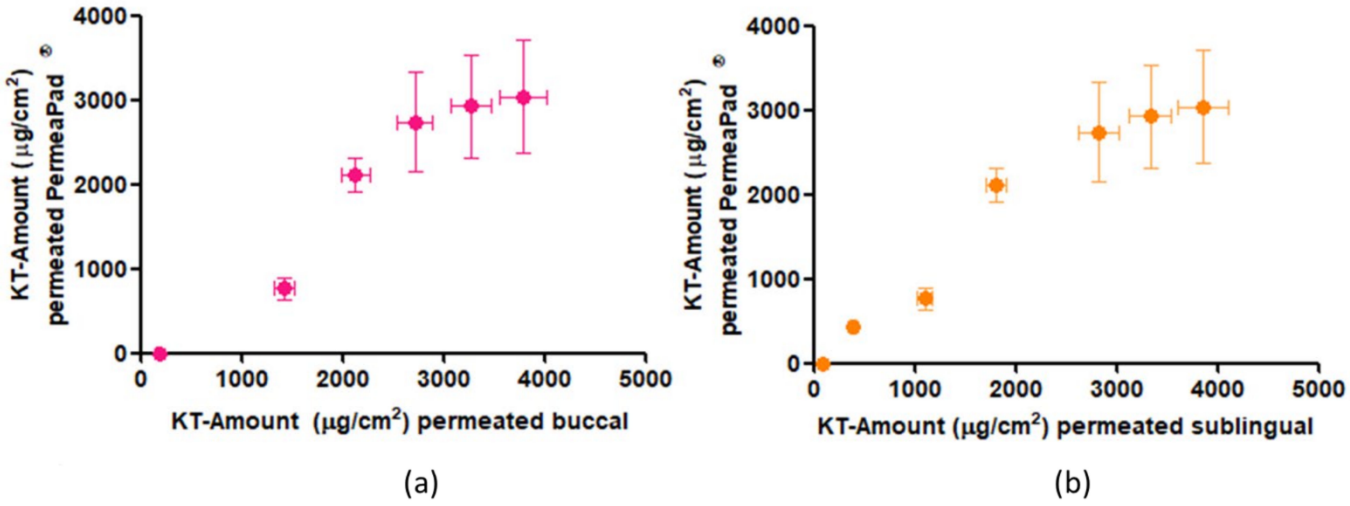

Figure 4. In vitro–ex vivo correlation: (**a**) correlation of in vitro permeation through PermeaPad® membrane and ex vivo permeation through buccal mucosa, (**b**) correlation of in vitro permeation through the PermeaPad® membrane and ex vivo permeation through sublingual mucosa.

Figure 3b shows the profiles of the permeation kinetics through the ex vivo tested mucosa and the PermeaPad® biomimetic membrane. It can be seen how the permeation kinetics through the mucosa and the PermeaPad® membrane are the same for up to 4 h. In the last 2 h, it seems as if a lesser amount had been permeating through the PermeaPad® membrane. Therefore, a correlation of the results was made at up to 4 h to see if it gave a better result than the correlation at 6 h. The r^2 at 4 h was 0.95 between the PermeaPad® membrane and buccal mucosa and 0.96 between the PermeaPad® and sublingual mucosa. As can be observed, the values of the correlation coefficients at 4 and 6 h practically do not differ practically; therefore, it can be concluded that the PermeaPad® biomimetic membrane can predict the permeation of alginate-HA-KT gel through the buccal and sublingual mucosa, for at least 6 h, with an excellent correlation.

In addition to the correlation study, a statistical study (one-way ANOVA) was performed between permeation parameters. The results were a *p*-value greater than 0.05 for all

parameters except for the retained amounts of KT in the tissues and biomimetic membrane and the Tlag (Table 2). Besides the ANOVA test, Tukey's multiple comparison test was carried out to determine which parameters differed. The results were that the biomimetic membrane reached the steady state just as quickly as the buccal mucosa (in about 10 min) but faster as the sublingual mucosa (about 23 min) and that the two mucosae were able to retain more than twice as much KT as the PermeaPad® membrane.

Taking into account all these results, it can be concluded that the PermeaPad® membrane is able to predict with a high correlation the permeation kinetics of KT both in buccal and sublingual mucosae, and it has a significantly lower drug retention capacity.

2.4. In Vitro Study of the Influence of Saliva on Drug Elimination

The in vitro simulation aims to determine the amount of KT that would be eliminated from the mucosa and would end up being swallowed under the influence of artificial saliva exposed to the mucosa by a peristaltic pump. Salivary flow is highly variable and depends on many factors and stimuli. Any value above 0.10 mL/min is considered acceptable, and the average is around 0.30 mL/min [24]. Taking into account the capacity of the available peristaltic pump, a continuous flow of 0.24 mL/min was established to perform the in vitro simulation. The study lasted 1 h, and samples of the saliva dropped down were extracted every 10 min. In Figure 5a, the elimination profile of KT is represented as a function of time.

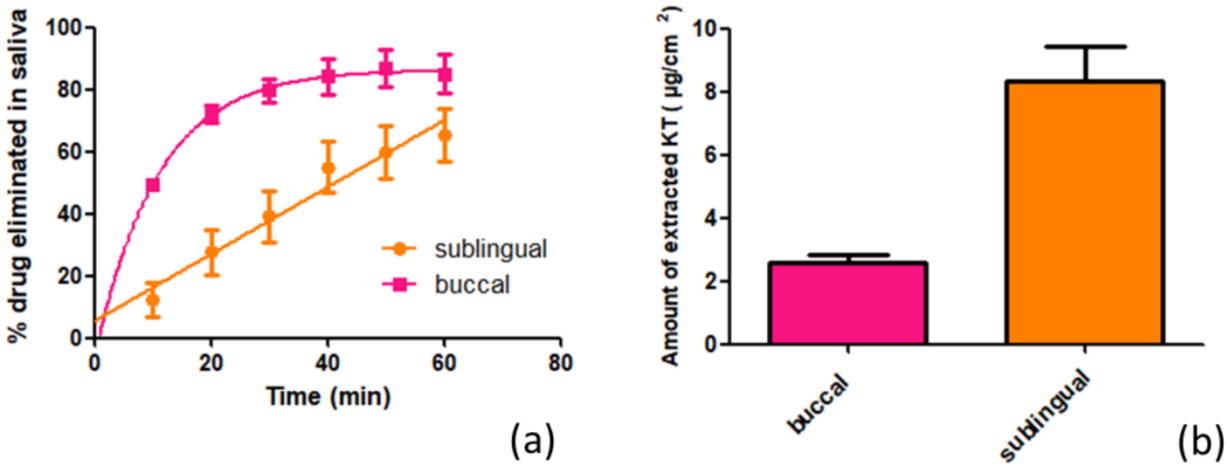

Figure 5. In vitro study of influence of saliva on drug elimination: (**a**) percentage of KT eliminated by the action of artificial saliva at a flow rate of 0.24 mL/min in buccal (pink curve) and sublingual (orange curve) mucosa as a function of time; (**b**) Amounts of KT extracted from the mucosa (buccal—pink; sublingual—orange) after the in vitro study. Results expressed as mean and SD (n = 3).

It is observed how the elimination through the buccal mucosa follows first-order kinetics (r^2 = 0.92), and through the sublingual mucosa, it follows zero-order kinetics (r^2 = 0.96). This differential behavior in the kinetics dissolution of the drug in the saliva is striking. The total amounts eliminated and therefore swallowed by the action of saliva after one hour of the hydrogel application were 2239.88 µg/cm^2, equivalent to 85.1% of the total KT applied (4656 µg), in the buccal mucosa, and 1931.01 µg/cm^2, equivalent to 65.2% of the total KT (5230 µg), in the case of the sublingual mucosa (p = 0.008). The results of the extraction of KT retained in the mucosa are represented in Figure 5b, in which it is seen that the sublingual mucosa is capable of retaining 8.34 µg/cm^2 of KT (2.01% of the total amount applied per unit area) and the buccal mucosa 2.58 µg/cm^2 (corresponding to 0.62% of the total amount applied per unit area), with a p-value of 0.006, which means that the sublingual mucosa is capable of retaining twice as much KT as the buccal mucosa.

2.5. In Vivo Study in Pigs and Histological Study

After the encouraging results obtained in the in vitro and ex vivo studies, we wanted to analyze the behavior of the hydrogel under the effect of salivation in live pigs. The ex vivo permeation study was carried out under an infinite dose regimen to determine the permeation capacity of the oral mucosae. In this case, to better analyze what the real application of the hydrogel would be like, a finite dose regimen was chosen. The dose applied was 5 mg/cm^2 of formulation, as recommended by the Organization for Economic Cooperation and Development (OECD) [25]. The test duration was established at two hours for the in vitro test results on the influence of saliva, where it was observed that after the first 60 min, a large part of the applied hydrogel had been eliminated by the action of saliva. Another concern was to avoid stress on the pigs, and thus not to lengthen the in vivo test with animals unnecessarily.

Figure 6a,b shows the TMWL values for the buccal and sublingual mucosae before applying the hydrogel (basal) and at 2 h post-application. There were no statistically significant differences ($p < 0.05$) between post-application and basal TMWL values, indicating that the 2% KT formulation did not cause the de-structuring of the mucosal epithelium.

Then, before euthanizing the animals, a blood sample was taken to assess whether systemic drug levels could be reached, as predicted in the ex vivo permeation study. Concentrations between 0.3 and 5 μg/mL of KT are considered concentrations within the therapeutic range [23]. After analysis by HPLC, no peak of KT was detected (quantification limit for KT = 0.011 μg/mL). The buccal and sublingual mucous membranes were extracted once the animals had been sacrificed to determine the amount of KT that could have been retained. As can be seen in Figure 6c, the buccal mucosa can retain 1.88 μg/cm^2 of KT, and the sublingual mucosa 0.48 μg/cm^2. Differences were statistically significant ($p = 0.0007$).

Histological Analysis

The histological study was carried out with two of the four pigs used for the in vivo test, extracting the buccal and sublingual mucosa, and analyzing the histology of the tissues in the microscope before and after the application of the alginate-HA gel. As can be seen in Figure 7, both mucous membranes do not present differences in their histology before and after the application of the gel. No severe cytopathic effects (alterations in cell morphology or epithelium structure) were found in treated samples (Figure 7b,d), which demonstrate that the transmucosal application of the alginate-HA and KT gel is safe and well tolerated by the target tissues.

2.6. Cytotoxicity

We examined the impact of alginate gel on the cell growth of the intestinal epithelial cell line Caco-2. For this, Caco-2 cells were exposed to different alginate-HA gel dilutions. The 2% KT alginate-HA gel was diluted in DMEM medium, and dilutions containing ketorolac ranging from 0.715 to 0.09 μg/mL were used in this analysis of cytotoxicity. Living cell numbers were calculated by the MTT assay carried after 24 h incubation. Results showed that cell viability was not altered by the alginate-HA gel, at the concentrations tested (Figure 6d). The viability of cells treated with a ketorolac drug solution used as a control (Figure 6e). In both cases, the viability profile was similar ($p > 0.05$).

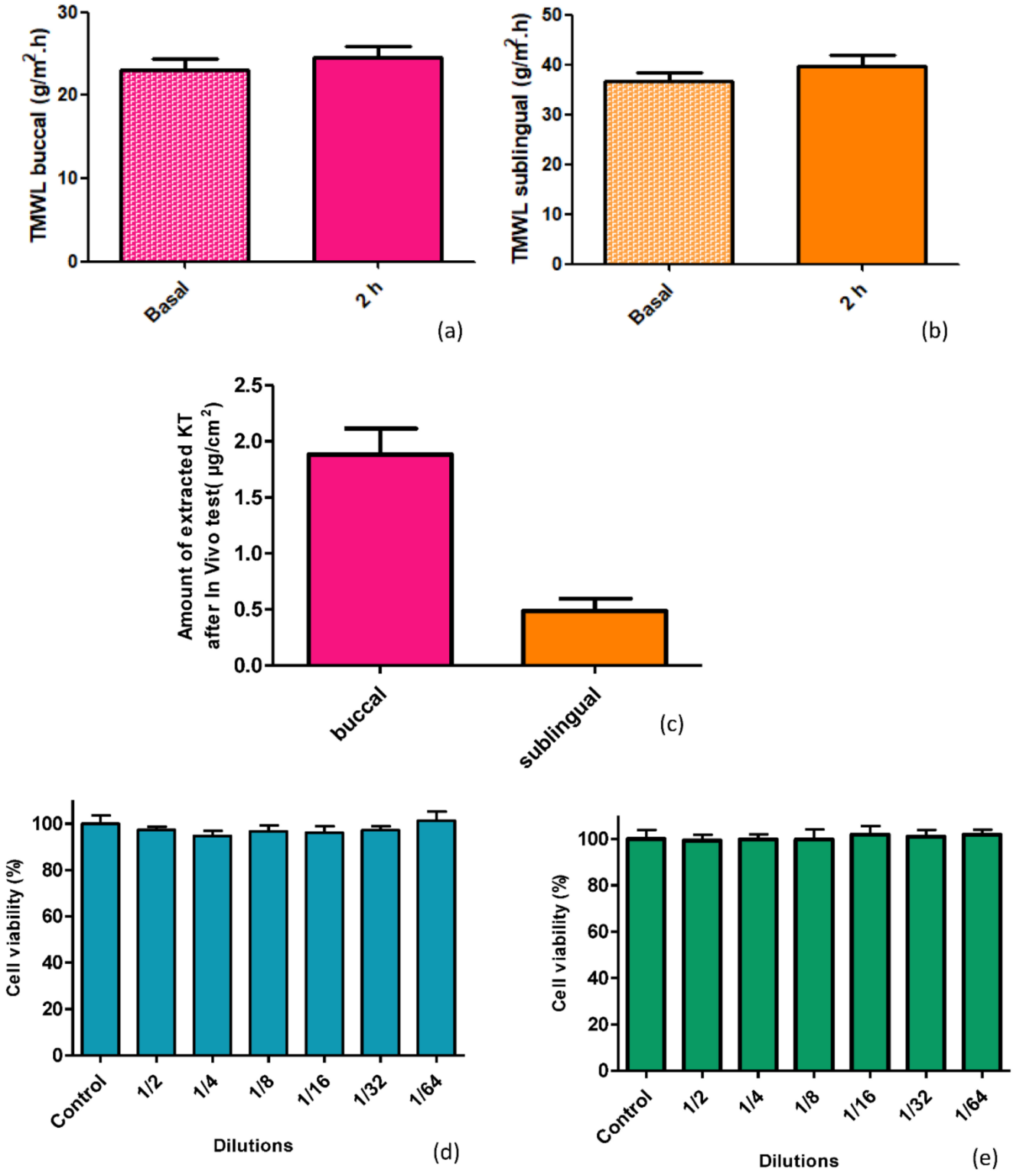

Figure 6. In vivo studies: Integrity of the buccal (**a**) and sublingual (**b**) mucosae. TMWL values taken before the alginate-HA 2% KT gel application (basal) and 2 h after application. (**c**) Amount of extracted KT (µg/cm^2) from the mucosae after in vivo test on pigs. Results represented as mean and SD (n = 3). (**d**,**e**) Cell viability (%) after the MTT test for different dilutions of the 2% KT alginate-HA gel and the KT-solution, respectively. Control: untreated cells in their environment. Results expressed as mean and SD (n = 8).

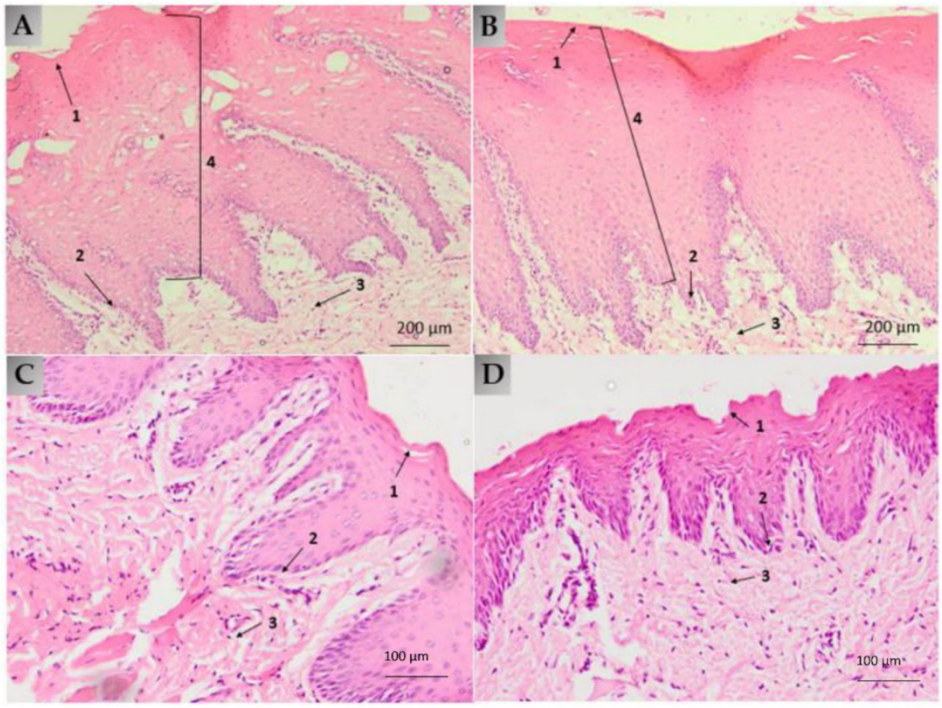

Figure 7. (**A**) Buccal mucosa histology under basal conditions, without gel (100× magnification); (**B**) buccal mucosa histology after 2 h gel exposure (100× magnification); (**C**) sublingual mucosa histology under basal conditions, without gel (200× magnification); (**D**) sublingual mucosa histology after 2 h gel exposure (200× magnification). (1) Keratinized or non-keratinized stratified squamous epithelium; (2) basal layer; (3) lamina propria; (4) dermal papilla.

3. Discussion

We elaborated a 2% ketorolac tromethamine hydrogel composed of sodium alginate as a polymer to be applied to the buccal and sublingual mucosae with the aim of treating pain and inflammation before, during, and after surgical, ablative, or extractive procedures in the oral cavity. The hyaluronic acid was incorporated into the formulation because of its well-known regenerative, moisturizing and strengthening properties [15]. Both, low and high molecular weight hyaluronic acids have been used. The low-molecular-weight HA can penetrate to slightly deeper layers, and there, it can act regeneratively, while the high-molecular-weight HA acts at a more superficial level [26].

The physicochemical, mechanical, and morphological characteristics of the gel have been analyzed. The pH was within the normal intraoral pH range (6.8–7.8) [16], thus no disruptions, neither the biota nor the functions of saliva in the oral cavity, are expected. The alginate-HA gel showed to be hygroscopic in nature since it is able to uptake 15-fold its weigh in solvent, and their components can disperse in the medium relatively quickly compared to other polymer-based hydrogels. Mallandrich et al. studied the degradation of a 2% carbopol hydrogel, which required 24 h to be thoroughly degraded [27].

When formulating gels, determining the extensibility is crucial to ensure that the formulation is pleasant to use and has a comfortable application. That is why very high (very fluid) or very low (very viscous) extensibility should be avoided. The patient's compliance will be affected by the sensory feeling of the formulation. Inoue and co-workers investigated the correlation between the physical properties of different formulations and the sensory feeling [28]. This means that rheological studies are essential to evaluate the galenic features and the suitability of a formulation. Despite the compact structure of the alginate-HA 2% KT gel observed by SEM, the gel exhibited good extensibility and an ideal rheological behavior for the indication of the hydrogel. Pseudoplastic behavior is interesting because it allows a smooth and easy extension application by dabbing without high pressure and, therefore, painlessly. Furthermore, thixotropy also displays interesting

behavior in semi-solid products because the formulation's change in structure results in fluidization that facilitates the product's application. This is an interesting outcome since the mucous membranes are already sensitive tissues per se and even more so after a surgical, ablative, or extractive intervention.

The biomimetic membrane PermeaPad® was tested and compared to the buccal and sublingual mucosae. It was observed that the biomimetic membrane correlated well with both mucosae. These results are in agreement with other researchers' work. Bibi et al. [19] investigated the use of PermeaPad® as a predictor in the buccal absorption of Metoprolol solution. The authors compared the apparent permeability obtained with PermeaPad® to the previous works performed by other authors, which evaluated the apparent permeability of metroprolol solution in cell culture, in ex porcine buccal mucosa and, finally, in in vivo studies conducted on minipigs. Bibi et al. found good in vitro–in vivo correlation between PermeaPad® and all the three systems evaluated.

Ketorolac tromethamine rapidly diffuses across the mucous membranes of the oral cavity, especially through the buccal mucosa. Under infinite doses and an exposure time of 6 h, ketorolac tromethamine would achieve therapeutic plasma concentrations. Nevertheless, the impact of saliva on drug elimination should not be disregarded, since the main drawback in buccal delivery is that the patient may swallow part of the applied dose before the drug is absorbed, even if it has been released [29]. The in vitro test showed that saliva dragged more than 60% of Ketorolac in 1 h, which is swallowed and follows on from an oral intake. Even despite the saliva's effect, Ketorolac tromethamine was able to penetrate both mucosae. The alginate-HA-hydrogel was formulated with Ketorolac in the tromethamine salt since this is more hydrophilic and allows it to be better integrated into the hydrogel. However, it is to be expected that once the gel is applied to the mucous membranes, the KT changes and, due to the environment in which it is found, protonates and/or ionizes and that, during the process, the different forms coexist until reaching a balance. These changes will affect the physicochemical properties of the drug, such as its solubility in saliva or the value of the log P partition coefficient, thus modifying its tissue affinity [18,30]. Given that the alginate-HA-hydrogel was formulated with the tromethamine salt, it is likely that this was the predominant form at the beginning of the study when applying the gel on the mucosa and therefore that the process of dissolving KT in saliva was favored. It should not be forgotten, however, that the KT of the formulation is simultaneously being absorbed through the mucosa. This absorption depends on different factors. On one hand, the mucosa histology, and on the other, the KT physicochemical properties. Taking into account that both the buccal and sublingual mucosae consist of a non-keratinized stratified squamous epithelium and that the main difference is the thickness of the said epithelium (the sublingual being between 100 and 200 μm, 8–12 cells thick, and between 500 and 800 μm, 40–50 cells thick, the buccal [24]), it is logical to think that the sublingual mucosa presents less resistance to the passage of KT. From the beginning, the amount of KT that is eliminated by the action of the saliva when the gel is applied on this mucosa is lower compared to when the gel is applied on the buccal mucosa. The kinetic dissolution profile is the result of the sum of these two processes. Through the buccal mucosa, it is observed how at the beginning, the KT dissolution in saliva predominates until after about 30 min, when a balance is reached between what is dissolved and what is absorbed by the mucosa. This behavior adjusts to first-order kinetics. On the other hand, in the sublingual mucosa, by presenting less resistance to the passage of KT through its structure, the dissolution and absorption processes are balanced from the beginning, and this therefore describes zero-order dissolution kinetics. These results show how, apart from the drug physicochemical properties and the mucosa physiological characteristics, other factors such as salivation play a significant role in the bioavailability of KT since, in both mucosae, much more than half of the applied dose was eliminated by the action of saliva, which can be explained, in part, by the high-water solubility of KT, which is eliminated from the mucosa by the action of saliva and ends up being ingested. It

is therefore considered that the KT is administered orally. In contrast, the amount that is retained in the mucosa is responsible for the local analgesic and anti-inflammatory action.

Thus, it is observed that the study in live animals and under a finite dose regimen does not reach systemic concentrations of KT. Besides the lower dose, this is probably due to the effect of saliva, as demonstrated in the in vitro study, which can influence by reducing the time that the alginate-HA gel is in contact with the mucous membranes and consequently with the amount of KT that could be permeated. It should be noted that the present study was carried out by administering a single drug dose in order to minimize the test time as much as possible and, therefore, the stress that could be caused to the animals. Other studies applying the alginate-HA gel in a multiple-dose regimen are necessary to analyze the behavior of the hydrogel more accurately in terms of bioavailability and permeability through the mucous membranes of the oral cavity.

When mucosae are damaged, their barrier functions are impaired, resulting in higher water loss [31]. This water loss can be measured by the transmucosal water loss (TMWL) method, which is well established in dermatology and used to assess the integrity of the mucosa barrier in vivo [32]. In the TMWL measurement, the water density gradient that evaporates through the tissue is indirectly measured by placing the measuring device perpendicular to the site of interest and reaching a stable TMWL reading in about 60 s. Before exposing the mucosa to alginate-HA hydrogel, the basal TMWL value was measured. The formulation was then applied to the mucosae, and after 2 h, the TMWL value was measured again. The TMWL values obtained, both basal and 2 h post-application, (around 30 $g/m^2 \cdot h$ for the buccal mucosa and around 40 $g/m^2 \cdot h$ for the sublingual mucosa) show the excellent condition of the mucosa since both have values close to 30 $g/m^2 \cdot h$, which is considered acceptable for the integrity of the oral mucosa [32]. Thus, the alginate-HA 2% KT does not cause mucosae disruption, being well-tolerated by the target tissues: the histological analysis revealed no differences between the treated and the untreated mucosae. Additionally, the cell viability showed that the alginate-HA 2% KT does not cause cytotoxicity in Caco-2 cells.

4. Materials and Methods

4.1. Materials

4.1.1. Reagents

Sodium alginate was purchased from Fagron Iberica (Terrassa, Spain). Ketorolac tromethamine and Nipagin were obtained from Sigma-Aldrich (Barcelona, Spain). Nipasol was acquired from Acofarma (Barcelona, Spain), Hyaluronic acids were obtained from Fagron Iberica (Terrassa, Spain); Na2HPO4 and KH2PO4 were supplied by Panreac (Barcelona, Spain), NaCl and KCl were from Merck (Darmstadt, Germany), CaCl from Ferosa (Spain) Hepes was obtained from Fagron Iberica (Terrassa, Spain) and glucose from Sigma-Aldrich (Barcelona, Spain). The Millipore Express® PLUS 0.45 µm PES Membrane was from Merck (Darmstadt, Germany), the Nylon membrane Filter with 0.45 µm pore size from Teknokroma (Barcelona, Spain) and the biomimetic membrane PermeaPad® from InnoME GmbH (Espelkamp, Germany).

The purified water was obtained from a Milli-Q1 Gradient A10 system apparatus (Millipore Iberica S.A.U., Madrid, Spain). All the other chemicals and reagents used in the study were of analytical grade.

4.1.2. Tissues for Ex Vivo Assays

The Bellvitge animal facility services provided the buccal and sublingual mucosae (Landrace Large White race). The Ethics Committee of Animal Experimentation of the University of Barcelona approved the Study Protocol (approved on 10 January 2019). A thickness of 500 µm was dermatomized (GA630, Aesculap, Tuttlingen, Germany) to carry out the test.

4.2. Preparation of the Sodium Alginate and Hyaluronic Acid Hydrogel

Drug-loaded hydrogel was prepared at laboratory scale with a KT concentration of 2% w/v. A concentration of 0.5% w/v of high molecular and 0.2% low molecular weight HA was used. Sodium alginate concentration was established at 4% w/v. Firstly, preservatives (nipagin and nipasol at 0.05% and 0.02%, respectively) and KT were added to purified water under continuous stirring. Separately, both HA were dispersed in ethanol (corresponding to a 5% of the final composition); then, the KT-preservatives solution was poured into the HA mixture, and finally, alginate was added gradually to avoid the formation of lumps. Then, the formulation was allowed to rest for 24 h at room temperature.

4.3. Gel Characterization

The alginate gel containing 2% ketorolac was characterized in terms of appearance, pH, extensibility, swelling and degradation ratio and rheological behavior.

4.3.1. Swelling and Degradation Tests

The swelling and degradation tests were carried out according to the methodology described by S. El Moussaoui et al. [18]. The swelling test evaluates the hydrogel's capacity to absorb water within its structure. First, the hydrogels were dehydrated at 40 °C until constant weight. The dehydrated hydrogels were immersed in PBS (pH 7.4) at room temperature for 14 min. The hydrogels were removed from the PBS at predetermined intervals (every 2 min). The excess PBS was removed, and the amount of captured PBS was weighed. The experiment was performed in triplicate. The swelling ratio (SR) was calculated using the following equation:

$$SR = \frac{W_s - W_d}{W_d} \quad (1)$$

where W_d is the weight of the dried hydrogel, and W_s is the weight of the swollen hydrogel at different times.

The degradation test aims to monitor weight loss (WL) as a function of time. The WL was calculated by incubating known amounts of fresh hydrogel (3.017 g) in PBS (pH = 7.4) at 37 °C for 115 min. Three replicates of hydrogel were removed, blotted, and weighed at the following times: 0, 5, 10, 15, 20, 25, 30, 35, 40, 45, 55, 65, 75, 85, 100, and 115 min. The weight loss was expressed as the percentage of weight loss concerning the freshly prepared hydrogel. It was calculated based on Equation (2):

$$WL(\%) = \frac{W_i - W_d}{W_i}\ 100\% \quad (2)$$

where W_i is the initial weight of hydrogel and W_d the weight of hydrogel at different times.

4.3.2. Extensibility

The extensibility was determined in triplicate at room temperature. The formulation was placed between two crystal platforms. Several weights (0, 2, 5, 10, and 20 g) were placed on the top platform for 2 min. The diameters (cm^2) of the circles which spread out were measured and recorded. The extensibility was calculated from the equation:

$$Ext = \frac{\pi \cdot (d^{-}2)}{4} \quad (3)$$

where Ext = extensibility; d = average diameter of the extended formulation.

4.3.3. Rheological Profile

The rheological properties of the Alginate-HA hydrogel containing 2% KT were determined by a rotational Haake RheoStress 1 rheometer (Thermo Fisher Scientific, Karlsruhe, Germany) equipped with cone-plate geometry (Haake C60/2° Ti, 60 mm diameter,

0.105 mm gap between cone-plate). Measurements were performed in duplicate at 25 °C (Thermo Haake Phoenix II + Haake C25P). An oscillatory study was carried out, for which a stress sweep of 0 to 500 Pa, at 1 Hz, was first performed to determine the linear viscolastic zone. For the following test, the shear was set at a value between 0.4 and 100 Pa (linear zone), and 10 Pa was chosen to perform the Frequency Sweep test, which allows how the product behaves at low and high frequencies to be determined and recorded.

For the rotational study, the program was adjusted to the following conditions: ramp-up from 0 to 15.0 s^{-1} for 3 min, constant shear rate at 15.0 s^{-1} for 1 min, and ramp-down from 15.0 to 0 s^{-1} for 3 min. The flow data obtained were fitted to different mathematical models (Table A2) to describe the flow curve and characterize the flow properties.

4.3.4. Morphological Study

In order to examine the hydrogel structure, Scanning Electron Microscopy (SEM) was carried out in a JSM-7100F (JEOL Inc., Peabody, MA, USA). The sample was coated with a thin layer of carbon in an Emitech K950 coater (Quorum Technologies Ltd., Kent, UK).

4.4. In Vitro Release Assay on Membranes and Biomimetic Membranes

The in vitro release profile was assessed by vertical Franz diffusion cells (FDC 400, Crown Glass, Somerville, NY, USA) with an active diffusion area of 1.77 cm^2. Hank's solution pH (7.02) was used as receptor fluid, which was thermostated at 37 ± 1 °C. The stirring rate was set at 500 rpm, and sink conditions were held throughout the experiments. A total of 400 mg ± 10 mg of KT hydrogel was accurately applied to the membranes.

The membranes used were PermeaPad®, and polyethersulfone (PES)—the selection of PES membrane was based on a previous study in which a solution of Ketorolac tromethamine was tested through Nylon and PES membranes. Samples of 300 µL from the receiver compartment were extracted over pre-established times (0.5, 1, 2, 3, 4, 5, and 6 h) and replaced with an equal volume of fresh solution. The KT content was analyzed by a validated HPLC method, described in Section 4.8.

The experimental data (cumulative amount of KT per cm^2) were fitted to different mathematical models (zero and first-order kinetics) so as to choose the best fitting model according to the correlation coefficient (r^2) value.

4.5. Ex Vivo Transmucosal Permeation Assay

The ex vivo permeation tests were conducted on porcine oral mucosa from the pigs' cheeks and sublingual tissues to evaluate the ability of KT to permeate through the mucosal membranes. The mucosae were dermatomed at a thickness of 500 µm.

The assays were performed on Franz diffusion cells with a diffusional area of 0.64 cm^2. They were conducted in the same conditions as in the release assay (Section 4.4), adjusting the sampling times to 1, 2, 3, 4, 5, and 6 h. Samples were analyzed with the same HPLC method. From the permeated amounts analyzed by HPLC, the permeation parameters were calculated according to the equations described in Appendix A (Table A3).

4.5.1. Amount of Ketorolac Retained in the Mucosa

Once the permeation assay was finished, the KT retained in the mucosa was extracted. To do this effectively, the residual hydrogel on the mucosa was removed with a swab and cleaned with a gauze soaked in 0.05% solution of sodium lauryl sulfate and rinsed three times with distilled water. The permeation area of the mucosa was cut, weighed, perforated by a thin needle, and incubated with 1 mL of methanol:water (1:1) solution and sonicated for 20 min. The supernatants were analyzed by the HPLC method.

4.5.2. In Vitro—Ex Vivo Correlation

To determine if the PermeaPad® biomimetic membrane can be comparable to the buccal and sublingual mucosae, the ex vivo permeation results and parameters were

compared with the release test results performed on the PermeaPad® membrane, and to achieve this, a one-way ANOVA statistical study was carried out.

Furthermore, the correlation between the amounts of KT permeated through PermeaPad® vs. through buccal and sublingual mucosae at each time was calculated with the help of GraphPad software.

4.6. In Vitro Study of the Influence of Saliva on Drug Elimination

To simulate the influence of saliva on the KT elimination once the hydrogel had been applied to the mucosa of the oral cavity, the buccal and sublingual mucosae were cut to an area of 2.83 cm^2 and placed vertically on a support point. A certain amount of KT hydrogel was carefully placed on the mucosa. Using a peristaltic pump, artificial saliva (Table A4) was passed over the mucosa at a 0.24 mL/min flow rate. The study lasted 1 h, taking samples of the artificial saliva that dropped every 10 min. The collected samples were analyzed by HPLC to determine the amount of KT that had been eliminated by the action of saliva, and the amount of KT that had been retained in the mucosa was determined as described in Section 4.5.1.

The KT extraction retained in the mucosa after the in vitro simulation of the influence of saliva on the elimination of KT was carried out according to Section 4.5.1.

4.7. In Vivo Study and Analysis of Tolerance through Histology

With the aim of assessing the tolerability of the alginate-HA gel, the formulation was applied to female pigs (Yorkshire-Landrace) of 45–50 kg. Transmucosal water loss (TMWL) (TEWL-Dermalab) was measured at basal conditions (before applying the formulation) by placing the measuring device perpendicular to the site of interest and reaching a stable TMWL reading in about 60 s. Four pigs were used. Two had the hydrogel applied to the buccal mucosa and two to the sublingual mucosa. The hydrogel was applied on the mucosa covering the most accessible area to facilitate the process and cause the least possible stress to the animals. After two hours, the TMWL value was measured again, and a blood sample was taken to determine whether, by means of buccal and/or sublingual application, therapeutic systemic levels could be reached. Then, all animals were euthanized, and the mucosa tissues were obtained immediately afterwards. The tissues from two treated animals were fixed by immersing them overnight in 4% paraformaldehyde in phosphate-buffered 20 mM, pH 7.4. Then the tissues were processed so as to embed them in paraffin, and vertical histological sections were cut to be stained with hematoxylin and eosin and observed under a Leica DMD 108 optical microscope. The tissues from the two remaining treated animals underwent the extraction procedure for determining the Ketorolac retained in the mucosa, according to Section 4.5.1. The study protocol was approved by the Animal Experimentation Ethics Committee of the University of Barcelona (code 10619, 10 January 2019).

4.8. Cytotoxicity

Cell viability was assessed by the MTT (3-(4,5-Dimethylthiazol-2-yl)-2,5-diphenyltetrazolium bromide) assay. This method is based on the mitochondrial reduction of tetrazolium to formazan which is directly proportional to the viable cell numbers. To achieve this, 1 × 104 Caco-2 cells in 100 µL of DMEM medium without phenol red were plated into each well in a 96-well plate and further incubated for five days at 37 °C before the addition of the compounds under study. The volume of each well was set to 0.1 mL, with eight duplicate wells for each specific sample under study. After 24 h, the cells were treated with 0.25% MTT (Sigma-Aldrich) in PBS and allowed to react for 2 h at 37 °C. The supernatant was then removed, and 0.1 mL of dimethyl sulfoxide (DMSO) was added (Applichem, Ecogen, Barcelona, Spain) to each well to fully dissolve the formazan produced by the living cell. For Cell viability determination, the optical density (OD) was measured at a wavelength of 570 nm in a Modulus™ Microplate Photometer (Turner BioSystems, Madrid, Spain). The results were expressed as percentage of cell survival relative to the control (untreated cells).

4.9. Analytical Method for the Determination of Ketorolac Tromethamine

To quantify the KT concentration described in previous sections, a HPLC method was used. The chromatographic conditions were the following: the column used was YMC-Pack Pro C18 (25 cm, 4.6 mm and 5 μm). The mobile phase consisted of acetonitrile (+0.065% triethylamine) and purified water (+0.165% acetic glacial acid), in an isocratic elution (1:1) at flux 1 mL/minute. The volume injected was 10 μL, and Ketorolac was determined at the wavelength of 314 nm. The standard range for the calibration line was from 0.39 to 300 μg/mL. Data were collected and processed using Empower Pro software (Walters, Milford, CT, USA).

4.10. Statistical Analysis

GraphPad Prism®, v. 5.00 software (San Diego, CA, USA), was used for all statistical calculations. If data followed a normal distribution, a *t*-test or an ANOVA (if more than two groups were being compared) was applied. If data followed a non-normal distribution, a Mann-Whitney (for two group comparison) or Kruskal-Wallis test (for more than two groups) was applied. The significance level was 0.05 in all cases.

5. Conclusions

The objective of this study was to comprehensively characterize a hydrogel based on sodium alginate and high and low molecular weight hyaluronic acid formulated with 2% ketorolac tromethamine. Organoleptic, morphological, and rheological studies showed the suitability of the formulation to be an excellent and easy topical application of the hydrogel on the mucosa of the oral cavity.

The release studies demonstrated the remarkable capacity of KT to be released from the alginate-HA hydrogel, releasing 51.59% of the drug per cm^2 in 6 h.

Ex vivo permeation studies demonstrated good oral and sublingual mucosal patency for KT and predicted systemic steady-state concentrations within the therapeutic range. Furthermore, when comparing the results of both mucosae, no statistically significant differences were observed.

An additional positive finding was that comparative studies of the PermeaPad® biomimetic membrane with the buccal and sublingual mucosae showed an excellent correlation but a significantly lower drug retention capacity.

Through in vitro simulation, the influence of saliva on the bioavailability of the drug was observed. It was shown how in one hour, artificial saliva at a constant flow of 0.24 mL/min was capable of eliminating more than half of the initially applied dose on the mucous membranes, which would end up being swallowed and considered as oral administration.

In in vivo studies with pigs and under a finite regime dose, it was not possible to quantify the systemic concentrations of the drug, but the amounts of KT retained in both mucosae showed the feasibility of the gel to provide an analgesic and anti-inflammatory locally, which is very useful in surgical and/or ablative processes such as the elimination of papillomatous lesions, treatment of certain oral carcinomas, dental extractions, etc. Further studies are needed in a multi-dose regimen to characterize the hydrogel's behavior better, and this would be more realistic since, in practice, a single application of the formulation would not be sufficient to obtain the desired effect.

Finally, the histological, cytotoxicity study and the measured TMWL values demonstrated the safety and innocuousness of the formulation, not showing any damage or alterations to the mucosal tissues.

Author Contributions: Conceptualization, M.M. and A.C.C.; methodology, A.C.C. and M.M.; software, M.M., N.G. and S.E.M.; validation, A.C.C.; formal analysis, A.C.C. and M.M.; investigation, S.E.M. and N.G.; resources, A.C.C. and M.M.; data curation, M.M. and S.E.M.; writing—original draft preparation, S.E.M.; writing—review and editing, M.M., A.C.C. and F.F.-C.; visualization, M.J.R.L.; supervision, A.C.C. and F.F.-C.; project administration, F.F.-C., M.M. and A.C.C.; funding acquisition, A.C.C. and M.J.R.L. All authors have read and agreed to the published version of the manuscript.

Funding: This research received no external funding.

Institutional Review Board Statement: The study was conducted according to the guidelines of the Declaration of Helsinki and approved by the Animal Experimentation Ethics Committee of the University of Barcelona (ethical code 10619 approved on 10 January 2019).

Informed Consent Statement: Not applicable.

Data Availability Statement: The data presented in this study are available on request from the corresponding authors. The data are not publicly available due to the fact that they are part of a doctoral thesis, and they will be available once the thesis has been published.

Acknowledgments: Our sincere thanks to Cristina Peralta for her time and help with the cytotoxicity study, Lyda Halbaut for her technical support in the rheological analysis, and to the innoME GmbH company for donating the PermeaPad® biomimetic membranes. We also want to thank Harry Paul for the English language editing.

Conflicts of Interest: The authors declare no conflict of interest.

Abbreviation

The abbreviations used in the manuscript are listed below:

ANOVA	One-way analysis of variance
AP	Amount permeated
AR	Amount retained
C_0	Initial concentration
CA	Condyloma acuminata
$CaCl_2$	Calcium chloride
Clp	Human plasma clearance
CO_2	Carbon dioxide
Css	Concentration at steady state
d	Diameter
Ext	Extensibility
HPLC	High Performance Liquid Chromatography
HPV	Human Papilloma Virus
J	Flux
Jss	Flux at steady state
K	Release rate constant
KCl	Potassium chloride
KH_2PO_4	Potassium dihydrogen phosphate
Kp	Permeability coefficient
KT	Ketorolac tromethamine
Log P	Octanol-water partitioning
NaH_2PO_4	Sodium hydrogen phosphate
Na_2HPO_4	Disodium phosphate
NaCl	Sodium chloride
NSAID	Non-steroidal anti-inflammatory drug
Pa	Pascals
PBS	Phosphate-buffered saline
PES	Polyethersulfone
r	Coefficient of regression
r^2	Correlation coefficient
R∞	Maximum amount released
Rt	Amount of drug released at time t
SD	Standard deviation
SEM	Scanning Electron Microscopy

SR	Swelling ratio
$t_{1/2}$	Half-life
TCA	trichloroacetic acid
Tlag	Lag time
TMWL	Trans-mucosal water loss
TSA	Theoretical surface area
Wd	Weight of dried hydrogel
Wi	Initial weigh of hydrogel
WL(%)	Weight loss
Ws	Weight of the swollen hydrogel at different times
Ymax	Total amount of drug released

Appendix A

Table A1 presents the results of the rheological data fit of alginate-HA 2% KT gel and the goodness of fit for each model.

Table A1. Results of rheological data fit in different mathematical models.

Flow Model	R^2 Ramp-up	Parameters-up	R^2 Ramp-down	Parameters-down
Newton	0.7401	η = 52.48 Pa·s	0.6865	η = 48.02
Bingham	0.9248	τ_0 = 179.5 Pa η_0 = 34.76 Pa·s	0.9727	τ_0 = 183.3 η_0 = 29.64
Ostwald-de Waele	0.9915	K = 200.3 n = 0.4314	0.9981	K = 164.4 n = 0.4744
Herschel-Bulkley	0.9969	τ_0 = 151 Pa K = 345.9 n = 0.3017	0.9999	τ_0 = 168.4 K =313.6 n = 0.3234
Casson	0.9641	τ_0 = 107.2 η_0 = 16.32 Pa·s n = 0.5	0.9887	τ_0 = 99.31 η_0 = 14.54 n = 0.5
Cross	0.9999	η_0 = 326.1 Pa·s η∞ = 16.41 Pa·s $\dot{\gamma}_0$ = 1.346 n = 0.6674	0.9999	η_0 = 290.9 η∞ = 0.1397 $\dot{\gamma}_0$= 0.994 n = 0.6876

τ is the shear stress (Pa); η is the dynamic viscosity (mPa·s); $\dot{\gamma}$ is the shear rate (1/s); τ_0 is the yield shear stress (Pa); η_0 is the zero-shear rate viscosity; ηp is a constant plastic viscosity (mPa·s); η∞ is the infinity shear rate viscosity; n is the flow index, and K is the consistency index. The goodness of fit was determined by correlation coefficient (r^2) by linear regression analysis of the flow plots.

Table A2 presents the different mathematical models fitted to the rheological data to characterize the flow curve and the flow properties of alginate-HA 2% KT gel.

Table A2. Mathematical models of the flow characterization by regression analysis.

Flow Curve—Models: $\tau = f(\dot{\gamma})$	
Newton	$\tau = \eta \cdot \dot{\gamma}$
Bingham	$\tau = \tau_0 + (\eta_0 \cdot \dot{\gamma})$
Ostwald-de Waele	$\tau = K \cdot \dot{\gamma}^n$
Herschel-Bulkley	$\tau = \tau_0 + K \cdot \dot{\gamma}^n$
Casson	$\tau = \sqrt[n]{\left(\tau_0^n + \left(\eta_0 \cdot \dot{\gamma}\right)^n\right)}$
Cross	$\tau = \dot{\gamma} \cdot (\eta_\infty + (\eta_0 - \eta_\infty)/(1 + (\dot{\gamma}/\dot{\gamma}_0)^n)$

τ is the shear stress (Pa); η is the dynamic viscosity (mPa·s); $\dot{\gamma}$ is the shear rate (1/s); τ_0 is the yield shear stress (Pa); η_0 is the zero-shear rate viscosity; ηp is a constant plastic viscosity (mPa·s); η_∞ is the infinity shear rate viscosity; n is the flow index, and K is the consistency index.

Table A3 describes the calculation of the permeation parameters flux, lag-time, predictive plasma concentration at the steady state and permeability coefficient.

Table A3. Permeation Parameters and Calculation of the Css upon Application of alginate-HA gel 2% KT.

Permeation Parameter	Equation	
Steady state plasma concentration	$Css = \frac{J \cdot TSA}{Cl_p \cdot A}$	(A1)
Permeability coefficient	$Kp = J \cdot C_0$	(A2)

The flux (Jss) corresponds to the slope of the permeation profile's linear section. The latency time (Tlag) was obtained from the extrapolation of the straight line resulting from the accumulated amounts as a function of time. The steady state plasma concentration (Css) was calculated assuming an area of application of 5 cm^2 according to the Equation (A1): where Css is the steady state plasma concentration (Css); J (µg/h) is the flux; TSA (cm^2) is the theoretical surface area of application; Cl_p (mL/min) is the human plasma clearance of ketorolac, and A (cm^2) is the diffusion area of the Franz cells.

The permeability coefficient was calculated in accordance with the Equation (A2): where Kp is the permeability coefficient of ketorolac through the membranes; J (µg/h) is the flux, and C_0 (µg/mL) is the initial concentration of ketorolac in the gel.

Table A4 shows the composition of the artificial saliva.

Table A4. Artificial saliva composition expressed in concentration (g/L).

Substance	Weight
Pure sodium chloride	8.00 g/L
Potassium dihydrogen phosphate	0.19 g/L
Anhydrous disodium hydrogen phosphate	2.38 g/L
Distilled water	1 L

The resulting pH was 6.8.

References

1. Betz, S.J. HPV-Related Papillary Lesions of the Oral Mucosa: A Review. *Head Neck Pathol.* **2019**, *13*, 80–90. [CrossRef] [PubMed]
2. Pina, A.; Fonseca, F.; Pontes, F.; Pontes, H.; Pires, F.; Taylor, A.; Aguirre-Urizar, J.; De Almeida, O. Benign epithelial oral lesions—Association with human papillomavirus. *Med. Oral Patol. Oral Cir. Bucal.* **2019**, *24*, e290–e295. [CrossRef] [PubMed]
3. Martínez, G.G.; Troconis, J.N. Tratamiento de las verrugas genitales: Una actualización. *Rev. Chil. Obstet. Ginecol.* **2015**, *80*, 76–83. [CrossRef]
4. Atienzo, P.C.; Memíje, M.E.V.; Galván, G.Z.; Calderón, A.G.G.; García, I.A.M.; González, J.C.C. Presencia del Virus Papiloma Humano en la Cavidad Oral: Revisión y Actualización de la Literatura. *Int. J. Odontostomatol.* **2015**, *9*, 233–238. [CrossRef]
5. Pringle, G.A. The Role of Human Papillomavirus in Oral Disease. *Dent. Clin. N. Am.* **2014**, *58*, 385–399. [CrossRef]
6. Syrjänen, S. Oral manifestations of human papillomavirus infections. *Eur. J. Oral Sci.* **2018**, *126*, 49–66. [CrossRef] [PubMed]
7. Buckley, M.M.-T.; Brogden, R.N. Ketorolac. A review of its pharmacodynamic and pharmacokinetic properties, and therapeutic potential. *Drugs* **1990**, *39*, 86–109. [CrossRef]
8. Vadivelu, N.; Gowda, A.M.; Urman, R.D.; Jolly, S.; Kodumudi, V.; Maria, M.; Taylor, R.; Pergolizzi, J.V. Ketorolac Tromethamine—Routes and Clinical Implications. *Pain Pract.* **2014**, *15*, 175–193. [CrossRef]
9. Hungund, S.; Thakkar, R. Effect of pretreatment with ketorolac tromethamine on operative pain during periodontal surgery: A case-control study. *J. Indian Soc. Periodontol.* **2011**, *15*, 55–58. [CrossRef]
10. DeAndrade, J.R.; Maslanka, M.; Maneatis, T.; Bynum, L.; Burchmore, M. The use of ketorolac in the management of postoperative pain. *Orthopedics* **1994**, *17*, 157–166. [CrossRef]
11. Alsarra, I.A.; Alanazi, F.K. Clinical evaluation of novel buccoadhesive film containing ketorolac in dental and post-oral surgery pain management. *Pharmazie* **2007**, *62*, 773–778.
12. Al-Hezaimi, K.; Al-Askar, M.; Selamhe, Z.; Fu, J.H.; Alsarra, I.A.; Wang, H.-L. Evaluation of Novel Adhesive Film Containing Ketorolac for Post-Surgery Pain Control: A Safety and Efficacy Study. *J. Periodontol.* **2011**, *82*, 963–968. [CrossRef]
13. Campisi, G.; Paderni, C.; Saccone, R.; di Fede, O.; Wolff, A.; Giannola, L.I. Human Buccal Mucosa as an Innovative Site of Drug Delivery. *Curr. Pharm. Des.* **2010**, *16*, 641–652. [CrossRef]
14. Zhang, H.; Zhang, J.; Streisand, J.B. Oral Mucosal Drug Delivery. Clinical Pharmacokinetics and Therapeutic Applications. *Clin. Pharmacokinet.* **2002**, *41*, 661–680. [CrossRef]
15. Salwowska, N.; Bebenek, K.A.; Żądło, D.A.; Wcisło-Dziadecka, D.L. Physiochemical properties and application of hyaluronic acid: A systematic review. *J. Cosmet. Dermatol.* **2016**, *15*, 520–526. [CrossRef]

16. Loke, C.; Lee, J.; Sander, S.; Mei, L.; Farella, M. Factors affecting intra-oral pH—A review. *J. Oral Rehabil.* **2016**, *43*, 778–785. [CrossRef]
17. Osswald, T.; Rudolph, N. Generalized newtonian fluid (GNF) models. In *Polymer Rheology Fundamentals and Applications*; Strohm, C., Ed.; Hanser Publications: Cincinnati, OH, USA, 2015; pp. 59–74.
18. El Moussaoui, S.; Fernández-Campos, F.; Alonso, C.; Limón, D.; Halbaut, L.; Garduño-Ramirez, M.; Calpena, A.; Mallandrich, M. Topical Mucoadhesive Alginate-Based Hydrogel Loading Ketorolac for Pain Management after Pharmacotherapy, Ablation, or Surgical Removal in Condyloma Acuminata. *Gels* **2021**, *7*, 8. [CrossRef] [PubMed]
19. Bibi, H.A.; Holm, R.; Bauer-Brandl, A. Use of Permeapad®for prediction of buccal absorption: A comparison to in vitro, ex vivo and in vivo method. *Eur. J. Pharm. Sci.* **2016**, *93*, 399–404. [CrossRef] [PubMed]
20. Limón, D.; Amirthalingam, E.; Rodrigues, M.; Halbaut, L.; Andrade, B.; Garduño-Ramírez, M.L.; Amabilino, D.B.; Pérez-García, L.; Calpena, A.C. Novel nanostructured supramolecular hydrogels for the topical delivery of anionic drugs. *Eur. J. Pharm. Biopharm.* **2015**, *96*, 421–436. [CrossRef] [PubMed]
21. Lau, W.; Ng, K. Finite and Infinite Dosing. Available online: https://www.researchgate.net/publication/316733922_Finite_and_Infinite_Dosing/link/59ca0d50aca272bb05074cc9/download (accessed on 4 August 2021).
22. Drugs: TORADOL T ROCHE Pill. Available online: https://www.drugs.com/imprints/t-toradol-t-roche-2369.html (accessed on 4 August 2021).
23. Cordero, J.A.; Alarcon, L.; Escribano, E.; Obach, R.; Domenech, J. A Comparative Study of the Transdermal Penetration of a Series of Nonsteroidal Antiinflammatory Drugs. *J. Pharm. Sci.* **1997**, *86*, 503–508. [CrossRef] [PubMed]
24. Humphrey, S.P.; Williamson, R.T. A review of saliva: Normal composition, flow, and function. *J. Prosthet. Dent.* **2001**, *85*, 162–169. [CrossRef]
25. OECD. *Guidance Document for the Conduct of Skin Absorption Studies*; OECD Series on Testing and Assessment, No. 28; OECD Publishing: Paris, France, 2004; Volume 28. [CrossRef]
26. Essendoubi, M.; Gobinet, C.; Reynaud, R.; Angiboust, J.F.; Manfait, M.; Piot, O. Human skin penetration of hyaluronic acid of different molecular weights as probed by Raman spectroscopy. *Ski. Res. Technol.* **2015**, *22*, 55–62. [CrossRef]
27. Mallandrich, M.; Fernández-Campos, F.; Clares, B.; Halbaut, L.; Alonso, C.; Coderch, L.; Garduño-Ramírez, M.L.; Andrade, B.; Del Pozo, A.; Lane, M.E.; et al. Developing Transdermal Applications of Ketorolac Tromethamine Entrapped in Stimuli Sensitive Block Copolymer Hydrogels. *Pharm. Res.* **2017**, *34*, 1728–1740. [CrossRef]
28. Inoue, Y.; Suzuki, K.; Maeda, R.; Shimura, A.; Murata, I.; Kanamoto, I. Evaluation of formulation properties and skin penetration in the same additive-containing formulation. *Results Pharma Sci.* **2014**, *4*, 42–49. [CrossRef] [PubMed]
29. Bredenberg, S.; Duberg, M.; Lennernäs, B.; Lennernäs, H.; Pettersson, A.; Westerberg, M.; Nyström, C. In vitro and in vivo evaluation of a new sublingual tablet system for rapid oromucosal absorption using fentanyl citrate as the active substance. *Eur. J. Pharm. Sci.* **2003**, *20*, 327–334. [CrossRef] [PubMed]
30. Bhati, R.; Nagrajan, R.K. A detailed review on oral mucosal drug delivery system. *Int. J. Pharm. Sci. Res.* **2012**, *3*, 659–681.
31. Netzlaff, F.; Kostka, K.-H.; Lehr, C.-M.; Schaefer, U.F. TEWL measurements as a routine method for evaluating the integrity of epidermis sheets in static Franz type diffusion cells in vitro. Limitations shown by transport data testing. *Eur. J. Pharm. Biopharm.* **2006**, *63*, 44–50. [CrossRef]
32. Amores, S.; Domenech, J.; Colom, H.; Calpena, A.C.; Clares, B.; Gimeno, Á.; Lauroba, J. An improved cryopreservation method for porcine buccal mucosa in ex vivo drug permeation studies using Franz diffusion cells. *Eur. J. Pharm. Sci.* **2014**, *60*, 49–54. [CrossRef]

3.3.- Artículo 3

pharmaceutics

MDPI

Article

Polymeric Nanoparticles and Chitosan Gel Loading Ketorolac Tromethamine to Alleviate Pain Associated with Condyloma Acuminata during the Pre- and Post-Ablation

Salima El Moussaoui [1,†], Ismael Abo-Horan [1,†], Lyda Halbaut [1], Cristina Alonso [2], Lluïsa Coderch [2], María Luisa Garduño-Ramírez [3], Beatriz Clares [4,5,*], José Luis Soriano [4], Ana Cristina Calpena [1,5], Francisco Fernández-Campos [6,‡] and Mireia Mallandrich [1,5,‡]

1 Department of Pharmacy, Pharmaceutical Technology and Physical-Chemistry, Faculty of Pharmacy and Food Sciences, University of Barcelona, Av. Joan XXIII 27-31, 08028 Barcelona, Spain; selmouel9@alumnes.ub.edu (S.E.M.); iabohora7@alumnes.ub.edu (I.A.-H.); halbaut@ub.edu (L.H.); anacalpena@ub.edu (A.C.C.); mireia.mallandrich@ub.edu (M.M.)
2 Institute of Advanced Chemistry of Catalonia-CSIC (IQAC-CSIC), 18-26 Jordi Girona St., 08034 Barcelona, Spain; cristina.alonso@iqac.csic.es (C.A.); luisa.coderch@iqac.csic.es (L.C.)
3 Centro de Investigaciones Químicas, Universidad Autónoma del Estado de Morelos, Avenida Universidad 1001, Cuernavaca 62209, Mexico; lgarduno@uaem.mx
4 Department of Pharmacy and Pharmaceutical Technology, School of Pharmacy, University of Granada, 18071 Granada, Spain; jlsoriano@correo.ugr.es
5 Institut de Nanociència i Nanotecnologia IN2UB, Universitat de Barcelona, 08028 Barcelona, Spain
6 Reig-Jofre Laboratories, Av. de les Flors s/n, 08970 Sant Joan Despí, Spain; ffernandez@reigjofre.com
* Correspondence: beatrizclares@ugr.es
† These authors contribute equally to this work.
‡ These authors contribute equally to this work.

Citation: El Moussaoui, S.; Abo-Horan, I.; Halbaut, L.; Alonso, C.; Coderch, L.; Garduño-Ramírez, M.L.; Clares, B.; Soriano, J.L.; Calpena,

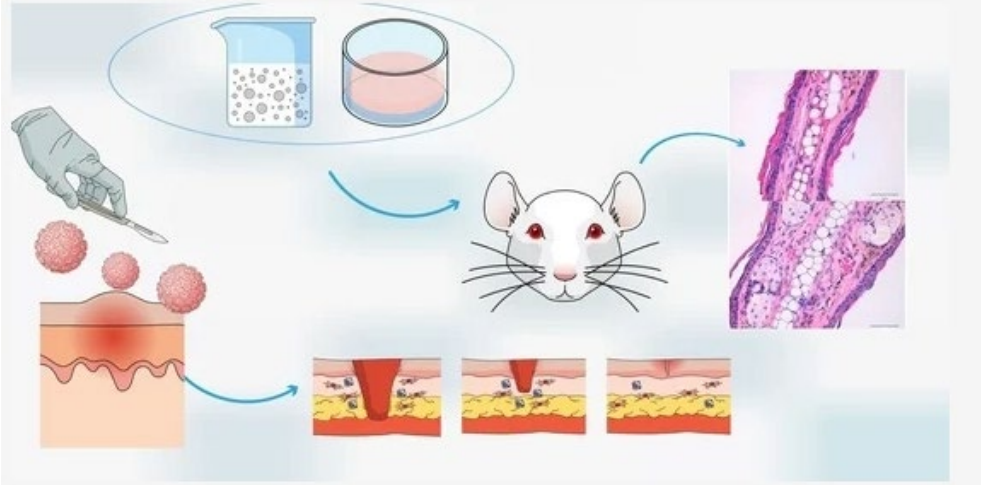

Graphical abstract

Current Impact Factor	JCR category rank
6.321	Q1 Pharmacology & Pharmacy

Resumen

Este estudio describe la preparación y evaluación de dos formulaciones, un hidrogel y un sistema nanoestructurado, que contienen ketorolaco trometamina como agente antiinflamatorio para la terapia local contra el proceso inflamatorio derivado de la escisión quirúrgica de Condyloma acuminata. Ambas formulaciones fueron caracterizadas fisicoquímicamente. Los perfiles de liberación in vitro muestran que las nanopartículas liberan el 92 % ± 2,3 del total de ketorolaco trometamina encapsulado, mientras que el gel de quitosano libera el 18,6 % ± 0,2. También se ensayó la permeación y distribución ex vivo a través de la piel humana y se observó cómo la mayor parte de ketorolaco trometamina se retiene en la epidermis. Se realizaron estudios in vivo para evaluar la eficacia antiinflamatoria en ratones que también incluyeron el análisis histológico para confirmar los resultados in vivo. Las nanopartículas presentan una eficacia antiinflamatoria significativamente mayor que el gel de quitosano. La tolerabilidad de las formulaciones desarrolladas se evaluó monitoreando las propiedades biomecánicas de la piel antes y después de la aplicación de ambas formulaciones. No se observaron diferencias estadísticas en la pérdida de agua transepidérmica y la hidratación de la piel con respecto a los valores basales y las formulaciones exhibieron una mayor actividad antiinflamatoria en comparación con una solución de ketotorlaco trometamina de referencia. Por lo tanto, se puede concluir que ambas formulaciones pueden proponerse como candidatas sobresalientes para ofrecer una herramienta terapéutica antiinflamatoria local con potencial aplicación clínica.

pharmaceutics

MDPI

Article

Polymeric Nanoparticles and Chitosan Gel Loading Ketorolac Tromethamine to Alleviate Pain Associated with Condyloma Acuminata during the Pre- and Post-Ablation

Salima El Moussaoui [1,†], Ismael Abo-Horan [1,†], Lyda Halbaut [1], Cristina Alonso [2], Lluïsa Coderch [2], María Luisa Garduño-Ramírez [3], Beatriz Clares [4,5,*], José Luis Soriano [4], Ana Cristina Calpena [1,5], Francisco Fernández-Campos [6,‡] and Mireia Mallandrich [1,5,‡]

1 Department of Pharmacy, Pharmaceutical Technology and Physical-Chemistry, Faculty of Pharmacy and Food Sciences, University of Barcelona, Av. Joan XXIII 27-31, 08028 Barcelona, Spain; selmouel9@alumnes.ub.edu (S.E.M.); iabohora7@alumnes.ub.edu (I.A.-H.); halbaut@ub.edu (L.H.); anacalpena@ub.edu (A.C.C.); mireia.mallandrich@ub.edu (M.M.)
2 Institute of Advanced Chemistry of Catalonia-CSIC (IQAC-CSIC), 18-26 Jordi Girona St., 08034 Barcelona, Spain; cristina.alonso@iqac.csic.es (C.A.); luisa.coderch@iqac.csic.es (L.C.)
3 Centro de Investigaciones Químicas, Universidad Autónoma del Estado de Morelos, Avenida Universidad 1001, Cuernavaca 62209, Mexico; lgarduno@uaem.mx
4 Department of Pharmacy and Pharmaceutical Technology, School of Pharmacy, University of Granada, 18071 Granada, Spain; jlsoriano@correo.ugr.es
5 Institut de Nanociència i Nanotecnologia IN2UB, Universitat de Barcelona, 08028 Barcelona, Spain
6 Reig-Jofre Laboratories, Av. de les Flors s/n, 08970 Sant Joan Despí, Spain; ffernandez@reigjofre.com
* Correspondence: beatrizclares@ugr.es
† These authors contribute equally to this work.
‡ These authors contribute equally to this work.

Abstract: This study describes the preparation and evaluation of two formulations, a hydrogel and a nanostructured system, containing ketorolac tromethamine as an anti-inflammatory agent for the local therapy against the inflammatory process derived from the surgical excision of Condyloma acuminata. Both formulations were physicochemically characterized. In vitro release profiles show that the nanoparticles release 92% ± 2.3 of the total ketorolac tromethamine encapsulated, while the chitosan gel releases 18.6% ± 0.2. The ex vivo permeation and distribution through human skin were also assayed and was observed how the main amount of ketorolac tromethamine is retained in the epidermis. In vivo studies were accomplished to evaluate the anti-inflammatory efficacy in mice which also involved the histological analysis to confirm the in vivo results. The nanoparticles present a significantly higher anti-inflammatory efficacy than chitosan gel. The tolerability of developed formulations was assessed by monitoring the biomechanical properties of the skin before and after application of both formulations. No statistical differences in trans-epidermal water loss and skin hydration with respect to the basal values were observed and the formulations exhibited higher anti-inflammatory activity compared to a reference ketotorlac tromethamine solution. Therefore, it can be concluded that both formulations can be proposed as outstanding candidates for offering a local anti-inflammatory therapeutical tool with potential clinical application.

Keywords: PLGA nanoparticles; chitosan gel; Condyloma acuminata; ketorolac tromethamine; anti-inflammatory; topical delivery

check for updates

Citation: El Moussaoui, S.; Abo-Horan, I.; Halbaut, L.; Alonso, C.; Coderch, L.; Garduño-Ramírez, M.L.; Clares, B.; Soriano, J.L.; Calpena, A.C.; Fernández-Campos, F.; et al. Polymeric Nanoparticles and Chitosan Gel Loading Ketorolac Tromethamine to Alleviate Pain Associated with Condyloma Acuminata during the Pre- and Post-Ablation. *Pharmaceutics* **2021**, *13*, 1784. https://doi.org/10.3390/pharmaceutics13111784

Academic Editor: Jesus Perez-Gil

Received: 31 August 2021
Accepted: 20 October 2021
Published: 25 October 2021

Publisher's Note: MDPI stays neutral with regard to jurisdictional claims in published maps and institutional affiliations.

1. Introduction

Sexually transmitted infections (STIs) represent nowadays a significant public health problem [1]. One of the most common STIs is the human papillomavirus (HPV) infection [2], being Condyloma acuminata (CA) its clinical manifestation [3]. To date, more than 200 HPV strains have been sequenced, of which 40 are known to cause genital infections [2]. There are two types of HPV in terms of the oncogenic risk, of which the virus subtypes 6 and 11,

are classified as of low oncogenic risk, and are those which are mainly responsible 90% of cases. It is noteworthy that subtypes 16 and 18 in contrast are deemed as high-risk strains, due to their oncogenic potential [4]. Patients aged 20 to 39 account for more than 70% of CA infections [5]. Children [6] and pregnant women can also be affected [7].

Even though asymptomatic Condyloma acuminata is common, certain cases might be accompanied by itching, pain, and bleeding [8]. The treatment strategy could be ablative or by using topical procedures based on the localization, size and morphology of the lesions [2]. In some cases, such as intra-anal involvement, the ablative strategy might be the only option [5]. However, Condyloma acuminate is known for its recurrence, particularly if HPV 11 has been diagnosed [9]. In previous studies, our research group investigated the use of topical ketorolac tromethamine (KT) as a good alternative for managing the inflammatory process following the excision of anogenital warts with promising results by loading the drug in alginate-based hydrogel [4]. KT is a non-steroidal anti-inflammatory drug (NSAID) belonging to the Aryl acetic acid derivatives. It is used for the relief of postoperative pain and the management of inflammation [10].

Stemming from the nanoparticles (NPs) having the property of sustained drug release, the drug can reach the skin over a prolonged time period and can be retained in the skin at the desirable concentration [11]. In this context poly (D, L-lactic-co-glycolic acid) (PLGA) has demonstrated immense potential among the matrixes used for NPs owing to its biocompatible and biodegradable properties, among others [12].

Chitosan (CTS), a natural polymer, is a promising candidate for controlled drug delivery systems and wound healing [13]. It being a strong candidate is due to their properties such as biocompatibility, biodegradability, antimicrobial activity, low immunogenicity, mucoadhesivity, hydrophilicity and ease modification [14]. Additionally, CTS can also provide antifungal properties and hemostatic properties as well as the anti-inflammatory effect [13,14]. All these properties are of great interest for the management and care of the areas treated post-surgically, thus positively influencing the reduction of complications such as bleeding and infections and this favors the wound healing process [15].

Skin is the largest human organ which accounts for roughly 10% of an average total body mass. The main function of skin is to act as a barrier preventing moisture and the loss of nutrients and protecting against ultraviolet (UV) radiation action, chemicals, allergens and microorganisms [16]. Transdermal Drug Delivery (TDD) offers various benefits over other traditional drug delivery routes such as it is painless and non-invasive with fewer side effects, and more patient compliance among other benefits [17]. *Stratum corneum* (SC) is the outer layer of the epidermis with a crucial barrier function. Many strategies have been investigated to overcome this barrier and facilitate the drug permeation [18,19]. However, overcoming the SC to reach the deeper layers of skin or the systemic circulation is not always appropriate. In certain cases, such as Condyloma acuminata, where the infection occurs in the epidermis, taking advantage of the drug accumulation in this skin layer would be a great strategy for local treatment.

Taking all the above into account, in this work, we formulated KT into a PLGA nanostructured system as a vehicle for preventing the inflammatory process during the surgical excision of warts. The KT-NPs may be easily sprayable onto warts without the need to contact them. At the same time, we formulated KT into a CTS-based hydrogel as a vehicle for managing the local inflammatory process stemming from the post-operative stage in the surgical excision of warts taking advantage of the mucoadhesive and regenerative properties of CTS. Both formulations were characterized and evaluated in vitro, ex vivo and in vivo.

2. Materials and Methods

2.1. Materials

KT, polyvinyl alcohol (PVA) with 90% hydrolyzation, ethyl acetate (EA), lactic acid solution 85%, phosphate buffer solution (PBS) pH 7.6, gentamicin sulphate and bovine serum albumin were purchased from Sigma-Aldrich (Barcelona, Spain). CTS was obtained from

FagronIberica (Terrassa, Spain). PLGA (Resomer® RG 503) was acquired from Boehringer Ingelheim (Ingelheim, Germany). Adhesive tapes were obtained from D-squame, (Cuderm Co., Dallas, TX, USA). Double distiller water was obtained from a Milli-Q1 Gradinet A10 system apparatus (Millipore Iberica S.A.U., Madrid, Spain). All the other chemicals and reagents used in the study were all of analytical grade (Panreac, Castellar del Vallès, Spain).

2.2. Preparation of Formulations

2.2.1. Preparation of CTS Gel

CTS gel was prepared weighting an accurate amount of CTS and dispersing the polymer in 1% lactic acid solution under continuous stirring so as to obtain a final concentration of 3% (*w/v*) until dissolution. Then, the mixture was allowed to swell in the fridge overnight. Appropriate amount of KT (2%; *w/v*) was added once the gel was swollen and gently homogenized. Table S1 in Supplementary Materials depicts the critical process parameters and Table S2 shows the Quality Target Product Profiles.

2.2.2. Preparation of NPs

NPs were prepared using the double emulsion-solvent evaporation method as described previously with modification [20,21]. The NPs were optimized by a two-level full factorial design for 3 factors in standard order, which led to 8 candidate formulations (Table S3). In brief, 250 µL of the inner aqueous phase pH 2.0 (W_1) consisting of a PVA 2% (*w/v*) and KT (80 mg/mL) solution were added to 1 mL of the oily phase (O), which contained 90 mg of PLGA in ethyl acetate. A probe Vibra-Cell® sonicator (Sonics and Materials, Inc., Newtown, CT, USA) was used to homogenize this mixture for 20 s in two 10 s cycles at 50 watts and 30% amplitude, resulting in a primary emulsion (W_1/O), in which 2 mL of external aqueous phase (W_2), PVA 2% (*w/v*), was added drop-wise and subjected to a second sonication process for 1.5 min, 10 s cycles (50 watts and 30% amplitude) to produce the double emulsion ($W_1/O/W_2$). Finally, a volume of 5 mL of PVA 0.3% (*w/v*) was added to the double emulsion before the organic solvent was evaporated under reduced pressure (Bücchi B-480, Flawil, Switzerland) for about 15 min at 36 °C and 74 mbar vacuum. For comparison studies, blank NPs were also fabricated. Table S1 shows the critical process parameters and Table S2 shows the Quality Target Product Profiles.

2.3. Physical Characterization of Formulations

2.3.1. Characterization of CTS Gel

pH Study

The pH was recorded in triplicate by pH meter micropH 2000 (Crison Instruments SA, Alella, Spain) at room temperature.

Swelling and Degradation Tests

The swelling ratio (SR) was assayed based on a gravimetric method. For this task, known amounts of dried hydrogel were immersed in PBS (pH = 5.5) for 3 h at 32 °C. Samples were removed and weighed (W_t) after blotting the surface water at pre-established times. The PBS uptake was measured in triplicate. The swelling ratio was determined using the following equation:

$$SR = \frac{W_s - W_d}{W_d} \quad (1)$$

where W_s is the weight of the swollen hydrogel at various times and W_d is the weight of dried hydrogel.

The gel degradation rate was evaluated in terms of percentage of weight loss (WL). Briefly, known amounts of dried hydrogel were immersed in PBS (pH = 5.5) at 32 °C for

3.75 h. Samples (n = 3) were then dried and weighed at pre-established time intervals. The following equation was used to calculate the WL:

$$WL(\%) = \frac{W_i - W_d}{W_i} 100\% \quad (2)$$

where W_i denotes the initial weight of the hydrogel and W_d denotes the weight of the hydrogel at various times.

Both, the swelling and the degradation were fitted to mathematical models. The best fit was chosen based on the determination coefficient value (R^2).

Morphological Studies

Scanning Electron Microscopy (SEM) was used to visualize the internal structure of developed hydrogel in a JEOL J-7100F (JEOL Inc., Peabody, MA, USA). Samples were carbon-coated with an Emitech K950X coater (Quorum Technologies Ltd., Kent, UK).

Rheological Study

The rheological properties of CTS gel were analyzed in a rotational HaakeRheo Stress 1 rheometer (Thermo Fisher Scientific, Karlsruhe, Germany) with cone-plate geometry (Haake C60/2° Ti, 60 mm diameter, 0.105 mm cone-plate gap). The shear profile was evaluated following a ramp-up stage (0–100 s^{-1} for 3 min), a constant shear rate stage (100 s^{-1} for 1 min), and a ramp-down stage (100–0 s^{-1} for 3 min). All measurements were taken in triplicate at room temperature and the steady-state viscosity was recorded at 100 s^{-1} (constant shear stretch).

Experimental results were then fitted to different mathematical models by regression analysis [4].

2.3.2. Characterization of the NPs

Physicochemical Characterization

Both, the mean particle size (Zave), the polydispersity index (PI) and the zeta potential (ZP) of the KT-NPs were determined by dynamic light scattering (DLS). The characterization was carried outby diluting the samples 1/20 in Milli-Q water and measuring by a Zetasizer Nano Zs (Malvern Instruments, Malvern, UK) at 25 °C with disposable cuvettes.

The pH of the resulting colloidal suspension of NPs was measured by pH metermicrop H 2000 (Crison Instruments SA, Alella, Spain).

Transmission electron microscopy (TEM) technology was used to evaluate the structure of KT-NPs with a JEOL 1010 (JEOL Inc., Tokyo, Japan) at 80 Kv. Uranyl acetate (1% *w/v*) was used as a staining solution to visualize the NPs. The image processing program Image J (1.53 e) was utilized to measure the particle size starting from the produced TEM image.

Encapsulation Efficiency

An indirect method was used to determine the KT encapsulated in the NPs based on the measuring of the non-entrapped KT in the dispersion medium. For this purpose, fresh KT-NPs were centrifuged for 15 min at 14,000 rpm (Sigma 301K, Sigma Laborzentrifugen GmbH, Osterode am Harz, Germany). Subsequently, free KT was separated using Ultracel YM-100 filters (Millipore, Bedford, MA, USA) and collected in the filtered solution.

The determination of the KT was performed using a high-performance liquid chromatography (HPLC) methodology which had been previously validated. The encapsulation efficiency (EE) was calculated using Equation (3).

$$EE\% = \frac{\text{Total amount of KT} - \text{free KT}}{\text{Total amount of KT}} \quad (3)$$

2.4. Stability Studies

The physical stability of KT-NPs stored at 4 °C was studied for 3 months by monitoring potential changes in Zave, PI and EE.

The stability of the KT-CTS gel was visually evaluated. The formulation was stored at room temperature for 3 months.

2.5. In Vitro Drug Release Study

To investigate the KT release from NPs and the CTS gel, vertical Franz diffusion cells (Vidrafoc, Barcelona, Spain) with a diffusion area of 2.54 cm^2 were used. A dialysis membrane (MWCO 12,000–14,000 Da., Medicell International Ltd., London, UK) was placed between the donor and receptor chambers in the case of NPs and nitrocellulose 0.45 μm pore size (Millipore Merck, Madrid, Spain) for CTS gel. The receptor medium was PBS solution pH 7.4. The system was kept at 32 ± 0.5 °C under continuous stirring, maintaining sink conditions throughout the course of the experiment. 200 μL of KT-NPs (n = 6) and 200 mg of CTS gel (n = 6) were put into the donor compartment. Aliquots of 300 μL were removed at predetermined intervals of up to 9 h and replaced with an equivalent volume of tempered receptor medium. The experimental data were fitted to first order, using the Prism software, v. 5 (GraphPad Software, Inc., San Diego, CA, USA).

2.6. Ex Vivo Permeation Studies

The penetration and permeation of KT in and through skin was evaluated ex vivo using human skin. The skin was obtained from abdominoplasties (protocol code N°001 approved on 20/01/2016 by Bioethics Committee of the Barcelona-SCIAS Hospital); which was frozen and kept at −20 ± 5 °C until the date of the permeation test. Then, specimens were dermatomed at 500 μm pieces. The human skin pieces were allowed to thaw at room temperature and then were placed between the donor and receptor chambers of Franz static diffusion cells (Lara-Spiral, Courtenon, France). The Franz cells consisted of a 3 mL receptor volume and 1.86 cm^2 diffusion area.

The experimental system used PBS (pH 7.6), gentamicin sulphate 0.04% (*w/v*) to prevent skin degradation [22] and bovine serum albumin 1% (*w/v*) as receptor fluid at 32 °C continuously stirred at 500 rpm by a magnetic bar allowing sink conditions throughout the test. 10 μL samples (either NPs or CTS gel) were placed on the donor chamber.

At the end of the experiment (24 h), skin membranes were demounted, and the remaining formulation amounts were recovered by a swab. Equally, the receptor fluid was collected to measure the amount of KT distributed at each skin layer [9]. KT was extracted from the skin samples by sonication in a water:methanol (1:1, *v/v*) medium for 20 min. KT was determined by HPLC. The extracted amount of KT is expressed as $\mu g/cm^2$ and percentage (%) of the applied dose. Control cells were also used to evaluate potential interferences in the sample analysis of the receptor fluid or skin samples using unloaded gel and blank NPs.

2.7. HPLC Analysis

KT in samples was determined using HPLC methodology validated in terms of linearity, accuracy, and precision according to ICH Q2 (R1) validation guidelines. The HPLC system consisted of a Waters 717 plus Autosampler with a detector Waters 2487 (Waters, Milford, MA, USA); a C18 column YMC-Pack Pro, 250 × 4.6 mm, 5 μm (YMC Co., LTD, Kyoto, Japan) was used with a flow rate of 1 mL/min at isocratic conditions. The mobile phase was carried out with acidified water (glacial acetic acid 1.65%) and acetonitrile with 0.065% of triethylamine at the elution conditions of 1:1 *v/v*. The volume of injection was 10 μL. The wavelength was set at 314 nm.

2.8. In Vivo Anti-Inflammatory Efficacy Evaluation

2.8.1. TPA-Induced Ear Oedema in Mice

Male Swiss CD-1 mice (20–25 g) purchased from Circulo AND, S.A. de C.V. (Coyacan D.F., Mexico) were kept under standard animal housing conditions in a 12 h dark-light cycle with access to food and water ad libitum. This study was approved by the animal research ethical committee of the Vivarium at University of Morelos (protocol code BIO-UAEM 03:2019 date of approval February 2019).

The protocol was carried out as previously reported by Domínguez-Villegas et al. [23]. A 12- O-detradecanoylphorbol-13-acetate (TPA) solution of 50 mg/mL in ethanol was used to induce mouse ear oedema inflammation. Animals were divided into three groups of three specimens each one (n = 3). 5 µL of TPA solution was applied to both sides of the right ear simultaneously with 100 mg of formulation (KT-CTS gel to group 1 and KT-NPs to group 2) as well as 5 µL of ethanol to both sides of the left ear. The control group was treated with an equal amount of KT solubilized in acetone applied to both sides of the right ear and 5 µL of acetone to both sides of the left ear. The animals were then sacrificed by cervical dislocation 4 h after treatment and 7 mm circular sections were cut from the left and right ears. These were weighted accurately. The anti-inflammatory activity expressed as a percentage of inhibition of the inflammatory process was calculated according to the Equation (4):

$$\text{Inhibition}(\%) = \left(\frac{\text{Weight control ear} - \text{Weight treated ear}}{\text{Weight control ear}}\right) \times 100 \quad (4)$$

2.8.2. Histological Analysis

Histological analysis of the circular sections was conducted after TPA-induced oedema in mice to evaluate the anti-inflammatory efficacy by observing whether immunologic cells were present in the tissues. Hence, the circular ear sections were fixed in 4% formaldehyde solution and then embedded in paraffin to obtain histological cuts which were stained with hematoxylin-eosin and observed by light microscopy.

2.9. In Vivo Tolerance Study

The study was carried out with 10 healthy-skinned female participants ranging in age from 21 to 64 years old. The study was authorized by the University of Barcelona's Ethics Committee (IRB00003099, approved on 20 March 2018), which followed the Declaration of Helsinki's guidelines. All the participants provided written informed consent forms. Volunteers were asked to not use cosmetic or another skin care products on the test areas during two days before the study. The subjects stayed in the test room for at least 30 min before taking the measurements. Several readings were collected from the flexor side of the left forearm before applying the formulation (baseline readings). Then, readings were collected newly just after application of a uniform layer (0.1 mL/cm^2) of formulation at1 h after application and at 2 h. The total quantity of water lost (TEWL) through the skin was measured using a Tewameter® TM 300. (Courage-Khazaka electronic GmbH, Cologne, Germany). The hydration of the stratum corneum (SCH) was determined using a Corneometer® CM 825. (Courage-Khazaka electronic GmbH, Cologne, Germany). All measurements were taken in accordance with published procedures.

2.10. Statistical Analysis

All statistical analyses were performed using the Prism® software, v. 5 (GraphPad Software Inc., San Diego, CA, USA). T-student tests were performed on the in vitro release and the ex vivo permeation studies to compare both formulations. Furthermore, analysis of variance (ANOVA) was conducted on the in vivo anti-inflammatory efficacy study to compare the formulations, as well as in the in vivo tolerance study to compare the biomechanical properties if the skin over time to the basal values. The level of statistical significance was set at $p < 0.05$.

3. Results

3.1. Characterization of Formulations

3.1.1. Characterization of CTS Gel

The resulting CTS gel was transparent and extremely viscous with poor flowability. The pH of the CTS gel was 4.4 ± 0.1 and 5.5 ± 0.1 for KT-CTS gel.

Figure 1 shows the swelling and degradation profiles of KT-CTS gel and blank CTS gel. Similar profiles were observed for both gels, indicating that the addition of KT in the gel does not affect the gel structure. Nevertheless, significant statistical differences were found between the KT-CTS gel and blank CTS gel in terms of the initial weight on the swelling study. It can be seen that the swelling is a linear and steady process following a zero-order kinetic with a lag-time of 10 min. This formulation was able to absorb PBS up to 4.5-fold its weight.

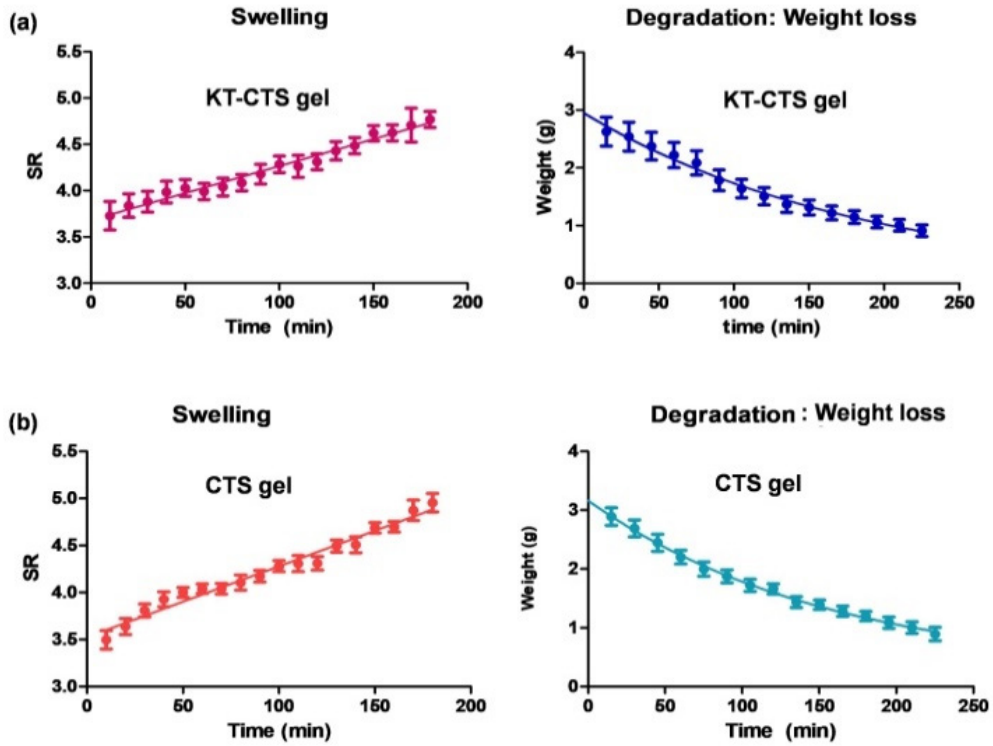

Figure 1. Swelling and degradation processes of KT-CTS gel. Modelling graphic expressed as mean ± SD (n = 3). Panel (**a**) shows the KT-CTS gel; and panel (**b**) the blank gel without KT (CTS gel).

After 3.75 h ± 0.22 h, the CTS gel had utterly degraded in the medium (PBS). The weight loss fitted to a one-phase exponential decay. Table 1 shows the fitted parameters values for both processes.

Table 1. Best-fit values of the swelling and degradation processes of CTS gel with and without KT.

	Parameter	Swelling	Degradation
KT-CTS gel	Y_0 (g) [1]	3.681 ± 0.050 *	2.952 ± 0.168
	K [2]	0.006 ± 0.001	0.005 ± 0.002
	R^2	0.9033	0.9322
CTS gel (blank)	Y_0 (g) [1]	3.526 ± 0.062	3.164 ± 0.183
	K [2]	0.008 ± 0.001	0.006 ± 0.002
	R^2	0.9085	0.9341

[1] Y_0 = initial weight; [2] K = degradation constant (g/min) or swelling constant (min^{-1}); * statistical differences between the KT-CTS gel and blank CTS gel (significance level set at $p < 0.05$).

The surface of the dried KT-CTS gel was evaluated by SEM. The gel presented a compact and dense appearance, with smooth surface which presented micro-irregularities where the water and KT may be interposed within the polymer structure (Figure 2).

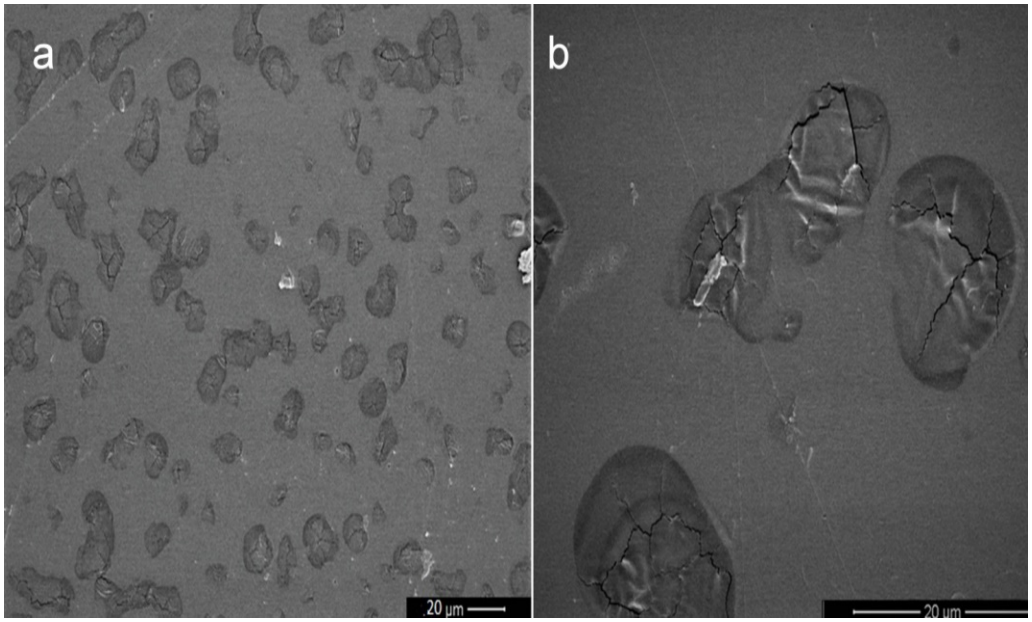

Figure 2. SEM images of the dried discs of KT-CTS gel. (**a**) Magnification 1000×; and (**b**) magnification 5000×; the scale bar is 20 µm length.

To predict the potential topical usage of KT-CTS gel, the rheological study was carried out. The mathematical model that best fitted experimental flow data was the Casson model (r^2 = 0.999), confirming a shear-thinning behavior of KT-CTS gel. In Figure 3 is depicted the rheological profile which revealed that the gel has a pseudoplastic behavior with a viscosity of 1.431 Pas ± 0.0004.

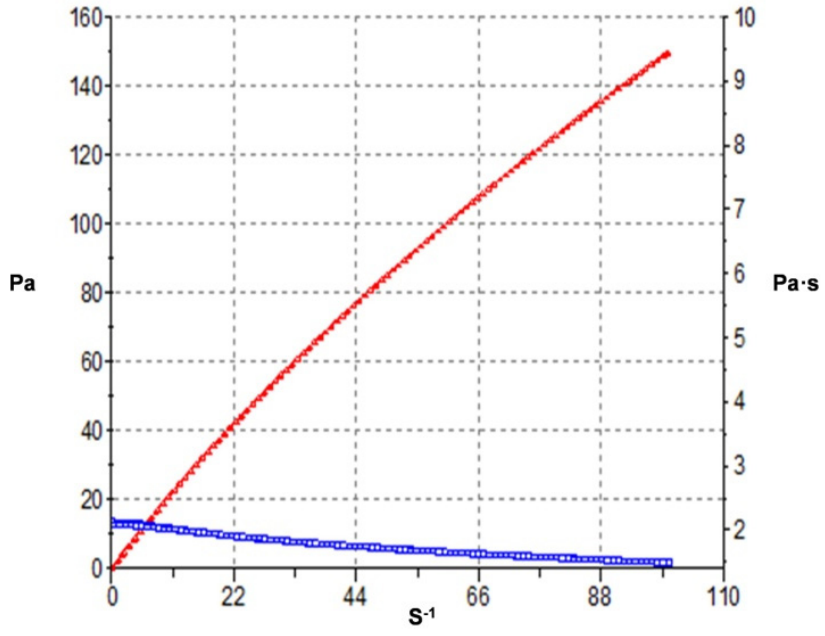

Figure 3. Rheological profile of KT-CTS gel. Blue curve represents the formulation viscosity. Red curve represents the shear stress of the formulation.

3.1.2. Characterization of NPs

The resulting KT-NPs showed a high EE, concretely 93.91%. The Zave was 108.9 ± 2.3 nm with a PI value of 0.061 indicative of narrow distribution, and a ZP of −6.20 mV. The pH of the external aqueous phase W_2 resulted in 5.2.

As depicted in Figure 4, the TEM image shows round-shaped structure of KT-NPs. The particle size associated was 51.9 ± 14.5 nm (26.4 nm was the minimum size, whereas the maximum was 92.7 nm).

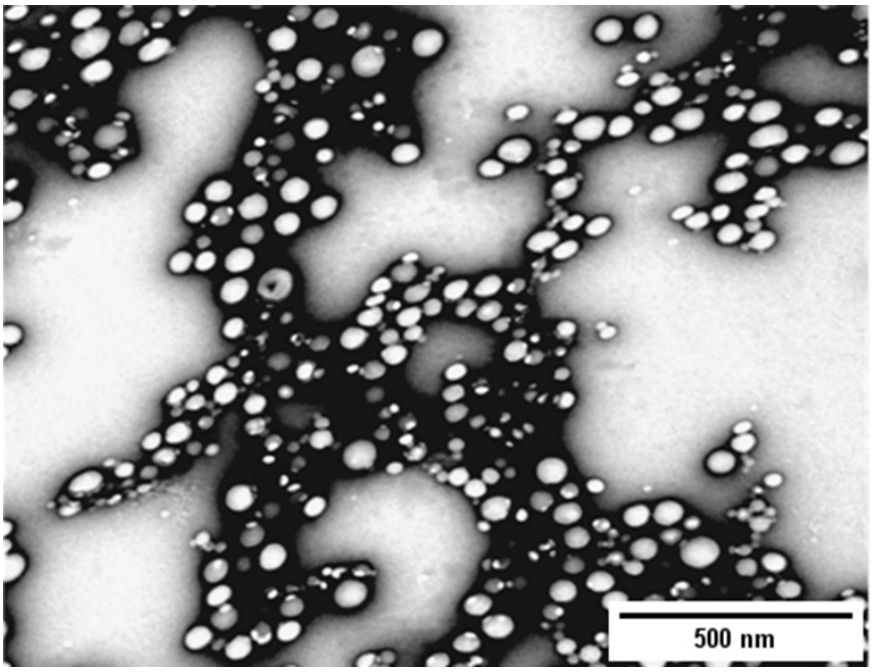

Figure 4. TEM image of KT-NPs.

3.2. Stability Studies

The stability of the formulations was evaluated at 3 months, stored at 25 °C and 4 °C for the KT-CTS gel and the KT-NPs, respectively. After 3 months of storage of KT-CTS gel at room temperature (25 °C), no visual changes in appearance were evidenced.

The KT-NPs stored at 4 °C for 3 months neither showed statistically significant changes in the Zave, the PI, the ZP nor the EE (Table 2). The statistical significance level was set at $p < 0.05$.

Table 2. Comparison of the particle size (Zave), polydispersity index (PI), zeta potential (ZP), pH of the external aqueous phase and encapsulation efficiency (EE) from the KT-NPs at time 0 and time 90 days ($n = 3$) stored at 4 °C. Results are expressed as mean ± standard deviation.

Parameter	KT-NPs Day 0	KT-NPs Day 90	*p*-Value
Zave (nm)	108.9 ± 2.3	111.2 ± 3.6	$p = 0.4039$
PI	0.061 ± 0.013	0.064 ± 0.018	$p = 0.8265$
ZP	−6.20 ± 0.48	−6.28 ± 0.39	$p = 0.8337$
pH aqueous external phase (W_2)	5.2 ± 0.1	5.2 ± 0.2	$p = 1.000$
EE%	93.9 ± 2.83	92.4 ± 2.45	$p = 0.5258$

3.3. In Vitro Drug Release Study

The release profiles of both formulations were investigated by the in vitro diffusion cells technique. The NPs allowed a higher degree of release of KT than the CTS gel (Figure 5).

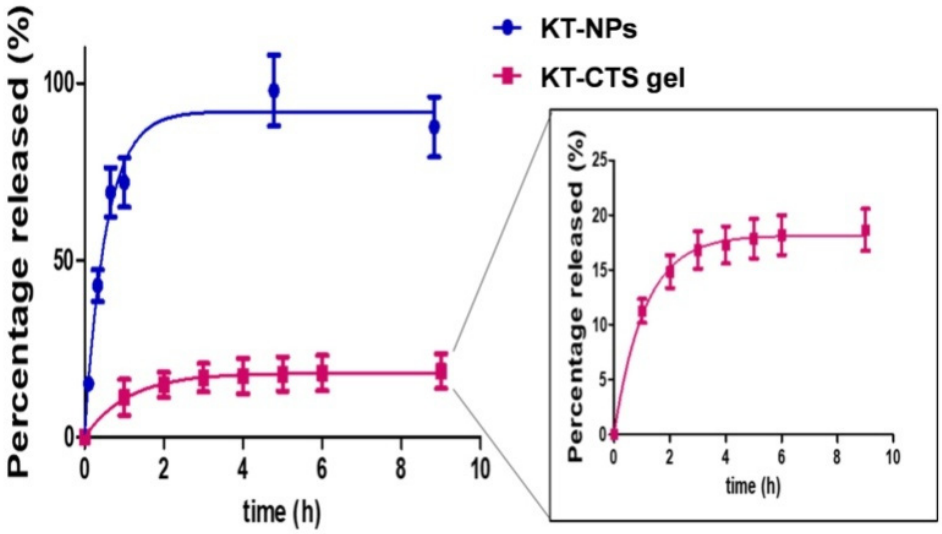

Figure 5. In vitro release profile of the formulations, KT-NPs and KT-CTS gel ($p < 0.001$). Each value represents mean ± SD ($n = 6$).

According to the drug release study, the best-fitted model to the experimental data was the first-order kinetic equation with a K value of 0.901 h^{-1} for KT-CTS gel and 1.841 h^{-1} for the KT-NPs (Table 3). Significant statistical differences were found for all the parameters evaluated.

Table 3. Parameters of KT release from KT-CTS gel and KT-NPs according to first-order kinetics. Values are expressed as the Mean ± standard deviation ($n = 6$).

Parameter	KT-CTS Gel	KT-NPs	*p*-Value
%R∞ (%) [1]	18.6 ± 0.3	92.0 ± 2.3	$p < 0.0001$
K (h^{-1}) [2]	0.9 ± 0.2	1.8 ± 0.1	$p < 0.0001$
Half-time (h)	0.8	0.4	$p = 0.0014$
R^2	0.9422	0.9287	-

[1] %R∞ represents the maximum percentage of KT released; [2] K represents the release rate.

3.4. Ex Vivo Permeation of KT through Human Skin

Ex vivo permeation studies were carried out to examine the permeability of KT through human skin and investigate the biodistribution of KT in the skin layers. A large percentage of KT was found on the skin surface in the residual formulation, for both, the NPs and the CTS gel as depicted in Table 4. NPs provided greater absorption of KT than the CTS gel. In the case of NPs, the KT was mainly retained in the epidermis whereas it was in the receptor fluid in the case of the CTS gel. The CTS gel led to higher percutaneous absorption of KT than the NPs. However, no significant statistical differences were found in the KT amount retained or in the epidermis or in the amount percutaneously absorbed. Statistical differences were only observed in the amount diffused into the receptor fluid and the amount penetrated in the *stratum corneum*.

Table 4. Skin distribution of KT (expressed as μg/cm^2) contained in the formulations with an in vitro test after an exposure time of 24 h. Values are expressed as mean ± SD (n = 6).

Biodistribution	KT-NPs (μg/cm^2)	KT-CTS Gel (μg/cm^2)	p-Value
Total applied	14.61	26.91	-
Skin surface	12.14 ± 1.31	26.51 ± 0.84	-
Stratum corneum	0.08 ± 0.02	0.04 ± 0.01	0.03 *
Epidermis	0.71 ± 0.32	0.32 ± 0.17	0.13
Dermis	0.001 ± 0.001	0.002 ± 0.001	0.57
Receptor Fluid	0.02 ± 0.01	0.49 ± 0.09	<0.01 *
Total recovery	12.95 ± 0.84	27.36 ± 0.85	-
Percutaneous Absorption	0.73 ± 0.32	0.81 ± 0.19	0.71

* Statistical differences between formulations ($p < 0.05$).

3.5. In Vivo Anti-Inflammatory Efficacy Evaluation

3.5.1. TPA-Induced Ear Oedema in Mice

The acute ear skin oedema model created by topical administration of TPA was used to assess the formulations anti-inflammatory activity. As a reference of inflammatory inhibition, a KT solution in acetone was used. Figure 6 shows the percentage of inhibition for each formulation.

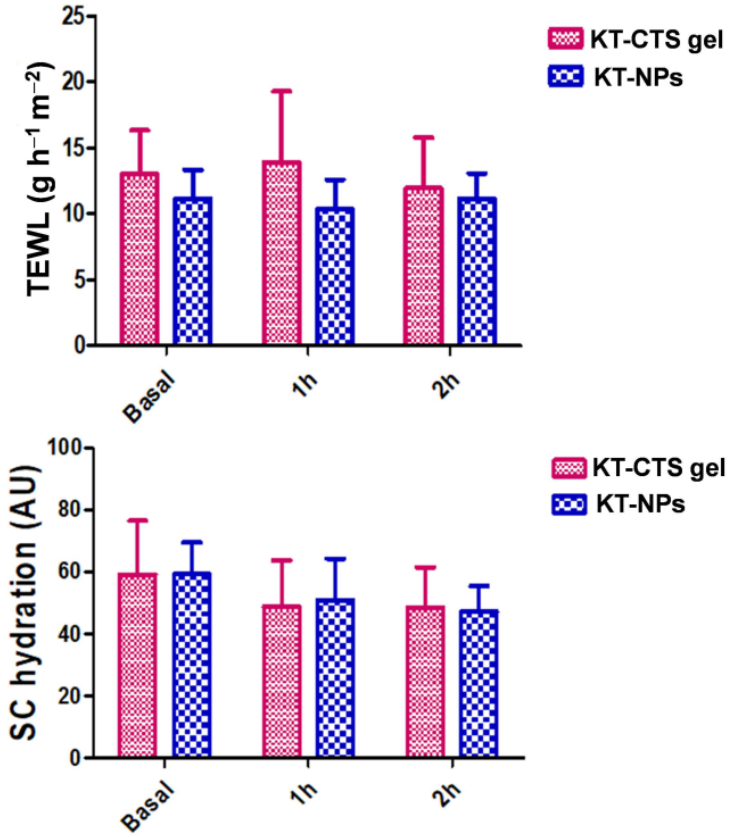

Figure 6. Biomechanical properties in human volunteers before the formulations applications (Basal) 1 h and 2 h post-application: TEWL for both formulations; and the evolution of the stratum corneum hydration for both formulations.

The formulation of the NPs was the one that exhibited the highest reduction in inflammation, and both formulations showed greater anti-inflammatory efficacy than the reference KT solution in acetone. All differences were statistically significant.

3.5.2. Histological Analysis

After the TPA-induced inflammation, a histological evaluation of the mice ears was conducted. Figure 7a,b shows the histological images for the negative and positive controls, respectively, as well as for the treated tissues with either KT-NPs (Figure 7c) or KT-CTS gel (Figure 7d). No immune system cells were found in the negative control sample (Figure 7a). On the contrary, the positive control shows immune system cells in blood vessels (Figure 7b). The ear treated with KT-NPs did not present immune system cells (Figure 7c). A limited number of immune cells systems were observed in the blood vessels of the ear treated with KT-CTS gel (Figure 7d).

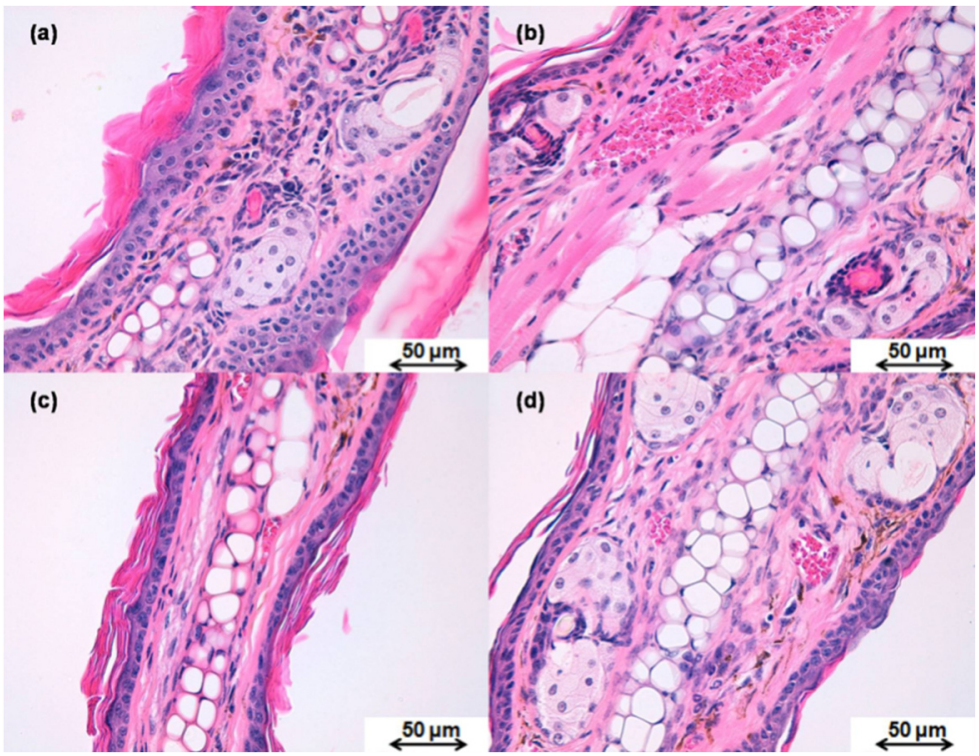

Figure 7. Histological images of the mice ear after the TPA-induced ear oedema in the (**a**) negative control ear, (**b**) positive control ear, (**c**) ear treated with KT-NPs, and (**d**) ear treated with KT-CTS gel. The scale bar is 50 µm in length. The small purple cells corresponding to the immune system cells.

3.6. *In Vivo Tolerance Study*

Figure 8 shows the evolution of biomechanical parameters as tracked before and after the formulations were applied for up to 2 h. This was to assess the impact of the formulations on the skin hydration and its integrity. TEWL is measured in grams per hour per square meter (g/h·m²) and the *stratum corneum* hydration is given in arbitrary units (AU). A slight decrease was observed in the *stratum corneum* after the application of the formulations whereas no changes in the TEWL values were observed. Neither were anystatistical differences found for TEWL and nor were they found in the process of *stratum corneum* hydration at 1 and 2 h compared to the basal values.

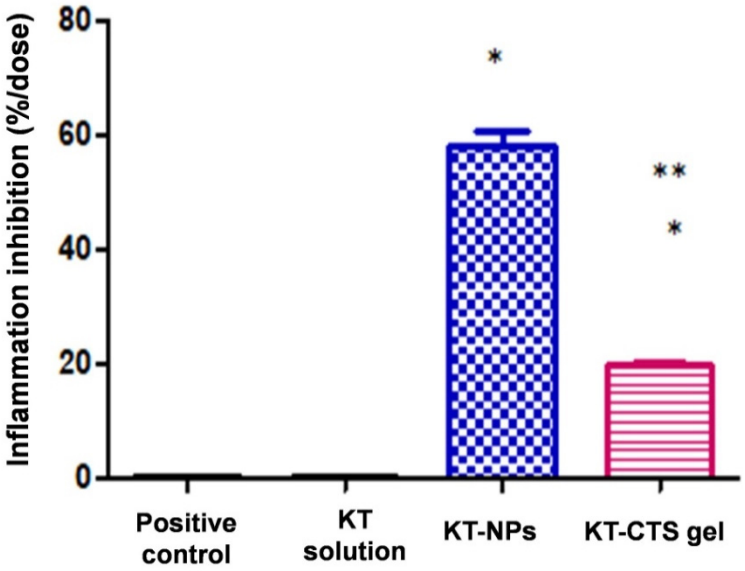

Figure 8. Anti-inflammatory efficacy of studied formulations expressed as a percentage reduction in in-flammation when compared to a control. The results are presented as the mean ± SD of three measurements. * stands for statistical differences between the formulations and the positive control and the KT solution, ** stands for statistical differences between KT-NPs and KT-CTS gel ($p < 0.0001$).

4. Discussion

The patients' health-related quality of life is negatively impacted by Condyloma acuminata and therefore finding appropriate and effective treatments is necessary. Improving this quality of life can be achieved by alleviating the pain associated with the disease, an aim which has been pursued with considerable effort. In this context, the current study is focused on developing two formulations containing KT as an anti-inflammatory agent to address this need, one for the pre-operative period and another for the post-operative period. KT was selected based on its promising results previously reported by our group [4], into which it was formulated into a topical sodium alginate-hydrogel and tested on human skin and porcine vaginal mucosa. This showed its capacity to be released from the formulation and to permeate through the tissues, and it also exhibited an optimal anti-inflammatory activity. Two carriers were chosen based on extensive research previously reported: polymeric NPs and CTS hydrogel. Several studies have shown the potential of KT in the management of postoperative pain and the impact of using it as a pre-operative agent and that it added towards achieving better outcomes during and after surgery [24–26]. The hypothesis was that the KT-NPs might be an appropriate choice in the pre-operative period as CTS might be used as a spray and facilitate their clinical applications whereas the KT-CTS gel would be beneficial in the post-operative period, due to the biodegradable, mucoadhesive, homeostatic and antibacterial properties of CTS, among its other properties.

Hydrogels are three-dimensional structure composed of hydrophilic polymeric networks, capable of absorbing large amounts of water or biological fluids. The polymers are water-insoluble due to the presence of chemical (covalent bonds) or physical crosslinks (non-covalent secondary interactions such as Van der Waals, hydrophobic, hydrogen bonding and electrostatic interactions). These crosslinks provide the structure of the network and its physical integrity. The hydrogels have thermodynamic compatibility with water, which allows them to swell in an aqueous medium [27,28]. The morphological characteristics of the KT-CTS gel showed that it has a compact and dense structure. This was also observed by Yanget al. [29]. Nevertheless, other researchers observed lamellar or porous structures in CTS gels [30–33]. The differences in the microstructure observed by the different authors may be attributed to the formulation or preparation of the sample.

Hydrogels can also show a swelling behavior that depends on the characteristics of the external environment and as a consequence the polymer complexes can break down, swell or show drastic changes in their swelling values as a result of changes in certain physiological stimuli. Some of the factors that influence the polymers that respond to certain physiological stimuli include pH, temperature, ionic strength, and electromagnetic radiation [34]. In our case, the KT-CTS gel swelling process followed a zero-order kinetic. This can be interpreted as being due to the excellent ability of CTS to absorb large volumes of water [33], a property which opens up the possibilities for drug delivery and wound healing applications [35]. Our findings indicate that the dehydrated gel is hygroscopic absorbing to an extent of up to 4.5 times its weight in water in less than 4 h. Several researchers have investigated the swelling phenomenon of polyionic or polyelectrolytic hydrogels. In some cases, the swelling balance and the mesh size were caused by the percentage of ionic component and by the degree of ionization of the active principle [36]. For example, Peniche et al. [28] verified the ability to complex salicylic acid and acrylic acid derivatives with cationic polyvalent ligands such as CTS. On the other hand, Gabrielii et al. [37] studied the swelling properties of CTS hydrogels under the influence of various pH and sodium chloride concentrations (0.075 M and 0.15 M). The authors deduced that the effect of adding sodium chloride could be explained by the increase in the total amount of ions that decreases the ratio between the ions inside the hydrogel and the external environment. Therefore, under extreme pH conditions (pH = 3 and pH = 12) the degree of swelling decreases when the ionic strength of the medium increases. Our findings demonstrate that the CTS gel diffuses into the media, indicating that it should be expected that this formulation degrades successfully when submerged in a biological medium.

The hydrogel viscosity plays a crucial role in controlling drug release and skin penetration [23]. The Casson rheological model describes the viscoelastic fluids flow [38]. This behavior supports the intended topical application of this formulation, thus facilitating its outpatient application. On key point in favor of it is that it be applied in the desired area precisely, without fear that it will disperse to other regions as soon as the patient changes postural position, and on the other hand, it can flow and its viscosity decrease when stress is applied, which is a desirable feature in the potential spread of dermatological products as it allows a smooth and painless application.

The preparation of NPs by the double emulsion method requires ultrasound or high-speed homogenization, followed by evaporation of the solvent either by continuous magnetic stirring at room temperature or under vacuum conditions. Generally, the polymer is dissolved in an organic solvent that is used in the oil phase, while the aqueous phase contains the stabilizer [39]. First, the hydrophilic drug and the chosen surfactant are dissolved in water and, a solution of the polymer is dissolved in an organic solvent. The primary emulsion is prepared by dispersing the aqueous phase in the organic phase. Afterwards, a re-emulsification is carried out with a second aqueous phase that also uses surfactant. Finally, the solvent is evaporated and the NPs are collected. Evaporation of the solvent can be carried outby magnetic stirring at room temperature for several hours or by rotary evaporation [39,40]. NPs production has many independent variables. The polymer used to formulate the NPs affects the structure, properties and applications of the particles, so there is no single polymer suitable for all drugs. The PLGA was chosen to design the NPs because of its various advantageous reported characteristics, especially biodegradability [41]. There are two characteristics that need to be considered when formulating polymeric NPs for a given route of administration: particle size and encapsulation efficiency. For example, if fast absorption is intended, the nanoparticle size should be 100 nm or below. The ZP is a measure of the particle charge, the greater the absolute value of ZP, the greater the charge on the NPs surface, and in turn, the greater stability of the particles [40]. In the case of KT-NPs the small ZP value was not critical because the KT-NPs were prepared with PVA as the stabilizer agent. The PVA mechanism of action to prevent particle aggregation relies on steric hindrance [42]. The obtained KT-NPs showed a high encapsulation efficiency, round-shaped structure and narrow distribution which indicates a monodisperse system.

The difference in the value of Zave between TEM and DLS measurements is attributed to the fact that the DLS measured the hydrodynamic diameter, whereas the TEM shows the real particle size [20]. Zambaux et al. [43] studied the influence of certain experimental parameters (preparation temperature, solvent evaporation method, surfactant concentration, polymer molecular weight) on the Zave, PI and the ZP of NPs prepared by the double emulsion method. The authors concluded that high concentrations of surfactant (3% *w/v*, or higher) guaranteed a successful emulsification process, and smaller particles which came with a satisfactory PI. Other factors influence the characteristics of PLGA NPs prepared by the double emulsion method W/O/W solvent evaporation. Bilati et al. [21] studied the influence of the sonication process, analyzing the modification of the size and distribution of NPs as a function of the duration and intensity of sonication. The work showed that the duration of the second homogenization step, the one that provides the double emulsion (W/O/W), had a greater influence on the particle size than the first homogenization (W/O emulsion). The particle size decreases with the increasing sonication time of the second emulsification. The results of the study also suggested that the intensity of sonication influenced the morphometry of the NPs as well. Additionally, the organic solvent used can also influence the final properties of NPs. Mainardes et al. [44] evaluated this effect in his work, comparing the particle size obtained when preparing the PLGA NPs with two organic solvents: methylene chloride or ethyl acetate. It was concluded that methylene chloride provided larger NPs than when ethyl acetate was used as organic solvent. The selection of the method depends, therefore, on several factors that must be evaluated in order to obtain the NPs with the desired characteristics and properties [40].

The pH of the external aqueous phase of the KT-NPs as well as of the KT-CTS gel were within the pH range of the healthy skin so the formulations are not expected to cause any disorder [45,46].

Whether a hydrogel is suitable as an active ingredient delivery system in a certain area depends to a large extent on its polymeric structure. The controlled release of active principles from polyionic hydrogels can respond to changes in environmental parameters, such as: pH, temperature and other stimuli. Thus, interpolymeric hydrogels such as polyacrylic acid/polyvinyl alcohol or polymethacrylic acid linked to polyethylene glycol can form reversible complexes depending on the temperature and pH conditions of the external environment [36,47]. Our findings revealed that the KT release from the NPs was significantly faster than CTS gel. A more outstanding level of release was observed from NPs in comparison to CTS gel ($p < 0.0001$). The KT-NPs release profile seems to be fitting with the hypothesis of our study as the KT fast release is crucial for the pre-operative application where a fast release is preferred. Meanwhile, the profile of KT-CTS gel, which could be due to the electrostatic interaction between KT and CTS, and the compact structure, seems to be suitable for the post-operative application, where a more sustained release is desirable.

Hydrogels have also been used as vehicles for active ingredients that can interact with the mucosa of the gastrointestinal tract, the colon, the vagina, the nasal mucosa, and other parts of the body thanks to their ability to prolong their times of residence in the body place of administration. In the present work, we have assessed the biodistribution of KT after the skin was exposed to both formulations under a finite dose approach for 24 h. To determine the amount of KT in each compartment, the skin was separated into its different layers, and both the receptor fluid and the residual formulation at the end of the experiment were recovered for further drug quantification. We observed that the greatest amount of KT remained on the skin surface for both formulations. This is in line with previous hydrogels works, and it is because of the primary barrier function of the *stratum corneum* against the drug penetration [4,48]. Both formulations seem to be adequate vehicles for the dermal delivery. In both cases, KT readily diffuses through the skin, and it is mainly retained in the epidermis, where it can exert its anti-inflammatory and analgesic properties. Similar profiles were observed for KT hydrogels formulated with different polymers [4]. When the distribution of KT into the human skin was tested with an alginate-based hydrogel,

the diffusion of KT was limited to the epidermis where similar amounts of KT were found with poor retention of KT in the dermis and not quantifiable KT in the receptor fluid. Nor was KT retained in the dermis from a Carbopol-based and Pluronic-based hydrogels, and there was also poor diffusion of KT into the receptor fluid. Among these polymers, CTS gel is the vehicle which most enhanced the diffusion of KT into the receptor fluid.

In order to evaluate the potential changes in the skin characteristics caused by the application of the formulations, the variations in the properties of the skin were studied using bio-metrological techniques. The parameters evaluated were the *stratum corneum* hydration and the TEWL. These parameters are indicative of a potential irritant or pro-inflammatory effect. TEWL measurement, due to passive diffusion of water through the skin, provides important information on skin barrier function and its integrity [49]. An increase in TEWL values reflects a possible deterioration in the barrier function, leading to decreased protection against water loss. The TEWL values 2 h after post-application of the formulations, showed slight variation with no significant statistical differences compared to the basal values. In healthy skin functioning normally as a barrier, TEWL should be directly proportional to skin hydration [50]. *Stratum corneum* hydration is determined as the conductance that free water provides to the skin surface [51]. Even though the *stratum corneum* hydration experienced a decrease after the application of the formulations, the differences observed were not found to be statistically significant. Our results show that the skin exhibit sufficiently hydrated values (above 45 AU), according to the skin hydration normal values in standard conditions [4,52]. In the case of the KT-CTS gel, the decrease can be probably related to the CTS gel swelling behavior when it is applied to the skin.

The anti-inflammatory efficacy study revealed that the KT-NPs exhibit statistically significantly higher anti-inflammatory efficacy than KT-CTS gel by an approximately three-fold ratio. These results agree with the histological analysis which showed the presence of the immune cells system in the positive control, in agreement with TPA-induced oedema. Thanks to the KT-NPs action, the infiltration of immune system cells is completely inhibited, while the ear treated with the KT-CTS gel histology shows a limited number of these cells in tissue blood vessels. Even so, the KT-CTS gel anti-inflammatory efficacy is evident, as shown in the histological images. It should be noted that the NPs loaded less KT than the KT-CTS gel. This demonstrates how NPs are an excellent formulation for the application of KT since we achieved a powerful effect without the need to apply a high dose, thus improving the side effects window and, therefore, patient satisfaction and adherence, for pain during treatment is one of the factors that affects treatment adherence [53–55].

Considering that the formulations show suitable characteristics for the topical delivery, are well-tolerated and exhibited a good anti-inflammatory profile, both formulations are candidates for offering a local anti-inflammatory activity in the clinical application. In this regard, future pre-clinical and clinical studies might be conducted.

5. Conclusions

Two polymeric formulations loading KT were developed to address the pain associated with the ablation of anogenital warts in Condyloma acuminata. The polymers were chosen based on their biocompatibility and biodegradability among other characteristics. The CTS was selected because of its muco-adhesivity, and hemostatic and antimicrobial activity, while the PLGA was selected because it is already approved by several medicine regulatory authorities.

The formulations, a CTS gel and a polymeric nanostructured system, were fully characterized. Both formulations exhibited suitable features for the dermal application and remained stable for at least 3 months. They showed a fast drug release, particularly the KT-NPs, and both formulations led to the accumulation of KT in the epidermis where the drug can exert its anti-inflammatory effect. Even though the NPs were prepared at a lower concentration of KT than the CTS gel, they showed greater retention of KT in the epidermis than the CTS gel.

Both formulations showed efficacy in reducing the inflammation in TPA-induced ear oedema in mice and both formulations were well-tolerated in healthy human volunteers.

The faster release, the greater amount of KT in the epidermis and the superior anti-inflammatory efficacy of the NPs over the KT-CTS gel led us to consider the KT-NPs as a good formulation in the pre-operative period, meanwhile, the viscosity and rheological profile of the KT-CTS gel in combination with the known mucoadhesive and antimicrobial properties of the CTS may confer some advantages for the post-operative period in the surgical removal of anogenital warts.

Supplementary Materials: The following are available online at https://www.mdpi.com/article/10.3390/pharmaceutics13111784/s1, Table S1: Critical Process Parameters (CPPs) and Critical Quality Attributes (CQAs) for the KT-formulations, Table S2: Quality Target Product Profiles (QTPPs) for the KT-formulations, Table S3: Optimization of the KT-NPs by a Two-level Full Factorial Design for 3 factors in standard order, and Table S4: Responses from KT-NPs formulated based on the Two-level Full Factorial Design for 3 factors.

Author Contributions: Conceptualization, M.M. and A.C.C.; methodology, A.C.C. and M.M.; software, M.M. and J.L.S.; validation, C.A.; formal analysis, A.C.C. and M.M.; investigation, S.E.M., I.A.-H., M.L.G.-R. and C.A.; resources, A.C.C., B.C., M.L.G.-R., L.C. and L.H.; data curation, M.M.; writing—original draft preparation, I.A.-H.; writing—review and editing, M.M.; J.L.S.; visualization, J.L.S.; supervision, A.C.C. and F.F.-C.; project administration, F.F.-C., M.M. and A.C.C.; funding acquisition, A.C.C. and L.C. All authors have read and agreed to the published version of the manuscript.

Funding: This research received no external funding.

Institutional Review Board Statement: The study was conducted according to the guidelines of the Declaration of Helsinki, and approved by the Ethics Committee University of Barcelona (protocol code IRB00003099 and date of approval 20 March 2018); the Bioethics Committee of the Barcelona-SCIAS Hospital (protocol code Nº001 and date of approval 20 January 2016); and the Academic Ethics Committee of the Vivarium at the Universidad Autónoma del Estado de Morelos (protocol code BIO-UAEM:03:2019 and date of approval 12 February 2019).

Informed Consent Statement: Informed consent was obtained from all subjects involved in the study.

Data Availability Statement: The data presented in this study are available on request from the corresponding author. The data are not publicly available due to they are part of a Doctoral Thesis and it will be available once the Thesis will be published.

Acknowledgments: The authors want to acknowledge Maria Luisa García for the PLGA donation and Noelia Pérez-González for their technical support.

Conflicts of Interest: The authors declare no conflict of interest. Francisco Fernández-Campos is the employee of Reig-Jofre Laboratories. The company had no role in the design of the study; in the collection, analyses, or interpretation of data; in the writing of the manuscript, and in the decision to publish the results.

References

1. Regional Committee for Africa Global Health Sector Strategy on Sexually Transmitted Infections: Implementation Framework for the African Region. Available online: https://apps.who.int/iris/handle/10665/260232 (accessed on 31 May 2021).
2. Kreuter, A.; Weyandt, G.; Wieland, U. Therapieoptionen Bei Condylomata Acuminata Und Analen Dysplasien. *Coloproctology* **2021**, *43*, 87–91. [CrossRef]
3. Gross, G.; Pfister, H. Role of Human Papillomavirus in Penile Cancer, Penile Intraepithelial Squamous Cell Neoplasias and in Genital Warts. *Med. Microbiol. Immunol.* **2004**, *193*, 35–94. [CrossRef]
4. El Moussaoui, S.E.; Fernández-Campos, F.; Alonso, C.; Limón, D.; Mallandrich, M. Topical Mucoadhesive Alginate-Based Hydrogel Loading Ketorolac for Pain Management after Pharmacotherapy, Ablation, or Surgical Removal in Condyloma Acuminata. *Gels* **2021**, *7*, 8. [CrossRef]
5. Fleischer, A.B.; Parrish, C.A.; Glenn, R.; Feldman, S.R. Condylomata Acuminata (Genital Warts): Patient Demographics and Treating Physicians. *Sex. Transm. Dis.* **2001**, *28*, 643–647. [CrossRef]
6. Giancristoforo, S.; Diociaiuti, A.; Tchidjou, H.K.; Lucchetti, M.C.; Carnevale, C.; Rotunno, R.; D'Argenio, P.; el Hachem, M. Successful Topical Treatment of Anal Giant Condylomata Acuminata in an Infant. *Dermatol. Ther.* **2020**, *33*, e13624. [CrossRef]

7. Sugai, S.; Nishijima, K.; Enomoto, T. Management of Condyloma Acuminata in Pregnancy: A Review. *Sex. Transm. Dis.* **2021**, *48*, 403–409. [CrossRef]
8. Patel, H.; Wagner, M.; Singhal, P.; Kothari, S. Systematic Review of the Incidence and Prevalence of Genital Warts. *BMC Infect. Dis.* **2013**, *13*, 39. [CrossRef] [PubMed]
9. D'Ambrogio, A.; Yerly, S.; Sahli, R.; Bouzourene, H.; Demartines, N.; Cotton, M.; Givel, J.C. Human Papilloma Virus Type and Recurrence Rate after Surgical Clearance of Anal Condylomata Acuminata. *Sex. Transm. Dis.* **2009**, *36*, 536–540. [CrossRef]
10. Ahuja, M.; Dhake, A.S.; Sharma, S.K.; Majumdar, D.K. Topical Ocular Delivery of NSAIDs. *AAPS J.* **2008**, *10*, 229–241. [CrossRef] [PubMed]
11. Elgadir, M.A.; Uddin, M.S.; Ferdosh, S.; Adam, A.; Chowdhury, A.J.K.; Sarker, M.Z.I. Impact of Chitosan Composites and Chitosan Nanoparticle Composites on Various Drug Delivery Systems: A Review. *J. Food Drug Anal.* **2015**, *23*, 619–629. [CrossRef]
12. Makadia, H.K.; Siegel, S.J. Poly Lactic-Co-Glycolic Acid (PLGA) as Biodegradable Controlled Drug Delivery Carrier. *Polymers* **2011**, *3*, 1377–1397. [CrossRef] [PubMed]
13. Shariatinia, Z. Pharmaceutical Applications of Chitosan. *Adv. Colloid Interface Sci* **2019**, *263*, 131–194. [CrossRef]
14. Ali, A.; Ahmed, S. A Review on Chitosan and Its Nanocomposites in Drug Delivery. *Int. J. Biol. Macromol.* **2018**, *109*, 273–286. [CrossRef]
15. Muxika, A.; Etxabide, A.; Uranga, J.; Guerrero, P.; de la Caba, K. Chitosan as a bioactive polymer: Processing, properties and applications. *Int. J. Biol. Macromol.* **2017**, *105*, 1358–1368. [CrossRef] [PubMed]
16. Benson, H.A.E. Skin Structure, Function, and Permeation. In *Topical and Transdermal Drug Delivery*; Benson, H.A.E., Watkinson, A.C., Eds.; John Wiley & Sons: Hoboken, NJ, USA, 2012; pp. 1–22.
17. Prausnitz, M.R. Microneedles for Transdermal Drug Delivery. *Adv. Drug Deliv. Rev.* **2004**, *56*, 581–587. [CrossRef] [PubMed]
18. Alkilani, A.Z.; McCrudden, M.T.C.; Donnelly, R.F. Transdermal Drug Delivery: Innovative Pharmaceutical Developments Based on Disruption of the Barrier Properties of the Stratum Corneum. *Pharmaceutics* **2015**, *7*, 438–470. [CrossRef] [PubMed]
19. Kanikkannan, N. Iontophoresis-Based Transdermal Delivery Systems. *BioDrugs* **2002**, *16*, 339–347. [CrossRef]
20. Mallandrich, M.; Calpena, A.C.; Clares, B.; Parra, A.; García, M.L.; Soriano, J.L.; Fernández-Campos, F. Nano-Engineering of Ketorolac Tromethamine Platforms for Ocular Treatment of Inflammatory Disorders. *Nanomedicine* **2021**, *16*, 401–414. [CrossRef]
21. Bilati, U.; Allémann, E.; Doelker, E. Sonication Parameters for the Preparation of Biodegradable Nanocapsulesof Controlled Size by the Double Emulsion Method. *Pharm. Dev. Technol.* **2003**, *8*, 1–9. [CrossRef]
22. Mallandrich, M.; Fernández-Campos, F.; Clares, B.; Halbaut, L.; Alonso, C.; Coderch, L.; Garduño-Ramírez, M.L.; Andrade, B.; del Pozo, A.; Lane, M.E.; et al. Developing Transdermal Applications of Ketorolac Tromethamine Entrapped in Stimuli Sensitive Block Copolymer Hydrogels. *Pharm. Res.* **2017**, *34*, 1728–1740. [CrossRef]
23. Domínguez-Villegas, V.; Clares-Naveros, B.; García-López, M.L.; Calpena-Campmany, A.C.; Bustos-Zagal, P.; Garduño-Ramírez, M.L. Development and Characterization of Two Nano-Structured Systems for Topical Application of Flavanones Isolated from EysenhardtiaPlatycarpa. *Colloids Surf. B Biointerfaces* **2014**, *116*, 183–192. [CrossRef] [PubMed]
24. De Oliveira, G.S.; Agarwal, D.; Benzon, H.T. Perioperative Single Dose Ketorolac to Prevent Postoperative Pain: A Meta-Analysis of Randomized Trials. *AnesthAnalg* **2012**, *114*, 424–433.
25. Donnenfeld, E.D.; Perry, H.D.; Wittpenn, J.R.; Solomon, R.; Nattis, A.; Chou, T. Preoperative Ketorolac Tromethamine 0.4% in Phacoemulsification Outcomes: Pharmacokinetic-Response Curve. *J. Cataract Refract. Surg.* **2006**, *32*, 1474–1482. [CrossRef]
26. El-Harazi, S.M.; Ruiz, R.S.; Feldman, R.M.; Villanueva, G.; Chuang, A.Z. Efficacy of Preoperative versus Postoperative Ketorolac Tromethamine 0.5% in Reducing Inflammation after Cataract Surgery. *J. Cataract Refract. Surg.* **2000**, *26*, 1626–1630. [CrossRef]
27. Peppas, N.A.; Bures, P.; Leobandung, W.; Ichikawa, H. Hydrogels in pharmaceutical formulations. *Eur. J. Pharm. Biopharm.* **2000**, *50*, 27–46. [CrossRef]
28. Peniche, C.; Elvira, C.; Roman, J.S. Interpolymer complexes of chitosan and polymethacrylic derivatives of salicylic acid: Preparation, characterization and modification by thermal treatment. *Polymer* **1998**, *39*, 6549–6554. [CrossRef]
29. Yang, Y.; Chen, G.; Murray, P.; Zhang, H. Porous Chitosan by Crosslinking with Tricarboxylic Acid and Tuneable Release. *SN Appl. Sci.* **2020**, *2*, 435. [CrossRef]
30. Modrzejewska, Z.; Skwarczyńska, A.; Maniukiewicz, W.; Douglas, T.E.L. Mechanism of Formation of Thermosensitive Chitosan Chloride Gels. *Prog. Chem. Appl. Chitin. Deriv.* **2014**, *19*, 125–134. [CrossRef]
31. Sharma, S.; Kumar, A.; Kumar, R.; Rana, N.K.; Koch, B. Development of a Novel Chitosan Based Biocompatible and Self-Healing Hydrogel for Controlled Release of Hydrophilic Drug. *Int. J. Biol. Macromol.* **2018**, *116*, 37–44. [CrossRef]
32. Orue, I.G.; Vizcaíno, E.S.; Etxeberria, A.E.; Uranga, J.; Hernandez, R.M. Development of Bioinspired Gelatin and Gelatin/Chitosan Bilayer Hydrofilms for Wound Healing. *Pharmaceutics* **2019**, *11*, 314. [CrossRef]
33. Bhattarai, N.; Gunn, J.; Zhang, M. Chitosan-Based Hydrogels for Controlled, Localized Drug Delivery. *Adv. Drug Deliv. Rev.* **2010**, *62*, 83–99. [CrossRef]
34. José, L.; Gastres, G. *Hidrogeles Poliiónicos De Chitosán Y Ácido Poliacrílico Como Nuevos Sistemas De Libreación Gástrica De Amoxicilina Para El Tratamiento De "H Pylori"*; Universidad Complutense de Madrid: Madrid, Spain, 2003.
35. Adewale, F.J.; Lucky, A.P.; Oluwabunmi, A.P.; Boluwaji, E.F. Selecting the Most Appropriate Model for Rheological Characterization of Synthetic Based Drilling Mud. *Int. J. Appl. Eng. Res.* **2017**, *12*, 7614–7629.
36. Bell, C.L.; Peppas, N.A. Modulation of drug permeation through interpolymer complexed hydrogels for drug delivery applications. *J. Control. Release* **1996**, *39*, 201–207. [CrossRef]

37. Gabrielii, I.; Gatenholm, P. Preparation and properties of hydrogels based on hemicellulose. *J. Appl. Polym. Sci.* **1998**, *69*, 1661–1667. [CrossRef]
38. Iglesias, N.; Galbis, E.; Valencia, C.; de-Paz, M.V.; Galbis, J.A. Reversible PH-Sensitive Chitosan-BasedHydrogels. Influence of Dispersion Composition on Rheological Properties and Sustained Drug Delivery. *Polymers* **2018**, *10*, 392. [CrossRef] [PubMed]
39. Rao, J.P.; Geckeler, K.E. Polymer nanoparticles: Preparation techniques and size-control parameters. *Prog. Polym. Sci.* **2011**, *36*, 887–913. [CrossRef]
40. Llabot, J.; Palma, S.D. Nanopartículas poliméricas sólidas. *Nuestra Farm.* **2008**, *53*, 40–47.
41. Ghitman, J.; Biru, E.I.; Stan, R.; Iovu, H. Review of Hybrid PLGA Nanoparticles: Future of Smart Drug Delivery and Theranostics Medicine. *Mater. Des.* **2020**, *193*, 108805. [CrossRef]
42. Lee, A.; Tsai, H.-Y.; Yates, Z.M. Steric Stabilization of Thermally Responsive NisopropylacrylamideParticles by Poly (vinyl alcohol). *Langmuir* **2010**, *26*, 18055–18060. [CrossRef]
43. Zambaux, M.F.; Bonneaux, F.; Gref, R.; Maincent, P.; Dellacherie, E.; Alonso, M.J.; Labrude, P.; Vignerona, C. Influence of experimental parameters on the characteristics of poly(lactic acid) nanoparticles prepared by a double emulsion method. *J. Control. Release* **1998**, *50*, 31–40. [CrossRef]
44. Mainardes, R.M.; Evangelista, R.C. Praziquantel-loaded PLGA nanoparticles: Preparation and characterization. *J. Microencapsul.* **2005**, *22*, 13–24. [CrossRef] [PubMed]
45. Schmid-Wendtner, M.H.; Korting, H.C. The PH of the Skin Surface and Its Impact on the Barrier Function. *Ski. Pharm.* **2006**, *19*, 296–302. [CrossRef]
46. Ali, S.M.; Yosipovitch, G. Skin PH: From Basic Science to Basic Skin Care. *Acta DermVenereol* **2013**, *93*, 261–267. [CrossRef] [PubMed]
47. Shin, H.S.; Kim, S.Y.; Lee, Y.M. Indomethacin release behaviors from pH and thermoresponsive poly (vinyl alcohol) and poly (acrylic acid) IPN hydrogels for site-specific drug delivery. *J. Appl. Polym. Sci.* **1997**, *65*, 685–693. [CrossRef]
48. Campbell, K.; Lichtensteiger, C. Structure and Function of The Skin. In *Small Animal Dermatology Secrets*; Elsevier: Amsterdam, The Netherlands, 2003; pp. 1–9.
49. Mohammed, D.; Hirata, K.; Hadgraft, J.; Lane, M.E. Influence of skin penetration enhancers on skin barrier function and skin protease activity. *Eur. J. Pharm. Sci.* **2014**, *51*, 118–122. [CrossRef] [PubMed]
50. Raney, S.G.; Hope, M.J. The Effect of Bilayer and Hexagonal HII Phase Lipid Films on Transepidermal Water Loss. *Exp. Derm.* **2006**, *15*, 493–500. [CrossRef] [PubMed]
51. Del Pozo, A.; Viscasillas, A. Efficacy Evaluation. In *Analysis of Cosmetic Products*, 1st ed.; Salvador, S., Chisvert, A., Eds.; Elsiever: Amsterdam, The Netherlands, 2007; pp. 462–474.
52. Constantin, M.M.; Poenaru, E.; Poenaru, C.; Constantin, T. Skin Hydration Assessment through Modern Non-Invasive Bioengineering Technologies. *Maedica* **2014**, *9*, 33–38.
53. Hammarlund, K.; Nyström, M.; Jomeen, J. Young women's experiences of managing self-treatment for anogenital warts. *Sex. Reprod. Healthc.* **2012**, *3*, 117–121. [CrossRef]
54. Linnehan, M.J.; Groce, N.E. Counseling and educational interventions for women with genital human papillomavirus infection. *AIDS Patient Care STDs* **2000**, *14*, 439–445. [CrossRef]
55. Kumar, A.; Dixit, C.K. Method for characterization of nanoparticles. In *Bool Advances in Nanomedicine for the Delivery of Therapeutic Nucleic Acids*; Nimesh, S., Chandra, R., Gupta, N., Eds.; Woodhead Publishing: Southston, UK, 2017; pp. 43–58.

pharmaceutics

Supplementary Materials: Polymeric Nanoparticles and Chitosan Gel Loading Ketorolac Tromethamine to Alleviate Pain Associated with Condyloma Acuminata during the Pre- and Post-Ablation

Salima El Moussaoui, Ismael Abo-Horan, Lyda Halbaut, Cristina Alonso, Lluïsa Coderch, María Luisa Garduño-Ramírez, Beatriz Clares, José Luis Soriano, Ana Cristina Calpena Francisco Fernández-Campos and Mireia Mallandrich

Table S1. Critical Process Parameters (CPPs) and Critical Quality Attributes (CQAs) for the KT-formulations.

	Critical Process Parameters (CPPs)	Specification	Critical Quality Attributes (CQAs)	Specification (value and range)
KT-CTS gel	pH	As described in section 2.2.1	pH of the final formulation	Eudermic (4.0 – 6.0)
			Swelling ratio (SR)	SR = 4.7 after 3h (4.0 – 5.4)
			Degradation rate	In 3.75h (3.10 – 4.40) CTS gel degraded in the medium (PBS).
	Order of raw materials addition			
	CTS concentration	3% (*w*/*v*)	Rheology behavior (viscosity)	Pseudoplastic behavior 1.431 Pas (1.420 – 1.440)
	mixing time and speed (homogenization)	Avoid stirring at high speed so as not to form air bubbles in the hydrogel. ca. 50 rpm 5 min.	Microscopy Morphology	compact and dense, with smooth surface.
			Release ability	K = 0.9h $^{-1}$ (0.3 – 1.2); %R∞ = 18.6% (16.8 – 20.4)
			Permeation capacity (skin retention)	Superficial skin layers, manly in the epidermis
KT-NPs	Order of addition of raw materials	As described in section 2.2.2	pH aqueous external phase (W_2)	5.2(4.0 – 6.0)
			particle size (Zave)	108.9 nm (95.1 – 122.7)
	Sonicator power and cycle length	W_1/O: 50 watts 30% amplitude for 20s in 10s cycles	polydispersity index (PI)	0.061 (≤ 0.1)
			efficiency (EE%)	93.9% (87.0 – 102.0)

Pharmaceutics **2021**, *13*, 1784. https://doi.org/10.3390/pharmaceutics13111784 www.mdpi.com/journal/pharmaceutics

Organic solvent and its evaporation method	$W_1/O/W_2$: 50 watts 30% amplitude for 1.5 min in 10s cycles	Release ability	$K = 1.8h^{-1}$ (1.5 – 2.1); $\%R\infty = 92.0\ \%$ (85 – 99)
	Ethyl acetate Rotary evaporation	Permeation capacity (skin retention)	Superficial skin layers, manly in the epidermis

Table S2. Quality Target Product Profiles (QTPPs) for the KT-formulations.

	Quality target product profiles (QTPPs)	Target
KT-CTS gel	Dosage form	Semisolid hydrogel. Easy to apply and conserve.
	Route of administration	Dermal. Non-invasive routewhich allows higher drug concentration on the application site avoiding systemic side effects.
	Site of activity	Superficial skin layers. Epidermis.
	Therapeutic effect	Analgesic and anti-inflammatory effect for the post-operative management of condyloma removal.
	Appearance	Homogeneous and transparent to ensure the aesthetic appearance and increase patient compliance.
	Viscosity	Sufficient consistency to not spread to unwanted areas as soon as the patient changes position, but it must fluidize just enough to allow an easy and painless application.
	Stability	No visible sign of instability at the time of preparation and after three months at room temperature (ca. 25°C).
	Release profile	Controlled drug release. A sustained release over time is desirable for the management of post-surgical pain and inflammation.
KT-NPs	Dosage form	Colloidal suspension suitable for sprayable application onto warts without the need to contact them.
	Route of administration	Dermal. Non-invasive route which allows higher drug concentration on the application site avoiding systemic side effects.
	Site of activity	Superficial skin layers. Epidermis.
	Therapeutic effect	Analgesic and anti-inflammatory effect for the pre-operative management of condyloma removal.
	Appearance	Homogeneous fluid with no visible suspended particles
	Stability	No visible sign of instability at the time of preparation and after three months at 4ºC storage conditions. pH, Z-awe, PI, ZP and EE% should not be altered.
	Release profile	Controlled drug release. Rapid drug release is desirable for management of pre-surgical pain and inflammation

Table S3. Optimization of the KT-NPs by a Two-level Full Factorial Design for 3 factors in standard order. .

Run	X_1	X_2	X_3	Amount KT (mg)	Amount PLGA (mg)	pH inneraqueousphase
F1	−1	−1	−1	20	90	2.0
F2	1	−1	−1	80	90	2.0
F3	−1	1	−1	20	110	2.0
F4	1	1	−1	80	110	2.0
F5	−1	−1	1	20	90	7.5
F6	1	−1	1	80	90	7.5
F7	−1	1	1	20	110	7.5
F8	1	1	1	80	110	7.5

X_1, X_2 and X_3 stands for the three factors evaluated: amount of KT in the formulation, amount of PLGA in the formulation and pH of the inner aqueous phase, respectively.

Table A4 shows the responses for each formulation. The following characteristics were measured: particle size (Zave), polydispersity index (PI), zeta potential (ZP), encapsulation efficiency (EE%) and the final pH of the external aqueous phase (W_2).

Table S4. Responses from KT-NPs formulated based on the Two-level Full Factorial Design for 3 factors.

	Factors			Responses				
Formulation	Amount KT (mg)	Amount PLGA (mg)	pH inneraqueousphase	Zave (nm)	PI	ZP (mV)	EE (%)	Final pH externalaqueousphase
F1	20	90	2.0	138.2	0.048	−8.35	92.3	4.0
F2	80	90	2.0	108.9	0.061	−6.20	93.9	5.2
F3	20	110	2.0	136.6	0.047	−11.00	80.7	3.6
F4	80	110	2.0	120.2	0.048	−0.27	71.8	4.8
F5	20	90	7.5	121.8	0.049	−12.40	72.4	5.2
F6	80	90	7.5	110.6	0.043	−7.29	65.2	5.1
F7	20	110	7.5	142.4	0.041	−13.60	35.0	4.7
F8	80	110	7.5	113.6	0.024	−5.57	74.5	5.6

Zave = average particle size; PI = polydispersity index; ZP = zeta potential and EE = Encapsulation efficiency.

The amount of KT or PLGA and the pH of the inner aqueous phase (W1) did not impact on the polydispersity index of the formulations.All of them presented PI values below 0.1 indicating that the colloidal suspension of KT-NPs was a monodisperse system with a narrow particle size distribution. The zeta potential is an important tool to predict NPs stability, the greater the values (positive or negative), the higher stability, with a cut off value of ±30 mV [54]. However, in the case of KT-NPs the ZP value was not critical because the KT-NPs were prepared with PVA as the stabilizer agent. The PVA's mechanism of action to prevent particle aggregation relies on steric hindrance [55].

Taking into account the above mentioned, F2 was selected as the optimized formulation. It was selected based on its smaller particle size and having the highest encapsulation efficiency. Additionally, the pH value was close to the skin's and so this was a desirable characteristic for the dermal delivery.

DISCUSIÓN

La calidad de vida relacionada con la salud de los pacientes se ve afectada negativamente por la aparición de lesiones cutáneas cómo pueden ser las generadas por el VPH, tomando relativa importancia los condilomas acuminados, dada su localización y el estigma asociado al tratarse de una ETS. La mejora de esta calidad de vida se puede conseguir aliviando el dolor asociado al tratamiento de la enfermedad. Varios estudios han demostrado el potencial del KT en el manejo del dolor posoperatorio y el impacto de su uso como agente preoperatorio y que contribuye a lograr mejores resultados durante y después de la cirugía [104][105][106].

En este contexto, el presente estudio se centra en desarrollar diferentes formulaciones tópicas mucoadhesivas que contengan KT como agente analgésico y antiinflamatorio para manejar el dolor y la inflamación asociado a procesos quirúrgicos y ablativos sobre piel y mucosas.

Primeramente, se elaboró un hidrogel a base de alginato de sodio como polímero gelificante mucoadhesivo, donde se formuló ketorolaco de trometamina al 2 %. Dicho hidrogel fue ampliamente caracterizado en términos de morfología, pH, estabilidad física y propiedades mecánicas, mostrando características adecuadas para una formulación tópica.

Al formular geles, determinar la extensibilidad y reología es crucial para garantizar que la formulación sea agradable de usar y tenga una aplicación cómoda. Es por eso por lo que debe evitarse una extensibilidad muy alta (muy fluida) o muy baja (muy viscosa). Inoue et.al. investigaron la correlación entre las propiedades físicas de diferentes formulaciones y la sensación sensorial, concluyendo que, el cumplimiento del paciente se ve afectado por la misma [107]. Los estudios reológicos son esenciales para evaluar las características galénicas y la idoneidad de una formulación. El hidrogel de alginato y KT al 2 % mostró un comportamiento reológico pseudoplastico, lo que se traduce en una aplicación suave y fácil, mediante frotamiento, sin necesidad de alta presión.

Los estudios de liberación del fármaco mostraron que hasta el 73 % de la cantidad total de KT en el hidrogel se puede liberar en menos de 6 h siguiendo un modelo exponencial de fase uno.

Se realizaron experimentos de permeación bajo un enfoque de dosis infinita usando piel humana y mucosa vaginal, demostrando que el KT contenido en el hidrogel puede penetrar exitosamente a través de ambos tejidos, revelando una penetración casi 7 veces más rápida a través de la mucosa vaginal (306.0 μg/h·cm^2) que a través de la piel humana (50,92 μg/h·cm^2). Estos resultados pueden explicarse por la rápida liberación de KT desde el hidrogel, así como por las propiedades fisicoquímicas del fármaco (QSAR). Por ejemplo, se considera que los fármacos con un peso molecular inferior a 500 Da, un coeficiente de partición octanol:agua (log P) por debajo de 5, menos de 5 donantes de enlaces de hidrógeno y menos de 10 aceptores de enlaces de hidrógeno, pueden penetrar con éxito a través del tejido de la piel [32][34]. Estas propiedades cambian cuando el fármaco está en su forma neutra (ketorolaco) o en forma de sal (ketorolaco trometamina). Por ejemplo, la forma de sal tiene un peso molecular más alto que la base (376,4 frente a 255,27 g/mol), más donantes de enlaces de hidrógeno (5 frente a 1), más aceptores de enlaces de hidrógeno (7 frente a 3), y aunque no se conoce el log P para la forma de sal, se espera que sea mucho más bajo que el de la forma neutra (1.9) [108][109]. Es cierto que el fármaco en contacto con el target puede cambiar su forma (y por lo tanto sus propiedades), alcanzando un equilibrio que depende de la concentración de la droga y la composición del medio en el que se disuelve. Los cambios pueden incluir el intercambio del resto catiónico (trometamina) para otros cationes, o protonación del grupo carboxilato del KTa un ácido carboxílico neutro. No obstante, el uso de la forma de sal en el hidrogel de KT puede inicialmente influir en una mayor proporción de moléculas de KTen forma de sal. Por esta razón, la penetración más rápida de KTa través de la mucosa vaginal puede estar especialmente relacionada con el comportamiento altamente hidrofílico de la sal (ketorolaco trometamina), ya que no encuentra una importante barrera lipofílica contra la penetración del tejido y permite altos flujos a través de la mucosa. Por el contrario, la penetración de KT a través de la piel se ve comprometida por el efecto barrera que produce la epidermis (especialmente el estrato corneo altamente lipofílico), lo que lleva a flujos más pequeños.

Además, el KTse retiene en el tejido (24 h en piel / 6 h en mucosa vaginal) después de la aplicación, mostrando una cantidad de fármaco retenido hasta 20 veces mayor en la mucosa vaginal (1090,42 μg/cm^2) que en la piel humana (52,54 μg/cm^2).

La aplicación tópica de este hidrogel, en general, no debería causar efectos secundarios sistémicos y, por lo tanto, puede considerarse segura.

Para evaluar los cambios potenciales en las características de la piel causados por la aplicación de las formulaciones, se estudiaron las variaciones en las propiedades de la piel mediante técnicas biometrológicas. Cuando las mucosas o la piel están dañadas, sus funciones de barrera se ven afectadas, lo que resulta en una mayor pérdida de agua [110]. Esta pérdida se puede medir mediante el método de pérdida de agua transdermal o transmucosa (*transepidermal water loss* TEWL o TMWL *transmucosal water loss*), que está bien establecido en dermatología y se utiliza para evaluar la integridad de la barrera de la mucosa y/o piel in vivo [111]. Un aumento en los valores de TEWL refleja un posible deterioro en la función de barrera, lo que lleva a una disminución de la protección contra la pérdida de agua En la medición de TEWL/TMWL, el gradiente de densidad de agua que se evapora a través del tejido se mide indirectamente colocando el dispositivo de medición perpendicular al sitio de interés y alcanzando una lectura estable en aproximadamente 60 s. El hidrogel fue bien tolerado in vivo cuando se aplicó en piel humana, sin mostrar alteraciones importantes en la función de barrera de la piel, como la hidratación y el TEWL. Además, el hidrogel no causó ninguna irritación visible. Todos estos resultados muestran que el hidrogel alginato de sodio con KT al 2 % es una formulación estable y adecuada para el tratamiento de procesos inflamatorios, como los que se producen durante o tras la extirpación química o quirúrgica de las verrugas anogenitales.

Dado los excelentes resultados obtenidos tras probar el hidrogel a base de alginato de sodio con KT al 2 % sobre piel humana y mucosa vaginal de cerdo, se quiso mejorar la formulación mediante la adición de ácido hialurónico (AH) tanto de alto como de bajo peso molecular. Dicha formulación fue testada sobre mucosa bucal y sublingual con el fin de tratar el dolor y la inflamación antes, durante y después de procedimientos quirúrgicos, ablativos o extractivos en la cavidad bucal, como pueden ser los condilomas acuminados orales.

El ácido hialurónico se incorporó a la formulación por sus conocidas propiedades regeneradoras, hidratantes y cicatrizantes [112]. Se optó por utilizar AH tanto de alto cómo de bajo peso molecular, dado que el AH de bajo peso molecular puede penetrar a capas más profundas y allí actuar regenerativamente, mientras que el AH de alto

peso molecular actúa a un nivel más superficial [113]. Las características fisicoquímicas, mecánicas y morfológicas del gel fueron estudiadas y analizadas. El pH estaba dentro del rango de pH intraoral normal (6,8–7,8) [38], por lo que no es de esperar alteraciones, ni en la biota ni las funciones de la saliva en la cavidad oral.

El gel de alginato-AH 2 % KT mostró ser de naturaleza higroscópica dada su capacidad de absorber 15 veces su peso en disolvente. Sus componentes pudieron dispersarse en el medio con relativa rapidez en comparación con otros hidrogeles basados en polímeros. Mallandrich et al. estudió la degradación de un hidrogel de carbopol al 2 %, que requirió 24 h para degradarse por completo [114], mientras que nuestra formulación mostró una degradación de más del 84 % en una hora.

A pesar de la estructura compacta del gel de alginato-HA 2 % KT observada por SEM, la formulación exhibió una buena extensibilidad y un comportamiento reológico ideal para la indicación del hidrogel. El comportamiento pseudoplástico es adecuado porque permite una aplicación suave y fácil mediante frotamiento sin alta presión y, por lo tanto, sin dolor. Además, la tixotropía presente en el hidrogel también muestra un comportamiento interesante en productos semisólidos, ya que el cambio de estructura de la formulación da como resultado una fluidización que facilita la aplicación del producto. Estos resultados son idóneos ya que las membranas mucosas son tejidos sensibles per se y más aún después de una intervención quirúrgica, ablativa o extractiva.

El KT difundió rápidamente a través de las membranas mucosas de la cavidad oral, especialmente a través de la mucosa bucal. A dosis infinitas y un tiempo de exposición de 6 h, el KT alcanzaría concentraciones plasmáticas terapéuticas. Sin embargo, no debe despreciarse el impacto de la saliva en la eliminación del fármaco, ya que el principal inconveniente en la administración bucal es que el paciente puede tragar parte de la dosis aplicada antes de que el fármaco se absorbe, incluso si se ha liberado [115]. La prueba in vitro mostró que la saliva arrastró más del 60 % de KT en 1 h, que se ingiere y se deriva de una ingesta oral. Incluso a pesar del efecto de la saliva, el KT pudo penetrar en ambas mucosas. El hidrogel de alginato-HA se formuló con la sal trometamina del KT ya que ésta es más hidrófila y permite una mejor integración en el hidrogel. Sin embargo, es de esperar que, una vez aplicado el gel sobre las mucosas, el KT cambie y, debido al medio en el que se encuentra, se protone y/o ionice y que, durante el proceso, coexistan las diferentes formas hasta alcanzar

un equilibrio. Estos cambios afectan las propiedades fisicoquímicas del fármaco, como su solubilidad en saliva o el valor del coeficiente de partición log P, modificando así su afinidad tisular[116] [117]. Dado que el hidrogel de alginato-HA se formuló con la sal de trometamina, es probable que esta fuera la forma predominante al inicio del estudio al aplicar el gel sobre la mucosa y por tanto que se favoreciera el proceso de disolución del KT en saliva. Sin embargo, no debe olvidarse que el KT de la formulación está siendo absorbido simultáneamente a través de la mucosa. Esta absorción depende de diferentes factores. Por un lado, la histología de la mucosa, y por otro, las propiedades fisicoquímicas del KT. Teniendo en cuenta que tanto la mucosa bucal como la sublingual están formadas por un epitelio escamoso estratificado no queratinizado y que la principal diferencia es el grosor de dicho epitelio (siendo la sublingual entre 100 y 200 µm, 8-12 células de espesor, y entre 500 y 800 µm, 40 – 50 células de espesor, la bucal [118]), es lógico pensar que la mucosa sublingual presenta menor resistencia al paso del KT. Desde un principio, la cantidad de KT que se elimina por acción de la saliva cuando se aplica el gel sobre esta mucosa es menor que cuando se aplica el gel sobre la mucosa bucal. El perfil cinético de disolución es el resultado de la suma de estos dos procesos. A través de la mucosa bucal se observa cómo al principio predomina la disolución de KT en saliva hasta que pasados unos 30 min se alcanza un equilibrio entre lo disuelto y lo absorbido por la mucosa. Este comportamiento se ajusta a una cinética de primer orden. Por otro lado, en la mucosa sublingual, al presentar menor resistencia al paso del KT a través de su estructura, los procesos de disolución y absorción están equilibrados desde el principio, por lo que describe una cinética de disolución de orden cero. Estos resultados muestran cómo, además de las propiedades fisicoquímicas del fármaco y las características fisiológicas de las mucosas, otros factores como la salivación juegan un papel importante en la biodisponibilidad del ketorolaco ya que, en ambas mucosas, mucho más de la mitad de la dosis aplicada fue eliminada por la acción de la saliva, que puede explicarse, en parte, por la alta hidrosolubilidad del KT.

La cantidad que se retiene en la mucosa es la responsable de la acción analgésica y antiinflamatoria local. Así, se observó que en el estudio en animales vivos y bajo un régimen finito de dosis no se alcanzan concentraciones sistémicas de KT. Además de la menor dosis, esto probablemente se deba al efecto de la saliva, como se demostró en el estudio in vitro, que puede influir al reducir el tiempo que el gel de alginato-HA 2 % KT está en contacto con las mucosas y, en consecuencia, con la cantidad de

principio activo que podría ser permeada. Cabe señalar que el presente estudio se realizó mediante la administración de una sola dosis de fármaco con el fin de minimizar al máximo el tiempo de prueba y, por tanto, el estrés que se pudiera ocasionar a los animales. Son necesarios otros estudios aplicando el gel de alginato-HA 2 % KT en un régimen de dosis múltiples para analizar con mayor precisión el comportamiento del hidrogel en términos de biodisponibilidad y permeabilidad a través de las membranas mucosas de la cavidad oral.

Los valores de TMWL obtenidos, tanto basales como a las 2 h postaplicación, (alrededor de 30 $g/m^2 \cdot h$ para la mucosa bucal y de 40 $g/m^2 \cdot h$ para la mucosa sublingual) muestran el excelente estado de la mucosa tras la aplicación del hidrogel, ya que ambos presentan valores cercanos a 30 $g/m^2 \cdot h$, que se considera aceptable para la integridad de la mucosa bucal [111]. Así, el gel alginato-HA 2 % KT no provoca disrupción de las mucosas, siendo bien tolerado por los tejidos diana.

El análisis histológico no reveló diferencias entre las mucosas tratadas y no tratadas. Adicionalmente, la viabilidad celular mostró que el gel alginato-HA 2 % KT no causa citotoxicidad en células Caco-2.

Paralelamente y aprovechando los estudios de permeación en mucosas de la cavidad oral, se evaluó la biocompatibilidad comparando la permeabilidad del hidrogel-AH 2 % KT sobre mucosa bucal y sublingual con la permeabilidad de la membrana sintética biomimética PermeaPad®. Se observó que la membrana biomimética se correlacionó muy bien con ambas mucosas, pero presentando una capacidad de retención de KT significativamente menor. Estos resultados están de acuerdo con el trabajo de otros investigadores. Bibi et al. investigó el uso de PermeaPad® como predictor de la absorción bucal de la solución de metoprolol [119]. Los autores compararon la permeabilidad aparente obtenida con PermeaPad® con trabajos previos realizados por otros autores, que evaluaron la permeabilidad aparente de la solución de metroprolol en cultivo celular, en mucosa bucal porcina y, finalmente, en estudios in vivo realizados en mini cerdos. Bibi et al. encontraron una buena correlación in vitro-in vivo entre PermeaPad® y los tres sistemas evaluados. La excelente correlación de la membrana PermeaPad con las mucosas de la cavidad oral muestra cómo dichas membranas sintéticas podrían llegar a ser una muy buena alternativa al uso de tejidos vivos de origen animal y/o humano, con todas las ventajas que eso supone.

Tras el éxito del hidrogel de alginato de sodio y KT al 2 % tanto en piel humana cómo en mucosas vaginal, bucal y sublingual, se quiso elaborar otras formulaciones con KT como principio activo, también dirigidas al manejo del dolor y la inflamación en cirugías sobre piel y mucosas. Para ello se optó por elaborar nanopartículas de PLGA portadoras de KT para el manejo del dolor y la inflamación prequirúrgico, dado que podrían usarse como spray y facilitar así su aplicación sin necesidad de entrar en contacto directo con la lesión evitando así posibles contaminaciones, y el chitosan como polímero gelificante y mucoadhesivo para la elaboración de un hidrogel con KT al 2 %, para el manejo del dolor y la inflamación postquirúrgico.

El quitosano o chitosan (CTS), un polímero natural, es un candidato prometedor para los sistemas de administración controlada de fármacos y la cicatrización de heridas [120]. Esto se debe a sus propiedades como biocompatibilidad, biodegradabilidad, actividad antimicrobiana, mucoadhesividad, hidrofilia y baja inmunogenicidad [121]. Además, el chitosan también posee propiedades antifúngicas y hemostáticas, así como un ligero efecto antiinflamatorio [120][121]. Todas estas propiedades son de gran interés para el manejo y cuidado de las áreas tratadas posquirúrgicamente, influyendo positivamente en la reducción de complicaciones como sangrado e infecciones, favoreciendo así el proceso de cicatrización de heridas [88].

Las características morfológicas del gel KT-CTS mostraron que tiene una estructura compacta y densa, lo cual también fue observado por Yanget al. [122]. Sin embargo, otros investigadores observaron estructuras lamelares o porosas en geles de chitosan [123][124]. Las diferencias en la microestructura observadas por los diferentes autores pueden atribuirse a la formulación o preparación de la muestra.

Los hidrogeles son estructuras tridimensionales compuestas por redes poliméricas hidrófilas, capaces de absorber grandes cantidades de agua o fluidos biológicos. Los hidrogeles tienen compatibilidad termodinámica con el agua, lo que les permite hincharse en un medio acuoso [83][125]. Los hallazgos indican que el gel deshidratado es higroscópico absorbiendo hasta 4,5 veces su peso en agua en menos de 4 h. El proceso de hinchamiento del gel KT-CTS siguió una cinética de orden cero. Esto fue debido a la excelente capacidad del CTS para absorber grandes volúmenes de agua [126]. El comportamiento de hinchamiento de los geles depende de las características del ambiente externo y como consecuencia los complejos poliméricos pueden romperse, hincharse o mostrar cambios drásticos en sus valores de hinchamiento.

Algunos de los factores que pueden afectar el comportamiento de polímeros son el pH, la temperatura, la fuerza iónica y la radiación electromagnética. Nuestros hallazgos demuestran que el gel chitosan se difunde en el medio, lo que indica que se debe esperar que esta formulación se degrade con éxito cuando se sumerge en un medio biológico.

La viscosidad del hidrogel juega un papel crucial en el control de la liberación del fármaco y la penetración en la piel. El modelo reológico de Casson describe el flujo de fluidos viscoelásticos [127]. Este comportamiento apoya la aplicación tópica pretendida de esta formulación, facilitando así su aplicación ambulatoria. Un punto clave a favor es que se aplique en la zona deseada con precisión, sin temor a que se disperse a otras regiones en cuanto el paciente cambie de posición postural, y, por otro lado, puede fluir y disminuir su viscosidad cuando se aplica estrés, lo cual es una característica deseable en la posible difusión de productos dermatológicos ya que permite una aplicación suave e indolora.

La producción de NPs tiene muchas variables independientes. El polímero utilizado para formular las NPs afecta a la estructura, propiedades y aplicaciones de las partículas, por lo que no existe un único polímero adecuado para todos los fármacos. El PLGA fue elegido para diseñar las NPs debido a sus diversas características ventajosas reportadas, especialmente la biodegradabilidad [128]. Hay dos características que deben tenerse en cuenta al formular NP poliméricas para una vía de administración determinada: el tamaño de partícula y la eficiencia de encapsulación. Por ejemplo, si se pretende una absorción rápida, el tamaño de las nanopartículas debe ser de 100 nm o menos. El PI es una medida de la carga de la partícula, cuanto mayor sea el valor absoluto de PI, mayor será la carga en la superficie de las NPS y, a su vez, mayor la estabilidad de las partículas [129]. En el caso de las KT-NP, el pequeño valor de PI no fue crítico porque las KT-NP se prepararon con PVA como agente estabilizador. El mecanismo de acción del PVA para prevenir la agregación de partículas se basa en el impedimento estérico [130]. Las KT-NP obtenidas mostraron una alta eficiencia de encapsulación, una estructura de forma redonda y una distribución estrecha que indica un sistema monodisperso.

La diferencia en el valor de Zave entre las mediciones TEM y DLS se atribuye al hecho de que el DLS midió el diámetro hidrodinámico, mientras que el TEM muestra el tamaño real de las partículas [97]. Zambaux et al. [100] estudiaron la influencia de

ciertos parámetros experimentales (temperatura de preparación, método de evaporación del solvente, concentración de surfactante, peso molecular del polímero) en el Zave, PI y ZP de las NPs preparadas por el método de doble emulsión. Los autores concluyeron que las altas concentraciones de tensioactivo (3 % p/v o más) garantizaban un proceso de emulsificación exitoso y partículas más pequeñas que llegaban a un PI satisfactorio. Otro factor que influye en las características de las NPs de PLGA preparadas por el método de doble emulsión W/O/W es la evaporación de solventes. Bilati et al. [101] estudiaron la influencia del proceso de sonicación, analizando la modificación del tamaño y distribución de las NPs en función de la duración e intensidad de la sonicación. El trabajo mostró que la duración del segundo paso de homogeneización, el que proporciona la doble emulsión (W/O/W), tuvo mayor influencia en el tamaño de partícula que la primera homogeneización (emulsión W/O). El tamaño de partícula disminuye con el aumento del tiempo de sonicación de la segunda emulsificación. Los resultados del estudio, asímismo sugirieron que la intensidad de la sonicación también afecta la morfometría de las NP. Además, el disolvente orgánico utilizado también puede tener un papel importanteen las propiedades finales de las NPs. Mainardes et al. [102] evaluó este efecto en su trabajo, comparando el tamaño de partícula obtenido al preparar las NPs de PLGA con dos disolventes orgánicos: cloruro de metileno o acetato de etilo. Se concluyó que el cloruro de metileno proporcionó NP más grandes que cuando se utilizó acetato de etilo como disolvente orgánico. La selección del método depende, por tanto, de varios factores que deben evaluarse para obtener las NPs con las características y propiedades deseadas.

El pH de la fase acuosa externa de las NP de KT así como del gel KT-CTS fueron dentro del rango de pH de la piel sana, por lo que no se espera que las formulaciones causen ningún trastorno [36][131].

Que un hidrogel sea adecuado como sistema de administración de ingredientes activos depende en gran medida de su estructura polimérica. La liberación controlada de principios activos a partir de hidrogeles poliiónicos puede responder a cambios en parámetros ambientales, tales como pH, temperatura y otros estímulos. Nuestros hallazgos revelaron que la liberación de KT de las NPs fue significativamente más rápida que del gel KT-CTS ($p < 0,0001$). El perfil de liberación de KT-NP parece encajar con la hipótesis de nuestro estudio, ya que la liberación rápida de KT es crucial

para la aplicación preoperatoria en la que se prefiere una liberación rápida. Mientras tanto, el perfil del gel KT-CTS, que podría deberse a la interacción electrostática entre KT y CTS, y la estructura compacta, parece ser adecuado para la aplicación postoperatoria, donde se desea una liberación más sostenida.

Asimismo, se evaluó la biodistribución de KT después de que la piel estuvo expuesta a ambas formulaciones bajo un enfoque de dosis finita durante 24 h. Para determinar la cantidad de KT en cada compartimento, la piel se separó en sus diferentes capas y tanto el líquido receptor como la formulación residual al final del experimento se recuperaron para una mayor cuantificación del fármaco. Se observó que la mayor cantidad de KT permaneció en la superficie de la piel para ambas formulaciones. Esto está en consonancia con trabajos previos sobre hidrogeles, y se debe a la función de barrera primaria del estrato córneo contra la penetración del fármaco [116][132]. Ambas formulaciones parecen ser vehículos adecuados para la administración dérmica. En ambos casos, el KT difundió fácilmente a través de la piel y se retuvo principalmente en la epidermis, donde puede ejercer sus propiedades antiinflamatorias y analgésicas. Se observaron perfiles similares para hidrogeles de KT formulados con diferentes polímeros [116]. Cuando se probó la distribución de KT en la piel humana con un hidrogel a base de alginato, la difusión de KT se limitó a la epidermis, donde se encontraron cantidades similares de fármaco, poca retención de KT en la dermis y KT no cuantificable en el líquido receptor. Tampoco se retuvo KT en la dermis de hidrogeles basados en Carbopol y Pluronic, y también hubo una mala difusión de KT en el líquido receptor. Entre estos polímeros, el gel CTS es el vehículo que mejoró la difusión de KT en el fluido receptor.

Los valores de TEWL 2 h después de la aplicación de las formulaciones mostraron una ligera variación sin diferencias estadísticas significativas en comparación con los valores basales. En una piel sana que funciona normalmente como barrera, el TEWL debería ser directamente proporcional a la hidratación de la piel [133]. La hidratación del estrato córneo se determina como la conductancia que proporciona el agua libre a la superficie de la piel. Si bien la hidratación del estrato córneo experimentó una disminución luego de la aplicación de las formulaciones, las diferencias observadas no resultaron ser estadísticamente significativas. Los resultados mostraron que la piel presenta valores suficientemente hidratados (superiores a 45 UA), acordes con los valores normales de hidratación de la piel en condiciones estándar [116][134]. En el

caso del gel KT-CTS, la disminución probablemente esté relacionada con el comportamiento de hinchamiento del gel CTS cuando se aplica sobre la piel.

El estudio de eficacia antiinflamatoria reveló que las KT-NP exhiben eficacia antiinflamatoria significativamente mayor que el gel KT-CTS en una proporción de aproximadamente tres veces. Estos resultados concuerdan con el análisis histológico que mostró la presencia de células del sistema inmunes en el control positivo, de acuerdo con el edema inducido por TPA. Gracias a la acción de las KT-NPs, la infiltración de las células del sistema inmunitario se inhibe por completo, mientras que la histología del oído tratado con el gel KT-CTS muestra un número limitado de estas células en los vasos sanguíneos de los tejidos. Aun así, la eficacia antiinflamatoria del gel KT-CTS es evidente, tal y como muestran las imágenes histológicas. Cabe señalar que las NP cargaron menos KT que el gel KT-CTS. Esto demuestra como las NPs son una excelente formulación para la aplicación de KT ya que conseguimos un potente efecto sin necesidad de aplicar una dosis alta, mejorando así la ventana de efectos secundarios y, por tanto, la satisfacción y adherencia del paciente, pues el dolor durante el tratamiento es uno de los factores que más afectan la adherencia al tratamiento [135][136]. Considerando que las formulaciones muestran características adecuadas para la administración tópica, son bien toleradas y exhiben un buen perfil antiinflamatorio, ambas formulaciones son candidatas para ofrecer una actividad antiinflamatoria local en la aplicación clínica. En este sentido, se podrían realizar futuros estudios preclínicos y clínicos.

Los resultados de los estudios realizados muestran cómo el diseño de formulaciones juega un papel crucial a la hora de elaborar y producir fármacos. Partiendo de un mismo principio activo, ketorolaco trometamina, se han elaborado 4 formulaciones tópicas distintas que presentan cada una sus particularidades que las hacen idóneas para ser aplicadas cada una de ellas en contextos determinados, permitiendo así adaptar el tratamiento a cada situación según mejor convenga.

CONCLUSIONES

Different topical KT formulations have been designed and prepared: sodium alginate hydrogel and KT at 2%, sodium alginate hydrogel, hyaluronic acid, and KT at 2%, chitosan hydrogel, and KT at 2%, and polymeric NPs of PLGA and KT.

Said formulations have been characterized organoleptically, morphologically, and physicochemically, showing suitable characteristics for their topical application on skin and mucous membranes.

The kinetic profile of the different formulations has been determined by in vitro release studies and modelling. In less than six hours and following a one-phase exponential model, 73.0%, 51.6%, 18.6%, and 92.0% of the total KT amount could be released from the sodium alginate gel and 2% KT, of the alginate-HA 2% KT gel, of the chitosan gel and 2% KT and of the KT-NP, respectively, responding and adapting, all of them, satisfactorily to the indication of each formulation.

KT's ex vivo penetration capacity from the formulations in different tissues was studied. The KT contained in the sodium alginate hydrogel showed adequate permeability in the skin and vaginal mucosa; the KT in the HA-alginate gel diffused rapidly through the buccal and sublingual mucosa, and the KT formulated in the chitosan gel, and the NPs presented optimal diffusion through the skin, being retained mainly in the epidermis.

The anti-inflammatory efficacy of the KT in the sodium alginate hydrogel, in the chitosan gel, and in the nanoparticles was evaluated through in vivo studies in mouse ears. In all formulations, the edema caused by TPA was effectively counteracted by KT.

The tissues' histological structure was observed after applying the sodium alginate-HA 2% KT gel, the chitosan 2% KT hydrogel, and the KT-NP. The tissues' histology in which the formulations were applied did not present differences before and after application, thus demonstrating the tested formulations' tolerability.

The impact of some formulations on the biomechanical properties of the skin and mucous membranes was analyzed. Sodium alginate 2% KT gel was well tolerated in vivo when applied to humans, showing no significant alterations in skin barrier function such as hydration and TEWL. The alginate-HA 2% KT hydrogel did not show

alterations in the TMWL after being applied to the buccal and sublingual mucosa, nor did the chitosan 2% KT gel nor the KT-NP after being tested on human skin.

Additionally, the innocuousness and safety of 2% KT-HA alginate gel were examined through in vitro cell cultures. The cell viability showed that the alginate-HA 2% KT gel does not cause cytotoxicity in Caco-2 cells.

BIBLIOGRAFÍA

[1] J. J. Bonica, “History of pain concepts and pain therapy,” *Mt. Sinai J. Med.*, vol. 58, no. 3, pp. 191–202, 1991, Accessed: Feb. 05, 2022. [Online]. Available: https://pubmed.ncbi.nlm.nih.gov/1875956/.

[2] R. M. John D Loeser and Until, “Pain: an overview,” *Lancet*, vol. 353, pp. 1607–1609, 1999.

[3] L. U. Sneddon, “Comparative Physiology of Nociception and Pain,” *Physiology*, vol. 33, pp. 63–67, 2018, doi: 10.1152/physiol.00022.2017.

[4] E. J. Cassel, “The Nature of Suffering and the Goals of Medicine,” *http://dx.doi.org/10.1056/NEJM198203183061104*, vol. 306, no. 11, pp. 639–645, Jan. 2010, doi: 10.1056/NEJM198203183061104.

[5] J. Vidal Fuentes *et al.*, *Manual de medicina del dolor : fundamentos, evaluación y tratamiento*. 2016.

[6] A. I. Basbaum, D. M. Bautista, G. Scherrer, and D. Julius, “Cellular and Molecular Mechanisms of Pain,” *Cell*, vol. 139, no. 2, p. 267, Oct. 2009, doi: 10.1016/J.CELL.2009.09.028.

[7] C. J. Woolf, “What is this thing called pain?,” *J. Clin. Invest.*, vol. 120, no. 11, p. 3742, Nov. 2010, doi: 10.1172/JCI45178.

[8] “Dolor.com,” *Clasificación del dolor*, 2021. https://www.dolor.com/para-sus-pacientes/tipos-de-dolor/clasificacion-dolor (accessed Feb. 06, 2022).

[9] A. Agita and M. Thaha, “Inflammation, Immunity, and Hypertension,” *Indones. J. Intern. Med.*, vol. 49, no. 2, pp. 158–165, 2017.

[10] R. M. Duarte Da Cruz *et al.*, “Thiophene-Based Compounds with Potential Anti-Inflammatory Activity,” *Pharmaceuticals*, vol. 14, p. 692, 2021, doi: 10.3390/ph14070692.

[11] A. G. D. E. L. Y. Mateos, J. L. Martínez, and Y. M. S. Castilla, “Respuesta inflamatoria sistémica : fisiopatología y mediadores,” pp. 353–360.

[12] J. J. G.-R. C. Juan A García Meijidea, “Fisiopatología de la ciclooxigenasa-1 y ciclooxigenasa-2 | Revista Española de Reumatología,” *Elsevier*, 2000. https://www.elsevier.es/es-revista-revista-espanola-reumatologia-29-articulo-fisiopatologia-ciclooxigenasa-1-ciclooxigenasa-2-8546 (accessed Feb. 15, 2022).

[13] E. Ricciotti and G. A. Fitzgerald, “Prostaglandins and Inflammation,” *Arterioscler. Thromb. Vasc. Biol.*, vol. 31, no. 5, p. 986, May 2011, doi: 10.1161/ATVBAHA.110.207449.

[14] H. Harizi, J.-B. B. Corcuff, and N. Gualde, “Arachidonic-acid-derived eicosanoids: roles in biology and immunopathology,” *Trends Mol. Med.*, vol. 14, no. 10, pp. 461–469, 2008, doi: 10.1016/j.molmed.2008.08.005.

[15] A. Salido, M. Abásolo, L. Bañares, “Revisión de los antiinflamatorios inhibidores selectivos de la ciclooxigenasa-2,” *Inf Ter Sist Nac Salud*, vol. 25, no. 2, pp. 46–52, 2001.

[16] S. Harirforoosh, W. Asghar, and F. Jamali, “Adverse effects of nonsteroidal antiinflammatory drugs: an update of gastrointestinal, cardiovascular and renal complications,” *J. Pharm. Pharm. Sci.*, vol. 16, no. 5, pp. 821–847, Dec. 2013, doi: 10.18433/J3VW2F.

[17] C. E. Inturrisi, “Clinical Pharmacology of Opioids for Pain,” *Clin. J. Pain*, vol. 18, no. 4, pp. 3–13, 2002.

[18] A. Garrote y R. Bonet, “Elsevier: Revista offarm,” *El papel de los AINE en el tratamiento*

analgésico, 2003. https://www.elsevier.es/es-revista-offarm-4-pdf-13043197 (accessed Feb. 16, 2022).

[19] V. R. Sinha, R. V. Kumar, and G. Singh, "Ketorolac tromethamine formulations: an overview," *Expert Opin. Drug Deliv.*, vol. 6, no. 9, pp. 961–975, Sep. 2009, doi: 10.1517/17425240903116006.

[20] J. C. Gillis and R. N. Brogden, "Ketorolac: A reappraial of its pharmacodynamic and pharmacokinetic properties and therapeutic use in pain management," *Drugs*, vol. 53, no. 1, pp. 139–188, 1997, doi: 10.2165/00003495-199753010-00012.

[21] F. Dastan, Z. M. Langari, J. Salamzadeh, A. Khalili, S. Aqajani, and A. Jahangirifard, "A Comparative Study of the Analgesic Effects of Intravenous Ketorolac, Paracetamol, and Morphine in Patients Undergoing Video-assisted Thoracoscopic Surgery: A Double-blind, Active-controlled, Randomized Clinical Trial," *Ann. Card. Anaesth.*, vol. 23, no. 2, p. 177, Apr. 2020, doi: 10.4103/ACA.ACA_239_18.

[22] E. J. Wladis, K. V. Dennett, V. H. Chen, and A. De, "Preoperative Intravenous Ketorolac Safely Reduces Postoperative Pain in Levator Advancement Surgery," *Ophthal. Plast. Reconstr. Surg.*, vol. 35, no. 4, pp. 357–359, Jul. 2019, doi: 10.1097/IOP.0000000000001265.

[23] B. Masoumi, B. Farzaneh, O. Ahmadi, and F. Heidari, "Effect of Intravenous Morphine and Ketorolac on Pain Control in Long Bones Fractures," *Adv. Biomed. Res.*, vol. 6, no. 1, p. 91, 2017, doi: 10.4103/2277-9175.211832.

[24] M. M-T Buckley, R. N. Brogden, and H. Bird, "Ketorolac: A Review of Evaluationits Pharmacodynamic and Pharmacokinetic Properties, and Therapeutic Potential," 1990.

[25] D. P. Orgill and D. Ph, "Ketorolac does not increase perioperative bleeding: A Meta-Analysis of randomized controlled trials," *Plast. Reconstr. Surg.*, vol. 133, no. 3, pp. 741–755, 2014, doi: 10.1097/01.prs.0000438459.60474.b5.

[26] M. B. Brown, G. P. Martin, S. A. Jones, and F. K. Akomeah, *Drug Delivery Dermal and Transdermal Drug Delivery Systems: Current and Future Prospects*. 2008.

[27] M. Ghosh, "Secreted Mucosal Antimicrobials in the Female Reproductive Tract that are Important to Consider for HIV Prevention," *J Reprod Immunol*, vol. 71, pp. 575–588, 2014, doi: 10.1111/aji.12250.

[28] K. Sharif and O. Olufowobi, "The Structure, Chemistry and Physics of Human Cervical Mucus," *Cervix Second Ed.*, pp. 155–168, May 2009, doi: 10.1002/9781444312744.CH11.

[29] M. T. Cook and M. B. Brown, "Polymeric gels for intravaginal drug delivery," *J. Control. Release*, vol. 270, pp. 145–157, Jan. 2018, doi: 10.1016/J.JCONREL.2017.12.004.

[30] M. J. GODLEY, "Quantitation of vaginal discharge in healthy volunteers," *BJOG An Int. J. Obstet. Gynaecol.*, vol. 92, no. 7, pp. 739–742, Jul. 1985, doi: 10.1111/J.1471-0528.1985.TB01457.X.

[31] M. E. Gómez and A. Campos, "Histología, embriología e Ingeniería Tisular Bucodental," *Histol. Embriol. en Ing. Tisular Bucodental*, vol. 4ta, p. 456, 2019.

[32] C. A. Lipinski, F. Lombardo, B. W. Dominy, and P. J. Feeney, "Experimental and computational approaches to estimate solubility and permeability in drug discovery and development settings i," 2012, doi: 10.1016/j.addr.2012.09.019.

[33] M. Mallandrich, "Estudio de formulaciones de ketorolaco de trometamina para aplicación sobre mucosas y piel," 2017.

[34] A. K. Ghose, V. N. Viswanadhan, and J. J. Wendoloski, “A Knowledge-Based Approach in Designing Combinatorial or Medicinal Chemistry Libraries for Drug Discovery. 1. A Qualitative and Quantitative Characterization of Known Drug Databases,” *J. Comb. Chem.*, vol. 1, no. 1, pp. 55–68, 1998, doi: 10.1021/CC9800071.

[35] J. L. Du Plessis, A. B. Stefaniak, and K. P. Wilhelm, “Measurement of Skin Surface pH,” *Curr. Probl. Dermatology*, vol. 54, pp. 19–25, 2018, doi: 10.1159/000489514.

[36] M. H. Schmid-Wendtner and H. C. Korting, “The pH of the Skin Surface and Its Impact on the Barrier Function,” *Skin Pharmacol. Physiol.*, vol. 19, no. 6, pp. 296–302, Nov. 2006, doi: 10.1159/000094670.

[37] E. Proksch, “pH in nature, humans and skin,” *J. Dermatol.*, vol. 45, no. 9, pp. 1044–1052, Sep. 2018, doi: 10.1111/1346-8138.14489.

[38] C. Loke, J. Lee, S. Sander, L. Mei, and M. Farella, “Factors affecting intra-oral pH - a review,” *J. Oral Rehabil.*, vol. 43, no. 10, pp. 778–785, 2016, doi: 10.1111/joor.12429.

[39] S. De Liberación Bioadhesivos, “Sistemas de liberación Bioadhesivos,” *Ars Pharm.*, vol. 1, no. 41, pp. 115–128, 2000.

[40] S. A. Garzón, “Estudio de la permeación de una serie de betabloqueantes a través de mucosa de cerdo,” 2012.

[41] C. A. Lesch, C. A. Squier, A. Cruchley, D. M. Williams, and P. Speight, “The Permeability of Human Oral Mucosa and Skin to Water,” *J. Dent. Res.*, vol. 68, no. 9, pp. 1345–1349, Nov. 1989, doi: 10.1177/00220345890680091101.

[42] P. Van Der Biji’’, I. O. C. Ttiompson’^, and C. A. Squier^, “Comparative permeability of human vaginal and buccal mucosa to water,” 1997.

[43] R. H. Guy, J. Hadgraft, and D. A. W. Bucks, “Transdermal drug delivery and cutaneous metabolism,” *http://dx.doi.org.sire.ub.edu/10.3109/00498258709043943*, vol. 17, no. 3, pp. 325–343, 2009, doi: 10.3109/00498258709043943.

[44] M. Stanley, “Pathology and epidemiology of HPV infection in females,” *Gynecologic Oncology*, vol. 117, no. 2 SUPPL. Academic Press Inc., p. S5, May 01, 2010, doi: 10.1016/j.ygyno.2010.01.024.

[45] G. González Martínez and J. Núñez Troconis, “Tratamiento de las verrugas genitales: una actualización,” *Rev. Chil. Obstet. Ginecol.*, vol. 80, no. 1, pp. 76–83, 2015, doi: 10.4067/s0717-75262015000100012.

[46] S. V. Graham, “The human papillomavirus replication cycle, and its links to cancer progression: A comprehensive review,” *Clinical Science*, vol. 131, no. 17. Portland Press Ltd, pp. 2201–2221, 2017, doi: 10.1042/CS20160786.

[47] A. O. Cutro and F. C. Scharn, *AEPC-Guía: Condilomas Acuminados.*, vol. 67, no. 13. 2015.

[48] S. M. Garland *et al.*, “Impact and effectiveness of the quadrivalent human papillomavirus vaccine: A systematic review of 10 years of real-world experience,” *Clin. Infect. Dis.*, vol. 63, no. 4, pp. 519–527, 2016, doi: 10.1093/cid/ciw354.

[49] F. Bouscarat, F. Pelletier, S. Fouéré, M. Janier, A. Bertolloti, and F. Aubin, “Verrues génitales (condylomes) externes External genital warts (condylomata),” *Ann. Dermatol. Venereol.*, vol. 143, no. 11, pp. 741–745, 2016, doi: 10.1016/j.annder.2016.09.013.

[50] H. Patel, M. Wagner, P. Singhal, and S. Kothari, “Systematic review of the incidence and prevalence of genital warts,” *BMC Infect. Dis.*, vol. 13, no. 39, pp. 1–14, 2013, doi:

10.1186/1471-2334-13-39.

[51] S. Sabeena, P. Bhat, V. Kamath, and G. Arunkumar, “Possible non-sexual modes of transmission of human papilloma virus,” *Journal of Obstetrics and Gynaecology Research*, vol. 43, no. 3. Blackwell Publishing, pp. 429–435, Mar. 01, 2017, doi: 10.1111/jog.13248.

[52] M. W. Report, *Sexually Transmitted Diseases Treatment Guidelines , 2015*, vol. 64, no. 3. 2015.

[53] S. J. Betz, “HPV-Related Papillary Lesions of the Oral Mucosa: A Review,” *Head Neck Pathol.*, vol. 13, no. 1, pp. 80–90, 2019, doi: 10.1007/s12105-019-01003-7.

[54] S. Syrjänen, “Oral manifestations of human papillomavirus infections,” *Eur. J. Oral Sci.*, vol. 126, pp. 49–66, 2018, doi: 10.1111/eos.12538.

[55] G. A. Pringle, “The Role of Human Papillomavirus in Oral Disease,” *Dent. Clin. NA*, vol. 58, pp. 385–399, 2014, doi: 10.1016/j.cden.2013.12.008.

[56] C. J. N. Lacey, S. C. Woodhall, A. Wikstrom, and J. Ross, “2012 European guideline for the management of anogenital warts,” *J. Eur. Acad. Dermatology Venereol.*, vol. 27, no. 3, pp. e263–e270, Mar. 2013, doi: 10.1111/j.1468-3083.2012.04493.x.

[57] P. C. Atienzo *et al.*, “Presencia del Virus Papiloma Humano en la Cavidad Oral: Revisión y Actualización de la Literatura,” *Int. J. Odontostomat*, vol. 9, no. 2, pp. 233–238, 2015.

[58] A. R. Piña *et al.*, “Benign epithelial oral lesions – association with human papillomavirus,” *Med. Oral Patol. Oral y Cir. Bucal*, vol. 24, no. 3, pp. e290–e295, May 2019, doi: 10.4317/medoral.22817.

[59] R. P. M. Alsina and C. Mu, “Nuevos tratamientos en la infección por virus del papiloma humano,” *Actas Dermosifiliogr.*, vol. 104, no. 10, pp. 883–889, 2013.

[60] M. Carmona Lorduy, J. Harris Ricardo, Y. Hernández Arenas, and W. Medina Carmona, “Use of trichloroacetic acid for management of oral lesions caused by human papillomavirus.,” *Gen. Dent.*, vol. 66, no. 2, 2018.

[61] J. B. Karnes, M. Dartmouth, F. Medicine, M. R. P. Usatine, T. Health, and S. Antonio, “Management of External Genital Warts,” *Am. Fam. Phsician*, vol. 90, no. 5, pp. 312–318, 2014.

[62] N. Sharma, S. Sharma, and C. Singhal, “A comparative study of liquid nitrogen cryotherapy as monotherapy versus in combination with podophyllin in the treatment of condyloma acuminata,” *J. Clin. Diagnostic Res.*, vol. 11, no. 3, pp. WC01–WC05, 2017, doi: 10.7860/JCDR/2017/23797.9339.

[63] N. Scheinfeld, “Genital warts,” 2006. https://escholarship.org/uc/item/7v57p744 (accessed Nov. 13, 2020).

[64] E. Thurgar, S. Barton, C. Karner, and E. Sj, “Clinical effectiveness and cost-effectiveness of interventions for the treatment of anogenital warts: systematic review and economic evaluation,” *Health Technol. Assess. (Rockv).*, vol. 20, no. 24, pp. 1–64, 2016, doi: 10.3310/hta20240.

[65] “Electrocoagulación: qué es, síntomas, causas, prevención y tratamiento | Top Doctors.” https://www.topdoctors.es/diccionario-medico/electrocoagulacion (accessed Nov. 22, 2020).

[66] G. Von Krogh and E. L. V, “Podophyllin office therapy against condyloma should be abandoned,” *Sex Transm. Infect.*, vol. 77, pp. 409–412, 2001.

[67] E. Longstaff and G. Von Krogh, “Condyloma Eradication: Self-Therapy with 0.15–0.5%

Podophyllotoxin versus 20–25% Podophyllin Preparations—An Integrated Safety Assessment," *Regul. Toxicol. Pharmacol.*, vol. 33, no. 3, pp. 117–137, 2001, doi: 10.1006/rtph.2000.1446.

[68] J. Yuan *et al.*, "Genital warts treatment: Beyond imiquimod," *Hum. Vaccines Immunother.*, vol. 14, no. 7, pp. 1815–1819, 2018, doi: 10.1080/21645515.2018.1445947.

[69] E. Stockfleth and T. Meyer, "The use of sinecatechins (polyphenon E) ointment for treatment of external genital warts," *Expert Opin. Biol. Ther.*, vol. 12, no. 6, pp. 783–793, Jun. 2012, doi: 10.1517/14712598.2012.676036.

[70] T. G. Tzellos, C. Sardeli, A. Lallas, G. Papazisis, M. Chourdakis, and D. Kouvelas, "Efficacy, safety and tolerability of green tea catechins in the treatment of external anogenital warts: A systematic review and meta-analysis," *J. Eur. Acad. Dermatology Venereol.*, vol. 25, no. 3, pp. 345–353, 2011, doi: 10.1111/j.1468-3083.2010.03796.x.

[71] L. Morales, A. Liliana, R. Rincón, F. Diego, and R. Orozco, "Avances en el desarrollo de nuevas vacunas profilácticas y terapéuticas contra el Virus del Papiloma Humano," *Rev. la Univ. Ind. Santander. Salud*, vol. 48, no. 3, pp. 385–391, 2016.

[72] A. S. Aldahan *et al.*, "Efficacy of intralesional immunotherapy for the treatment of warts : A review of the literature," *Dermatologyc Ther.*, vol. 29, no. 6, pp. 197–207, 2016.

[73] S. Sharma and S. Agarwal, "Intralesional Immunotherapy with Measles Mumps Rubella Vaccine for the Treatment of Anogenital Warts: An Open-label Study.," *J. Clin. Aesthet. Dermatol.*, vol. 13, no. 8, pp. 40–44, Aug. 2020, Accessed: Feb. 09, 2021. [Online]. Available: http://www.ncbi.nlm.nih.gov/pubmed/33178381.

[74] A. Nofal and R. Alakad, "Intralesional immunotherapy for the treatment of anogenital warts in pediatric population," *J. Dermatolog. Treat.*, pp. 1–5, Aug. 2020, doi: 10.1080/09546634.2020.1800573.

[75] T. D. Horn, S. M. Johnson, R. M. Helm, and P. K. Roberson, "Intralesional immunotherapy of warts with mumps, Candida, and Trichophyton skin test antigens: A single-blinded, randomized, and controlled trial," *Arch. Dermatol.*, vol. 141, no. 5, pp. 589–594, May 2005, doi: 10.1001/archderm.141.5.589.

[76] S. Gupta, A. Malhotra, K. Verma, and V. Sharma, "Intralesional immunotherapy with killed *Mycobacterium w* vaccine for the treatment of ano-genital warts: an open label pilot study," *J. Eur. Acad. Dermatology Venereol.*, vol. 22, no. 9, pp. 1089–1093, Sep. 2008, doi: 10.1111/j.1468-3083.2008.02719.x.

[77] Y. Lee and E. D. Baron, "Photodynamic therapy: current evidence and applications in dermatology.," *Seminars in cutaneous medicine and surgery*, vol. 30, no. 4. Semin Cutan Med Surg, pp. 199–209, 2011, doi: 10.1016/j.sder.2011.08.001.

[78] B. Wang *et al.*, "Gain with no pain? Pain management in dermatological photodynamic therapy," *Br. J. Dermatol.*, vol. 177, no. 3, pp. 656–665, 2017, doi: 10.1111/bjd.15344.

[79] R. Kollipara, E. Ekhlassi, C. Downing, J. Guidry, M. Lee, and S. Tyring, "Advancements in Pharmacotherapy for Noncancerous Manifestations of HPV," *J. Clin. Med.*, vol. 4, no. 5, pp. 832–846, 2015, doi: 10.3390/jcm4050832.

[80] G. Andrei, R. Snoeck, D. Schols, and E. De Clercq, "Induction of apoptosis by cidofovir in human papillomavirus (HPV)-positive cells," *Oncol. Res.*, vol. 12, no. 9–10, pp. 397–408, 2000, doi: 10.3727/096504001108747855.

[81] T. Fernández-Morano, J. Del Boz, M. Frieyro-Elichegui, J. B. Repiso, L. Padilla-España, and M.

De Troya-Martín, “Tratamiento de verrugas anogenitales con cidofovir tópico,” *Enferm. Infecc. Microbiol. Clin.*, vol. 31, no. 4, pp. 222–226, 2013, doi: 10.1016/j.eimc.2012.09.015.

[82] C. Derancourt and N. D. Andre, “Local Management of Anogenital Warts in Non-immunocompromised Adults : A Systematic Review and Meta-analyses of Randomized Controlled Trials,” *Dermatol Ther*, vol. 9, pp. 761–774, 2019, doi: 10.1007/s13555-019-00328-z.

[83] N. A. Peppas, P. Bures, W. Leobandung, and H. Ichikawa, “Hydrogels in pharmaceutical formulations.”

[84] M. L. B. Palacio and B. Bhushan, “Bioadhesion: a review of concepts and applications,” *Trans. R. Soc. A*, vol. 370, pp. 2321–2347, 2012, doi: 10.1098/rsta.2011.0483.

[85] H. H. Tønnesen, J. Karlsen, H. H. Tønnesen, and J. Karlsen, “Alginate in Drug Delivery Systems,” *Drug Dev. Ind. Pharm.*, vol. 28, no. 6, pp. 621–630, 2002, doi: 10.1081/DDC-120003853.

[86] M. Y. Gorshkova, I. F. Volkova, L. V. Vanchugova, I. L. Valuev, and L. I. Valuev, “Sodium Alginate Based Mucoadhesive Hydrogels,” *Appl. Biochem. Microbiol. 2019 554*, vol. 55, no. 4, pp. 371–374, Jul. 2019, doi: 10.1134/S0003683819040045.

[87] M. E. Abd El-Hack *et al.*, “Antimicrobial and antioxidant properties of chitosan and its derivatives and their applications: A review,” *Int. J. Biol. Macromol.*, vol. 164, pp. 2726–2744, Dec. 2020, doi: 10.1016/J.IJBIOMAC.2020.08.153.

[88] A. Muxika, A. Etxabide, J. Uranga, P. Guerrero, and K. De La Caba, “Chitosan as a bioactive polymer: Processing, properties and applications,” *Int. J. Biol. Macromol.*, vol. 105, pp. 1358–1368, 2017, doi: 10.1016/j.ijbiomac.2017.07.087.

[89] E. Fakhri *et al.*, “Chitosan biomaterials application in dentistry,” 2020, doi: 10.1016/j.ijbiomac.2020.06.211.

[90] V. Patrulea, V. Ostafe, G. Borchard, and O. Jordan, “Chitosan as a starting material for wound healing applications,” *Eur. J. Pharm. Biopharm.*, vol. 97, pp. 417–426, Nov. 2015, doi: 10.1016/J.EJPB.2015.08.004.

[91] L. M. Hemmingsen, K. Julin, L. Ahsan, P. Basnet, M. Johannessen, and N. Škalko-Basnet, “Chitosomes-in-chitosan hydrogel for acute skin injuries: Prevention and infection control,” *Mar. Drugs*, vol. 19, no. 5, May 2021, doi: 10.3390/MD19050269/S1.

[92] W. H. De Jong and P. J. Borm, “Drug delivery and nanoparticles: Applications and hazards,” 2008.

[93] S. Parveen, R. Misra, and S. K. Sahoo, “Nanoparticles: a boon to drug delivery, therapeutics, diagnostics and imaging,” 2012, doi: 10.1016/j.nano.2011.05.016.

[94] C. Gómez-Gaete, “Nanopartículas Poliméricas: Tecnología y Aplicaciones Farmacéuticas,” *Polímeros. Rev. Farm. Chile*, vol. 7, no. 2, pp. 7–16, 2014.

[95] J. P. Rao and K. E. Geckeler, “Polymer nanoparticles: Preparation techniques and size-control parameters,” *Prog. Polym. Sci.*, vol. 36, pp. 887–913, 2011, doi: 10.1016/j.progpolymsci.2011.01.001.

[96] U. Bilati, E. Allémann, and E. Doelker, “Sonication Parameters for the Preparation of Biodegradable Nanocapsulesof Controlled Size by the Double Emulsion Method,” *Pharm. Dev. Technol.*, vol. 8, no. 1, pp. 1–9, 2003, doi: 10.1081/PDT-120017517.

[97] M. Mallandrich *et al.*, “Nano-engineering of ketorolac tromethamine platforms for ocular treatment of inflammatory disorders,” *https://doi.org/10.2217/nnm-2020-0403*, vol. 16, no.

5, pp. 401–414, Feb. 2021, doi: 10.2217/NNM-2020-0403.

[98] M. C. Urrejola *et al.*, “Sistemas de Nanopartículas Poliméricas II: Estructura, Métodos de Elaboración, Características, Propiedades, Biofuncionalización y Tecnologías de Auto-Ensamblaje Capa por Capa (Layer-by-Layer Self-Assembly) Polymeric Nanoparticle Systems: Structure, Elaboration Methods, Characteristics, Properties, Biofunctionalization and Self-assembly Layer by Layer Technologies,” 2018.

[99] M. Danaei *et al.*, “Impact of particle size and polydispersity index on the clinical applications of lipidic nanocarrier systems,” *Pharmaceutics*, vol. 10, no. 2, pp. 1–17, 2018, doi: 10.3390/pharmaceutics10020057.

[100] M. F. Zambaux, F. Bonneaux, R. Gref, P. Maincent, E. Dellacherie, and M. J. Alonso, “Influence of experimental parameters on the characteristics of poly (lactic acid) nanoparticles prepared by a double emulsion method,” *J. Control. Release*, vol. 50, pp. 31–40, 1998.

[101] U. Bilati, E. Allémann, and E. Doelker, “Sonication Parameters for the Preparation of Biodegradable Nanocapsulesof Controlled Size by the Double Emulsion Method,” *Pharm. Dev. Technol.*, vol. 8, no. 1, pp. 1–9, 2003, doi: 10.1081/PDT-120017517.

[102] R. M. Mainardes and R. C. Evangelista, “Journal of Microencapsulation Micro and Nano Carriers Praziquantel-loaded PLGA nanoparticles: preparation and characterization,” 2008, doi: 10.1080/02652040400026285.

[103] J. B. Mayoral, A. C. Moreno, and E. San Martín-Martínez, “Potencial zeta en la determinación de carga superficial de liposomas,” *Am. J. Phys. Educ*, vol. 8, no. 4, 2014, Accessed: May 31, 2022. [Online]. Available: http://www.lajpe.org.

[104] G. S. De Oliveira, D. Agarwal, and H. T. Benzon, “Perioperative single dose ketorolac to prevent postoperative pain: A meta-analysis of randomized trials,” *Anesth. Analg.*, vol. 114, no. 2, pp. 424–433, 2012, doi: 10.1213/ANE.0b013e3182334d68.

[105] S. M. El-Harazi, R. S. Ruiz, R. M. Feldman, G. Villanueva, and A. Z. Chuang, “Efficacy of preoperative versus postoperative ketorolac tromethamine 0.5% in reducing inflammation after cataract surgery,” *J. Cataract Refract. Surg.*, vol. 26, no. 11, pp. 1626–1630, 2000, doi: 10.1016/S0886-3350(00)00519-8.

[106] E. D. Donnenfeld, H. D. Perry, J. R. Wittpenn, R. Solomon, A. Nattis, and T. Chou, “Preoperative ketorolac tromethamine 0.4% in phacoemulsification outcomes: Pharmacokinetic-response curve,” *J. Cataract Refract. Surg.*, vol. 32, no. 9, pp. 1474–1482, Sep. 2006, doi: 10.1016/J.JCRS.2006.04.009.

[107] K. Y, Inoue; K, Suzuki; R, Maeda; A, Shimura; I, Murata; I, “Evaluation of formulation properties and skin penetration in the same additive-containing formulation,” *Results Pharma Sci.*, vol. 4, pp. 42–49, Sep. 2014, doi: 10.1016/J.RINPHS.2014.09.003.

[108] “Ketorolac tromethamine | C19H24N2O6 - PubChem.” https://pubchem.ncbi.nlm.nih.gov/compound/Ketorolac-tromethamine (accessed Jun. 02, 2022).

[109] “Ketorolac | C15H13NO3 - PubChem.” https://pubchem.ncbi.nlm.nih.gov/compound/3826 (accessed Jun. 02, 2022).

[110] U. F. S. Frank Netzlaff, Karl-Heinz Kostka, Claus-Michael Lehr, “TEWL measurements as a routine method for evaluating the integrity,” *Eur. J. Pharm. Biopharm.*, vol. 63, pp. 44–50, 2006, doi: 10.1016/j.ejpb.2005.10.009.

[111] S. Amores, J. Domenech, H. Colom, A. C. Calpena, B. Clares, and Á. Gimeno, “An improved

cryopreservation method for porcine buccal mucosa in ex vivo drug permeation studies using Franz diffusion cells," *Eur. J. Pharm. Sci.*, vol. 60, pp. 49–54, 2014, doi: 10.1016/j.ejps.2014.04.017.

[112] N. M. Salwowska, K. A. Bebenek, D. A. Żądło, and D. L. Wcisło-Dziadecka, "Physiochemical properties and application of hyaluronic acid: a systematic review," *J. Cosmet. Dermatol.*, vol. 15, no. 4, pp. 520–526, 2016, doi: 10.1111/jocd.12237.

[113] M. Essendoubi, C. Gobinet, R. Reynaud, J. F. Angiboust, M. Manfait, and O. Piot, "Human skin penetration of hyaluronic acid of different molecular weights as probed by Raman spectroscopy," *Ski. Res. Technol.*, vol. 22, no. 1, pp. 55–62, 2016, doi: 10.1111/srt.12228.

[114] M. Mallandrich *et al.*, "Developing Transdermal Applications of Ketorolac Tromethamine Entrapped in Stimuli Sensitive Block Copolymer Hydrogels," *Pharm Res*, no. 34, pp. 1728–1740, 2017, doi: 10.1007/s11095-017-2181-8.

[115] S. Bredenberg *et al.*, "In vitro and in vivo evaluation of a new sublingual tablet system for rapid oromucosal absorption using fentanyl citrate as the active substance," *Eur. J. Pharm. Sci.*, vol. 20, no. 3, pp. 327–334, 2003, doi: 10.1016/j.ejps.2003.07.002.

[116] F. El Moussaoui, Salima; Fernández-Campos *et al.*, "Topical Mucoadhesive Alginate-Based Hydrogel Loading Ketorolac for Pain Management after Pharmacotherapy, Ablation, or Surgical Removal in Condyloma Acuminata," *gels*, 2021. https://doi.org/10.3390/gels7010008.

[117] Radha Bhati and Raja K Nagrajan, "A detailed Review on oral mucosal drug delivery system," *Int. J. Pharm. Sci. Res.*, vol. 3, no. 03, pp. 659–681, 2012.

[118] S. P. Humphrey and R. T. Williamson, "A review of saliva: Normal composition, flow, and function," *J. Prosthet. Dent.*, vol. 85, no. 2, pp. 162–169, Feb. 2001, doi: 10.1067/MPR.2001.113778.

[119] H. A. Bibi, R. Holm, and A. Bauer-Brandl, "Use of Permeapad® for prediction of buccal absorption: A comparison to in vitro, ex vivo and in vivo method," *Eur. J. Pharm. Sci.*, vol. 93, pp. 399–404, 2016, doi: 10.1016/j.ejps.2016.08.041.

[120] Z. Shariatinia, "Pharmaceutical applications of chitosan," *Adv. Colloid ans Interface Sci.*, vol. 263, pp. 131–192, 2018, doi: 10.1016/j.cis.2018.11.008.

[121] A. Ali and S. Ahmed, "A review on chitosan and its nanocomposites in drug delivery," *Int. J. Biol. Macromol.*, vol. 109, pp. 273–286, 2018, doi: 10.1016/j.ijbiomac.2017.12.078.

[122] Y. Yang, G. Chen, P. Murray, and H. Zhang, "Porous chitosan by crosslinking with tricarboxylic acid and tuneable release," *SN Appl. Sci.*, vol. 2, no. 3, pp. 1–10, Mar. 2020, doi: 10.1007/S42452-020-2252-Z/FIGURES/7.

[123] S. Sharma, A. Kumar, Deepak, R. Kumar, N. K. Rana, and B. Koch, "Development of a novel chitosan based biocompatible and self-healing hydrogel for controlled release of hydrophilic drug," *Int. J. Biol. Macromol.*, vol. 116, pp. 37–44, Sep. 2018, doi: 10.1016/J.IJBIOMAC.2018.05.020.

[124] I. Garcia-Orue *et al.*, "Development of Bioinspired Gelatin and Gelatin/Chitosan Bilayer Hydrofilms for Wound Healing," *Pharm. 2019, Vol. 11, Page 314*, vol. 11, no. 7, p. 314, Jul. 2019, doi: 10.3390/PHARMACEUTICS11070314.

[125] C. Peniche, C. Elvira, and J. S. Roman, "Interpolymer complexes of chitosan and polymethacrylic derivatives of salicylic acid: preparation, characterization and modification by thermal treatment."

[126] N. Bhattarai, J. Gunn, and M. Zhang, “Chitosan-based hydrogels for controlled, localized drug delivery,” *Adv. Drug Deliv. Rev.*, vol. 62, no. 1, pp. 83–99, Jan. 2010, doi: 10.1016/J.ADDR.2009.07.019.

[127] N. Iglesias, E. Galbis, C. Valencia, M. V. de-Paz, and J. A. Galbis, “Reversible pH-Sensitive Chitosan-Based Hydrogels. Influence of Dispersion Composition on Rheological Properties and Sustained Drug Delivery,” *Polym. 2018, Vol. 10, Page 392*, vol. 10, no. 4, p. 392, Apr. 2018, doi: 10.3390/POLYM10040392.

[128] J. Ghitman, E. I. Biru, R. Stan, and H. Iovu, “Review of hybrid PLGA nanoparticles: Future of smart drug delivery and theranostics medicine,” *Mater. Des.*, vol. 193, p. 108805, Aug. 2020, doi: 10.1016/J.MATDES.2020.108805.

[129] J. Llabot and S. D. Palma, “Nanopartículas poliméricas sólidas,” *Nuestra Farm.*, vol. 53, pp. 40–47, 2008.

[130] A. Lee, H. Y. Tsai, and M. Z. Yates, “Steric stabilization of thermally responsive N-isopropylacrylamide particles by poly(vinyl alcohol),” *Langmuir*, vol. 26, no. 23, pp. 18055–18060, Dec. 2010, doi: 10.1021/LA1039128/ASSET/IMAGES/MEDIUM/LA-2010-039128_0008.GIF.

[131] S. M. Ali and G. Yosipovitch, “Skin pH: From basic science to basic skin care,” *Acta Derm. Venereol.*, vol. 93, no. 3, pp. 261–267, Mar. 2013, doi: 10.2340/00015555-1531/.

[132] K. L. Campbell and C. A. Lichtensteiger, “Structure and Function of The Skin,” *Small Anim. Dermatology Secrets*, pp. 1–9, Dec. 2003, doi: 10.1016/B978-1-56053-626-0.50005-7.

[133] S. G. Raney and M. J. Hope, “The effect of bilayer and hexagonal HII phase lipid films on transepidermal water loss,” *Exp. Dermatol.*, vol. 15, no. 7, pp. 493–500, Jul. 2006, doi: 10.1111/J.1600-0625.2006.00432.X.

[134] M.-M. Constantin, S. Bucur, E.-D. Serban, R. Olteanu, O. G. Bratu, and T. Constantin, “Measurement of skin viscoelasticity: A non-invasive approach in allergic contact dermatitis.,” *Exp. Ther. Med.*, vol. 20, no. 6, p. 184, Dec. 2020, doi: 10.3892/etm.2020.9314.

[135] M. J. Linnehan and N. E. Groce, “Counseling and Educational Interventions for Women with Genital Human Papillomavirus Infection,” *https://home.liebertpub.com/apc*, vol. 14, no. 8, pp. 439–445, Jul. 2004, doi: 10.1089/108729100416650.

[136] K. Hammarlund, M. Nyström, and J. Jomeen, “Young women’s experiences of managing self-treatment for anogenital warts,” *Sex. Reprod. Healthc.*, vol. 3, no. 3, pp. 117–121, Oct. 2012, doi: 10.1016/J.SRHC.2012.07.002.